High resolution characterization of human erythroid progenitor's heterogeneity : implications for understanding physiological and pathological erythropoiesis.

Hongxia Yan

▶ **To cite this version:**

Hongxia Yan. High resolution characterization of human erythroid progenitor's heterogeneity : implications for understanding physiological and pathological erythropoiesis.. Human health and pathology. Université Montpellier, 2021. English. NNT : 2021MONTT045 . tel-03539472

HAL Id: tel-03539472
https://theses.hal.science/tel-03539472

Submitted on 21 Jan 2022

HAL is a multi-disciplinary open access archive for the deposit and dissemination of scientific research documents, whether they are published or not. The documents may come from teaching and research institutions in France or abroad, or from public or private research centers.

L'archive ouverte pluridisciplinaire **HAL**, est destinée au dépôt et à la diffusion de documents scientifiques de niveau recherche, publiés ou non, émanant des établissements d'enseignement et de recherche français ou étrangers, des laboratoires publics ou privés.

THÈSE POUR OBTENIR LE GRADE DE DOCTEUR DE L'UNIVERSITÉ DE MONTPELLIER

En Biologie-Santé

École doctorale Sciences Chimiques et Biologiques pour la Santé

Unité de recherche Institut de Génétique Moléculaire de Montpellier (IGMM) – UMR 5535

High resolution characterization of human erythroid progenitor heterogeneity: Implications for understanding physiological and pathological erythropoiesis

Présentée par Hongxia YAN
Le 03 Décembre 2021

Sous la direction de Sandrina KINET et Narla MOHANDAS

Devant le jury composé de

Eric SOLER, PhD, HDR, DR2 INSERM- IGMM UMR5535 Montpellier	Président
Frédérique VERDIER, PhD, HDR, DR2 Institut Cochin, Paris	Rapportrice
Loïc GARÇON, MD, PhD, PU-PH, CHU, Amiens	Rapporteur
Lionel BLANC, PhD, HDR- Feinstein Insitutes for Medical Research	Examinateur
Lydie DA COSTA, Pr, MD, PhD, AP-HP, Université de Paris	Examinatrice
Naomi TAYLOR, MD, PhD, DR1, IGMM (Montpellier)	Examinatrice
Sandrina KINET, PhD, HDR, CRCN, IGMM (Montpellier)	Directrice de Thèse
Narla MOHANDAS, DSc, New York Blood Center	Co-Directeur de Thèse

UNIVERSITÉ DE MONTPELLIER

Dedication:

To my husband, Gang, and my children, Qianqian and Ethan.

When we have each other, we have everything.

RESUME

RESUME

L'érythropoïèse est un processus qui permet la production de globules rouges à partir de cellules souches de la moelle osseuse. Ce processus complexe finement régulé est généralement divisé en 3 phases successives : l'érythropoïèse précoce, la différenciation érythroïde terminale (TED) et la maturation réticulocytaire. La première est la phase la moins bien définie ; l'hétérogénéité des progéniteurs érythroïdes restant à être mieux caractérisée.

Cette thèse à articles présente 2 études centrées sur la caractérisation et la régulation des progéniteurs érythroïdes dans l'érythropoïèse humaine normale et pathologique.

Nous avons d'abord exploré le mécanisme d'action des glucocorticoïdes dans la lignée érythroïde et la résistance aux stéroïdes chez les patients atteints de l'anémie de Diamond-Blackfan (ADB). Les glucocorticoïdes sont une des principales options thérapeutiques pour traiter ces patients et leur effet dans l'activation de l'érythropoïèse est bien connu. Cependant, les mécanismes moléculaires sous-jacent restent encore relativement incompris. Nous avons découvert que la dexaméthasone (dex), un glucocorticoïde synthétique, augmente la prolifération érythroïde des cellules souches/progénitrices $CD34^+$ dérivées de sangs périphériques d'adultes (SPA), mais pas celles de sangs de cordon (SC). En décryptant l'hétérogénéité d'une population de progéniteurs prédominant uniquement dans le SPA, nous avons identifié une population immature de CFU-E $CD71^{hi}CD105^{med}$ comme principale cible de la dex. L'analyse protéomique a révélé une augmentation spécifique de l'expression de régulateurs du cycle cellulaire dans les $CD34^+$ dérivées de SPA traités avec la dex, notamment du facteur $p57^{kip2}$, un inhibiteur de la kinase cycline-dépendante Cip/Kip. En accord avec une étude récente, nous avons observé une diminution significative des cellules en phase S dans les CFU-E immatures dérivées de SPA traités avec la dex. De plus, nous avons montré que la diminution de l'expression de $p57^{kip2}$ atténuait de manière significative l'effet de la dex. Il est important de noter que l'expression dérégulée de $p57^{kip2}$ a été observée dans les progéniteurs érythroïdes de patients ADB présentant une résistance aux stéroïdes. Ces données suggèrent que la dex induit spécifiquement l'expansion des CFU-E immatures $CD71^{hi}CD105^{med}$ par le biais d'un rôle conservé de $p57^{kip2}$ dans la régulation négative du cycle cellulaire.

Nous avons ensuite décrit l'hétérogénéité des progéniteurs érythroïdes via un immunophénotypage caractérisant le continuum des progéniteurs érythroïdes précoces dans la moelle osseuse humaine. En utilisant les marqueurs de surface CD71 et CD105, nous avons divisé les populations de progéniteurs érythroïdes précédemment définies par IL3R, GPA, CD34 et CD36 en sous-groupes et avons effectué leur caractérisation fonctionnelle. Ainsi, nous avons disséqué le continuum des progéniteurs érythroïdes en 4 populations distinctes : EP1, EP2, EP3 et EP4. De plus, nous avons montré que la diminution marquée de l'expression de CD105 pendant la TED pouvait discriminer les 5 stades d'érythroblastes : les pro-érythroblastes, les érythroblastes basophiles précoces et tardif ainsi que poly- et ortho-chromatiques. Cette stratégie permet ainsi la détection plus fine des étapes de la différenciation érythroïde allant du stade BFU-E aux réticulocytes. En appliquant cette stratégie expérimentale à des cellules de moelle osseuse provenant de patients atteints du syndrome myélodysplasique (SMD), nous avons identifié des défauts précédemment non encore identifiés à divers stades des progéniteurs érythroïdes.

Ainsi, mes résultats ont permis de définir avec une meilleure résolution l'hétérogénéité des progéniteurs érythroïdes ainsi que de mieux comprendre le mécanisme d'action de la dex dans le traitement de l'ADB, contribuant ainsi à une meilleure compréhension de la biologie des progéniteurs érythroïdes dans le contexte des érythropoïèses normale et pathologique.

Mots clés : érythropoïèse précoce, hétérogénéité des progéniteurs érythroïdes, résistance aux stéroïdes, anémie de Diamond-Blackfan (ABD), syndrome myéloblastique (SMD)

ABSTRACT

ABSTRACT

Erythropoiesis is a process by which red blood cell are produced from hematopoietic stem cell present in the bone marrow. It is a complex process subject to tight regulation, which could be divided into three successive phases: early erythropoiesis, terminal erythroid differentiation (TED), and reticulocyte maturation. Of those three phases, early erythropoiesis is the least characterized and the heterogeneity of erythroid progenitors remains to be better characterized.

This thesis presents the results of two paralleled studies that center around the characterization and regulation of erythroid progenitors in normal and disordered human erythropoiesis, in the form of published articles.

In article 1, we explored the mechanism of action of glucocorticoids in the erythroid lineage and steroid resistance in patients with Diamond Blackfan anemia (DBA). As one of the main therapeutic options for treatment of patients with DBA, the effect of glucocorticoids in promoting erythropoiesis is well known, but the underlying mechanism remains elusive. We found that dexamethasone, a synthetic glucocorticoid, enhanced the erythroid proliferation of $CD34^{+}$ hematopoietic stem/progenitor cells (HSPCs) derived from peripheral blood (PB) but not cord blood (CB). By resolving the heterogeneity of a progenitor population predominating in PB but not CB, we identified an immature CFU-E population $CD71^{hi}CD105^{med}$ as the principal target of dexamethasone. Proteomics analysis revealed specific up-regulation of several cell cycle regulators in PB derived cells treated with dexamethasone including $p57^{kip2}$, a Cip/Kip cyclin-dependent kinase inhibitor.

Consistent with a recent study, we observed a significant decrease of S-phase cells in PB derived immature CFU-Es treated with dexamethasone and down-regulation of $p57^{kip2}$ significantly attenuated the effect of dexamethasone. Importantly, dysregulated expression of $p57^{kip2}$ was observed in erythroid progenitors from DBA patients with steroid resistance. Altogether, these data suggested that dexamethasone specifically induces expansion of immature CFU-Es $CD71^{hi}CD105^{med}$ through a conserved role of $p57^{kip2}$ in negative regulation of cell cycle in murine and humans.

In the paralleled study presented in article 2, we further delineated the heterogeneity of erythroid progenitors through comprehensive immunophenotyping on the continuum of early erythropoiesis in human bone marrow. Using the two surface markers used in the above study, CD71 and CD105, we divided erythroid progenitor

populations previously defined by IL3R, GPA, CD34 and CD36 into more subsets and performed functional characterization on these subsets. On this basis, we dissected the erythroid progenitors continuum into four distinct populations, EP1, EP2, EP3 and EP4. Moreover, we demonstrated that the marked decrease of CD105 expression during TED could discriminate the five stages of erythroblasts including pro-erythroblast, early and late basophilic erythroblast, poly- and ortho-chromatic erythroblasts. Thus, we developed an efficient flow cytometry-based strategy for stage-wise detection of erythroid differentiation from the BFU-E stage to the reticulocytes. Applying this strategy to primary bone marrow cells from patients with myelodysplastic syndrome (MDS), we identified previously unrecognized defects at varied stages of erythroid progenitors.

Taken together, the findings delineated the heterogeneity of erythroid progenitors at a better resolution, and demonstrated the mechanism of current therapeutic drug for treatment of DBA, contributing to a better understanding of erythroid progenitors biology in the context of normal and disordered erythropoiesis.

Key words: early erythropoiesis; heterogeneity of erythroid progenitors; steroid resistance; Diamond Blackfan Anemia (DBA); myelodysplastic syndrome (MDS).

RESUME GRAND PUBLIC/ ABSTRACT GENERAL PUBLIC

Résumé grand public

L'érythropoïèse désigne le processus de production des globules rouges à partir de cellules souches de la moelle osseuse. Actuellement, les progéniteurs précoces de ce processus restent à être mieux caractérisés. J'ai d'abord montré qu'un glucocorticoïde synthétique utilisé pour traiter les patients atteints d'anémie de Diamond-Blackfan, induit spécifiquement l'expansion d'une population immature de cellules érythroïdes via une régulation négative du cycle cellulaire. J'ai ensuite mieux décrit l'hétérogénéité des progéniteurs érythroïdes en disséquant le continuum des étapes de différenciation allant des stades très précoces à celui précédant le globule rouge mature. Utilisant cette stratégie, j'ai identifié des défauts méconnus dans la moelle osseuse de patients atteints du syndrome myélodysplasique. Ainsi, mes résultats décrivent le continuum de ces progéniteurs avec une meilleure résolution et soulignent la complexité de leur régulation dans l'érythropoïèse normale et pathologique.

General public abstract

Erythropoiesis refers to the process of red cell production from stem cell in the bone marrow. Presently, erythroid progenitors that constitute early stage of this process remain to be better characterized. In a first study, I demonstrated that dexamethasone, a synthetic glucocorticoid used to treat patients with Diamond Blackfan anemia, specifically induces the expansion of an immature population by a negative regulation of the cell cycle. In a second study, I delineated the heterogeneity of erythroid progenitors by dissecting the entire continuum of erythroid progenitors from early stages to the stage preceding the mature red blood cell. Using this strategy, I identified unrecognized defects of erythroid progenitors in the bone marrow of patients with myelodysplastic syndrome. Overall, these findings depicted the continuum of erythroid progenitors at a higher resolution and highlighted the complexity of regulation of those progenitors in normal and disordered erythropoiesis

ACKNOWLEDGEMENT

ACKNOWLEDGEMENT

First, I would like to thank all the members of my thesis jury. Dr. Frédérique Verdier, Dr. Loïc Garçon, Dr. Naomi Taylor, Dr. Lydie Da Costa, Dr. Eric Soler and Dr. Lionel Blanc, thank you for offering your knowledge, your expertise and your valuable time to evaluate my research work, your contribution and your presence are very important to me, and it's a great honor to have each of you on the jury of my thesis.

I am extremely grateful to my amazing supervisors, Dr. Sandrina Kinet and Dr. Mohandas Narla. Thank you both for accepting me as a PhD candidate under your guidance and providing me endless supports. During last three year, these two great people have taught me how to learn, to practice, to think and to prepare for a future career development in the research field.

Sandrina, I'm deeply grateful for everything that you have done for me. From the beginning of my enrollment to the eventual completion of my thesis, you have always been there for me whenever I needed help or support. I sincerely appreciate the tremendous amount of time that you spent for me or with me. In the number of scientific discussions, emails, and more recent ZOOM meetings, I learnt a lot from you, scientifically and personally. Your constructive criticism, inspired questions and your encouraging words are irreplaceable for the completion of my thesis. Specifically, I want to thank you for your care and understanding when I had setbacks. Thank you for being a rigorous scientist, a warm person, a great supervisor.

Mohan, I cannot count how many times I said "thank you" since I joined your lab, my gratitude is beyond words. Behind every "thank you", there's your unreserved teaching, full support, and generous help. Thank you for taking me under your wings and guiding me throughout the project; thank you for answering my questions and sharing your profound knowledge without reservation; thank you for bringing me to the red cell field and offering me incredible opportunities to communicate and collaborate with many great scientists; thank you for your trust and respect; thank you for keeping faith in me all the time; thank you for being so passionate and dedicated to science that has inspired me to pursue an academic career in the research field… I am lucky to join your lab and work with you.

Very special thank you to Dr. Naomi Taylor, you're the one who brought to my attention to the possibility of being a PhD candidate at the University of Montpellier. Thank you for opening me this precious opportunity and helping me make the dream a

reality. Also, thank you for your time and effort as a member of my thesis committee, your valuable comments and your expert advice on my project are very important for me. More than that, thank you for being my reliable supporter in times of need, I truly appreciate all the non-scientific support and enthusiastic help, and I was really touched every year when I open the New Year greeting from the Sitbon-Taylors.

I must also thank Dr. Marc Sitbon, I am deeply honored to have you as the chair of my thesis committee. Thank you for your time organizing the meetings and evaluating my progress, I appreciate your constructive feedback during every thesis committee meeting. Additionally, thank you for the warm opening remarks before my presentations, that's very helpful relieving my nervousness and making me perform better.

A big thank you to Dr. Lionel Blanc, thank you for making me a priority for bone marrow samples, thank you for your constant support, for your prompt response to my questions and requests of manuscript revisions, I deeply appreciate your help with the preparation of the manuscripts. Your participation and contribution throughout my thesis project means a lot to me.

Many thanks to our incredible collaborators, it's my pleasure to have the chance working with you.

To the Blanc lab at the Feinstein Institute for Medical Research, thank you Ryan for working together with me on the dexamethasone journey, thank you Julien for coordinating the marrow samples, and experimental skills and discussing scientific thoughts.

To Dr. Anupama Narla and her Lab at Stanford University. Thank you Anu for your help whenever I needed, thank you for providing crucial clinical data to the study and for your important contributions to the manuscript. Thanks to Nan for your hard work, and for sharing exciting results.

To the Naomi Taylor Lab at Montpellier, I should have worked there for part of my project research, if there was no pandemic…Nevertheless, thanks to Pedro González Menéndez, for your hard work and the beautiful data you generated for our collaborative study.

To Dr. Patrick Gallagher and your excellent team members Kimberly Lezon-Geyda and Vincent Schulz, from Yale University, school of medicine. Thank you for sharing

the experimental techniques and helping the analysis of high-throughput sequencing data and productive discussions.

To Dr. Azra Raza and Dr. Ali Abdullah from Columbia University, thank you for providing the precious samples from patients with MDS and carrying your clinical expertise into this research and ongoing collaboration. Special thanks to Azra for teaching me the way you treat your patients, and I will always treat patient samples with respect and responsibility. Hope our continuing collaboration will bring new insights into the prognosis and treatment of the disease.

To all the donors and patients, I am grateful for all your contribution to this research, thank you for your belief that, in addition to physicians, basic medical researchers are also dedicated to making changes to alleviate the suffering of patients.

Thanks to my colleagues at New York blood center. Thank you Erjing and John for the days working together in the culture room and in front of flow cytometer, for the team work during long sorting days and for doing great job supporting my research. I would like to thank Dr. Christopher Hillyer, the CEO and President of the New York Blood Center and member of our red cell physiology laboratory, for participating in this research project and your continuous encouragement and support. Thanks to Mr. Barry Greene, the Vice President of the New York Blood Center, for offering excellent facility supports and all the help to ensure the progress of my project. Thanks to Mihaela and Zannatul at the flow facility core for providing excellent expertise service and accommodating my late sorting! Thanks to all the people that I met at NYBC, for accommodating flow time, sharing knowledge and techniques, and food!

The last, most important thank you to my family, to my parents and parents-in-law, to my husband Gang, to my angels Qianqian and Ethan, for your trust, hope and love!

TABLE OF CONTENTS

LIST OF FIGURES & TABLES

FIGURES

TABLES

LIST OF ABBREVIATIONS

#

2-DG: 2-deoxyglucose

A

ABCC4: ATP Binding Cassette Subfamily C Member 4

α-KG: α-ketoglutarate

ALAS: δ-aminolevulinic acid synthase

AML: Acute myeloid leukemia

ARC: Absolute reticulocyte count

ARNT: Aryl hydrocarbon receptor nuclear translocator

ASCT2: Solute Carrier Family 1 Member 5, glutamine importer

ATP: Adenosine triphosphate

B

BFU-E: Burst forming unit-Erythroid

BM: bone marrow

BMP: Bone morphogenetic protein

C

Cat: Catalase

CAT1: Solute Carrier Family 7 Member 1, arginine importer

CB: Cord blood

CD: Cluster of differentiation

CDK: Cyclin-dependent kinase

CEN: Core erythroid network

CFA: Colony forming assay

CFU-E: Colony forming unit-Erythroid

CHIP: Clonal hematopoiesis of indeterminate potential

CIP/KIP: CDK interacting protein/Kinase inhibitory protein

CLP: Common lymphoid progenitor

CMP: Common myeloid progenitor

CoA: Coenzyme A

D

DBA: Diamond Blackfan anemia

DCYTB: Duodenal Cytochrome B

DMT1: Divalent metal transporter 1

DNA: Deoxyribonucleic acid

DNMTs: DNA methyltransferases

E

E2A: Transcriptional factor E2-alpha

EBI: Erythroblastic island

EdU: 5-ethynyl-2′-deoxyuridine

EEP: Early Erythroid Progenitor

EKLF: Erythroid Kruppel-like factor

EMA: European medicines agency

EMP: Erythroblast macrophage protein

ENT1: Equilibrative nucleoside transporter 1

EP: Erythroid progenitor

EPAS1: Endothelial PAS domain containing protein 1

EPO: Erythropoietin

EPOR: Erythropoietin receptor

Er: Erythroid

ERK: Extracellular signal regulated kinase

ESA: Erythropoiesis-stimulating agents

EZH2: Enhancer of Zeste 2 Polycomb Repressive Complex 2

F

FACS: Fluorescence-activated cell sorting

FAD: Flavin adenine dinucleotide

FDA: Food and Drug Administration

FLVCR: Feline leukemia virus C receptor

FMN: Flavin mononucleotide

FOG1: Friend of GATA1

G

GATA1: GATA-binding factor 1

GATA1s: A short form of GATA1

GATA2: GATA-binding factor 2

GATA3: GATA-binding factor 3

GC: Glucocorticoid

G-CSF: Granulocyte colony-stimulating factor

GDF1: Growth differentiation factor 1

GDF11: Growth differentiation factor 11

GFI1B: Growth Factor Independent 1B

GLUT1: Solute Carrier Family 2 Member 1, Glucose transporter

GM-CSF: Granulocyte-macrophage colony-stimulating factor

GMP: Granulocyte/macrophage progenitor

GPA: Glycophorin A

GPx: glutathione peroxidase

GR: Glucocorticoid receptor

GRE: glucocorticoid response element

GSH: Reduced glutathione

GSSG: Oxidized glutathione

GVHD: Graft versus host disease

H

HATs: Histone acetyltransferases

Hb: Hemoglobin

HDACs: Histone deacetylases

HDMs: Histone demethylases

HIF: Hypoxia-inducible factor

HMA: hypomethylating agent

HMTs: Histone methyltransferases

HREs: Hypoxia response elements

HSC: Hematopoietic stem cell

HSCT: Hematopoietic stem cell transplantation

HSP70: Heat shock protein 70

HSPC: Hematopoietic stem progenitor cell

I

ICAM: Intercellular adhesion molecule

IDH1: Isocitrate dehydrogenase 1

IL-3: Interleukin-3

IPSS: the International Prognostic Scoring System for MDS

J

JAK2: Janus kinase 2

K

KLF1: Kruppel-like factor

L

LDB1: LIM Domain Binding 1

LEP: Late Erythroid Progenitor

LMO2: LIM Domain Only 2

M

MAPK: Mitogen-activated protein kinase

MDS: Myelodysplastic syndrome

MEP: Megakaryocyte/Erythrocyte progenitor

MGG: May-Grünwald Giemsa

miRNA: microRNA

Mk: Megakaryocyte

MMP: mitochondria membrane potential

MPL: Myeloproliferative Leukemia Protein, thrombopoietin transporter

MPP: Multipotent progenitor

MSCs: Mesenchymal stem cells

N

NAC: N-acetyl-cysteine

NLRP3: NOD-like receptor protein 3

NR4A1: Nuclear Receptor Subfamily 4 Group A Member 1

NuRD: Nucleosome remodeling and histone deacetylase

O

OS: Overall survival

OXPHOS: Oxidative phosphorylation

P

PB: Peripheral blood

PDK: Pyruvate dehydrogenase kinase

PER1: Period Circadian Regulator 1

PHDs: Prolyl hydroxylase domain proteins

PI3K: Phosphoinositide 3-kinase

PiT1: Phosphate importer 1

PiT2: Phosphate importer 2

PPP: Pentose phosphate pathway

Prdxs: Peroxiredoxins

PS: Phosphatidylserine

R

RBC: Red blood cell

RBC-TI: RBC transfusion independence

RBD: Receptor binding domain

RFVT1/2: Riboflavin importer 1/2

RNA: Ribonucleic acid

ROS: Reactive oxygen species

RP: Ribosomal protein

rRNA: Ribosomal RNA

RS: Ring sideroblast

S

SCF: Stem cell factor

shRNA: Short hairpin RNA

SOD: Superoxide dismutase

S-phase: synthesis phase

STAT5: Signal transducer and activator of transcription 5

T

TAL1: T-cell acute lymphocytic leukemia 1

TCA: Tricarboxylic acid cycle

TED: Terminal erythroid differentiation

TET: Ten-elven translocation

TFs: Transcription factors

TGF-β: Transforming growth factor-β

TO: Thiazole Orange

TPO: Thrombopoietin

TPO-R: Thrombopoietin receptor

TSR2: TSR2 Ribosome Maturation Factor

U

UCP2: Uncoupling protein 2

V

VCAM: Vascular cell adhesion molecule

X

XPR1: Phosphate exporter 1

INTRODUCTION

With approximately 2.5×10^{13} circulating cells in a healthy adult weighing 70kg, red blood cells (RBCs) are the most abundant cell type in human body (Palis, 2014). Their primary function is to transport oxygen from the lungs to the tissues. Decreased production or increased destruction of RBCs leads to anemia, a global health care problem affecting more than 1.6 billion people worldwide (Miller, 2013).

Human RBCs have a lifespan of approximately 120 days (Franco, 2012) and ~ 2 billion new RBCs need to be produced in adults by the bone marrow every day to maintain the homeostatic levels in circulation and replace aged cells eliminated by the spleen. Production of red cells from hematopoietic stem cells (HSCs) is a tightly regulated biological process designated as erythropoiesis.

In humans and other vertebrate animals, three sequential waves of erythropoiesis generate different type of erythroid cells to ensure oxygen transport at different developmental stages (McGrath & Palis, 2008) (Barminko, Reinholt, & Baron, 2016) (Nandakumar, Ulirsch, & Sankaran, 2016). The first wave of erythropoiesis, termed “primitive” erythropoiesis, emerges from the yolk sac blood islands, and generates large erythroid cells during early embryogenesis. These primitive erythroblasts complete their maturation in the circulation, including enucleation, and they predominantly express embryonic globin type, Hb Gower I (ζ2ε2) at week 5 of gestation before switching to Hb Gower II (α2ε2) (Peschle et al., 1985). Due to ethical concerns, very little is known about human primitive erythropoiesis, and most of our understanding comes from extensive studies in different mouse models.

The second wave of erythropoiesis arises following switching from the yolk sac to the fetal liver in the second gestational month in humans, in conjunction with generation of smaller “definitive” erythroid cells in circulation and the switch of hemoglobin from embryonic to fetal types (α2γ2) (Iturri et al., 2021; S. J. Lu & Lanza, 2019; S. J. Lu, Park, Feng, & Lanza, 2009).

As the fetus develops, hematopoietic niches begin to form in the bones and HSCs colonize these niches, with the bone marrow becoming the primary site of erythropoiesis during late fetal life, postnatal life and through adulthood. This constitutes the third wave of erythropoiesis (Gritz & Hirschi, 2016). In humans, a second switch from fetal globin (α2γ2) to adult globin (α2β2) takes place more gradually than in the murine system with the switch completed 9 months following birth and less than 5% of fetal hemoglobin expressed throughout life (Edoh, Bosaiko, & Amuzu, 2006; Oneal et al., 2006).

The work accomplished during my Ph. D focused on normal and disordered human definitive erythropoiesis. In this introduction, after a description of erythropoiesis at steady state (1. Human Definitive Erythropoiesis) and current advances in the regulatory machinery (2. Regulation of erythropoiesis.), I will discuss specific red cell disorders with ineffective erythropoiesis (3. Inherited and acquired disorders of erythropoiesis), such as Diamond Blackfan anemia (DBA) and myelodysplastic syndromes (MDS). Unless otherwise indicated, erythropoiesis refers to human definitive erythropoiesis in these chapters.

1. Human Definitive Erythropoiesis

Definitive erythropoiesis is characterized by the sequential maturation of a continuum of erythroid progenitors and precursors. A pre-requisite for the study of erythropoiesis in normal and pathological conditions is the identification and characterization of human erythroid progenitors and precursors at distinct developmental stages. While this process has been studied for decades, the continuum in humans has only recently been comprehensively characterized (J. Hu et al., 2013; J. Li et al., 2014; Yan et al., 2018).

According to the established models, human erythropoiesis can be divided into three distinct phases: early erythropoiesis, terminal erythroid differentiation (TED), and reticulocyte maturation (**Figure 1**).

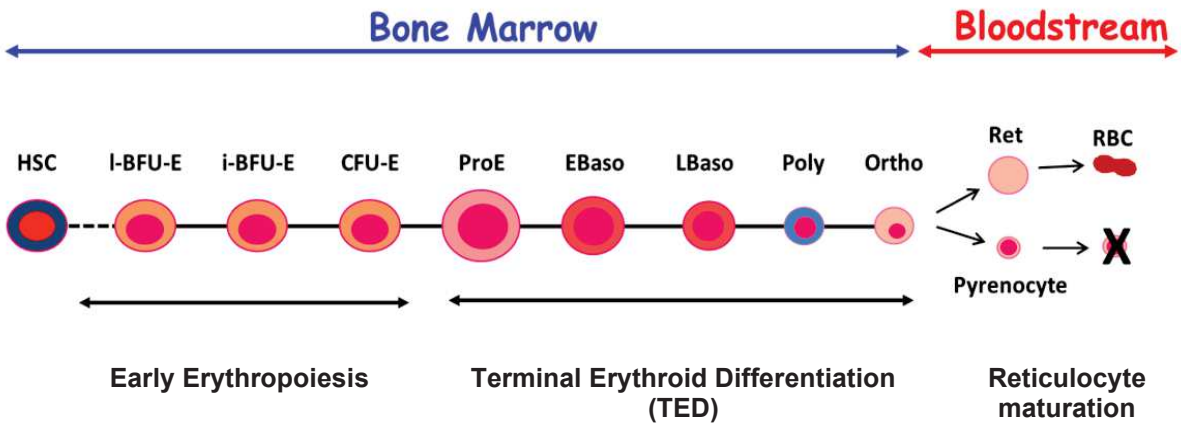

Figure 1. Human adult erythropoiesis. This process consists of three phases. While the early erythropoiesis and TED occur exclusively in the bone marrow, reticulocytes maturation begins in the bone marrow and is completed in blood stream. Proliferative erythroid progenitors from immature Burst forming unit-Erythroid (BFU-E) to more mature Colony forming unit-Erythroid (CFU-E) constitute early erythropoiesis. The proliferation ability of erythroid progenitor cells decreases with differentiation, and accordingly, their colony size declines from large BFU-E (l-BFU-E), intermediate BFU-E (i-BFU-E) to CFU-E. Terminal Erythroid Differentiation (TED) is composed of erythroblasts with distinguishable morphologies. Reticulocytes released from the bone marrow into the bloodstream following enucleation of orthochromatic erythroblasts mature into functional RBCs in the circulation.

1.1 Early erythropoiesis

1.1.1 Erythroid lineage commitment of HSCs

The conventional model of hematopoiesis has been described as a cellular hierarchy maintained by self-renewing of HSCs at the apex, which progressively give rise to multipotent progenitors (MPP) and then oligopotent, bipotent and unipotent

progenitors (**Figure 2, figure at the top**). The first major step of lineage bifurcation is the segregation of two oligopotent progenitors, the common myeloid progenitor (CMP) and the common lymphoid progenitor (CLP). In this model, CMP is the direct predecessor of bivalent granulocyte-monocyte progenitors (GMP) and megakaryocyte-erythroid progenitors (MEP), through which CMP generate all the cell types in the myeloid lineage. MEP eventually differentiates into unipotent progenitors of erythroid and megakaryocyte lineage. Thereafter, the generation of most immature erythroid progenitors, BFU-E initiates the first step of erythroid differentiation.

Despite the use of this model over many decades, recent findings have begun to challenge this stepwise progression of hematopoietic stem and progenitor cells (HSPCs) and have led to key revisions to this model. In 2013, Yamamoto R et al found that murine HSCs could directly differentiate into megakaryocyte, megakaryocyte and erythroid, or CMP via asymmetric division (Yamamoto et al., 2013). More recently, Notta et al noticed an unexpected low proportion of oligopotent progenitors (CMP and CLP) in the human bone marrow, with multipotent and unipotent progenitors predominating (Notta et al., 2016). Moreover, the megakaryocyte and erythroid lineages branched directly from the MPP, by passing the conventional CMP/MEP trajectory. In contrast, the oligopotent progenitors were a prominent component of the fetal liver hierarchy, and the megakaryocyte/erythroid (Mk/Er) lineage originates from not only the stem cell compartment, but also from the oligopotent and bipotent progenitors. Based on these findings, a redefined model of hematopoiesis has been proposed (**Figure 2, figure at the bottom**). From previously identified oligopotent CMP $Lin^{-}CD34^{+}CD38^{+}IL3R^{low}CD45RA^{-}$, Kohta Miyawaki et al (Miyawaki et al., 2017) identified a subpopulation possessing unipotent to megakaryocyte lineage based on expression of CD41 and these $CD41^{+}$ cells can contribute significantly to both normal and malignant megakaryopoiesis, without going through the conventional MEP stage. Interestingly, a most recent study revealed a transcriptional continuum of murine

hematopoietic progenitors, instead of discrete states. Furthermore, the investigators demonstrated that, in addition to the megakaryocytic fates, erythroid fate was also coupled with the basophil and mast cell fates, which proposed potential refinements over current model (Tusi et al., 2018). Thus, hematopoiesis appears to be a more complex process than it was originally postulated by the conventional hierarchy model, and that the Mk and Er lineages may arise via multiple different pathways.

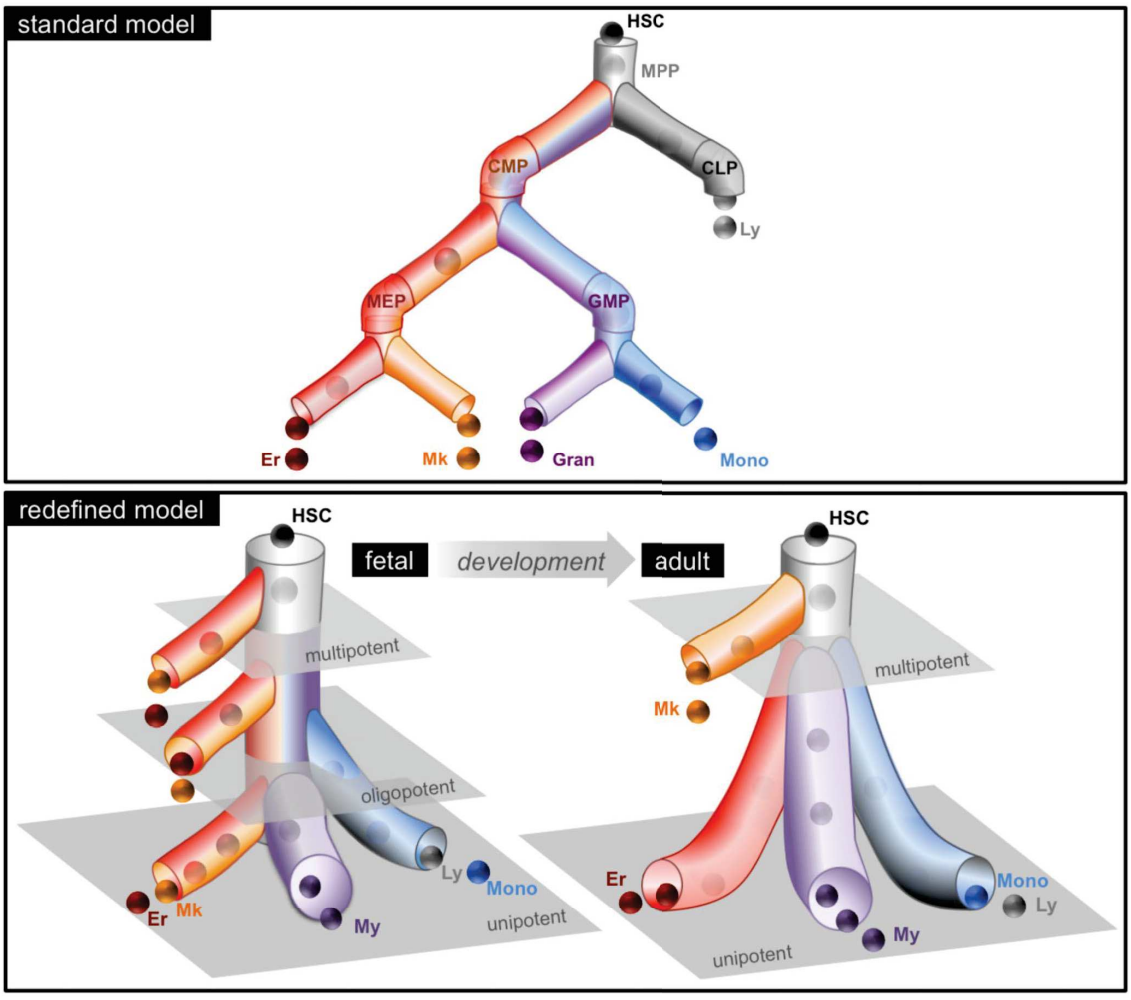

Figure 2. The classical model (top) and redefined model (bottom) of human hematopoiesis. A graphical representation of the redefined model that encompasses the predominant lineage potential of the newly defined progenitor subsets. The redefined model envisions a developmental shift in the progenitor cell architecture resulting in a two-tier hierarchy by adulthood. The standard model is shown at the **top** for comparison (Notta et al., 2016).

These recent findings have led to a controversy over the existence of the MEP in human hematopoiesis, which is closely associated with erythroid lineage specification. Using immunophenotyping, Markus G. Manz (Manz, Miyamoto, Akashi, & Weissman, 2002) identified $Lin^{-}CD34^{+}CD38^{+}IL3R^{-}CD45RA^{-}$ cells as the MEP in human bone marrow, which are widely used for quantification and isolation of bipotent Mk/Er progenitors for further analyses. However, functional assays from several recent studies revealed that this population is actually a mixed population greatly enriched for unipotent erythroid progenitors and committed megakaryocyte progenitors, with only low levels of "true" MEP (Mori, Chen, Pluvinage, Seita, & Weissman, 2015; C. J. H. Pronk et al., 2007). Not surprisingly, single cell RNA-seq on this population showed that most of these cells are transcriptionally primed to generate exclusively single-lineage output, erythroid predominantly, with a minority giving rise to mixed-lineage colonies (Miyawaki et al., 2017; Psaila et al., 2016).

One way to resolve this controversy is to identify Mk/Er bipotential in single cells (Xavier-Ferrucio & Krause, 2018). Chad Sanada and Juliana Xavier-Ferrucio et al (C. Sanada et al., 2016) developed a specific dual Mk/Er function assay to identify true MEP with Mk/Er bipotential. Consistent with the previous studies, the dual functional assay on individual cells revealed that the conventionally defined MEP is a heterogeneous mixture with only ~15% real MEP with bipotential. Using this assay, they found the true MEPs are mainly enriched in $Lin^{-}CD34^{+}CD38^{mid}$ population, characterized by expression of MPL, the receptor for Thrombopoietin (TPO). They further improved the isolation strategy by using $Lin^{-}CD34^{+}Flt3^{-}CD45RA^{-}CD38^{mid}MPL^{+}CD36^{-}CD41^{-}$ for bipotent MEP enrichment, which yielded 45-60% of CFU-Mk/Er, compared to ~15% of conventional approach.

Thus, bipotent progenitors do exist, but are a rare population with a proportion of <1% in human $CD34^{+}$ cells. In addition, the improved approach that enables more

efficient enrichment of purer MEP should facilitate a better understanding of fate decisions involved in commitment of MEPs towards to erythroid lineage.

Finally, the development of single cell multi-omics technologies in recent years should enable a more comprehensive analysis of the highly heterogeneous cell population present in human bone marrow. Future studies based on these technologies should provide multi-faceted insights into underlying mechanism of erythroid lineage specification via multiple pathways and the relative contribution of these different pathways under steady state and stress conditions (Y. Hu et al., 2018).

1.1.2 Erythroid progenitors: heterogeneity and developmental trajectory

Since their first description in murine system by Axelrod's lab in 1970s (Axelrad, Mcleod, Shreeve, & Heath, 1973; Stephenson, Axelrad, Mcleod, & Shreeve, 1971), erythroid progenitors BFU-E and CFU-E have been functionally defined by their ability to generate hemoglobinized colonies in the colony forming assay system (CFA). To perform a CFA, an appropriate number of HSPCs are seeded in the semi-solid methylcellulose media formulated for optimal proliferation and differentiation and incubated at 37℃, in 5% CO_2, with ≥ 95% humidity for ~7 days and ~15 days for CFU-E and BFU-E colony maturation, respectively. The number and the morphology of the colonies formed by a fixed number of input cells provide preliminary information about the ability of tested progenitors to differentiate and proliferate.

Based on extensive studies on murine erythroid progenitors (C. J. Gregory, 1976; Mcleod, Shreeve, & Axelrad, 1974), Connie J. Gregory and Allen C. Eaves (Connie J Gregory & Eaves, 1977) were the first to describe different types of erythroid colonies generated by human bone marrow cells, which could be distinguished by the time of maturation and cluster composition (**Table 1**).

Table 1. The three types of human erythroid colonies (Connie J Gregory & Eaves, 1977).

Colony type	Time of maturation	Number of clusters
Large BFU-E	17-20 days	>16
Small BFU-E	10-12 days	3-8
CFU-E	7-8 days	1-2

These fundamental studies and subsequent work on the effects of different growth factors on colony forming ability of human cells *in vitro* has greatly improved our understanding of early erythropoiesis and led to the following consensus in erythroid progenitor biology.

The BFU-E are the first committed erythroid progenitors, which generate large hemoglobinized colonies with multiple clusters of erythroid cells in semi-solid medium in the presence of essential growth factors including interleukin-3 (IL-3), stem cell factor (SCF) and erythropoietin (EPO) (C. H. Dai, Krantz, Means, Horn, & Gilbert, 1991; Chun Hua Dai, Krantz, & Zsebo, 1991; M. J. Koury & Bondurant, 1991; Sawada et al., 1987). Further differentiation of BFU-E leads to the generation of more mature erythroid progenitors, the CFU-E, which form smaller condensed colonies of one to two clusters in the presence of EPO only (Mark J. Koury, 2015; Stephenson et al., 1971). The differentiation of CFU-E leads to the first morphologically identifiable erythroblast, the Pro-erythroblast, and marks the transition from early erythropoiesis to TED. BFU-Es require at least 14 days to form well-hemoglobinized colonies typically containing thousands of erythroblasts, while CFU-Es need only 7 days to generate mature colonies containing 8-200 erythroblasts, highlighting a continuum of erythroid progenitors with different proliferation potentials.

To date, colony-forming assays are still the gold standard approach for identification of erythroid progenitors. However, these assays are time-consuming and the classification and scoring of colonies can be subjective. Moreover, they do not allow the isolation and use of highly enriched populations required for their detailed characterization at the molecular level.

Since 1980s, with the development of flow cytometry, several studies attempted to immunophenotype BFU-E and CFU-E enabling their potential isolation. Recently, our group developed a flow cytometry-based method for the identification and isolation of BFU-E and CFU-E (J. Li et al., 2014), based on the changes in the surface expression of a defined set of antigens during *in vitro* erythroid differentiation of $CD34^+$ HSPCs. BFU-E and CFU-E were immunophenotyped as $IL3R^-CD34^+CD36^-GPA^-$ and $IL3R^-CD34^-CD36^+GPA^-$, respectively. Further study identified a transitional population of $IL3R^-CD34^+CD36^+GPA^-$ as a mixture containing both BFU-E and CFU-E from *in vitro* cultures of adult-derived $CD34^+$ cells (**Figure 3**) (Yan et al., 2018). In addition, while present in cultures of both cord blood (CB) or adult peripheral blood (PB) derived $CD34^+$ cells, this transitional population was predominant and maintained only in adult-derived cultures.

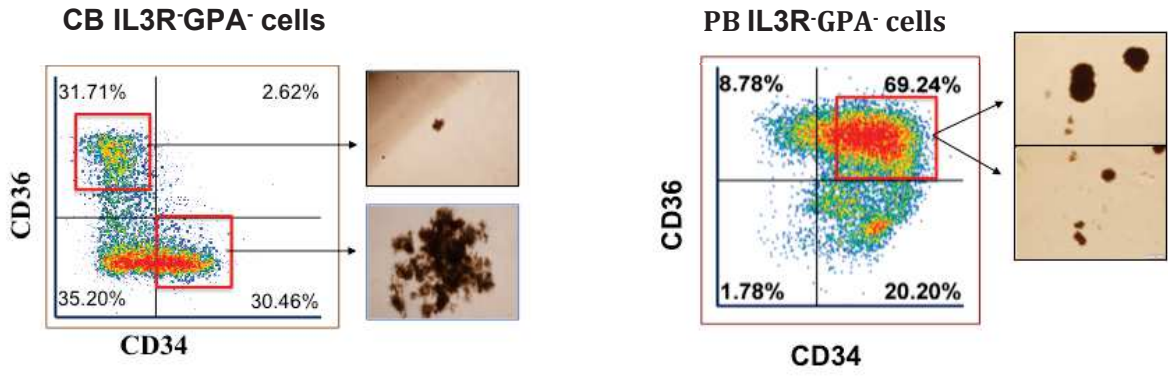

Figure 3. Erythroid progenitor populations identified from *in vitro* culture of $CD34^+$ cells. After 5 days of differentiation with presence of EPO, SCF and IL3, cells derived from CB (left) and PB (right) were collected and analyzed. Gated populations of erythroid progenitors were

isolated by fluorescence-activated cell sorting (FACS) -based cell sorting and CFA was performed as described (Yan et al., 2018).

Other groups also documented the prospective isolation of BFU-E and CFU-E from $CD34^+$ HSPCs. Based on the expression of CD36 and CD105, in the so-called MEP population ($Lin^-CD34^+CD38^+CD45RA^-IL3R^-$), Iskander and colleagues identified Early Erythroid Progenitor (EEP) as $CD105^-CD36^-$ and Late Erythroid Progenitor (LEP) as $CD105^+CD36^+$, generating BFU-E and CFU-E colonies, respectively (Iskander et al., 2015). Moreover, Mori and colleagues documented that, in the $Lin^-CD34^+CD38^+CD45RA^-IL3R^-$ population, $CD71^+$ $CD105^-$ MEPs primarily generated large erythroid colonies while $CD71^{int/+}$ $CD105^+$ MEPs gave rise mostly to CFU-E colonies (Mori et al., 2015). Both studies used CD105 as a potential marker for the discrimination between BFU-E and CFU-E. It is noteworthy that, in contrast to the $CD34^-CD36^+$ CFU-E defined by Jie Li et al (J. Li et al., 2014), the two above described studies identified CFU-E populations in the $CD34^+$ population. These results imply the potential existence of immunophenotypically different CFU-Es, highlighting the heterogeneity of human erythroid progenitors and the incomplete definition of BFU-E and CFU-E.

To address these heterogeneity issues and further improve our understanding of the continuum of erythroid progenitors, a systematic identification and characterization of intermediate progenitor populations is essential. This issue was one of the primary objectives of my project and we made significant progress as will be described in the RESULTS section. Briefly, four successive distinct erythroid progenitor populations were identified by a novel flow cytometry-based strategy, using a specific set of surface markers that included CD34, CD117 (c-Kit), IL3R, CD45RA, CD41a, CD71, CD105 and Glycophorin-A (GPA). These four populations constitute the continuum of early erythropoiesis, and the developmental trajectory of these populations was comprehensively validated *in vitro*

and *in vivo*. Importantly, the most mature CFU-E, redefined as EP4 (Erythroid Progenitor 4), underwent EPO-induced differentiation and generated proerythroblasts in 24 hours, implying the successive transition of late stage erythroid progenitor to TED.

1.2 Terminal erythroid differentiation (TED)

In striking contrast to the characterization of erythroid progenitors, terminal erythroid differentiation has been previously well-characterized (Jingping Hu et al, 2013). Terminal erythroid differentiation consists of morphologically distinct erythroid precursors starting with proerythroblasts. Proerythroblasts undergo 4-6 mitoses to sequentially generate early and late basophilic, polychromatophilic and orthochromatic erythroblasts (**Figure 1**). During this process, each cell division generates two daughter cells that are morphologically and functionally distinct to the mother cell. The essential criteria distinguishing these erythroblasts rely on morphological changes along with decrease in cell size, increased hemoglobin content and progressive nuclear condensation.

Terminal erythroid differentiation culminates with the enucleation process, resulting in the expulsion of the pyrenocyte from orthochromatic erythroblast and generation of enucleate reticulocyte. This process occurs within erythroblastic islands, niches for erythropoiesis, composed of a central macrophage surrounded by differentiating erythroblasts (Lévesque et al., 2021). In addition to serving as a nurse cell to provide iron to erythroblasts for hemoglobin production, the central macrophage has another critical function, which is to phagocyte the pyrenocyte through an “eat-me” signaling pathway (Yoshida et al., 2005). Although some progress has been made in last few decades (C. An et al., 2021; Gnanapragasam et al., 2016; Ji, Yeh, Ramirez, Murata-Hori, & Lodish, 2010; S. T. Koury, Koury, & Bondurant, 1989; Nowak et al., 2017; Ouled-Haddou et al., 2020), the mechanism of enucleation is still not fully understood.

Currently, efficient enucleation is the major technical bottleneck for the *in vitro* production of RBCs for use in transfusion.

To isolate erythroid precursors at distinct developmental stages for downstream molecular studies, our group monitored the dynamic changes of membrane protein expression on the surface of differentiating erythroblasts and used these insights to develop a method to isolate erythroblasts at distinct differentiation stages (J. Hu et al., 2013). Based on the expression of GPA, α4-integrin and band3, large numbers of erythroblasts at specific stages could be isolated with a high purity not only from *in vitro* $CD34^+$ HSPCs culture, but also directly from primary bone marrow samples. In addition, these surface markers also enabled detection and quantitation of TED *in vivo*, an important issue to identify stage-specific defects in disorders associated with impaired TED, such as MDS (**Figure 4**).

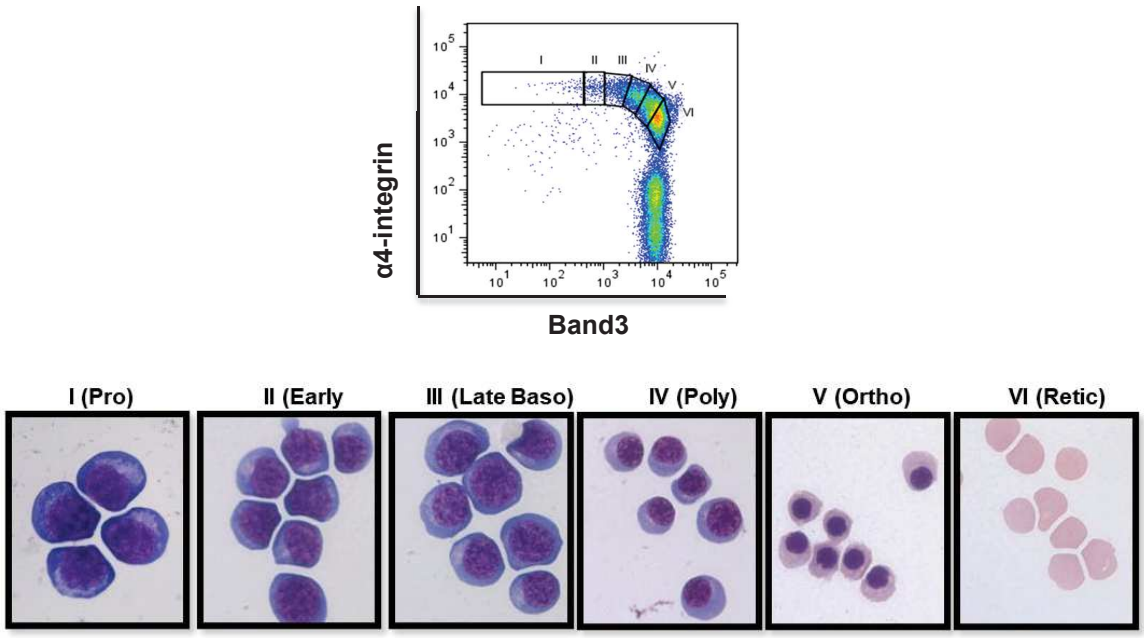

Figure 4. Isolation of erythroblasts at distinct differentiation stages. $CD45^-$ cells were isolated from bone marrow mononuclear cells for antibody staining. GPA^+ cells were gated for analysis and five stages of erythroblasts were isolated based on expression of α4-integrin and band3. May Grünwald-Giemsa (MGG) staining of purified erythroblasts showed distinctive cell morphologies (Lower panel), characterized by decrease of cell size, increase of hemoglobin

content and progressive nuclear condensation from proerythroblast, early and late basophilic erythroblast, to poly- and ortho- chromatic erythroblast (J. Hu et al., 2013).

Transcriptomic analysis on these purified populations of erythroblasts revealed marked changes in gene expression during TED with stage-specific transcriptomes. These data from high-throughput RNA-sequencing provided a useful resource for furthering our understanding of erythropoiesis (X. An et al., 2014).

While this immunophenotyping method was helpful to answer questions related to erythroid precursors, it could not resolve the whole continuum from the earliest stages to the reticulocyte. Therefore, I decided to develop an efficient and feasible FACS strategy for stage-wise detection of erythropoiesis. During my thesis, I highlighted CD105 as a key marker to resolve the entire erythroid continuum at a stage-wise manner, and these findings will be detailed in the RESULTS section.

1.3 Reticulocyte maturation

The final step of erythropoiesis is reticulocyte maturation. Following enucleation of the orthochromatic erythroblast, nascent motile reticulocyte (also known as R1) undergoes maturation over 2-3 days to generate mature red cell. Two third of this maturation process takes place in the bone marrow, and the later stage stomatocytic reticulocyte (also known as R2) reach the blood stream where they acquire their biconcave shape, characteristic of mature red cells (Malleret et al., 2013; Mel, Prenant, & Mohandas, 1977).

During reticulocyte maturation all internal organelles are lost, and extensive membrane remodeling occurs. Reticulocytes lose about 20% of their membrane surface area during the maturation process and there is significant remodeling of the cytoskeleton (Blanc, Gassart, Géminard, Bette-Bobillo, & Vidal, 2005; Costa,

Mohandas, Sorette, & Tchernia, 2001; J. Liu, Guo, Mohandas, Chasis, & An, 2010; WAUGH et al., 1995).

Distinguishing features of reticulocytes are mostly their morphology and their RNA content. The use of Thiazole Orange (TO), a fluorescent nucleic acid intercalating dye, provided a “visualized” reticulocyte classification system through detection of the fluorescence intensity by flow cytometry (L G Lee, Cytometry, 1986). The use of flow cytometry overcame the time-consuming disadvantage of microscope-based visualization and classification and enabled rapid analysis on large numbers of blood cells. However, this method had a significant drawback in that TO stains not only RNA but also DNA, which can cause false positive results in certain conditions, such as presence of hemoparasites or Howell-Jolly bodies in mature red cells in certain pathological states (Roger S. Riley, 2001, JCLA).

Malleret et al (2013) recently reported an improved FACS-based classification of reticulocyte maturation. Based on the expression of CD71, the transferrin receptor, reticulocytes were classified into four populations ($CD71^{high}$, $CD71^{medium}$, $CD71^{low}$ and $CD71^{negative}$) and their morphology, membrane antigens, biomechanical properties and metabolomic profiles were phenotyped. The mature erythrocytes R3 are negative for both CD71 expression and TO staining, as there is no residual RNA in these cells. This study not only provided more efficient and feasible method for determination and isolation of maturing reticulocytes, but also provided more comprehensive insights for a more detailed understanding in reticulocytes biology (**Figure 5**).

With that being said, the mechanisms and molecular actors involved in the process of reticulocytes maturation such as membrane reorganization and organelle clearance are still not fully understood.

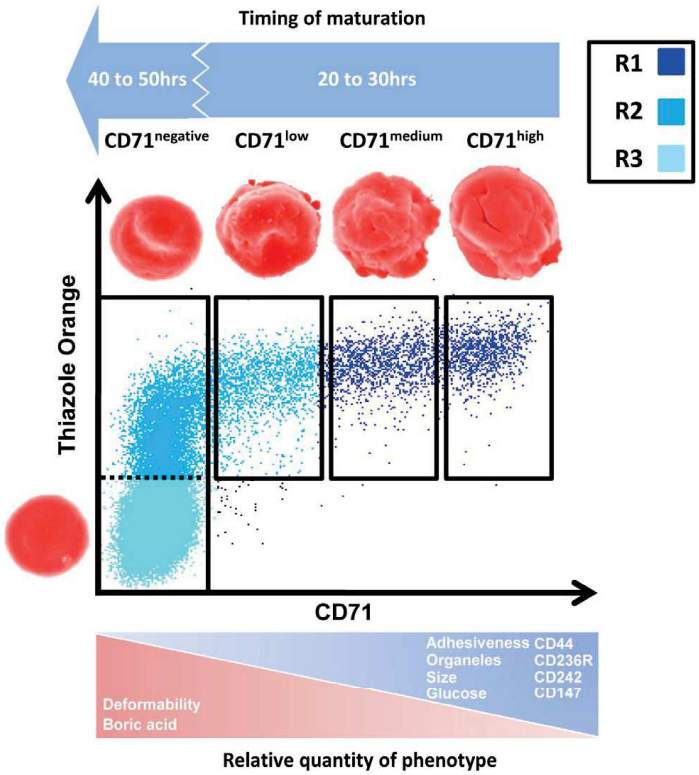

Figure 5. Phenotypic changes of maturing reticulocytes in human cord blood samples. Along with decrease in CD71 expression and TO staining, morphologies of maturing reticulocytes change. At the last stage, there's a loss of CD71 surface expression and bi-concave shape of functional red cells arise (Malleret et al., 2013).

2. Regulation of erythropoiesis

To maintain homeostatic numbers of RBCs in circulation under steady state conditions, and increased production of red cells under stress conditions, a tight regulation of erythropoiesis is required. Over the last several decades, accumulating evidence indicates that this complex process is controlled at multiple levels involving transcriptional factors (TFs), growth factor-driven signaling and cell-cell/cell-matrix interaction in the bone marrow niche (Gutiérrez, Caballero, Fernández-Calleja, Karkoulia, & Strouboulis, 2020; Lodish, Flygare, & Chou, 2010; Marieke von Lindern, Schmidt, & Beug, 2004; Yuan et al., 2020). Epigenetic modifications also heavily influence erythroid differentiation through epigenetic modifiers including but not limited

to DNA methyltransferases (DNMTs), Ten-eleven translocation (TET) enzymes, histone methyltransferases (HMTs) and demethylases (HDMs), histone acetyltransferases (HATs) and deacetylase (HDACs) (DeVilbiss et al., 2015; L. Ge et al., 2014; Liang Ge et al., 2014; Hewitt et al., 2014; Ji et al., 2010; Myers et al., 2020; Okano, Bell, Haber, & Li, 1999; Yan et al., 2017). In addition to these well-documented regulators, more recent studies reveal that, metabolic enzymes and metabolites as well as their transport and utilization, also play important roles in the regulation of erythropoiesis (N. J. Huang et al., 2018; Mikdar et al., 2021; Oburoglu, Romano, Taylor, & Kinet, 2016; A. Richard et al., 2019). Notably, responsive changes in the status of epigenetic modifications could be triggered by extrinsic factors like growth factors, hormones or metabolites, and epigenetic regulators could mediate regulation of TFs and metabolic status, highlighting the interlinkage between multiple players of the complex regulatory machinery(Guo et al., 2015; M. Y. Kim, Yan, Huang, & Qiu, n.d.; Kohrogi et al., 2021; Ling et al., 2019; L. Wang, Di, & Noguchi, 2014; Zwifelhofer et al., 2020).

2.1 Transcription factors (TFs)

Transcription factors are fundamental regulators of hematopoiesis, which function by recognizing and binding to specific DNA sequences of promoters or enhancers of targeted genes to stimulate or repress gene transcription. Three DNA-binding TFs, GAGA-binding factor 1 (GATA1), T-cell acute lymphocytic leukemia 1 (TAL1) and Kruppel-like factor 1 (KLF1) are considered master regulators of erythroid differentiation by activating the transcription of erythroid specific genes and suppressing genes regulating other lineages. Deficiency in any of these TFs leads to severely impaired erythropoiesis, as evidenced by mouse embryonic death caused by any of these TFs knockouts, and multiple anemia phenotypes in humans carrying deficiency in one of these TFs. Together with their cofactors LIM Domain Binding 1

(LDB1) (Love PE 2014) and LIM Domain Only 2 (LMO2), these TFs form a core erythroid network (CEN), which functions in concert at chromatin binding sites and tightly regulate the transcription of erythroid specific genes (Liang & Ghaffari, 2016; Nandakumar et al., 2016).

2.1.1 GATA1

Among the 6 members of the GATA family, only GATA1, 2 and 3 are expressed in hematopoietic lineages. GATA3 is expressed in T lymphocytes, while GATA1 and GATA2 play important roles in self-renewal and survival of HSPCs as well as in erythroid differentiation. GATA2 is expressed in HSPCs and erythroid progenitors while GATA1 is expressed abundantly in more mature cells of several blood lineages including erythrocytes, megakaryocytes, eosinophils and mast cells (Katsumura & Bresnick, 2017). The reciprocal expression of GATA2 and GATA1 is essential for the proper progress of erythroid differentiation and is commonly known as the “GATA switch” (Kaneko, Shimizu, & Yamamoto, 2010; M. Suzuki et al., 2013). It has long been presumed that the GATA switch from GATA2 to GATA1 occurs at the proerythroblast stage due to the increased abundance of GATA1. However, a recent study on absolute quantification of TFs revealed that GATA1 is more abundant than GATA2 at the protein level, even early in hematopoiesis (Gillespie et al., 2020). These data indicate that the GATA switch in genomic binding is more likely mediated by a decrease in GATA2 levels rather than its competition with GATA1.

GATA1, the funding member of GATA family, has three functional domains, two Zinc finger domains at C-terminal for DNA binding (WGATAR motif) and one N-terminal transactivation domain for binding of its main cofactor, Friend of GATA1 (FOG1) (Gutiérrez et al., 2020). FOG1 modulates the affinity of GATA1 to its binding sites, and binding of GATA1 to FOG1 is required for many of GATA1-regulated events including activation of globin gene expression. Several studies have linked a truncated

form of GATA1 to DBA, a model of ineffective erythropoiesis (Gutiérrez et al., 2020; Ling et al., 2019). A recent study highlighted a role for GATA1 in decreased globin production and consequent imbalance between globin and heme synthesis (Rio et al., 2019). These studies will be discussed in detail in the third section of INTRODUCTION entitled “Inherited and acquired disorders of erythropoiesis”. The N-terminus of FOG1 interacts with the nucleosome remodeling and histone deacetylase (NuRD) complex to repress expression of GATA1 targeted genes including *Gata-2*, *Myc* and *Kit* (Hong et al., 2005; Miccio et al., 2010).

In addition, GATA1 was found to form a complex with other master regulators of hematopoiesis. GATA1 interacts with TAL1 via its N-terminal zinc finger, and recruits other TFs including LMO2, LDB1 and transcriptional factor E2-alpha (E2A) to form a transcriptional complex that regulates erythropoiesis as well as the functions of HSCs (Fujiwara, 2017; Lahlil, Lécuyer, Herblot, & Hoang, 2004; Stadhouders et al., 2015; Wilkinson-White et al., 2011). GATA1 also interacts with other erythroid transcription factors such as KLF1, PU.1, SP1, Growth Factor Independent 1B (GFI1B) and chromatin modifiers histone methyltransferases SetD8 and EZH2 (Katsumura & Bresnick, 2017).

2.1.2 TAL1

TAL1 is a core member of the CEN family of TFs, which mainly functions with other TFs as a complex to form enhancer to promoter loops to activate erythroid gene expression (Capellera-Garcia et al., 2016). Before GATA1 is produced abundantly, TAL1 binds to many genomic locations in erythroid progenitor cells and multilineage precursors (Kassouf et al., 2010). At early stages of erythropoiesis, TAL1 and GATA2 co-occupy the GATA switch sites in the *Gata2* and *Kit* loci to drive the transcription of these genes, which are crucial for erythroid progenitor proliferation (W. Wu et al.,

2014). Also, TAL1 and GATA1 interact with GFI1B and NuRD to suppress target gene expression (Liang & Ghaffari, 2016).

2.1.3 KLF1

KLF1, also known as EKLF (Erythroid Kruppel-like factor), is the founding member of the KLF family of transcription factors and is the only family member required during erythropoiesis. In erythroid cells, *Klf1* is a direct target of the bone morphogenetic protein 4 (BMP4)/Smad pathway and GATA1 (Xue, Galdass, Gnanapragasam, Manwani, & Bieker, 2014). In the human β-globin locus, KLF1 stabilizes GATA1 and TAL1 occupancy, contributing to the generation of active chromatin structure, which is critical for activation of β-globin transcription (Kang, Kim, Yun, Shin, & Kim, 2015). In addition to regulating *globin* genes, recent studies highlighted the role of KLF1 in cell cycle regulation (Siatecka & Bieker, 2011). KLF1 regulates many cell cycle genes, and is present in both self-renewing erythroid progenitors and in terminal differentiating erythroblasts. A recent study suggested a KLF1- dependent biphasic model - KLF1 directs the expression of transcription factor E2F2 during the early phase for erythroid progenitor proliferation (Tallack, Keys, Humbert, & Perkins, 2009). E2F2 is a transcription factor that controls S-phase entry and DNA synthesis, and it favors the cell cycle exit of erythroblasts at the late stage by directing expression of cyclin-dependent kinases (CDK) inhibitors, which is critical for enucleation (Gnanapragasam et al., 2016). Moreover, KLF1 also plays a role in facilitating commitment of MEPs into erythroid lineage by suppressing megakaryopoiesis (Doré & Crispino, 2011).

2.1.4 HIF2

Hypoxia-inducible factor 2 (HIF2) is another key transcription factor for erythropoiesis. HIF2 is a heterodimeric complex constituted of an oxygen-sensitive α subunit (also known as endothelial PAS domain containing protein 1 (EPAS1)) and a

constitutively expressed β subunit (also known as aryl hydrocarbon receptor nuclear translocator (ARNT)) (Watts et al., 2020). HIF2α is synthesized and constantly degraded under normoxic condition. The degradation is regulated by prolyl hydroxylase domain proteins (PHDs), mainly PHD1 (Appelhoffl et al., 2004; Berra et al., 2003). When local oxygen level decreases, HIF2α is stabilized and translocate to the nucleus to form heterodimeric complex with HIFβ, which sequentially binds hypoxia response elements (HREs) in the promoters/enhancers of targeted genes to activate their transcription (Wielockx, Grinenko, Mirtschink, & Chavakis, 2019). The most famous target of HIF2α is *Epo*, the gene encoding Erythropoietin (EPO), the key hormone involved in regulation of erythropoiesis. HIF2-mediated EPO upregulation augments RBCs production to meet oxygen demand when oxygen delivery is diminished (Tomc & Debeljak, 2021). In addition to the well-established HIF-EPO axis, HIF2 also plays a pivotal role in promoting cellular iron uptake for hemoglobin synthesis in erythroid cells. HIF2 can increase the transcription of Divalent Metal Transporter 1 (DMT1), the predominant iron importer in mammalian cells, and Duodenal Cytochrome B (DCYTB), a ferric reductase, both of which are important enzymes for dietary iron uptake (A. Kim & Nemeth, 2015; Nemeth, 2008). Moreover, HIF2 can suppress hepcidin transcription to increase iron availability (Q. Liu, Davidoff, Niss, & Haase, 2012). Recently, HIF stabilizers acting by restoring EPO levels and reducing hepcidin have been used in anemic patients with chronic kidney disease to enhance hemoglobin levels (Watts et al., 2020).

2.2 Growth factors

Growth factors are molecules that play essential roles in the regulation of cell proliferation, immune response and hematopoietic development. Among multiple growth factors supporting erythropoiesis, stem cell factor (SCF) and EPO are indispensable for survival, proliferation and differentiation of erythroid progenitors and

early precursors. Both factors initiate signaling via binding to their cognate receptor subunits, triggering the activation of downstream signaling pathways and activate specific gene expression programs. In general, SCF acts on proliferation of erythroid progenitor and more primitive HSPCs, while EPO promotes survival and maturation of late erythroid progenitors CFU-E and early erythroblasts proerythroblasts/basophilic erythroblasts, with substantial overlap with SCF during early erythropoiesis and triggering similar signaling pathways such as phosphoinositide-3 kinase (PI3K)/ protein kinase B (AKT) and Janus Kinase 2 (JAK2)/ Signal transducer and activator of transcription 5 (STAT5) (Karayel et al., 2020; Marieke von Lindern et al., 2004; W. Wang, Horner, Chen, Zandstra, & Audet, 2008).

2.2.1 EPO

EPO is the most essential factor governing erythropoiesis. Epo or Epo receptor (Epo-R)-deficient mice die in utero at day 13–15, when definitive erythropoiesis begins (N. Suzuki et al., 2002). Human EPO is a glycoprotein of molecular weight 34kD, which was purified in 1977 by Goldwasser's group from urine of patients with aplastic anemia and was approved for therapeutic use in humans by U. S. Food and Drug Administration in 1989 (Miyake, Kung, & Goldwasser, 1977; Suresh, Rajvanshi, & Noguchi, 2020). EPO was primarily produced by fibroblast-like interstitial peritubular cells in adult kidney or fetal hepatocytes, in response to anemia, ischemic stress or high altitude (**Figure 6**) (Liang & Ghaffari, 2016). The elaborate oxygen-sensitive regulation of EPO production by transcription factor HIF2 and PHD has been described in the previous section (2.1.4 HIF2). In this section I will focus on the current understanding of how EPO works on erythroid progenitors and precursors.

EPO acts on erythropoiesis via multiple signaling pathways mediated by EPO receptor (EPOR). EPO binding to EPOR induces a change of EPOR dimmers conformation that triggers JAK2, which then activates the transcription factor

STAT5(Remy, Wilson, & Michnick, 1999). Dimers of STAT5 migrate to the nucleus where they interact with erythroid master TFs to activate transcription of important erythroid genes to enhance erythroid cell survival, proliferation and differentiation (Sathyanarayana et al., 2008; Witthuhn et al., 1993). Additionally, EPOR can activates the canonical Ras/mitogen-activated protein kinase (MAPK) and PI3K/AKT pathways, which are also involved in the differentiation and expansion of erythroid progenitors (Adlung et al., 2021; Miura, Miura, Ihle, & Aoki, 1994; Watowich, 2011; Y. Zhang et al., 2014).

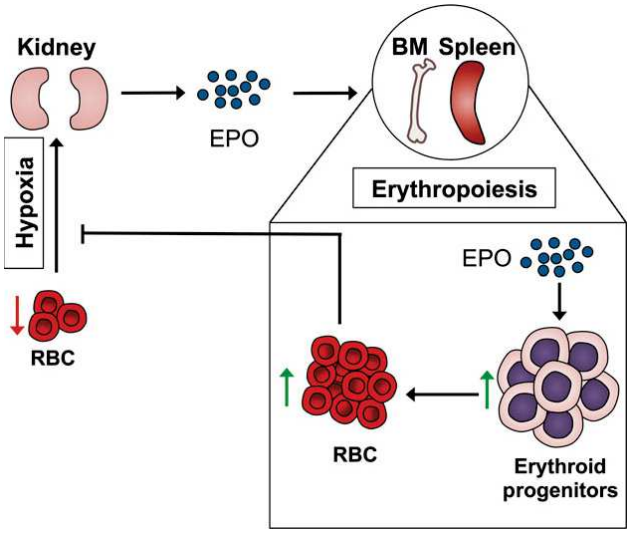

Figure 6. Systemic regulation of erythropoiesis through EPO. Under hypoxic conditions, the kidney will produce EPO, which is carried through the blood to the bone marrow and spleen (in mice but not human) to enhance proliferation and survival of erythroid progenitors. Expansion of the erythroid-committed progenitor pool leads to increased RBC production and sequentially reduced EPO production back to normal levels (Liang & Ghaffari, 2016).

EPO primarily promotes the survival and maturation of CFU-E and early erythroblasts in which EPOR is highly expressed (Broudy, Lin, Priestley, Nocka, & Wolf, 1996). The dependence of erythroblasts on EPO decreases during late stages of erythroblast maturation. Polychromatic and orthochromatic erythroblasts do not express EPOR and they do not need EPO for their survival (Hasan et al., 2018; Wickrema, Krantz, Winkelmann, & Bondurant, 1992). Although earlier studies in the

murine system showed that EPO/EPOR is not required for generation of BFU-E and CFU-E (H. Wu, Liu, Jaenisch, & Lodish, 1995), studies revealed a lineage instructive role of EPO through suppression of non-erythroid fate options (Grover et al., 2014). EPO stimulation changed broad gene expression in HSPCs from MPP, bi-potent and erythroid committed progenitors, reprograming of uncommitted primitive progenitors towards erythroid lineage at the expense of other lineages (Tusi et al., 2018).

2.2.2 SCF

Human SCF gene was identified in 1990 (E. Huang et al., 1990; Martin et al., 1990) and production of recombinant SCF significantly facilitated the development of *in vitro* model of human erythropoiesis by augmenting the expansion of $CD34^+$ HSPCs in liquid culture (Anna Rita Migliaccio, 2018; G. Migliaccio et al., 1992). SCF is produced by endothelial cells, fibroblasts, and bone marrow stromal cells, which also produce other growth factors important for hematopoiesis like Granulocyte-macrophage colony-stimulating factor (GM-CSF) and Granulocyte colony-stimulating factor (G-CSF) (Giovanni Migliaccio et al., 1991).

Like EPO and EPOR deficient mice, deficiency of either SCF or its cognate receptor c-Kit leads to anemia and fetal death in utero in the murine system (Munugalavadla & Kapur, 2005). Importantly, SCF was required for differentiation from BFU-E to CFU-E in both human (Chun Hua Dai et al., 1991) and mice (Broudy et al., 1996). Early studies indicated that recombinant human SCF can interact with other growth factor such as IL-3, G-CSF and EPO to enhance proliferation of early progenitors cells with multiple lineage potential and lineage committed progenitors like myeloid progenitors and erythroid progenitors (Hoffman et al., 1993; McNiece, Langley, & Zsebo, 1991; Giovanni Migliaccio et al., 1991). SCF also augments the expansion of *in vitro* cultured erythroid progenitors, delay their differentiation, and

protect erythroid cells from apoptosis (Endo et al., 2001). Although some studies have suggested that p38, ERK, Bcl-2/Bcl-XL and Notch 2 are involved into SCF-modulated regulation of erythroid differentiation, the detailed mechanisms of action still remain to be fully defined (Endo et al., 2001; Kapur, Chandra, Cooper, McCarthy, & Williams, 2002; A. Zeuner et al., 2011; Ann Zeuner et al., 2003).

As the two most recognized growth factors regulating erythroid differentiation, synergistic effects of SCF and EPO have been documented in both human and murine systems. Although, the exact mechanism underlying the synergy still needs to be fully defined, earlier studies indicated that SCF and EPO share common downstream signaling pathways including PI3K/AKT, JAK2/STAT5 and Ras-Erk (Matsuzaki, Aisaki, Yamamura, Noda, & Ikawa, 2000; Schmidt, Fichelson, & Feller, 2004; Weiler et al., 1996). However, the results from murine bone marrow cells indicate that SCF and EPO have distinct and sequential effects on erythroid differentiation, without co-signaling effects (W. Wang et al., 2008).

As such, further studies are needed to fully elucidate the mechanism of synergistic effects of SCF and EPO on erythropoiesis. A comprehensive phenotyping of human erythropoiesis presented in the thesis that enables efficient isolation of erythroid cells at distinct developmental stages should facilitate future studies in this area of research. Use of purified cells at specific stages of erythroid differentiation will facilitate a clearer understanding in the mechanisms underlying effects of SCF and EPO, and other growth factors such as IL-3, GDF1 in regulating proliferation of erythroid progenitors (Barth et al., 2019).

2.3 Metabolic regulation of erythropoiesis

Given the extensive cell expansion of erythroid cells and astonishing amount of hemoglobin synthesis leading to production of 270 million hemoglobin molecules in

each red cell (Korolnek & Hamza, 2015), it is to be expected that metabolism plays an important role in human erythropoiesis.

Early studies have focused on iron metabolism, as iron is the indispensable building block for heme synthesis and hemoglobin production. Significant progress has been made in this context, and the interaction between iron metabolism and erythropoiesis has been well summarized in recent reviews (Camaschella & Pagani, 2018; Ganz, 2019; A. Kim & Nemeth, 2015; C. Richard & Verdier, 2020; Rivella, 2019). Here I will focus on recent advances on energy metabolism and nucleotide metabolism.

2.3.1 Energy metabolism and erythroid lineage specification

Recently, energy metabolism emerged as a critical factor implicated in HSC's maintenance, self-renewal, and lineage commitment (Mochizuki-Kashio, Shiozaki, Suda, & Nakamura-Ishizu, 2021). HSCs reside in the hypoxic micro-niches in the bone marrow, an environment that favors glycolysis over mitochondrial oxidative phosphorylation (OXPHOS). Previous studies showed that HSCs are hypersensitive to reactive oxygen species (ROS), reducing the production of ROS associated with improved stem cell maintenance (Bigarella, Liang, & Ghaffari, 2014). Indeed, OXPHOS is one of the main generators of endogenous ROS, as a byproduct of ATP production. OXPHOS is suppressed in HSCs either by uncoupling protein 2 (UCP2) mediated substrate shunting mechanism or HIF1α activated expression of pyruvate dehydrogenase kinases (PDK2/PDK4) via blocking of pyruvate entry into the mitochondrial OXPHOS pathway (Takubo et al., 2013; J. Zhang et al., 2011), and HSCs mostly rely on anaerobic glycolysis for energy production. A recent study demonstrated that HSCs with greatest potential have the lowest level of mitochondria membrane potential (MMP), further implicated the role of mitochondria in the regulation of HSCs quiescence and maintenance of potency (Qiu et al., 2021).

Beyond the maintenance of HSC stemness, metabolism is also involved in cell fate decision. Oburoglu and colleagues revealed a critical role for glucose and glutamine in governing the lineage specification of human HSPCs toward erythroid lineage (Oburoglu, Tardito, Fritz, Phanie, et al., 2014). They demonstrated that blocking glutamine metabolism skewed erythropoietin treated HSPCs towards a myeloid fate. Mechanistically, glutamine-dependent *de novo* nucleotide biosynthesis is required for erythroid lineage specification. Recent work has also showed that succinyl-CoA required for heme biosynthesis mainly produced from glutamine derived α-ketoglutarate (α-KG) (JS et al., 2018). Oburoglu et al showed that glucose catabolism is essential for the specification of HSC towards the erythroid lineage. Indeed, they showed that erythroid commitment was associated with an increased shunting of glucose through the pentose phosphate pathway (PPP) and that diverting glucose into PPP by using 2-deoxyglucose (2-DG) accelerated erythropoiesis by providing five-carbon sugars for nucleotide biosynthesis (Oburoglu, Tardito, Fritz, Phanie, et al., 2014). Thus, it prompted us to focus our studies on developing detailed understanding in OXPHOS activity and the regulation machinery of OXPHOS-induced ROS in human erythroid differentiation.

2.3.2 Energy metabolism and redox homeostasis in erythroid cells

The dormant HSCs are hypersensitive to ROS, which could be activated by the low level OXPHOS-induced ROS to enter cell cycle and differentiation. Upon differentiation, OXPHOS increases in committed progenitors and becomes the major source of energy production. At late stage of terminal erythropoiesis, glycolysis regains dominance as mitochondria activity and biomass decreases (Daud, Browne, Al-Majmaie, Murphy, & Al-Rubeai, 2016; A. Richard et al., 2019). However, Luo Shuntao et al recently showed that lactic acid promoted *in vitro* erythroid differentiation by increasing ROS levels and reducing ROS levels abolished erythroid differentiation

induced by lactic acid (Luo et al., 2017). Consistently, Liang et al demonstrated that low mitochondria activity fueled by pyruvate, but not *in situ* glycolysis, is one of the key for erythroblasts enucleation (Liang et al., 2021).

Presumably, the increase in OXPHOS will lead to increased levels of ROS in erythroid progenitors. Under normal conditions, the redox homeostasis is maintained by antioxidant molecules, such as reduced and oxidized glutathione (GSH/GSSG), and antioxidant enzymes, such as superoxide dismutase (SOD), catalase (Cat), glutathione peroxidase (GPx), and peroxiredoxins (Prdxs) (KuhnViktoria et al., 2017; Romanello et al., 2018). Uncontrolled ROS production will cause oxidative damage to cells. For instance, the presence of pathological free iron in β-thalassemia leads to ineffective erythropoiesis and erythrocyte hemolysis; iron-overload in transfusion-dependent patients with DBA, MDS or β-thalassemia result in increase of cellular ROS, activation of apoptosis signaling, and subsequent tissue damage (Grootendorst et al., 2021). Therefore, the maintenance of redox homeostasis is critical for effective erythropoiesis. Indeed, deficiencies in several ROS scavengers cause anemia, and deficiency of FLVCR, the heme exporter expressed on cell surface of CFU-E/proerythroblast, leads to erythroid defects in mice at CFU-E/proerythroblast stage (Doty et al., 2015). In a recent study, Zhao and colleagues reported EPO-induced production of ROS at the early stages of TED and a decrease in ROS level at later stages in a mouse model(Zhao, Mei, Yang, & Ji, 2016). Importantly, ROS quenching by antioxidant N-acetyl-cysteine (NAC) improved enucleation. However, the mechanism of regulation of redox balance during human erythropoiesis remains to be fully defined.

Working with our colleagues, we found that, during normal erythroid differentiation, the use of glutamine was augmented early in erythropoiesis, which supports the tricarboxylic acid (TCA) cycle and downstream OXPHOS via the cataplerotic utilization

of α-KG (Gonzalez-Menendez et al., 2021). At late stages of erythroblasts maturation, glutamine uptake and OXPHOS levels are significantly decreased. Even if the mitochondria activity is low, the mitochondria still play an important role during late stage erythroblasts maturation and enucleation (Liang et al., 2021). In the recent published study, we showed that perturbations in the levels of α-KG and isocitrate dehydrogenase 1 (IDH1) resulted in augmented ROS production and subsequent ineffective erythropoiesis with defective enucleation. Importantly, Vitamin C, a well-known ROS scavenger, restored the redox homeostasis and rescued terminal erythroid differentiation. These findings implied the dynamic changes in OXPHOS levels to adapt to the energy needs at different developmental stages and revealed a critical role for IDH1 as a regulator of redox homeostasis during terminal erythropoiesis. Moreover, these findings highlighted the therapeutic potential of vitamin C in human erythroid disorders associated with oxidative stress. The detailed results are presented as a published paper in the ANNEX.

2.3.3 Nucleotide metabolism

As nucleotides are indispensable for RNA and DNA synthesis, they are extremely important for cell division. Oburoglu and colleagues identified a significant role of nucleotide metabolism in erythroid lineage specification(Oburoglu, Tardito, Fritz, Phanie, et al., 2014). Blocking glutamine-dependent *de novo* nucleotide biosynthesis by down-regulation of glutamine importer (ASCT2) skewed erythropoietin treated HSPCs towards a myeloid fate. Furthermore, a recent study demonstrated that nucleotide homeostasis is also crucial for TED. In addition to the *de novo* biosynthesis of nucleotides, uptake of its extracellular precursor, nucleosides, can contribute to the cytoplasmic level of nucleotides. The equilibrative nucleoside transporter 1 (ENT1), the major plasma membrane transporter of nucleosides, plays a critical role in nucleotide homeostasis. Deficiency of ENT1 resulted in abnormal erythropoiesis in both human

and mice, with reduced erythroid progenitors and impaired enucleation (Mikdar et al., 2021). Furthermore, mechanistic studies revealed a functional link between ENT1 and ATP Binding Cassette Subfamily C Member 4 (ABCC4) mediated cyclic nucleotide metabolism. ABCC4, a cyclic nucleotide transporter is highly expressed in erythroid precursors. In two ENT1-deficient patients with mild symptoms, ABCC4 mutation was also identified. Furthermore, *in vitro* inhibition of ABCC4 enhanced erythroid differentiation. These results suggest that the loss-of-function mutation of ABCC4 may compensate for the deficiency of ENT1 in patients, further highlighting the significance of nucleotide metabolism in regulating erythropoiesis.

Although continued progress is being made in defining mechanistic basis for metabolic regulation of erythropoiesis, there are still significant gaps in our understanding. Indeed, cell metabolism is not restricted to iron, energy and nucleotide metabolism, other nutrients/metabolites could also be essential for erythroid differentiation and more comprehensive investigations are needed to identify these metabolites, the involved metabolic pathways as well as their interplay with those previously established. Therefore, I explored the metabolic dynamics during erythropoiesis by detection of a set of nutrients transporters on the surface of erythroid progenitors and precursors, and discussed the preliminary results in the DISCUSSION section.

2.4 Erythroblastic island

Human bone marrow has a complex microenvironment containing highly heterogeneous populations of cells, where HSCs proliferate and differentiate into different blood cell lineages. Accumulating evidences suggest that there are multiple micro-niches in the bone marrow supporting the generation of cells of distinct hematopoietic lineages. Among those, a specialized niche for erythroid cells' maturation was first described by Marcel Bessis in 1958 and termed "erythroblastic

island" (EBI) (Bessis, 1958). This island consists of a central macrophage surrounded by developing erythroid cells, as illustrated by Joel Anne Chasis and Narla Mohandas (**Figure 7**), based on the transmission/scanning electron microscopy pictures of reconstituted erythroblastic island isolated from rat (Chasis & Mohandas, 2008; Mohandas & Prenant, 1978).

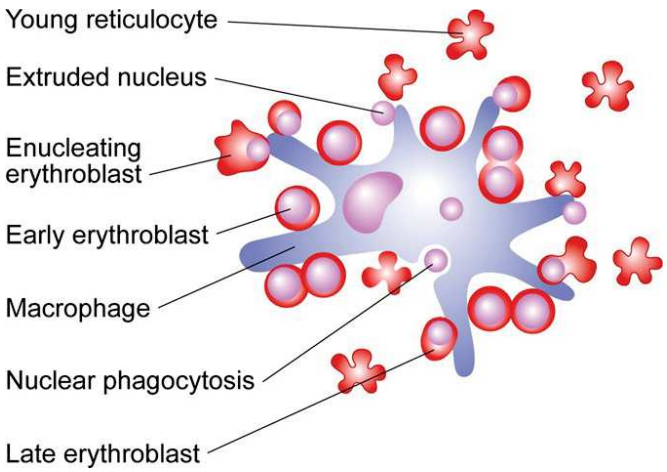

Figure 7. Proliferation and erythroid differentiation processes within the erythroid niche-erythroblastic island. CFU-E and proerythroblasts start to attach to the central macrophage and initiated irreversible differentiation towards generation of reticulocytes. The extruded nuclei are engulfed by the central macrophage soon after enucleation and the newly formed reticulocytes are released from the island (Chasis & Mohandas, 2008).

Further studies identified multiple pairs of adhesion molecules on the surface of central macrophage and erythroblasts by which the macrophage interacts with erythroblasts and regulates erythroid cell maturation, including but not limited to erythroblast-macrophage protein (EMP)/EMP, VCAM-1/α4β1 and ICAM-4/ α5 (Manwani & Bieker, 2008; Rhodes, Kopsombut, Bondurant, Price, & Koury, 2008). It has been shown that central macrophage plays a critical role in providing iron to surrounding erythroblasts for heme synthesis and in phagocytosing extruded nuclei (Korolnek & Hamza, 2015). Although *in vitro* cultured erythroblasts could enucleate in the absence of the macrophage, the efficiency of enucleation is low. Thus the way to

increase it remains a challenge for the *in vitro* production of RBCs. Further investigations on the functional sequel of the interaction of central macrophage with erythroblasts may provide further important insights for this and other questions.

Of note, earlier studies showed that the erythroid cells in EBI range from CFU-E to nascent reticulocytes (Seu et al., 2017). Considering the rarity of BFU-E in bone marrow, it's reasonable that more abundant CFU-E, but not BFU-E, have been shown to interact with macrophages. As the number of erythroid cells per human EBI ranges from 5 to 30 (H. Lee et al., 1988), the CFU-E population interacting with macrophage is likely to be a mature CFU-E. In this thesis, disrupted differentiation from immature CFU-E to mature CFU-E was observed in some MDS patients with impaired TED, suggesting that reduction in number of mature CFU-E limits the formation of EBI and can consequently lead to abnormal TED.

However, it remains unclear which adhesion molecule(s) on the central macrophage are involved in its interaction with CFU-E and start the process of TED. Currently, studies are ongoing to comprehensively characterize the defined progenitor populations by RNA-sequencing and proteomic analysis. It is anticipated these studies will provide further insights into ineffective erythropoiesis and anemia in MDS.

3. Inherited and acquired disorders of erythropoiesis

3.1 Ineffective erythropoiesis in Diamond-Blackfan anemia (DBA)

DBA is a rare congenital erythroid aplasia characterized by erythroblastopenia, with an incidence rate of 7 per million live births, and no difference among ethnicities and genders has been noted (Da Costa, Leblanc, & Mohandas, 2020). Approximately 90% of patients with DBA are diagnosed within the first year of life with 35% diagnosed within the first month. Patients usually present with progressive macrocytic anemia, without evident defects in other hematopoietic lineages. Other clinical features

of DBA include growth retardation and cancer predispositions with patients at higher risk of developing acute myeloid leukemia (AML), myelodysplastic syndromes (MDS) and solid tumors (Da Costa et al., 2020; Engidaye, Melku, & Enawgaw, 2019)

3.1.1 Pathogenesis of DBA

DBA is a genetic disease caused by heterozygous genetic mutations, mostly in ribosomal proteins genes encoding either the small or large ribosomal subunit. Mutations in up to 20 ribosomal protein genes have been identified to date in approximately 60-70% of DBA patients, and no genotype was identified in ~20% of patients. Of these 20 ribosomal protein genes, Ribosomal Protein S19 (RPS19) was the first gene identified in DBA (Draptchinskaia et al., 1999) and is the most commonly mutated gene (25% of the cases) (Da Costa et al., 2020, 2018). Other identified DBA genes include RPL5, RPL9, RPL11, RPL15, RPL18, RPL26, RPL27, RPL31, RPL35a and RPS7, RPS10, RPS15, RPS17, RPS24, RPS26, RPS27a, RPS27, RPS28 and RPS29. A recent review by Lydie Da Costa summarized these different mutations (**Figure 8**).

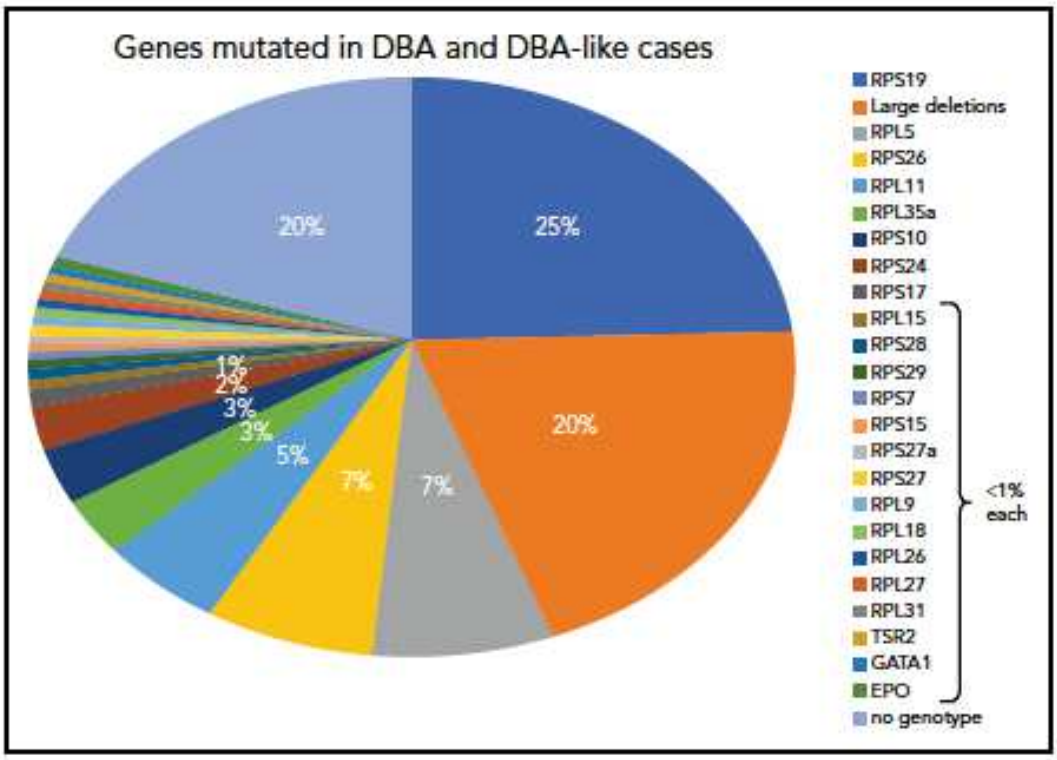

Figure 8. Summary of DBA genotypes. Summary of the frequency of various mutant ribosomal protein (RP) genes in DBA-affected patients compiled from published data from national registries. RPS19 is the most frequently mutated gene and was identified in 25% of patients with DBA. In ~20% o the DBA cases, no genotype was identified after extensive sequencing and screening for large deletions(Da Costa et al., 2020).

Haploinsufficiency in these ribosomal proteins can cause defects in ribosomal RNA maturation and result in stabilization and activation of p53, which in turn leads to activation of its target genes resulting in cell-cycle arrest and apoptosis of erythroid progenitors (Antunes et al., 2015). Nevertheless, many questions remain unanswered. Among these are: How haploinsufficiency of one RP gene affects rRNA maturation and ribosomal biogenesis? Why mutations in different RP genes led to similar reduction in ribosome level without affecting the ribosome composition? How the reduction of ribosomes levels primarily affects the erythroid lineage? What is mechanistic basis for the noted skeletal defects and cancer predisposition?

In addition to the haploinsufficiency of ribosomal proteins, other gene mutations including master transcription factor of erythroid lineage, GATA1, and TSR2 Ribosome Maturation Factor (TSR2), a direct binding partner of RPS26, were also identified in patients with DBA-like phenotype, which imply other plausible underlying mechanisms for erythroblastopenia and resultant anemia (Gripp et al., 2014; Khajuria et al., 2018; Sankaran et al., 2012).

GATA1 has two splice variants, the long form (GATA1l) and short form (GATA1s), with a difference in the splicing of exon 2. Mutations in exons 2 impaired splicing and the resultant frame shift of the full-length GATA1, favored the production of a short form GATA1 (GATA1s). GATA1s lacks the first 83 amino acids at the N terminus, including the transactivation domain of this erythroid master transcription factor, which resulted in the impaired ability of GATA1s to promote erythropoiesis in DBA (Chlon, McNulty, Goldenson, Rosinski, & Crispino, 2015; Ling et al., 2019; Sankaran et al., 2012).

GATA1 activity was also reduced in patients with DBA with ribosomal protein deficiency. Sankaran et al found that the haploinsufficiency of ribosomal protein can reduce the translation of GATA1 mRNA, as reflected by decreased transcription of GATA1 target genes (Ludwig et al., 2014). Further studies revealed that in HSPC, decrease in available ribosomes selectively alters translation of a select subset of transcripts, including GATA1, thereby impairing erythroid lineage commitment, but not other lineages (Khajuria et al., 2018) (**Figure 9**). While it could explain the erythroid specific defects of this disease, this finding does not address other defects observed in these patients, in compartments where *GATA1* is not expressed, such as skeletal, cardiac and gastrointestinal progenitor cells.

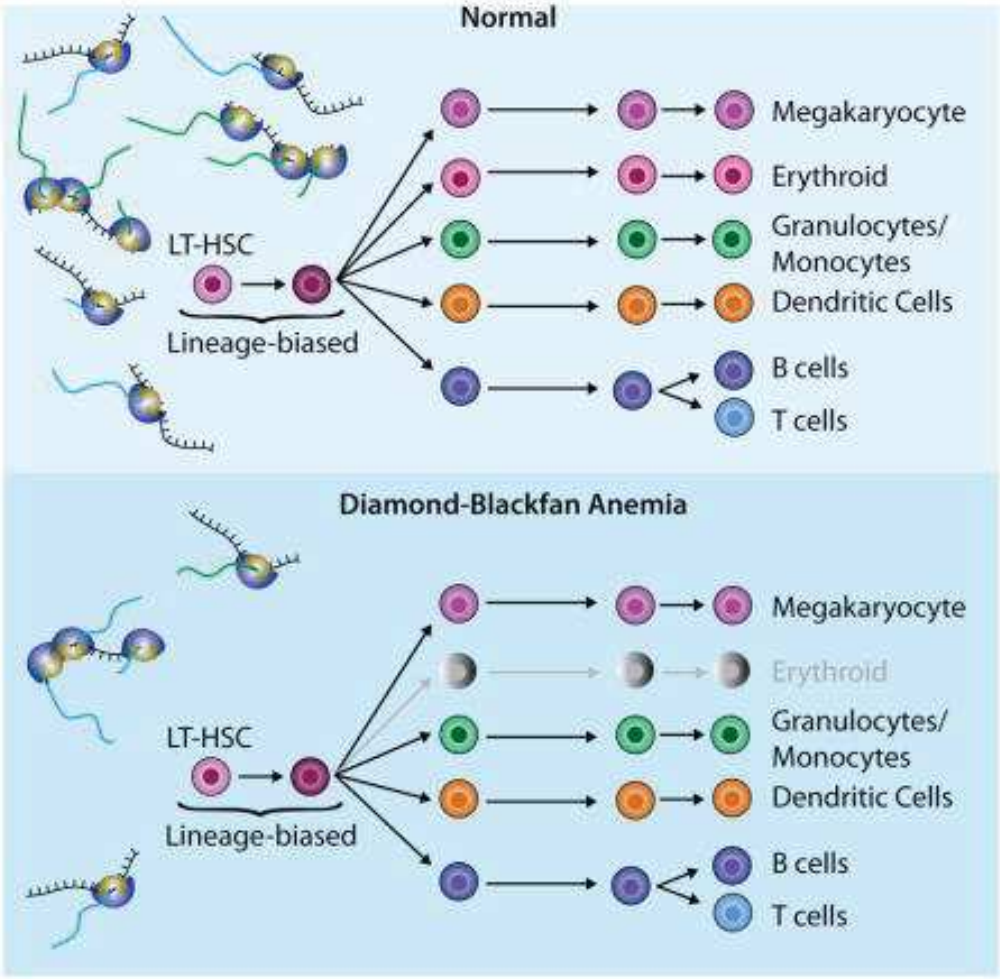

Figure 9. Reduced ribosome levels impaired translation of GATA1 in patients with DBA. Haploinsufficiency of ribosomal protein in DBA reduced ribosome levels in hematopoietic cells, and the reduction selectively impaired translation of a subset of mRNAs including GATA1, sequentially led to impaired erythropoiesis (Khajuria et al., 2018).

Regarding the decreased levels of GATA1 in DBA, recent studies demonstrated that the degradation of heat shock protein 70 (HSP70) plays a crucial role in this pathophysiological process (Gastou et al., 2017). Despite general erythroblastopenia at the time of presentation, the phenotype of DBA patients is highly heterogeneous and no genotype/phenotype correlation could be established (Farrar & Dahl, 2011). Lydie Da Costa et al found that *RPS19* haploinsufficiency decreased erythroid proliferation but did not affect erythroid differentiation, while haploinsufficiency of *RPL5*

or *RPL11* led to severely impaired erythroid cell proliferation and apoptosis. Further studies revealed that proteasomal degradation of polyubiquitinylated HSP70 caused decreased level of HSP70 in *RPL5* or *RPL11* deficient progenitor cells, but not in *RPS19* deficient progenitor cells (Gastou et al., 2017). As a chaperone molecule of GATA1, HSP70 is known to protect GATA1 from caspase-3 mediated cleavage during normal erythropoiesis (Ribeil et al., 2007). The degradation of HSP70 in RPL5/RPL11 deficient cells thereby leads to caspase-3 induced GATA1 cleavage, which could partially explain the more severe phenotype observed in *RPL5* or *RPL11* deficient cells (**Figure 10**).

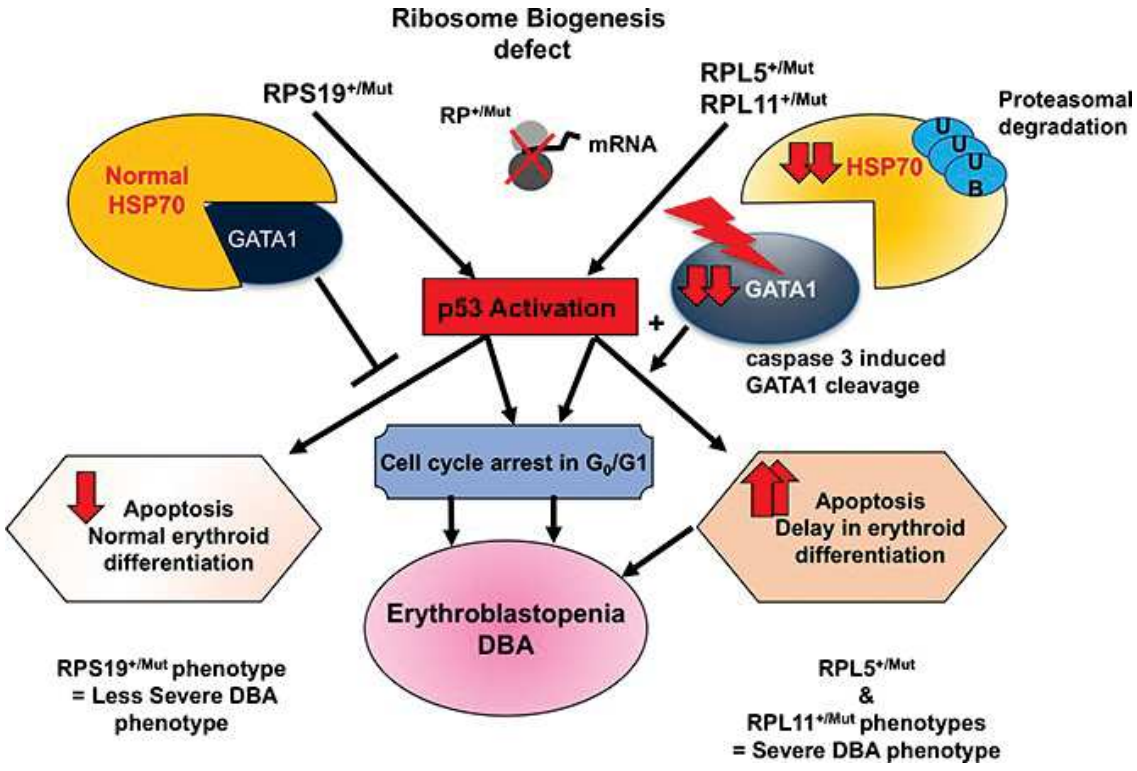

Figure 10. HSP70 plays a key role in determining the severity of the erythroid phenotype in RP-mutation-dependent DBA. Degradation of HSP70 led to caspase 3 induced GATA1 cleavage and resulted in increased apoptosis and delay in erythroid differentiation (Gastou et al., 2017).

Further studies on GATA1/HSP70-involved defective erythropoiesis in DBA revealed a novel pathological mechanism independent of the p53 pathway (Rio et al.,

2019). During normal erythroid differentiation, balanced production of globin and cellular heme is tightly regulated to avoid cell toxicity caused by excess of free heme, which contributes to the ROS production and increases apoptosis. In *RPL5* or *RPL11* mutated erythroid cells, degradation of HSP70 causes caspase 3 cleavage of GATA1, the master transcription factor controlling production of globin, leading to decreasd globin production. Due to the profound reduction in globin production, the tight balance between globin and heme synthesis is lost, and the excess of free heme in progenitor cells leads to increased ROS level and erythroid cell apoptosis. This excess in free heme also led to the up-regulation of FLVCR1, the heme exporter. Moreover, over-expression of HSP70 rescued the expression of GATA1 and restored the globin/heme balance, leading to decreased apoptosis of DBA erythroid cells. Excess of free heme was also detected in *RPS19* deficient cells, although this excess was minimal when compared to the one detected in *RPL5* or *RPL11* deficient cells.

These studies provided the first evidence of a genotype/phenotype correlation, in terms of proliferation and differentiation during erythropoiesis in patients with DBA. Importantly, HSP70 overexpression rescued erythroid defect in cells from DBA patients, suggesting modulation of HSP70 expression might be a new therapeutic target in DBA.

Since the degradation of HSP70 is not due to the activation of p53 but is the consequence of excess of free heme, these findings suggests that the initial imbalance between globin and heme synthesis caused by reduced GATA1 triggers a “self-sustaining” state of excess free heme in ribosomal protein-deficient erythroid cells. As such, the initial excess of free heme leads to a decrease of HSP70, which in turn exaggerates the imbalance between globin and heme synthesis that could not be restored by FLVCR1 mediated heme export (Rio et al., 2019)(**Figure 11**).

HSP70 is a molecular chaperone ubiquitously expressed and plays a crucial role in maintaining protein homeostasis in cells. Upon stress conditions like heat shock, oxidative stress, hypoxia or heavy metals exposure, HSP70 expression could be induced robustly to provide resistance to stresses. In the erythroid lineage, HSP70 is constitutively expressed in human erythroblasts and protect GATA1 from caspase 3 cleavage (Ribeil et al., 2007). In the context of DBA, the HSP70 levels were not up-regulated due to the oxidative stress caused by the excess of free heme in *RPL5* or *RPL11* deficient cells. Instead, its protein levels are down-regulated by proteasomal degradation (Rio et al., 2019). Therefore, further studies on the regulating machinery leading to the proteasomal degradation of HSP70 in DBA will promote the discovery of novel therapeutic targets for DBA treatment and drug development.

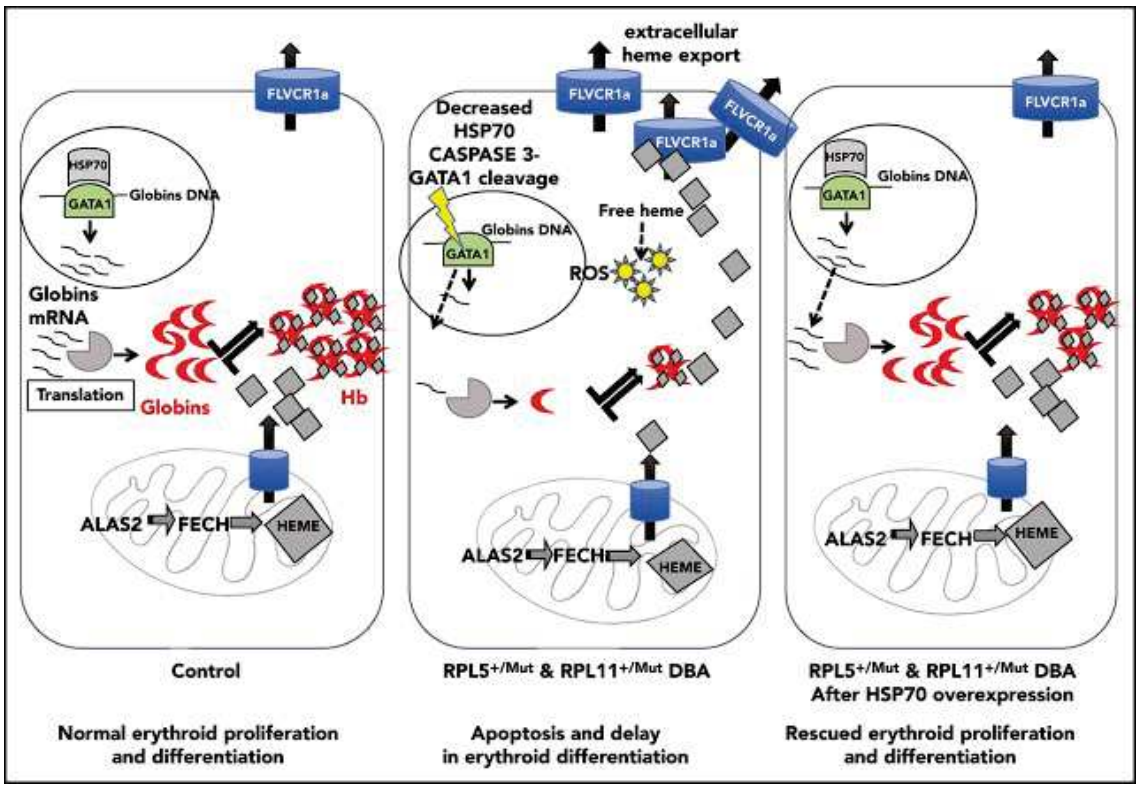

Figure 11. The involvement of globin-heme balance in DBA pathophysiology. Decreased levels of HSP70 and GATA1 led to reduced production of hemoglobin and accumulation of excess free heme in DBA erythroblasts with RPL5 or RPL11 haploinsufficiency, which sequentially led to increased ROS level and apoptosis (Rio et al., 2019).

The decrease of GATA1 levels, caused by either direct gene mutation, impaired translation or caspase-3 induced cleavage due to HSP70 degradation, profoundly contributes to DBA pathology. These novel insights into the mechanism of ineffective erythropoiesis in DBA also highlighted the fundamental role for GATA1 in erythropoiesis.

3.1.2 Glucocorticoid treatment in DBA

To date, the only curative treatment for DBA is allogeneic bone marrow/stem cell transplantation (HSCT). Of note, HSCT is not always possible for most patients and associated with possible complications such as graft versus host disease (GVHD). Moreover, HSCT does not protect from the cancer predisposition observed in patients with DBA. Recent advances in gene therapy provided promising new alternatives to transplant, but the therapeutic efficacy and safety of gene therapy is still under investigation (Jaako et al., 2014; Y. Liu et al., 2020; M et al., 2021).

Currently, Glucocorticoids and red cells transfusion are the main therapeutic treatment options for DBA (Tyagi, Gupta, Dutta, Potluri, & Batti, 2020). Red cells transfusion is the initial treatment of choice for patients under one year of age. After the age of 1 year, the patient's response to glucocorticoids is evaluated. Approximately 80% of patients initially respond to glucocorticoids, but half of the responding patients become refractory to the treatment over time and need to switch to chronic red cells transfusion therapy (Orgebin et al., 2020). No correlation has been identified between the DBA gene mutation and response to glucocorticoids.

Available synthetic glucocorticoids such as dexamethasone and prednisone are synthesized in 1950s based on the structure of cortisol (H. H & EP, 1992; C. H. Kim, Chen, & Coleman, 2017). Glucocorticoids have multiple important functions in human physiology like mediating stress response, anti-inflammation, regulating metabolic

homeostasis, among others (H. H & EP, 1992). Numerous cell types and cellular pathways have been proposed as important targets of glucocorticoids.

The first success of glucocorticoid in patients was reported by Gasser and Allen DM and Diamond LM reported patients responding in a follow-up study (Allen & Diamond, 1961; Narla, Vlachos, & Nathan, 2011). Apoptosis of erythroid progenitors has long been considered as the major cause of this anemia, and numerous studies since 1970s have noted that corticosteroids appear to exert anti-apoptotic effect on erythroid progenitors. Presence of dexamethasone in *in vitro* culture of HSPCs led to the accumulation of erythroid progenitors (M von Lindern et al., 1999) and consistently, dexamethasone treatment increased the expression of erythroid progenitors related genes, accompanied with the decrease of genes specific to non-erythroid lineages (Ebert et al., 2005). Variable and seemingly inconsistent effects of dexamethasone on colony formation of erythroid progenitors have been reported in earlier studies (Gidari & Levere, 1979; Papoff, Christensen, Harcum, & Li, 1998; Roodman, Lee, & Gidari, 1983). Most of these inconsistent effects can be explained by different cell sources, culture systems, study models, exposure time and concentrations of glucocorticoids used in these studies.

Effects of glucocorticoids on enhancing erythroid progenitor self-renewal cooperatively with EPO and SCF was documented by Marieke von Lindern (M von Lindern et al., 1999), and this finding is supported by the increased number of erythroid progenitors and red cell mass in patients with DBA following steroid treatment (C H A N, Saunders, & Freedman, 1982; Iskander et al., 2015).

3.1.3 Mechanisms of glucocorticoid action in human erythropoiesis

It is generally considered that most of the effects of glucocorticoids are mediated via the glucocorticoid receptor (GR), a member of the nuclear receptor superfamily of

ligand-dependent transcription factors. The fat-soluble glucocorticoids can easily enter into the cells and bind to GR in cytoplasm and the assembled complex translocate to the nucleus and activates/suppresses target gene transcription by binding to glucocorticoid response elements (GREs), the specific DNA sequences located upstream of transcription initiation site of the target genes, and/or by physically associating with other transcription factors (Hardy, Raza, & Cooper, 2020).

GR has been identified as a key regulator of chicken erythroid progenitors' self-renewal (Wessely, Deiner, Beug, & Von Lindern, 1997), and is also upregulated in mouse BFU-E cells following dexamethasone treatment (H.-Y. Lee et al., 2015), suggesting a canonical mode of action of glucocorticoids on erythropoiesis. Other studies also showed that GR acts synergistically with SCF and EPO to maintain erythroid progenitors at a self-renewal state instead of undergoing terminal erythroid differentiation (Kolbus et al., 2003; Stellacci et al., 2009; Varricchio et al., 2012; M von Lindern et al., 1999).

However, our understanding of the mechanism of action of glucocorticoids on human erythropoiesis is far from complete, let alone the mechanism accounting for differential responses of patients to glucocorticoids or the mechanism of developing steroids resistance in some patients. Dexamethasone is widely used for the *in vitro* expansion of erythroid progenitors (England, McGrath, Frame, & Palis, 2011; X. Huang et al., 2014), while long-term glucocorticoid treatment in patients with DBA is associated with severe side effects such as growth retardation, hypertension, and diabetes (Narla et al., 2011). Therefore, further progress in identifying cellular targets and clarifying molecular mechanism of glucocorticoids action is needed for developing more specific and effective treatment of DBA with fewer side effects.

While there is a general consensus for a role for dexamethasone at the erythroid progenitor stages, there is some controversy regarding whether its action takes place

at early (i.e., BFU-E) or late (i.e., CFU-E) progenitor stages. The earliest report on the effects of dexamethasone during erythropoiesis demonstrated its effect on EPO-dependent CFU-E formation in mouse fetal liver cells, as well as in the bone marrow from both adult mice and humans (Golde, Bersch, & Cline, 1976). A recent study also demonstrated that dexamethasone acts on murine CFU-E in an EPO-dependent manner through cell cycle regulation (Hwang et al., 2017). In contrast, others have identified the earlier BFU-E progenitor as the cellular target of dexamethasone (Flygare, Estrada, Shin, Gupta, & Lodish, 2011; Gao et al., 2016; H.-Y. Lee et al., 2015; H. Li et al., 2019). Thus, there is a critical need to define how steroids function during human erythropoiesis and precisely define the progenitor population(s) targeted by the drug.

As described earlier, erythroid progenitors are functionally heterogeneous cells and as such this heterogeneity must be resolved to better define dexamethasone responsive target cells. **During my Ph. D, I aimed at resolving the heterogeneity of erythroid progenitors with the goal to better understand the effects of dexamethasone in normal and disordered erythropoiesis. The detailed findings will be presented as a published paper in the RESULTS section** (Ashley et al., 2020)**.**

3.2 Ineffective erythropoiesis in Myelodysplastic Syndromes (MDS)

MDS is a heterogeneous group of hematopoietic disorders characterized by ineffective hematopoiesis, variable cytopenia, morphological dysplasia and increased risk of transformation to AML. Blood cytopenias, paradoxically in combination with bone marrow hypercellularity, is the hallmark of MDS, as a consequence of bone marrow dysfunction (Cazzola, 2020).

Diagnosis of MDS is based on morphological evidence of dysplasia upon blood and bone marrow examination. Additional information from karyotype, flow cytometry and molecular genetics are used to refine diagnosis (Garcia-Manero, Chien, & Montalban-Bravo, 2020). Defined dysplastic changes for each lineage of the bone marrow are listed below (**Table 2**).

Table 2. Signs of dysplasia in MDS (Fenaux et al., 2021).

Peripheral blood	
• Granulocytes	Pseudo Pelger-Huet cells, abnormal chromatin clumping, hypo-/degranulation, left shift
• Platelets	Giant platelets, anisometry of platelets
• Red cells	Anisocytosis, poikilocytosis, dimorphic erythrocytes, polychromasia, hypochromasia, megalocytes, basophilic stippling, presence of nucleated erythroid precursors, tear drop cells, ovalocytes, fragmentocytes
Bone marrow	
• Cellularity of the marrow	Typically hypercellularity, rarely hypocellularity
• Erythropoiesis	Megaloblastoid changes, multinuclearity, nuclear budding, non-round nuclei, karyorrhexis, nuclear bridges, atypical mitoses, sideroblastosis, ring sideroblasts, periodic acid-Schiff-positive red cell precursors
• Megakaryopoiesis	Micromegakaryocytes, mononuclear megakaryocytes, dumbbell-shaped nuclei, hypersegmentation, multinuclearity with multiple isolated nuclei
• Granulocytopoiesis	Left shift, increased medullary blast count, Auer rods or Auer bodies, hypo-/degranulation, pseudo-Pelger cells, nuclear anomalies (e.g. hypersegmentation, abnormal chromatin clumping), deficiency of myeloperoxidase, increase and morphological abnormality of monocytes

MDS is one of the most frequently encountered acquired bone marrow failures in the elderly (median age at diagnosis is ~70 years), but it can occur in all age groups. The average incidence of MDS is about 4 cases /100,000 inhabitants/ year, and it

reaches to 40-50/100,000 in the elderly (aged ≥70 years) (Fenaux et al., 2021). At all ages, it affects males more than females (F. Wang et al., 2019). Risk of developing MDS is also increased in patients with inherited blood marrow failure syndromes such as DBA, where the observed risk of MDS is reported to increase by 300 fold (Dutt et al., 2011).

3.2.1 Pathogenesis of MDS

During the last two decades, our knowledge of the pathogenesis of MDS has been significantly improved by identifying somatic mutations in MDS patients (Chen-Liang, 2021). MDS are clonal neoplasms that arise from the expansion of mutated HSCs. Although the cause of mutations is not clear for most patients, driver mutations have been identified in more than 90% of patients with MDS (Ogawa, 2019). Apart from the genetic and epigenetics alterations caused by driver mutations, the bone marrow microenvironment and the immune system are also involved in the development of MDS. The complex interplay between genetic mutations, epigenetic alterations, bone marrow microenvironment and the immune system, leads to the accumulation of the origin cells of clonal hematopoiesis in MDS, followed by increased apoptosis and eventually resulting in the cytopenia and morphological dysplasia (**Figure 12**) (Hellström-Lindberg, Tobiasson, & Greenberg, 2020).

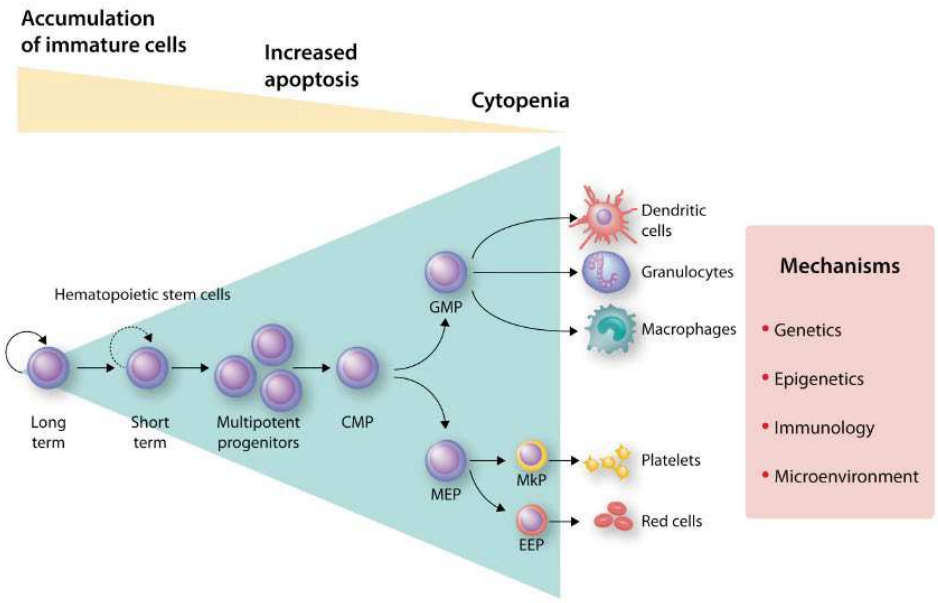

Figure 12. Pathogenesis of MDS. MDS cells accumulate in the bone marrow as a result of a complex interplay between genetic and epigenetic alterations, the bone marrow microenvironment, and the immune system, a process that can develop over several years (Hellström-Lindberg et al., 2020).

Presently, more than 30 driver genes, involved in DNA methylation, DNA repair, chromatin modification, transcription, RNA splicing, and signal transduction among others have been identified from patients with MDS. The most commonly mutated genes are *TET2, SF3B1, ASXL1, SRSF2, DNMT3A* and *RUNX1*, with > 10% mutation frequency (**Figure 13**) (Steensma, 2015).

Some of these mutations, such as *DNMT3A, TET2* and *ASXL1,* are observed in elderly healthy individuals with a condition termed clonal hematopoiesis of indeterminate potential (CHIP), in which one somatic mutation occurs, but the clinical manifestations of MDS (i.e., dysplasia and ineffective hematopoiesis) are not observed yet. CHIP is strongly associated with age and increased risk of hematological malignancies including MDS. The sequential accumulation of mutations drives disease evolution from asymptomatic clonal hematopoiesis like CHIP to MDS, and, ultimately, to secondary AML (Sperling, Gibson, & Ebert, 2016).

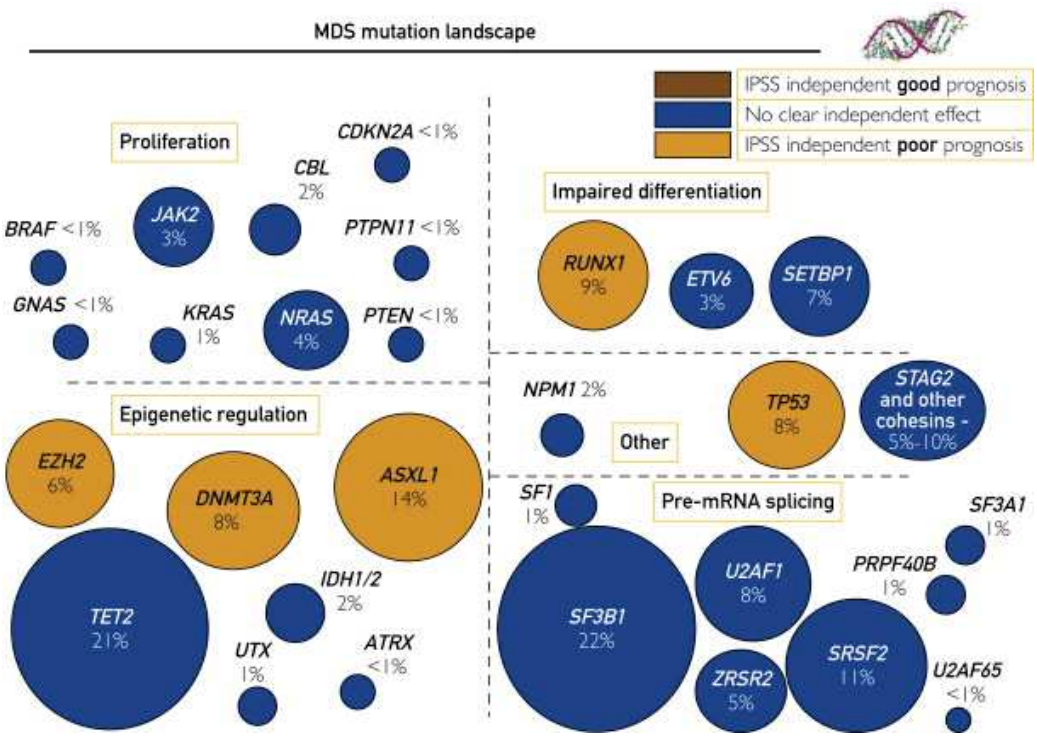

Figure 13. **Recurrent somatic mutations in MDS**. Some mutations influence the phenotype and are, therefore, more common in specific subtypes of MDS. For example, *SF3B1* mutations are found in more than 50% of patients with refractory anemia with ring sideroblasts (RS). *SRSF2* mutations are more common in myeloproliferative neoplasm/MDS overlap syndromes, such as chronic myelomonocytic leukemia (Steensma, 2015).

The deletion of the long arm of chromosome 5 (del(5q)) is also one of the most common cytogenetic abnormalities in MDS (Nagata & Maciejewski, 2019). The deletion cause loss of a large chromosomal region encompassing more than 30 genes, including *RPS14* (Venugopal, Mascarenhas, & Steensma, 2021). In general, del(5q) MDS patients are associated with a favorable outcome, but it could also be related to poor prognosis when the patients have complex karyotypes (Zemanova et al., 2018). Of note, Lenalidomide, an immunomodulatory drug, could effectively target the del(5q) clone in MDS and has been approved for treatment of del(5q) MDS patients (Platzbecker, 2019; Ximeri et al., 2010).

Most mutations, except for the ones in *SF3B1*, are associated with a poor prognosis, and 40% of MDS patients have more than one mutation, which leads to worse prognosis. The different combination of mutations adds further complexity to this heterogeneous disease.

3.2.2 Ineffective erythropoiesis and prognostic evaluation of MDS

As a highly heterogeneous group of disorders, different classification systems have been developed for MDS. In 1997, the International MDS Risk Analysis Workshop established a classification system, the International Prognostic Scoring System for MDS (IPSS), based on the main risk factors in MDS including number and severity of cytopenias, marrow blasts percentage and cytogenetic subgroup (P. Greenberg et al., 1997). IPSS was revised in 2012 and referred as IPSS-R, which stratified patients into five risk groups, very low risk, low risk, intermediate risk, high risk and very high risk (P. L. Greenberg et al., 2012). According to the more recent WHO 2016 classification, MDS is classified into six subtypes, based on the morphological examination dysplastic features in hematopoietic cells, the presence of ring sideroblast (RS) and the percentage of bone marrow blasts. However, considerable variations are noted in the overall survival and the rate of transformation into AML within same subtypes.

Considering the predominance of anemia in MDS symptoms, it is not surprising that evaluation of the severity of ineffective erythropoiesis could be another novel marker for prognostic assessment of MDS. One recent study attempted to quantify cells at different stages of TED (Ali et al., 2018). Detailed analysis using established surface markers for TED (GPA, Band3 and α4-integrin) identified a strong correlation between absence of TED and poor overall survival across all IPSS-R categories, indicating TED as a powerful independent prognostic marker for MDS. More importantly, the study revealed that the absence of TED was more frequently observed in patients bearing *SRSF2* mutations.

In a very recent study, Hunjun Huang et al found that the absolute reticulocyte count (ARC) in peripheral blood can be used to evaluate the severity of ineffective erythropoiesis (H. Huang et al., 2020). The results from 776 patients demonstrated that patients with lower ARC ($< 20 \times 10^9$/L) had more severe impaired erythropoiesis and significantly shorter overall survival (OS), with a median OS of 14 months, than that of patients with higher ARC, with a median OS 48 months. Therefore, ARC could also serve as an independent prognostic factor of MDS.

3.2.3 Mechanisms of ineffective erythropoiesis and treatment of anemia in MDS

Anemia is the defining characteristic in most patients with MDS, affecting >90% MDS patients and impacts their quality of life (Platzbecker, Kubasch, Homer-Bouthiette, & Prebet, 2021). **Therefore, understanding the mechanism that results in ineffective erythropoiesis in MDS patients is critical for improving existing therapies and identifying novel therapies.**

Erythropoiesis is a complicated continuum encompassing multiple developmental stages, defects at any of the multiple stages could affect the production of red cells and eventually lead to anemia, which therefore may require different treatment options according to the specific affected stages. However, currently MDS patients have very limited treatment options and most of them are largely treated with risk-adapted supportive care to decrease transfusion needs and improve survival (Cazzola, 2020). In addition to RBCs transfusion and allogeneic HSCT, other treatment options for MDS, include hypomethylating agents (HMAs), Azacitidine and Decitabline for high-risk disease, immunomodulatory drug lenalidomide for patients with low-risk MDS and del(5q), erythropoiesis-stimulating agents (ESAs) and erythroid maturation agent luspatercept for patients with lower-risk MDS. Except for the HMAs, which aims at

eliminating the clonal cells by switching off DNA methyltransferase, lenalidomide, EPO and luspatercept all stimulate erythropoiesis through different signaling pathways.

Most patients with MDS belong to the low-risk category (IPSS-R score ≤ 3.5), and for many of them, single-agent ESAs represent the first line of therapy. An early study showed that the overall response rates to ESAs is only 20%-40%, and even lower in patients who are transfusion dependent or with EPO serum level >200U/L (Hellström-Lindberg et al., 2003). In a recent study, the initial response rate to ESAs reached 61.5% but 29% relapsed after a median response duration of 17 months (Park et al., 2017). As described in an earlier section (2.2 Growth factors), EPO exert its effects by specifically targeting CFU-E and early-stage erythroblasts that express EPOR. Therefore, patients with defects at early stages such as the BFU-E, which do not rely on EPO for survival, or at late-stage erythroblasts like poly- or ortho-chromatic erythroblasts, that do not express EPOR, do not respond to EPO. In a recent phase 3 trial in ESA-resistant and RBC transfusion dependent patients, combination of lenalidomide and ESAs greatly improved the overall RBC transfusion independence (RBC-TI) rate, as compared to lenalidomide monotherapy (Toma et al., 2016), suggesting potential multiple defects in MDS erythropoiesis that couldn't be restored by monotherapy. Indeed, in addition to its well-recognized immunomodulatory and anti-angiogenic effects, increasing evidence indicated that lenalidomide exert its effect on erythropoiesis by targeting BFU-E or the transition from BFU-E to CFU-E (Dulmovits et al., 2016, 2017). These results suggested the existence of multiple diverse defects of erythroid differentiation in MDS and further highlighted the heterogeneous nature of MDS.

Over the years, several key defects associated with dyserythropoiesis in MDS have been identified, including the overactivation of transforming growth factor beta (TGF-β) signaling pathway (Bhagat et al., 2013; Zhou et al., 2011, 2008), reduction of

GATA1 expression level (Frisan et al., 2012), disruption of histone release from nuclear required for chromatin condensation and enucleation of erythroblast (Zhao et al., 2019), and inflammatory changes and altered microenvironment in the bone marrow niche (E. Pronk & Raaijmakers, 2019; Sallman & List, 2019; Teodorescu, Pasca, Dima, Tomuleasa, & Ghiaur, 2020).

Inflammatory alterations in the marrow, particularly S100A9-mediated NOD-like receptor protein 3 (NLRP3) inflammasome activation, led to an inflammatory milieu, which favors the MDS clone expansion but inhibits the activity of normal HSPCs (Cluzeau et al., 2017). The heterodimeric S100A8/S100A9 proteins are significantly increased in erythroblasts from a mouse model of del(5q) MDS, accompanied by a p53-dependent erythropoiesis defect, specifically, apoptosis at the transition from poly- to ortho-chromatic erythroblasts(Giudice et al., 2019). Moreover, recombinant S100A8 directly induced defective erythroid differentiation and inactivation of S100A8 rescued erythroid differentiation defect in *Rps14* haploinsufficient HSCs (Schneider et al., 2016). Thus, there appears to be a direct link between activation of the inflammatory molecules S100A8/S100A9 and ineffective erythropoiesis in a sub-class of MDS, termed del(5q) MDS and suggests that S100A8/S100A9 could be potential targets for treatment of anemia in del(5q) MDS. In addition, mutations in multiple epigenetic modifiers (*TET2, DNMT3A, EZH2, ASXL1*) and RNA spicing factors (*SF3B1, SRSF2 and U2AD1*) are involved in innate and inflammasome signaling (Sallman & List, 2019; Trowbridge & Starczynowski, 2021).

In a recent study, bone marrow-derived mesenchymal stem cells (MSCs) from patients with MDS, but not from normal individuals, could maintain MDS clones effectively (Medyouf et al., 2014), suggesting that the bone marrow environment is a also a contributor to MDS pathogenesis.

As mentioned above, hyperactivity of TGF-β signaling is observed in many MDS patients, as indicated by the increased levels of SMAD2/SMAD3 phosphorylation (Zhou et al., 2008). TGF-β signaling is triggered by binding of TGF-β superfamily ligands (TGF-β, activins, BMPs, and growth differentiation factor 11 (GDF11) to type I and type II receptors, in some cases with the assistance of a coreceptor (type III). The activated receptors phosphorylate SMAD2/SMAD3, which then dissociate from their receptors and form a complex with SMAD4. The complexes translocate into nucleus and binds to chromatin to regulate target genes expression (Verma et al., 2020) (**Figure 14**). Activation of TGF-β signaling will block the proliferation of erythroid progenitors and accelerate erythroid differentiation via induction of cell cycle arrest and apoptosis (Zermati et al., 2000). Thus, TGF-β signaling is an important regulator of erythropoiesis, impacting the balance between proliferation and differentiation of erythroid progenitors.

In a series of studies, Amit Verma's group investigated the dysregulated TGF-β signaling in MDS (Bhagat et al., 2013; Zhou et al., 2011, 2008). They found that SMAD2 is constitutively activated and overexpressed in hematopoietic precursors from MDS patients, and that the inhibition of SMAD2 promoted erythropoiesis *in vitro*. Follow up studies explored the mechanistic bases of SMAD2/SMAD3 overactivation in MDS. SMAD7, an important negative regulator of SMAD2/SMAD3 activity was markedly decreased in MDS. Furthermore, the investigators revealed a binding site of microRNA-21 (miR-21) in the 3'-UTR of *SMAD7* gene and elevated level of miR-21 in the bone marrow samples from MDS patients. miR-21 plays crucial roles in diverse biological functions including anti-apoptosis and is upregulated in many disease conditions such as AML, cardiovascular diseases, and inflammation (Kumarswamy, Volkmann, & Thum, 2011). In addition, inhibition of miR-21 increased SMAD7 expression in cells from MDS patients and promoted erythropoiesis *in vitro*. These

findings strongly suggested that the inhibition of the SMAD2/3 pathway could be a potential therapeutic target for anemia in MDS.

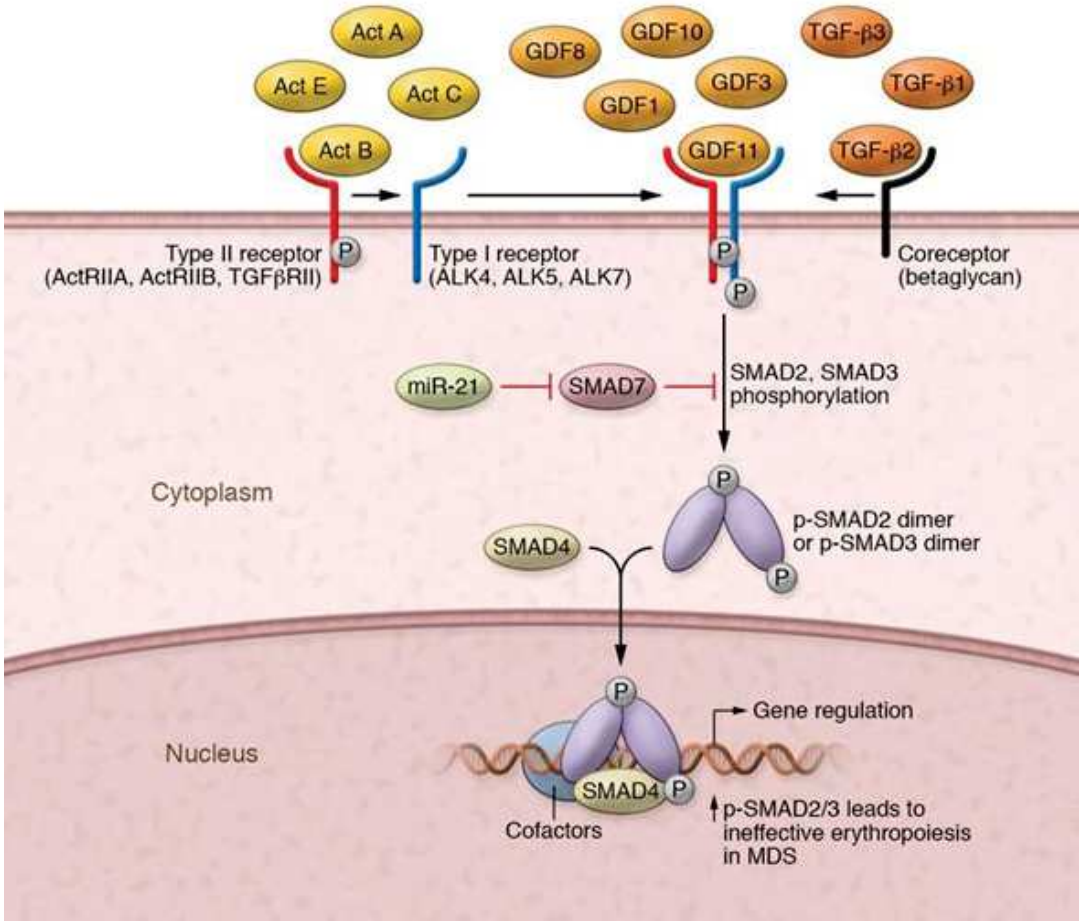

Figure 14. Canonical signaling by SMAD2/3-pathway ligands. Ligand binding leads to multimerization of type I and II receptors, in some cases with the assistance of type III receptor and I. Activated type I receptors phosphorylate SMAD2/3, which dissociate from type I receptor and oligomerize with SMAD4 to form a heterodimeric complex that translocates into the nucleus and regulate cellular responses. SMAD7 is an inhibitory regulator of SMAD2/3 and regulated by miR21 (Verma et al., 2020).

Indeed, a ligand-trap fusion protein, luspatercept, has been developed to correct the overactivated SMAD2/3 and alleviate anemia in MDS. Luspatercept is the first and only erythroid maturation agent effective for low-risk MDS patients with ring sideroblasts (RS) and/or SF3B1 mutations and transfusion dependent after ESA

failure, and has recently been approved by FDA in April 2020 and European medicines agency (EMA) in June 2020 (Kubasch, Fenaux, & Platzbecker, 2021).

In contrast to ESAs which improve erythropoiesis by expanding proliferation of erythroid progenitors, luspatercept improve red cell parameters mainly by acting on TED. Luspatercept contains a modified extracellular domain of activin receptor type IIB attached to the Fc domain of human IgG1. Luspatercept competes with the cell surface receptors for binding of TGF-β superfamily ligands and trapped ligands before they bind to the receptors on the surface of erythroblasts, thereby inhibit SMAD2/3 signaling (Kubasch et al., 2021)(**Figure 15**).

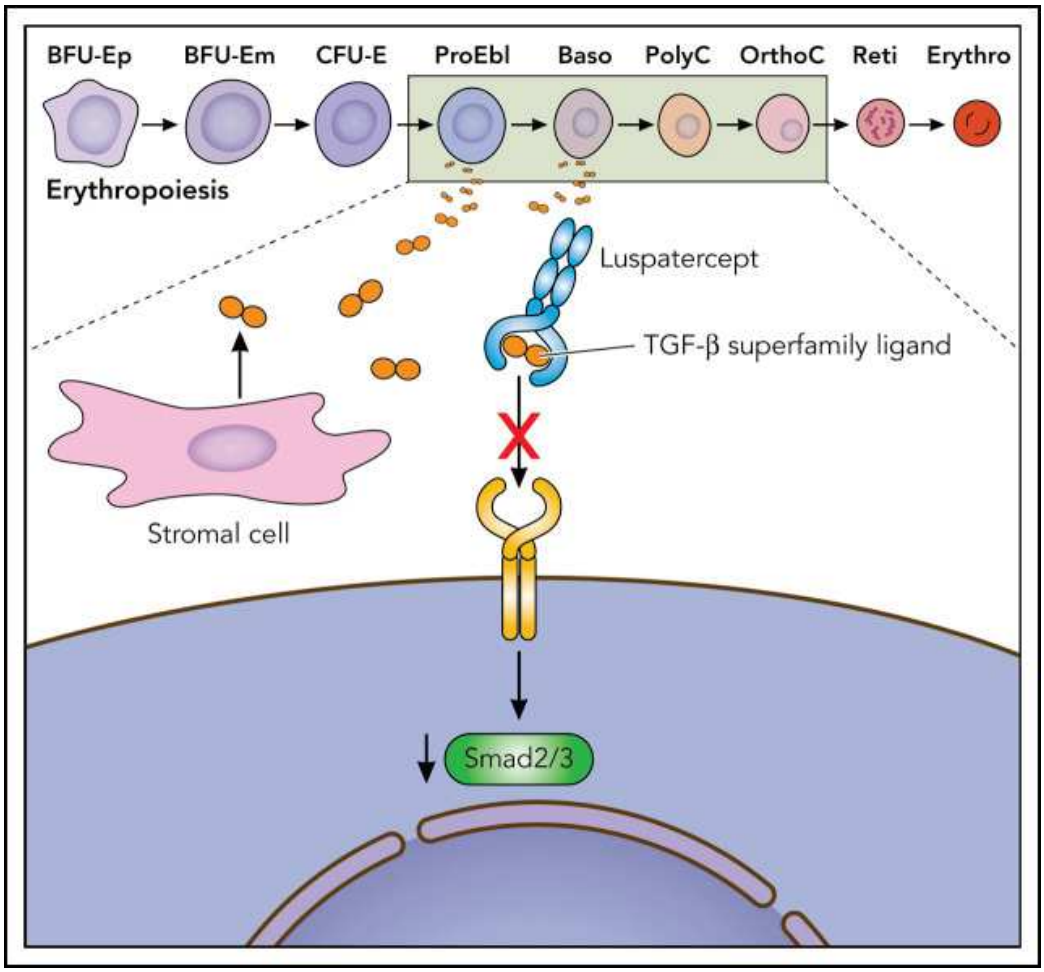

Figure 15. Putative mechanism of action of luspatercept to improve ineffective erythropoiesis. Luspatercept, a TGF-β superfamily ligand trap, blocks the activation of

SMAD2/3 signaling by competitively binding to TGF-β superfamily ligand, and thus improve ineffective erythropoiesis (Kubasch et al., 2021).

In addition to the above mentioned mechanism(s) of action of TGF-β signaling, a recent study documented the effect of TGF-β on early erythroid progenitors in mice (Gao et al., 2016). A transient upregulation of TGF-β signaling occurs during early erythropoiesis, and blocking the TGF-β signaling increased BFU-E self-renewal and the total number of erythroblasts produced. Another recent study found that TGF-β1 has a dose-dependent activity on erythropoiesis (Kuhikar et al., 2020). TGF-β1 at a concentration of 2 ng/ml was shown to inhibit the growth of $CD36^{+}$ cells, while a lower concentration of TGF-β1 (10pg/ml) accelerated the *in vitro* erythroid differentiation without inhibitory effect on the proliferation of erythroid progenitors.

Although luspatercept was approved for clinical treatment of transfusion-dependent MDS patients with RS after ESA failure, further studies are needed for a more thorough understanding in the mechanism of its action. What is the mechanism of TGF-β effect on erythroid progenitors? Does luspatercept influence early erythropoiesis? Which TGF-β receptors are expressed on erythroid progenitors? Which ligand could be trapped by luspatercept? Answers to these questions will provide useful information for expanding the use of luspatercept on other subtypes of MDS without RS.

In this section, I described our current understanding of abnormal erythropoiesis and the available therapeutical drugs for anemia treatment in MDS. Despite these recent advances, the underlying mechanisms of action remain to be fully defined. The development of luspatercept highlights the significance of understanding the mechanistic basis of ineffective erythropoiesis for identifying novel therapies.

Identification of defects in erythropoiesis at a stage-specific manner is the prerequisite to obtain further cellular and molecular understanding of the impaired erythropoiesis in MDS. Most current studies focused on TED, as impaired TED is the well-known feature of MDS. Whether there are defects in early erythropoiesis and if they contribute to the abnormal TED has not been adequately explored. **Thus, a flow cytometry-based assessment using sets of surface markers will enable quantitative evaluation on the whole continuum of erythroid differentiation and identify the stages where differentiation blockage/disturbances occur.** This is a prerequisite to obtain further cellular and molecular understanding by downstream analysis such as single cells sequencing, and such insights can provide useful information for phenotype-adapted therapy design.

OBJECTIVES

Over the last several decades, our knowledge in terminal erythroid differentiation has advanced significantly. However, our understanding of erythroid progenitor biology is still very limited, largely due to the heterogeneity of erythroid progenitors and insufficient immunophenotyping on these cells.

Erythroid progenitors can be functionally defined as BFU-Es and CFU-Es, based on their ability to form erythroid colony in the semi-solid methylcellulose medium. However, it had been very difficult to isolate these cells for further studies. Several years ago, Dr. Narla's lab developed a FACS based method for identification and isolation of BFU-E and CFU-E. According to the expression of a set of surface antigens, they defined $IL3R^{-}GPA^{-}CD34^{+}CD36^{-}$ as BFU-E and $IL3R^{-}GPA^{-}CD34^{-}CD36^{+}$ as CFU-E.

In studies preceding this PhD work, I had studied the differences between adult and neonatal erythropoiesis in Dr. Narla's lab. Interestingly, I identified a transitional population of $CD34^{+}CD36^{+}$ between the defined BFU-E and CFU-E. Notably, this population contains both BFU-E and CFU-E, and is a dominant feature of adult erythropoiesis but not neonatal erythropoiesis. Coincidentally, we observed that dexamethasone, a synthetic glucocorticoid, augmented adult erythropoiesis but not neonatal erythropoiesis. These preliminary findings suggest that the heterogeneous transition population may associate with the dexamethasone augmentation on adult erythropoiesis. Glucocorticoids is the main therapeutic option for the treatment of DBA, however the mechanism of action remains to be fully understood and cellular targets of glucocorticoids have not been clearly identified. Thus, detailed characterization of the heterogeneity of erythroid progenitors can help us to identify the specific cells responding to dexamethasone, characterize the erythroid defects in DBA, and improve our understanding in the regulation of early erythropoiesis under normal and

pathological conditions. The specific objectives pursued during my PhD studies include:

1. To delineate the heterogeneity of human erythroid progenitors using additional markers.
2. To identify the dexamethasone-targeted cell population.
3. To identify molecular player(s) /pathways mediating the effect of dexamethasone on human adult erythropoiesis.

Our limited understanding of early erythropoiesis has impeded our understanding not only of the mechanism(s) determining erythroid progenitors' self-renewal and differentiation under normal conditions, but also in the pathogenesis of diseases with erythroid progenitor defects, such as DBA, and mechanism of action of therapeutic drugs, such as Dexamethasone.

The achievement of these goals should enable us to elucidate the continuum of erythroid progenitors with a stage-specific resolution, improve our understanding in the mechanism of action of dexamethasone, and facilitate a better understanding of the regulation of early erythropoiesis under normal, pathological, or pharmacological conditions.

RESULTS

Original article 1.

Steroid resistance in Diamond Blackfan anemia associates with p57Kip2 dysregulation in erythroid progenitors

Ryan J. Ashley,1,2 **Hongxia Yan**,3,8 Nan Wang,4 John Hale,3 Brian M. Dulmovits,1,2 Julien Papoin,2 Meagan E. Olive,5 Namrata D. Udeshi,5 Steven A. Carr,5 Adrianna Vlachos,1,2,6 Jeffrey M. Lipton,1,2,6 Lydie Da Costa,7 Christopher Hillyer,3 Sandrina Kinet,8 Naomi Taylor,8,9 Narla Mohandas,3 Anupama Narla,4 and Lionel Blanc1,2,6

1Department of Molecular Medicine and Pediatrics, Donald and Barbara Zucker School of Medicine, Hofstra/Northwell, Hempstead, New York, USA. 2Center for Autoimmunity, Musculoskeletal and Hematopoietic Diseases, The Feinstein Institutes for Medical Research, Manhasset, New York, USA. 3Red Cell Physiology Laboratory, New York Blood Center, New York, New York, USA. 4Department of Pediatrics, Stanford University School of Medicine, Stanford, California, USA. 5Proteomics Platform, Broad Institute, Massachusetts Institute of Technology and Harvard University, Cambridge, Massachusetts, USA. 6Pediatric Hematology/Oncology, Cohen Children's Medical Center, New Hyde Park, New York, USA. 7Hôpital Universitaire Robert Debré, Paris, France. 8Institut de Génétique Moléculaire de Montpellier, University of Montpellier, Montpellier, France. 9Pediatric Oncology Branch, Center for Cancer Research, National Cancer Institute, NIH, Bethesda, Maryland, USA.

Authorship note: RJA and HY are co–first authors. NM, AN, and LB are co–senior authors.

https://doi.org/10.1172/JCI132284.

Introduction of original article 1

The work on this article originated from a comparative study of human adult and neonatal erythropoiesis. The *in vitro* differentiation of $CD34^+$ HSPCs has been used as a main model of human erythropoiesis, but significant functional differences exist between different sources of HSPCs. As documented in our previous work, CB and PB derived HSPCs exhibited different proliferation capacity and differentiation kinetics during *in vitro* differentiation, especially the predominance of the transition population $CD34^+CD36^+$ from BFU-E $CD34^+CD36^-$ to CFU-E $CD34^-CD36^+$ in adult but not neonatal erythropoiesis. Comparative transcriptomic analysis revealed that gene expression differs at early erythropoiesis and very late differentiation stages (polychromatic and orthochromatic erythroblasts), and genes exhibiting the most significant differences in expression between CB and PB HSPCs clustered into cell cycle- and autophagy-related pathways (Yan et al., 2018).

In addition to above differences, we observed that $CD34^+$ HSPCs derived from PB and CB have different responses to dexamethasone in culture. Specifically, only PB-derived $CD34^+$ cells demonstrated an enhanced proliferation upon dexamethasone treatment. We then sought to explore the molecular basis of the different responses.

To identify erythroid cell targets of dexamethasone, we examined the differentiation kinetics of PB derived $CD34^+$ cells, with or without dexamethasone treatment. We observed an acceleration of $CD34^+CD36^-$ BFU-E and an increase of the transition population $CD34^+CD36^+$ and CFU-E $CD34^-CD36^+$ in dexamethasone treated cells, comparing to untreated control. By dissecting the heterogeneity of the transition population $CD34^+CD36^+$ using two additional markers CD71 and CD105, we identified that a population of immature CFU-Es characterized by

$CD71^{hi}CD105^{med}$ are the principal responders to dexamethasone. Importantly, clinical data from steroid-responsive patients with DBA showed that reticulocytosis was observed within 7-11 days of steroid treatment. As human BFU-E maturation requires at least 14 days and mature CFU-E maturation requires only 7 days, these clinical data support our finding from *in vitro* model that immature CFU-Es are the main targets of dexamethasone.

Further investigation by global proteomics analysis revealed several cell cycle regulators in PB derived cells treated with dexamethasone, including $p57^{kip2}$, a Cip/Kip cyclin-dependent kinase inhibitor, nuclear receptor subfamily 4 group 1 member 1 (NR4A1), and Period Circadian Regulator 1 (PER1). A recent study has identified $p57^{kip2}$ as a target of glucocorticoids that mediated the expansion of murine CFU-Es (Hwang et al., 2017). Consistently, we observed dysregulated expression of $p57^{kip2}$ in erythroid progenitors from DBA patients with steroid resistance, and down-regulation of $p57^{kip2}$ significantly attenuated the effect of dexamethasone on erythroid differentiation and expansion. These results indicated a conserved role of $p57^{kip2}$ in mice and humans in the mechanism of action of dexamethasone through negative regulation of cell cycle.

In brief, this work revealed that an immature CFU-E population $CD71^{hi}CD105^{med}$ from adult erythropoiesis are the principal cellular target of dexamethasone, and 57^{kip2} mediated negative regulation of cell cycle plays a critical role in the modulation of erythroid progenitor expansion and differentiation. Findings from this work may explain some of the mechanism behind steroid resistance in patients with DBA.

JCI The Journal of Clinical Investigation

Steroid resistance in Diamond Blackfan anemia associates with p57^{Kip2} dysregulation in erythroid progenitors

Ryan J. Ashley, … , Anupama Narla, Lionel Blanc

J Clin Invest. 2020;130(4):2097-2110. https://doi.org/10.1172/JCI132284.

Research Article | Development | Hematology

Graphical abstract

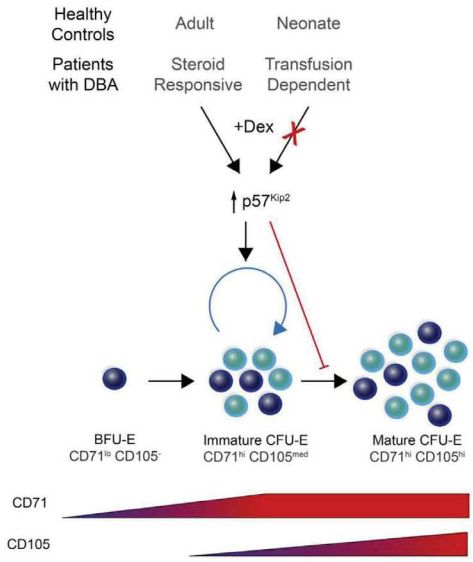

Find the latest version:

https://jci.me/132284/pdf

Steroid resistance in Diamond Blackfan anemia associates with p57^{Kip2} dysregulation in erythroid progenitors

Ryan J. Ashley,[1,2] Hongxia Yan,[3,8] Nan Wang,[4] John Hale,[3] Brian M. Dulmovits,[1,2] Julien Papoin,[2] Meagan E. Olive,[5] Namrata D. Udeshi,[5] Steven A. Carr,[5] Adrianna Vlachos,[1,2,6] Jeffrey M. Lipton,[1,2,6] Lydie Da Costa,[7] Christopher Hillyer,[3] Sandrina Kinet,[8] Naomi Taylor,[8,9] Narla Mohandas,[3] Anupama Narla,[4] and Lionel Blanc[1,2,6]

[1]Department of Molecular Medicine and Pediatrics, Donald and Barbara Zucker School of Medicine, Hofstra/Northwell, Hempstead, New York, USA. [2]Center for Autoimmunity, Musculoskeletal and Hematopoietic Diseases, The Feinstein Institutes for Medical Research, Manhasset, New York, USA. [3]Red Cell Physiology Laboratory, New York Blood Center, New York, New York, USA. [4]Department of Pediatrics, Stanford University School of Medicine, Stanford, California, USA. [5]Proteomics Platform, Broad Institute, Massachusetts Institute of Technology and Harvard University, Cambridge, Massachusetts, USA. [6]Pediatric Hematology/Oncology, Cohen Children's Medical Center, New Hyde Park, New York, USA. [7]Hôpital Universitaire Robert Debré, Paris, France. [8]Institut de Génétique Moléculaire de Montpellier, University of Montpellier, Montpellier, France. [9]Pediatric Oncology Branch, Center for Cancer Research, National Cancer Institute, NIH, Bethesda, Maryland, USA.

Despite the effective clinical use of steroids for the treatment of Diamond Blackfan anemia (DBA), the mechanisms through which glucocorticoids regulate human erythropoiesis remain poorly understood. We report that the sensitivity of erythroid differentiation to dexamethasone is dependent on the developmental origin of human CD34$^+$ progenitor cells, specifically increasing the expansion of CD34$^+$ progenitors from peripheral blood (PB) but not cord blood (CB). Dexamethasone treatment of erythroid-differentiated PB, but not CB, CD34$^+$ progenitors resulted in the expansion of a newly defined CD34$^+$CD36$^+$CD71^{hi}CD105^{med} immature colony-forming unit–erythroid (CFU-E) population. Furthermore, proteomics analyses revealed the induction of distinct proteins in dexamethasone-treated PB and CB erythroid progenitors. Dexamethasone treatment of PB progenitors resulted in the specific upregulation of p57^{Kip2}, a Cip/Kip cyclin–dependent kinase inhibitor, and we identified this induction as critical; shRNA-mediated downregulation of p57^{Kip2}, but not the related p27^{Kip1}, significantly attenuated the impact of dexamethasone on erythroid differentiation and inhibited the expansion of the immature CFU-E subset. Notably, in the context of DBA, we found that steroid resistance was associated with dysregulated p57^{Kip2} expression. Altogether, these data identify a unique glucocorticoid-responsive human erythroid progenitor and provide new insights into glucocorticoid-based therapeutic strategies for the treatment of patients with DBA.

Introduction

Diamond Blackfan anemia (DBA) is an inherited bone marrow (BM) failure syndrome with an incidence of 5 to 10 cases per million live births and is characterized by red cell aplasia, a range of physical anomalies, developmental bone defects, and cancer predisposition (1, 2). More than 70% of the patients diagnosed with DBA have defects in ribosome biogenesis due to mutations in genes encoding ribosomal proteins. In addition, mutations in the *GATA1* transcription factor, a key regulator of erythroid development, and *TSR2*, a pre-rRNA processing protein, have recently been identified in several families with DBA (3, 4). The genetic landscape of DBA is heterogeneous, but genotype and phenotype correlations have been noted in association with mutations in the *RPL5* and *RPL11* ribosomal proteins in patients (5).

The standard of care for patients with DBA after the first year of life is glucocorticoids. Notably, a majority of treated patients have an increase in red cell production and have a reduced dependency on blood transfusions (6–8). However, the therapeutic dose is extremely variable among patients, and many become refractory to treatment over time. Once patients are glucocorticoid refractory they become dependent on chronic RBC transfusions unless they enter remission or undergo curative hematopoietic stem cell transplantation (7). The actions of glucocorticoids have been well studied in many disease contexts. These molecules interact with the glucocorticoid receptor (GR), leading to nuclear translocation of the resulting complex, which binds DNA at glucocorticoid response elements (GREs) and ultimately activates gene transcription (9). However, the specific mechanisms of action of glucocorticoids in the erythroid system in both healthy individuals and patients with DBA remain to be fully elucidated. Several studies have demonstrated that glucocorticoids act at the erythroid progenitor level, but the precise stages of erythroid differentiation at which they exert their effects have not been identified (10–13). This is due in part to the considerable heterogeneity of erythroid progenitor populations and the different markers and model sys-

Authorship note: RJA and HY are co-first authors. NM, AN, and LB are co-senior authors.
Conflict of interest: The authors have declared that no conflict of interest exists.
Copyright: © 2020, American Society for Clinical Investigation.
Submitted: August 21, 2019; **Accepted:** January 14, 2020; **Published:** March 16, 2020.
Reference information: *J Clin Invest*. 2020;130(4):2097–2110.
https://doi.org/10.1172/JCI132284.

tems that are used for studying glucocorticoid effects on erythropoiesis. Indeed, early burst-forming unit–erythroid (BFU-E) and colony-forming unit–erythroid (CFU-E) progenitors are often characterized on the basis of their functional ability to form erythroid colonies in colony-forming assays (CFAs), and immunophenotypic evaluations (14–18) are still in progress.

A further difficulty in evaluating the impact of glucocorticoids on BFU-E and CFU-E progenitors is due to important differences in murine versus human erythroid differentiation. In mice, the vast majority of research has focused on fetal liver progenitors, with a detailed characterization of early and late populations of fetal liver BFU-Es (19–21). Although several studies performed on murine fetal liver cells have suggested that dexamethasone acts at the BFU-E stage (11, 13, 19), a more recent study showed that dexamethasone enhances the maintenance of proliferative murine CFU-Es by upregulating $p57^{Kip2}$, a member of the Cip/Kip cyclin–dependent kinase (CDK) inhibitor (CKI) protein family (10). Under these conditions, the proliferative CFU-E population is maintained, and there is a delayed differentiation to the less proliferative proerythroblast (pro-EB) stage. However, it is not clear whether these data in fetal murine erythroid progenitors translate to humans, as regards both the potential ex vivo heterogeneity of BFU-E and CFU-E populations and, more important, the diversity of erythroid progenitor subpopulations in human BM. These limitations have made it challenging to elucidate the mechanisms through which glucocorticoids act at different stages of erythroid progenitor development, under both physiological and pathological conditions.

In the present study, we identified significant differences in the potential of dexamethasone to affect physiological as well as disordered human erythropoiesis. In the context of physiological differentiation, we found that, although it affected terminal erythropoiesis independently of the source, dexamethasone had an effect on the expansion of $CD34^+$ hematopoietic stem and progenitor cells (HSPCs) isolated from adult peripheral blood (PB), but not from cord blood (CB). Dexamethasone did not affect BFU-Es, but using a new set of cell-surface markers, we identified a unique, PB progenitor–generated subset of transitional $CD34^+$ $CD36^+CD71^{hi}CD105^{med}$ CFU-Es that were dexamethasone responsive. Mass spectrometry–based quantitative proteomics analyses revealed substantial differences in the effects of dexamethasone on PB and CB progenitors, with upregulation of nuclear receptor subfamily 4 group A member 1 (NR4A1), a negative cell-cycle regulator (22), in the former cell type. Furthermore, we found that the $p57^{Kip2}$ Cip/Kip CKI was specifically upregulated by dexamethasone in PB-derived CFU-Es and that its downregulation significantly attenuated the effects of this glucocorticoid. Even more notably, we found that $p57^{Kip2}$ was not upregulated by dexamethasone in CFU-Es isolated from steroid-resistant patients with DBA. These findings open new avenues for the development of specific therapeutic strategies for these patients.

Results

Dexamethasone increases the proliferation of adult human CFU-Es. It has previously been shown that dexamethasone increases the proliferation of erythroid progenitors derived from both healthy and DBA HSPCs (23–25). However, the differentiation stage at which dexamethasone exerts its effects is still unclear. Using a serum-free expansion medium that allowed for the effective erythroid differentiation of HSPCs under steady-state conditions (without dexamethasone), we studied the effects of dexamethasone on human erythropoiesis (18, 26). Notably, we found that dexamethasone (100 nM) increased the expansion of $CD34^+$ cells isolated from adult PB by 7-fold as compared with control conditions (Figure 1A). Surprisingly, though, we did not detect a dexamethasone-mediated increase in the expansion of CB-derived $CD34^+$ cells. In fact, total numbers of precursors differentiating from CB $CD34^+$ cells were approximately 4-fold lower in the presence versus absence of dexamethasone (Figure 1A), strongly suggesting marked developmental differences in the responsiveness of human PB and CB progenitors to this glucocorticoid.

To further elucidate the erythroid differentiation stage at which dexamethasone acts, we used our recently developed experimental strategy for the characterization of BFU-E and CFU-E progenitors, based on surface expression levels of glycophorin A (GPA), IL-3R, CD34, and CD36. The absolute numbers of BFU-Es and CFU-Es generated from 10^6 PB and CB $CD34^+$ cells were enumerated on the basis of cell-surface marker expression in the absence and presence of dexamethasone (Figure 1B). Beginning on day 7, the number of BFU-Es (defined as $GPA^-IL3R^-CD34^+CD36^-$) cells decreased in cultures starting with PB as well as CB $CD34^+$ progenitors, in the absence and presence of dexamethasone, and the extent of this decrease was enhanced by dexamethasone. In marked contrast, the absolute number of CFU-Es (defined as $GPA^-IL3R^-CD34^-CD36^+$) increased over time, and this increase was more pronounced in dexamethasone-treated adult PB $CD34^+$ cells. Notably, dexamethasone decreased the appearance of terminally differentiated GPA^+ cells in both PB- and CB-derived cultures. These data indicate that erythroblasts from both sources were responsive to this glucocorticoid, resulting in a delayed transition to terminal erythroid differentiation (Supplemental Figure 1, A and B). However, cells derived from PB were more affected, possibly because of additional effects at the progenitor levels and at this transitional stage. We also detected this decrease in terminal erythroid differentiation as a function of α4-integrin/band 3 profiles as well as reduced hemoglobinization (Supplemental Figure 1A).

To further validate that the CFU-E was the population primarily responding to dexamethasone, we sorted CFU-Es derived from PB and CB cultures of $CD34^+$ cells and studied their potential for expansion in serum-free expansion media. As shown in Figure 1C, the expansion of CFU-Es purified from adult $CD34^+$ cells increased by 5-fold in the presence of dexamethasone. Once again, dexamethasone had little to no effect on the proliferation of purified CFU-Es derived from CB, supporting the idea that the response to dexamethasone is linked to the specific developmental stage of erythroid progenitors. We performed the same experiments using increasing concentrations of dexamethasone on sorted populations of erythroid progenitors derived from adult PB cultures and observed that the effect on proliferation was maximal at the 100-nM dose (Supplemental Figure 2).

Functional assays using methylcellulose cultures with erythropoietin (Epo) only, a culture condition that supports the growth of CFU-Es but not BFU-Es (requiring both stem cell factor [SCF]

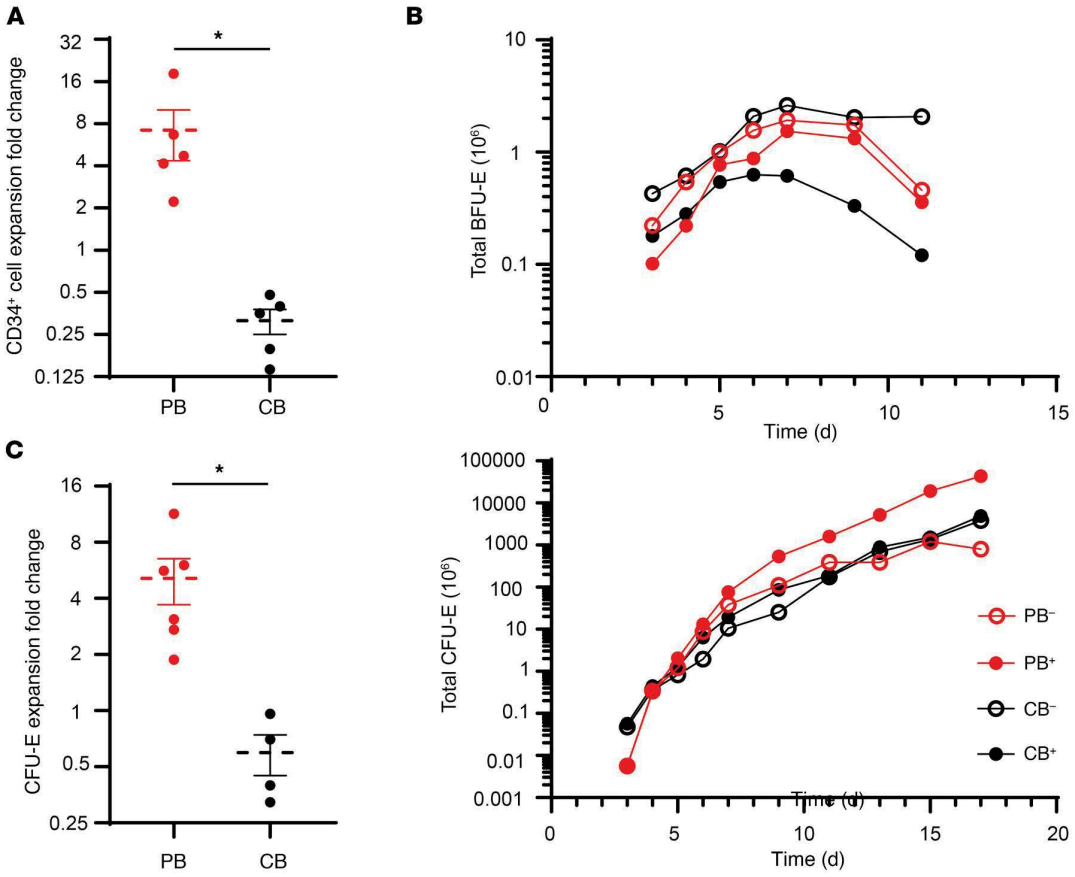

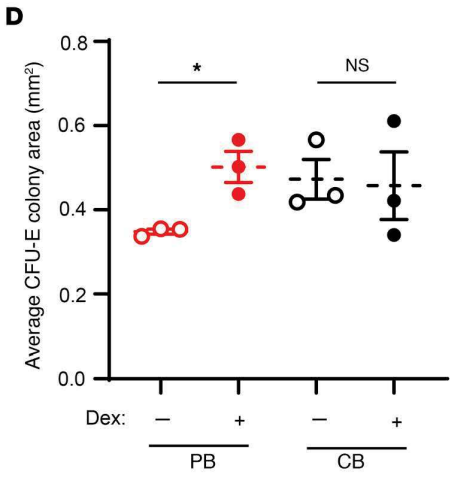

Figure 1. Dexamethasone enhances the proliferation of human CFU-Es derived from PB CD34⁺ cells. (**A**) Fold change in total expansion of PB-derived (red) and CB-derived (black, $n = 5$) CD34⁺ cells upon erythroid differentiation in the presence or absence of dexamethasone for 14 days. Data represent the mean ± SEM. (**B**) Total numbers of BFU-Es and CFU-Es generated from PB and CB cultures in the absence (PB–, CB–) or presence (PB+, CB+) of dexamethasone. Data are representative of 1 of 3 independent experiments. (**C**) Fold change in purified CFU-Es derived from PB ($n = 6$) and CB ($n = 4$) in the presence of dexamethasone relative to untreated controls after 14 days of expansion. Data represent the mean ± SEM. (**D**) Average size (area) of colonies generated from purified CFU-Es derived from untreated PB and CB after 5 days of culture in the absence (open circles) or presence (solid circles) of dexamethasone ($n = 3$). Data represent the mean ± SEM. Dex, dexamethasone. (**E**) Percentages of reticulocytes in 3 patients with DBA following treatment with prednisone, beginning on day 0. $^*P < 0.05$, by 2-tailed Student's t test (**A**, **C**, and **D**).

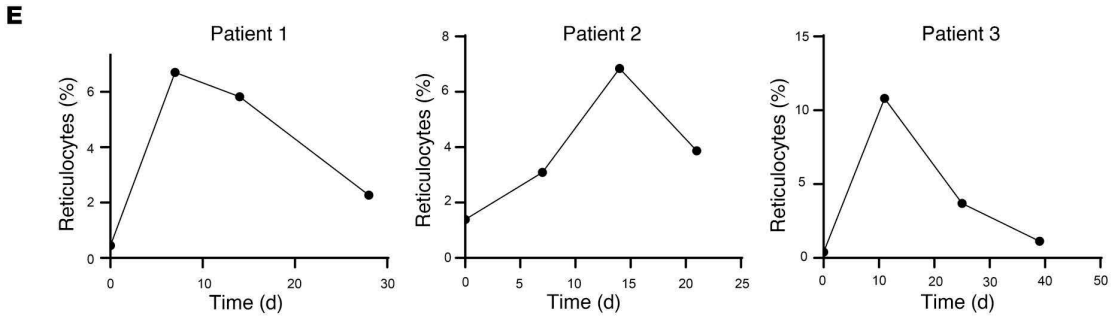

and Epo [ref. 18]), revealed that treatment with dexamethasone markedly increased the colony size of PB-derived CFU-Es but had very little or no effect on CB-derived CFU-E colony size (Figure 1D and Supplemental Figure 3), despite the fact that in the absence of dexamethasone the colony size of purified CB-derived CFU-Es was larger than that generated by PB-derived CFU-Es. Taken together, these data imply that only human CFU-Es derived from adult PB respond to dexamethasone by increasing proliferation.

Previous studies have shown that it takes at least 2 weeks in vivo for healthy BM to produce reticulocytes from the BFU-E stage and approximately 7 to 10 days from the CFU-E stage (27–29). We hypothesized that if the CFU-E is the progenitor population that responds to glucocorticoids in vivo, then patients treated with steroids should present with reticulocytosis in less than 2 weeks. We followed patients with DBA over a 1-month period before and after treatment with prednisone. We observed that in each patient, the reticulocyte count increased within 7 to 11 days after initiation of the treatment, strongly suggesting that in vivo, the CFU-E is indeed the glucocorticoid-responsive population (Figure 1E). We further noticed a decline in the reticulocyte response in a similar time frame, in association with a decrease in the dose of prednisone administered to the patient. Our finding that patients with DBA develop reticulocytosis within less than 2 weeks of starting prednisone treatment strongly suggests the presence of a mature, steroid-responsive progenitor, such as a CFU-E.

Dexamethasone targets a subpopulation of adult-derived CFU-Es. We previously described that, given the surface expression of CD34 and CD36, we could obtain a highly enriched population of BFU-Es ($GPA^-IL\text{-}3R^-CD34^+CD36^-$) and CFU-Es ($GPA^-IL\text{-}3R^-CD34^-CD36^+$) (18). More recently, we reported a transitional progenitor population defined as $GPA^-IL\text{-}3R^-CD34^+CD36^+$, which is more predominant during differentiation of adult PB than that of CB (30). Notably, the kinetics of progression through these differentiation states were also altered with dexamethasone treatment (Figure 2A).

Having identified 2 phenotypically different CFU-E populations ($CD34^+CD36^+$ and $CD34^-CD36^+$), we sought to determine whether there were additional cell-surface markers that would provide further insights into the heterogeneity of these CFU-E populations. We focused on CD71, the transferrin receptor, and CD105 (endoglin), both of which demonstrated large differences in their RNA expression during erythroid differentiation at the progenitor stages (Supplemental Figure 4A).

On the basis of the expression patterns of CD71 and CD105 on $CD34^+CD36^+$ cells, we identified a continuum of cells with 2 distinct populations: $CD71^{hi}CD105^{med}$ and $CD71^{hi}CD105^{hi}$ (Figure 2B). We then sorted these different cell populations and performed colony-forming assays in the presence of either Epo alone, to produce colonies with the traditional definition of a CFU-E, or in complete medium with SCF, Epo, IL-3, IL-6, granulocyte CSF (G-CSF), and granulocyte-macrophage–CSF (GM-CSF). Interestingly, although both sorted populations from $CD34^+CD36^+$ cells generated colonies in the presence of Epo only (Figure 2C), only $CD71^{hi}$ $CD105^{med}$ cells showed marked responsiveness to SCF in complete medium, whereas SCF had little or no effect on $CD71^{hi}$ $CD105^{hi}$ cells (Figure 2C). $CD71^{hi}CD105^{hi}$ cells from $CD34^+CD36^+$ cell populations responded similarly to $CD3^-CD36^+$ cell populations, with a minimal response to SCF. Given these findings, we propose that $CD71^{hi}CD105^{med}$ cells should be termed immature CFU-Es and $CD71^{hi}CD105^{hi}$ cells mature CFU-Es. Importantly, immature CFU-Es functionally responded to dexamethasone by increasing their colony size in a methylcellulose culture system (Figure 2D). In marked contrast, mature CFU-Es responded marginally to dexamethasone in the same functional colony-forming assays, and this increase was not statistically significant. When treated with dexamethasone, PB-derived $CD34^+$ cells preferentially maintained this immature CFU-E population. Indeed, although both untreated and treated cells expressed comparable levels of CD71 on their surface, approximately 50% of the PB cells treated with dexamethasone were still $CD105^{med}$ compared with untreated controls, approximately 30% of which were $CD105^{med}$ by day 4 (Figure 2, E and F, left). Consequentially, the population of $CD105^{hi}$ cells was decreased in PB cells treated with dexamethasone (Figure 2F, right). Taken together, these data demonstrate that in human erythropoiesis, dexamethasone treatment preferentially maintains the immature CFU-E progenitor population for an extended period to increase the proliferative capacity of this cell population.

Proteomics studies highlight previously unidentified erythroid dexamethasone targets. To begin exploring the mechanisms regulating the differential impact of dexamethasone on PB- and CB-derived progenitors, we elected to use a global, comparative proteomics approach. PB- and CB-derived $CD34^+$ cells were cultured in vitro for 5 days to allow for the acquisition of sufficient numbers of flow-sorted purified CFU-Es (~20×10^6 cells) and then subjected to proteomics evaluation. We treated biological triplicates of PB- and CB-derived CFU-Es in the absence or presence of dexamethasone (100 nM) for 24 hours. These cells were then processed for proteomics analysis by liquid chromatography–tandem mass spectrometry (LC-MS/MS). Proteomics quantified 10,045 proteins in PB samples and 10,028 proteins in CB samples (Supplemental Table 1). Proteomic evaluation of PB and CB samples was performed in 2 separate tandem mass tag–6 (TMT-6) plexes. This allowed for precise measurements of changes in protein abundance due to drug treatment in the PB-plex and the CB-plex, but less precise comparisons between PB and CB plexes. Therefore, the observed differences between PB and CB samples were subsequently validated in follow-up experiments.

Importantly, both PB- and CB-derived CFU-Es responded to dexamethasone as demonstrated by the upregulation of the gene for period 1 (PER1) (Figure 3, A and B), a major component of the mammalian circadian clock that has long been known to be regulated by glucocorticoids (31, 32). Notably, however, the majority of dexamethasone-upregulated proteins in PB- and CB-derived CFU-Es differed (Figure 3, C and D), consistent with the distinct phenotypic responses of these CFU-Es. One of the proteins whose abundance was upregulated by dexamethasone in PB-derived CFU-Es, but not CB-derived CFU-Es, was NR4A1 (Figure 3, C and D), a negative cell-cycle regulator. NR4A1 is an interesting target, given its role as a regulator of the cell cycle (22) and of T cell differentiation (33). NR4A1 also binds to HIF1α (34), an important regulator of erythroid differentiation (35). Identification of NR4A1 as a target of dexamethasone was confirmed by Western blot analysis (Figure 3E). Interestingly, the transcription profiles of NR4A1 as well as of 2 other cell-cycle inhibitors, $p27^{Kip1}$ and $p57^{Kip2}$, showed a

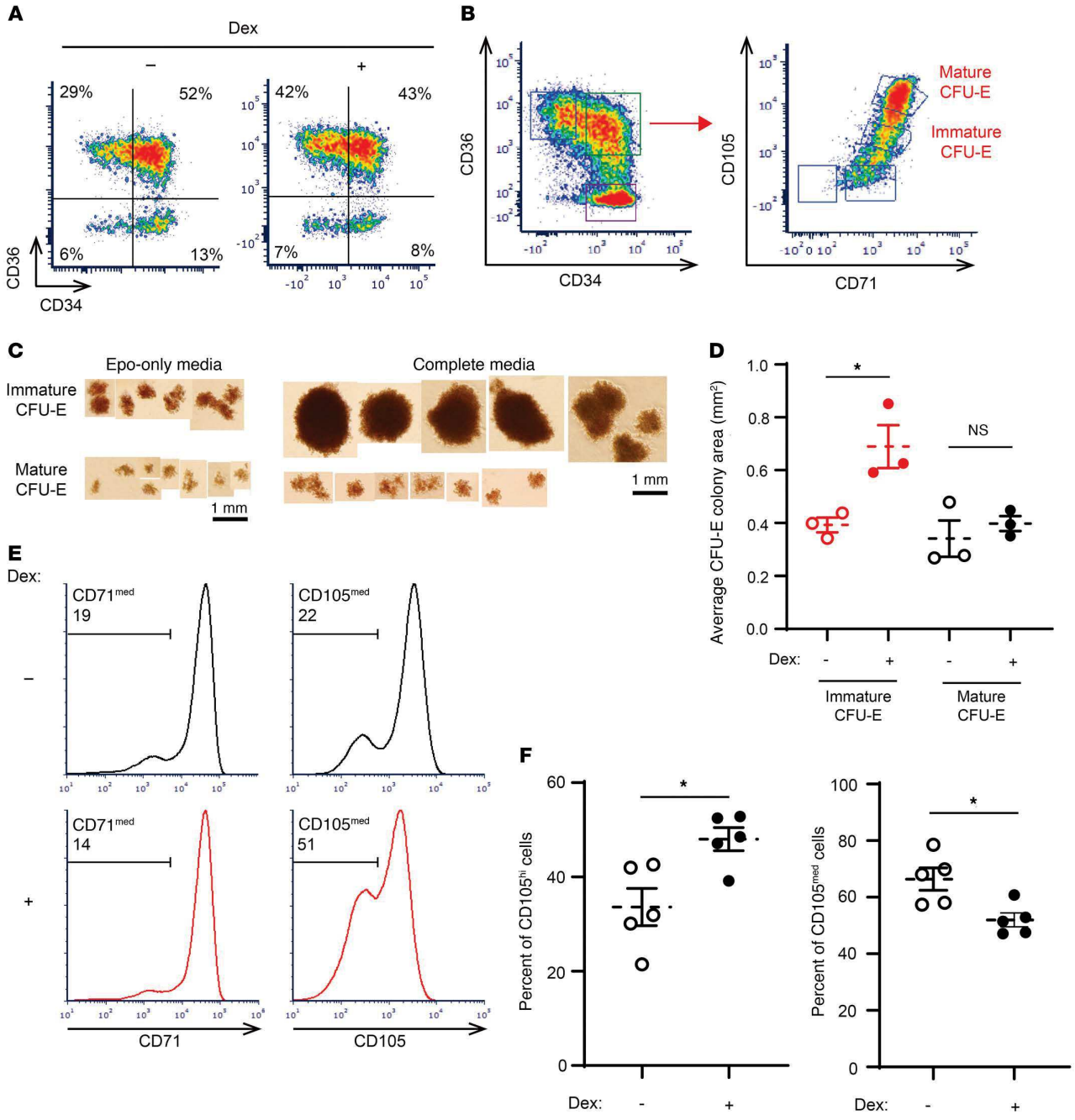

Figure 2. Dexamethasone specifically targets a transitional subpopulation of human CFU-Es derived from PB CD34⁺ cells. (**A**) PB-derived CD34⁺ cells differentiated in the presence or absence of dexamethasone were evaluated as a function of their CD36 and CD34 expression profiles. Representative plots on day 4 of differentiation are presented. Data shown are representative of 1 of 3 independent experiments. (**B**) Gating strategy to define mature and immature transitional CFU-E progenitor populations based on the CD71/CD105 profiles of the CD34⁺CD36⁺ subset. Data are representative of 1 of 3 independent experiments. (**C**) Representative images of colonies formed by immature and mature CFU-Es as defined in **B**, in the presence of Epo alone or Epo, SCF, IL-3, IL-6, G-CSF, and GM-CSF ($n = 3$). Scale bars: 1 mm. (**D**) Colony size (area) generated by immature (red) and mature (black) CFU-Es, defined as in **B** and formed in the presence of Epo alone, in the absence (open circles) or presence (solid circles) of dexamethasone ($n = 3$). Data represent the mean ± SEM. (**E**) Representative histograms show CD71 and CD105 expression in PB-derived CD34⁺ cells differentiated in the absence (black) or presence (red) of dexamethasone (unsorted, day 4). Percentages of $CD71^{med}$ and $CD105^{med}$ are shown in the upper left quadrant of each plot. Data are representative of 1 of 3 independent experiments. (**F**) Quantification of $CD105^{med}$ and $CD105^{hi}$ cells following differentiation of PB-derived CD34⁺ cells in the absence (control, open circles) or presence (solid circles) of dexamethasone (day 4, $n = 5$). Data represent the mean ± SEM. *$P < 0.05$, by 2-tailed Student's t test (**D** and **F**).

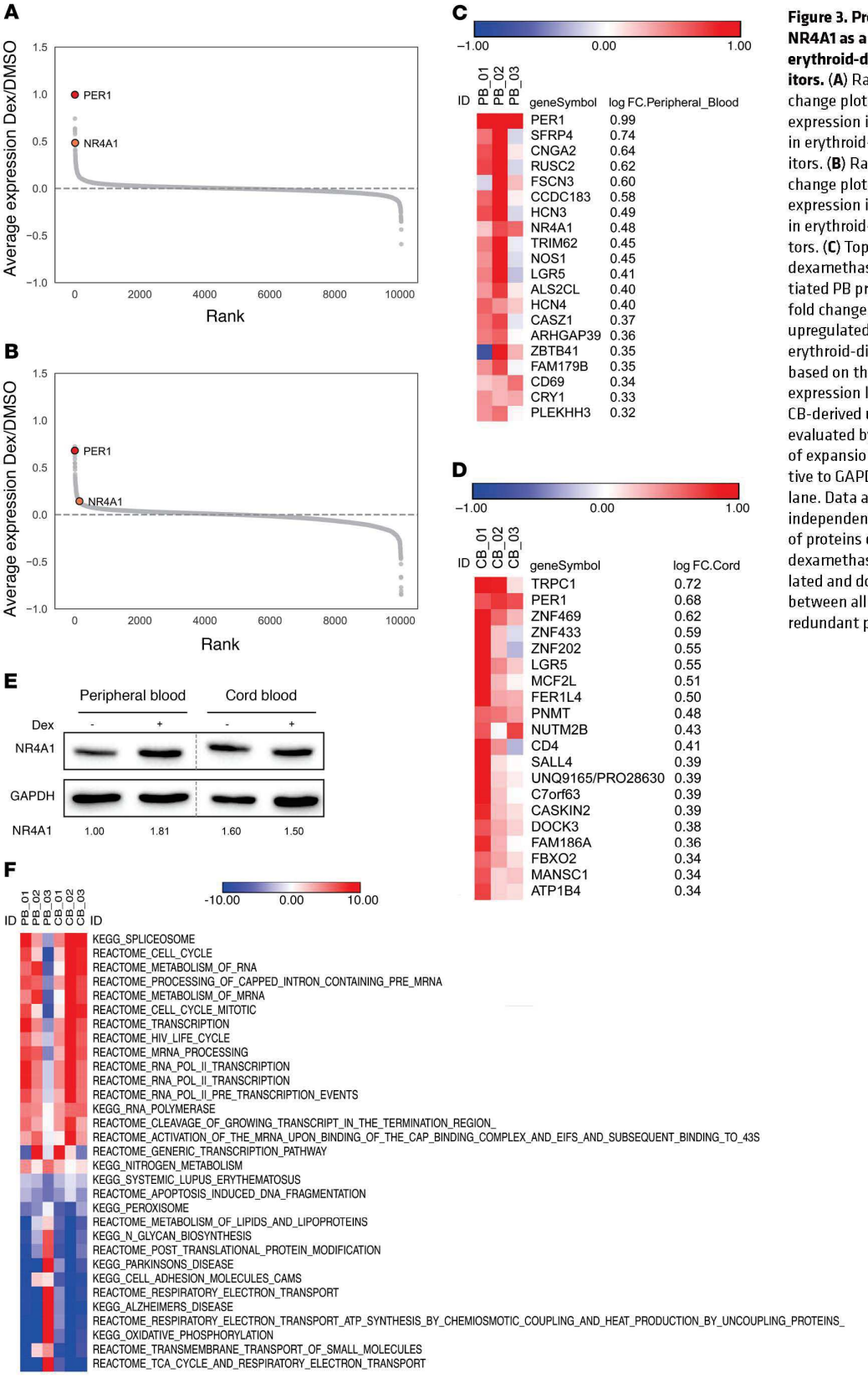

Figure 3. Proteomics studies highlight NR4A1 as a dexamethasone target in erythroid-differentiated PB progenitors. (**A**) Ranked average log fold-change plots of differences in protein expression induced by dexamethasone in erythroid-differentiated PB progenitors. (**B**) Ranked average log fold-change plots of differences in protein expression induced by dexamethasone in erythroid-differentiated CB progenitors. (**C**) Top-20 proteins upregulated by dexamethasone in erythroid-differentiated PB progenitors based on the log fold change (log FC). (**D**) Top-20 proteins upregulated by dexamethasone in erythroid-differentiated CB progenitors based on the log fold change. (**E**) NR4A1 expression levels in purified PB- and CB-derived unsorted progenitors were evaluated by Western blotting on day 4 of expansion. Expression of NR4A1 relative to GAPDH is quantified below each lane. Data are representative of 1 of 3 independent experiments. (**F**) ssGSEA of proteins differentially regulated by dexamethasone. The top-10 upregulated and downregulated pathways between all samples are listed, and redundant pathways were eliminated.

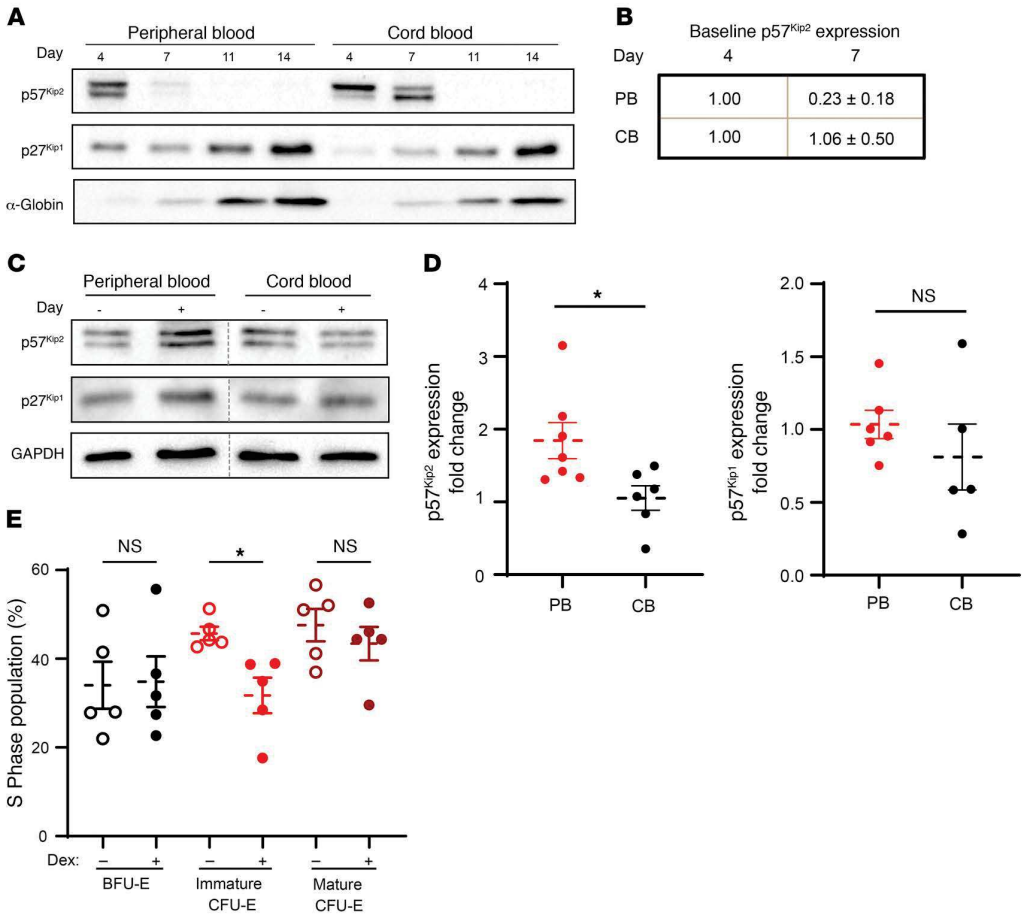

Figure 4. Dexamethasone increases p57^{Kip2} expression in Epo-induced PB CD34$^+$ cells. (**A**) Expression of p57^{Kip2} and p27^{Kip1} was evaluated by Western blotting in CD34$^+$ progenitors during Epo-induced erythroid differentiation. Erythroid differentiation was controlled by evaluating α-globin expression. Data are representative of 5 independent experiments. (**B**) Quantification of the differences in p57Kip2 protein levels in PB and CB cultures between days 4 and 7 of erythroid differentiation (n = 5; values for day 4 were arbitrarily set at 1.). (**C**) Expression of p57^{Kip2}, p27^{Kip1}, and GAPDH in PB-derived and CB-derived progenitors was evaluated in sorted CFU-Es following 4 days of Epo-induced differentiation in the absence (–) or presence (+) of dexamethasone. Representative Western blots from 1 of 3 independent experiments are shown. (**D**) Quantification of the fold changes in p57^{Kip2} and p27^{Kip1} expression in purified PB-derived (n = 7, red circles) and CB-derived (n = 6, black circles) CFU-Es in the presence of dexamethasone relative to control conditions (arbitrarily set at 1). Data represent the mean ± SEM. (**E**) Quantification of the percentages of PB-derived BFU-Es, immature CFU-Es, and mature CFU-Es that were in S phase in the absence (open circles) and presence (solid circles) of dexamethasone. S phase was quantified by Hoechst 33342 staining (n = 5). Data represent the mean ± SEM. *P < 0.05, by 2-tailed Student's t test (**D** and **E**).

substantial decrease between the CD34$^+$ and BFU-E stages (Supplemental Figure 4B). Although we did not detect p57^{Kip2} in the proteomics screen, it is notable that only p57^{Kip2} was expressed at markedly higher levels in PB than in CB CD34$^+$ progenitors (Supplemental Figure 4B). We also performed single-sample gene set enrichment analysis (ssGSEA) to identify the pathways most differentially affected by dexamethasone treatment in both PB and CB samples (Figure 3F). Notably, we observed an increase in proteins involved in the cell cycle and RNA processing as well as a decrease in proteins implicated in oxidative phosphorylation and biosynthetic pathways. Together, these data point to potential differences in the roles of cell-cycle inhibitors in CD34$^+$ progenitors as a function of their developmental origin.

Dexamethasone increases p57^{Kip2} expression in human CFU-Es. The data presented above, together with an elegant previous study showing that p57^{Kip2} regulates steroid responsiveness in murine erythroid progenitors (10), suggested that dexamethasone would act through p57^{Kip2} in PB-derived erythroid progenitors. We first evaluated the expression levels of p57^{Kip2} protein as a function of erythroid differentiation from PB and CB CD34$^+$ cells (Figure 4A). Although p57^{Kip2} was expressed in early erythroid progenitors derived from both PB and CB CD34$^+$ cells (unsorted, day 4), the loss of p57^{Kip2} was substantially more rapid in the CB cells. p57^{Kip2} levels in PB erythroid progenitors were reduced by 77% by day 7, whereas expression persisted in CB progenitors (Figure 4, A and B). Conversely, p27^{Kip1}, a related Cip/Kip family member, was expressed at minimal levels during early differentiation, but its expression increased dramatically in terminally differentiating erythroblasts (Figure 4A). These distinct expression profiles are in agreement with previous studies showing that p57^{Kip2} is associated with the quiescence of stem and progenitor cells, whereas p27^{Kip1} plays a role in the cell-cycle exit that occurs during terminal eryth-

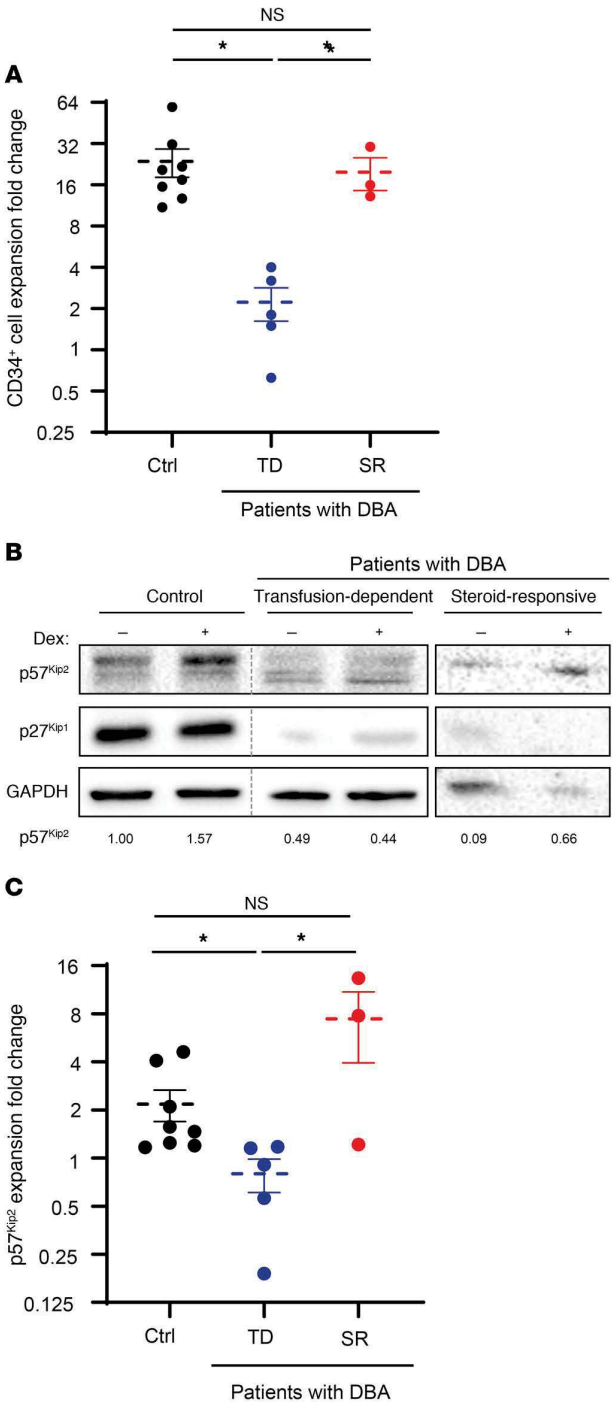

Figure 5. Aberrant steroid-mediated induction of p57^{Kip2} in erythroid progenitors from transfusion-dependent patients with DBA. (**A**) The expansion of CD34$^+$ cells derived from healthy controls (Ctrl) (black, $n = 8$), transfusion-dependent (TD) patients with DBA (blue, $n = 5$), and steroid-responsive (SR) patients with DBA (red, $n = 3$) is presented following a 7-day stimulation. Data represent the mean ± SEM. (**B**) Expression of p57^{Kip2} and p27^{Kip1} in erythroid progenitors from healthy controls and patients with DBA, either transfusion dependent or steroid responsive, was evaluated by Western blotting on day 7 of differentiation. Expression of p57^{Kip2} relative to GAPDH is quantified below each lane, with control levels in the healthy donor arbitrarily set at 1. (**C**) Quantification of the fold change in dexamethasone-induced p57^{Kip2} expression following expansion of CD34$^+$ cells from healthy controls ($n = 8$) as compared with transfusion-dependent patients with DBA ($n = 5$) and steroid-responsive patients with DBA ($n = 3$). Data represent the mean ± SEM. *$P < 0.05$, by Kruskal-Wallis test with Dunn's post hoc analysis with corrections for multiple comparisons (**A** and **C**).

roid differentiation (36, 37). Notably, however, differences in the kinetics of p57^{Kip2} downregulation in CB and PB erythroid progenitors have not thus far been appreciated.

Given these findings, it was of interest to assess whether p57^{Kip2} levels would be differentially affected by dexamethasone in purified PB-derived and CB-derived progenitors. To this end, progenitors derived from both sources were treated with dexamethasone, and the expression of p57^{Kip2} was quantified by Western blotting. We evaluated total CFU-Es, because the numbers of immature CFU-Es were insufficient in the absence of dexamethasone, particularly in CB cultures, in which the kinetics of differentiation is increased (30). Notably, within CFU-Es, we found that p57^{Kip2} protein levels were increased by 1.8-fold in PB-derived progenitors but remained unchanged in CB-derived progenitors ($P < 0.05$; Figure 4, C and D). These data are even more striking in light of the finding that p27^{Kip1} levels were not significantly altered in progenitors derived from either PB or CB sources (Figure 4, C and D). Altogether, these data strongly suggest a role for p57^{Kip2} in mediating the dexamethasone-induced changes in PB-derived, but not CB-derived, progenitors.

Given that p57^{Kip2} is a regulator of the cell cycle, we inhibited the transition from the G_1 to the S phase (38) to determine whether dexamethasone-mediated changes in p57^{Kip2} are associated with differences in the cell-cycle dynamics of PB erythroid progenitors. We found that the percentages of progenitors in the S phase of the cell cycle increased significantly between the BFU-E and CFU-E stages, from a mean of 35% to 48% ($P < 0.05$; Figure 4E). Notably however, dexamethasone significantly decreased S-phase cells in immature CFU-Es, but not in the BFU-Es or mature CFU-E subsets (Figure 4E and Supplemental Figure 5). In addition, the percentages of cells in the non–S phase of the cell cycle were increased in immature CFU-Es (Supplemental Figure 5B). Thus, in agreement with our data showing that the immature PB-derived CFU-E subset preferentially undergoes a dexamethasone-mediated expansion (Figure 2), only this subset responded to upregulated p57^{Kip2} levels with a significant decrease in the number of cells in the S phase. Despite this reduction of cells in the S phase, immature CFU-Es continued to divide, with increases in G_2/M, before further differentiating into mature CFU-Es and then proerythroblasts and resulting in increased expansion.

p57^{Kip2} expression is altered in erythroid progenitors from transfusion-dependent patients with DBA. We further hypothesized that the resistance of patients with DBA to glucocorticoids is mediated, at least in part, by p57^{Kip2}. To test this hypothesis, we compared dexamethasone-induced changes in p57^{Kip2} levels in unsorted cells on day 7 of culture in response to dexamethasone in CD34$^+$ cells from healthy controls and transfusion-dependent patients with DBA. Given the strong reduction in growth of cells from transfusion-

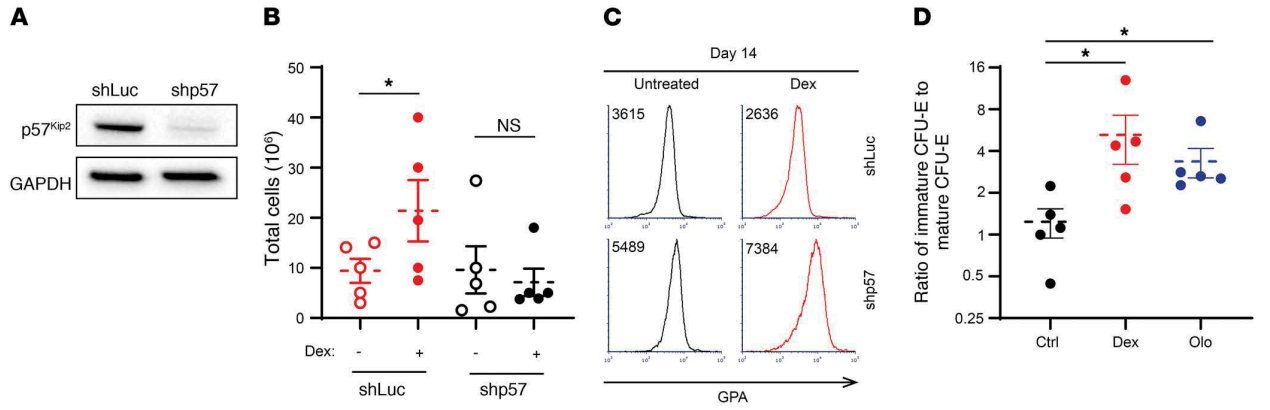

Figure 6. Downregulation of *CDKN1C* ($p57^{Kip2}$) in CD34$^+$ progenitors attenuates the impact of dexamethasone, accelerating erythroid differentiation, whereas olomoucine, a CKI, mimics the effect of dexamethasone. (**A**) CD34$^+$ progenitors were transduced with a lentiviral vector harboring an shRNA targeting luciferase (shLuc) or $p57^{Kip2}$ (shp57). Expression of $p57^{Kip2}$ was evaluated by Western blotting relative to GAPDH levels on day 7 after transduction. Data are representative of 1 of 3 independent experiments. (**B**) Expansion of control (shLuc) and $p57^{Kip2}$-downregulated (shp57) PB CD34$^+$ cells was evaluated in the absence (open circles) or presence (solid circles) of dexamethasone after 14 days of culture (n = 5). Data represent the mean ± SEM. *P < 0.05, by 2-tailed Student's t test. (**C**) Representative histograms of GPA expression in control (shLuc) and $p57^{Kip2}$-downregulated (shp57) progenitors on day 14 of differentiation. MFIs are indicated. Data are representative of 1 of 3 independent experiments. (**D**) Quantification of the ratio of immature CFU-Es to mature CFU-Es following expansion of PB-derived CD34$^+$ cells in the absence (black circles) or presence of 100 nM dexamethasone (red circles) or 1 μM olomoucine (blue circles) on day 4 of culture. n = 5. Data represent the mean ± SEM. *P < 0.05, by Kruskal-Wallis test with Dunn's post hoc analysis with corrections for multiple comparisons.

dependent patients with DBA, we evaluated $p57^{Kip2}$ levels in unsorted progenitors on day 7 of expansion (Figure 5A). Importantly, $p57^{Kip2}$ levels, which were increased in healthy controls and steroid-responsive patients with DBA in response to dexamethasone, were not affected in transfusion-dependent patients with DBA (Figure 5, B and C). As expected from the data presented in Figure 4C, $p27^{Kip1}$ levels were not affected by dexamethasone, but it is notable that they were dysregulated and pointedly higher or lower in samples from patients with DBA, probably due to early differentiation or defective terminal erythroid differentiation, respectively, in these unsorted cells. Most critically, $p57^{Kip2}$ levels in progenitors derived from steroid-responsive patients with DBA were upregulated in response to dexamethasone, similar to what was observed in healthy controls (Figure 5, B and C). Notably, the expansion of PB-derived CD34$^+$ cells from healthy controls and steroid-responsive patients with DBA was similar after 7 days of culture, whereas cells from transfusion-dependent patients with DBA showed significantly less expansion (Figure 5A). Taken together, these results suggest a critical role for $p57^{Kip2}$-associated cell-cycle changes in the steroid responsiveness of both physiological and pathological human erythropoiesis.

Dexamethasone responsiveness is mediated by CDK activity. In order to directly assess the role of $p57^{Kip2}$ in mediating dexamethasone effects on erythroid progenitors, we used a lentivirus-mediated shRNA approach to induce downregulation of $p57^{Kip2}$ levels. Following transduction, $p57^{Kip2}$ was downregulated by 80% as compared with cells transduced with a control luciferase–targeting shRNA construct (Figure 6A). Notably, $p57^{Kip2}$ downregulation abrogated the ability of PB-derived CD34$^+$ cells to respond to dexamethasone, monitored as a function of their expansion (Figure 6B). Moreover, we observed that erythroid differentiation was accelerated, as demonstrated by 1.5- and 3-fold increases in GPA expression levels in control- and dexamethasone-treated progenitors, respectively (Figure 6C). Finally, this effect on erythroid progenitors was specific to the $p57^{Kip2}$ CKI, as downregulation of $p27^{Kip1}$ did not alter the expansion of these progenitors (Supplemental Figure 6, A and B). The effect on $p27^{Kip1}$ was only noticed at later stages and was indicated by a delay in terminal differentiation measured by the surface markers α4-integrin and band3 (Supplemental Figure 6C). Altogether, these data reveal the function of $p57^{Kip2}$ in regulating the balance between human erythroid progenitor proliferation and differentiation and, furthermore, in controlling glucocorticoid responsiveness under both physiological and pathological conditions.

Given our finding that an increase in levels of $p57^{Kip2}$, a CKI, is critical for dexamethasone responsiveness, we hypothesized that inhibiting cyclin kinases would have the same effect as increasing $p57^{Kip2}$. Notably, treatment of PB-derived CD34$^+$ cells with olomoucine (1 μM), a small-molecule CDK1 and CDK2 inhibitor (39), resulted in a significant increase in the ratio of immature CFU-Es/mature CFU-Es to levels similar to those induced by dexamethasone (Figure 6D). Together, these data demonstrate the importance of CDK/CKI balance in the expansion of the immature CFU-E population.

Dexamethasone upregulates $p57^{Kip2}$ expression in erythroid progenitors derived from human BM. To assess the effects of dexamethasone on populations of cells that are directly targeted by the drug in vivo, we repeated key experiments with erythroid progenitors derived from human BM. In culture with serum-free expansion media, we found that the expansion of BM-derived CD34$^+$ cells increased significantly in the presence of dexamethasone (Figure 7A). When examining the expression of CD105 in BM-derived progenitors, we observed that dexamethasone treatment maintained the population of CD105^{med} cells and correspondingly decreased the population of CD105^{hi} cells (Figure 7B). Furthermore, treatment of BM-derived CFU-Es with dexamethasone

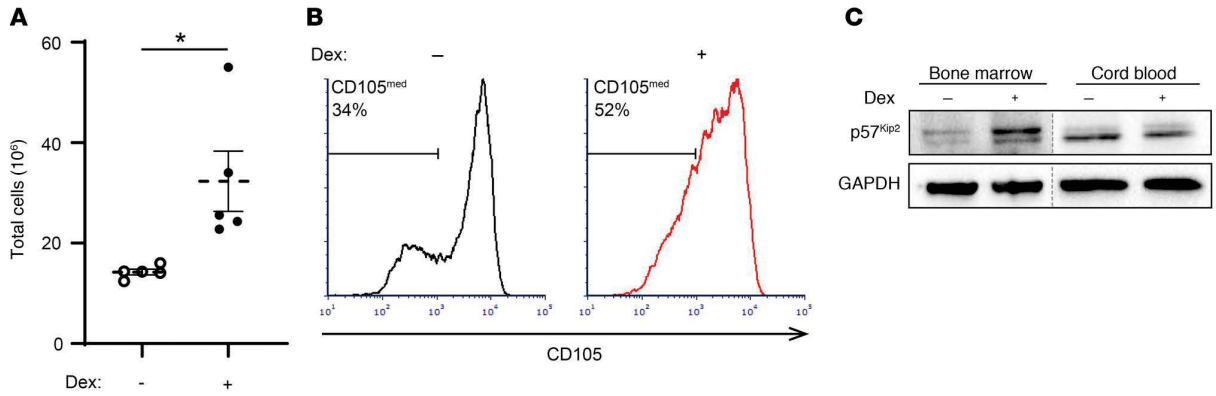

Figure 7. Dexamethasone increases p57^{Kip2} levels in Epo-induced, BM-derived progenitors, expanding the immature CD105^{med} CFU-E subset. (**A**) BM CD34$^+$ progenitors were differentiated in the absence (open circles) or presence (solid circles) of dexamethasone, and total cell numbers on day 14 are presented (n = 5 independent experiments). Data represent the mean ± SEM. *P < 0.05, by 2-tailed Student's t test. (**B**) Representative histograms of CD105 expression in BM-derived CD34$^+$ cells differentiated in the absence (black) or presence (red) of dexamethasone on day 4 are shown, and the percentages of CD105^{med} cells are indicated. (**C**) Expression of p57^{Kip2} and GAPDH in purified BM-derived and CB-derived mature CFU-Es, generated in the absence or presence of dexamethasone, was evaluated by Western blotting (blots from 1 of 3 independent experiments are shown).

led to an increase in p57^{Kip2} expression that we did not observe in CB-derived CFU-Es treated with dexamethasone (Figure 7C). Overall, these data indicate that PB- and BM-derived erythroid progenitors respond to dexamethasone in a similar manner and that the phenotypes we observed may be relevant in the clinical use of dexamethasone for the treatment of red cell disorders.

Discussion

We believe the present study, which focused on identifying the role of dexamethasone during physiological and pathological human erythropoiesis, has generated several unique insights. Our finding that dexamethasone markedly enhanced the erythroid proliferation of CD34$^+$ cells from adult PB but not from CB was unexpected and very surprising. In this context, it is of interest that the transition trajectories from BFU-E to CFU-E differ considerably following erythroid differentiation of CD34$^+$ cells derived from adult PB and CB (30). Together, these data strongly suggest that dexamethasone has differential effects on transitional erythroid progenitor populations that are regulated by the source of the CD34$^+$ progenitors. Importantly, these findings are relevant to BM populations, as we found that CFU-Es from BM-derived CD34$^+$ cells had dexamethasone-induced responses that were similar to those detected in PB-derived CFU-Es (Figure 7).

Although BFU-Es derived from human either PB or CB were not responsive to dexamethasone, BFU-Es from murine fetal liver have been shown to be dexamethasone responsive (19). Murine CFU-Es have also been shown to be specifically dexamethasone responsive (10), suggesting that dexamethasone-dependent erythroid developmental stages may be species dependent. Collectively, these previous studies (10, 19), together with the present work, point to important differences between murine and human systems and, moreover, demonstrate the importance of the developmental origin of hematopoietic stem and progenitor cells in regulating their responsiveness to glucocorticoids during erythropoiesis. These developmental differences as well as steroid resistance in DBA may be mediated by epigenetic regulators (40–43), and further investigations of the mechanisms may offer additional insights into the heterogeneity of progenitor cell populations. Finally, our data show the importance of the p57^{Kip2} cell-cycle inhibitor in mediating dexamethasone effects during human erythroid differentiation and reveal the critical nature of the p57^{Kip2} axis in the dexamethasone responsiveness of patients with DBA.

The marked heterogeneity of human erythroid progenitors has long been recognized (44, 45). Indeed, it has been known for decades that erythroid progenitors give rise to colonies of different sizes and morphology in the methylcellulose culture system, which led to the concept of large, intermediate, and small BFU-E colonies, with the small BFU-E–forming cells further differentiating into CFU-Es (46). The recent progress of single-cell technologies has enabled stringent analyses of these varied cell populations with regard to both steroid sensitivity and cell-fate decisions (12, 47). Although we previously found that human BFU-Es and CFU-Es can be immunophenotypically defined on the basis of IL-3R, GPA, CD34, and CD36 cell-surface markers, this characterization did not allow us to fully resolve the heterogeneity of human erythroid progenitors. In the present study, we found that the CD71 and CD105 markers allowed for further immunophenotyping, discriminating subpopulations of erythroid BFU-Es and CFU-Es. Using this method, we identified a transitional human progenitor CFU-E population, resulting in the designation of immature and mature CFU-Es.

Using this optimized immunophenotyping assay, we identified the immature CFU-E population as the steroid-responsive erythroid progenitor subset, as determined by both proliferation and a decrease in the percentages of cells in the S phase of the cell cycle. This cell-cycle phenotype was due to a dexamethasone-mediated increase in p57^{Kip2}, and under these conditions, differentiation was delayed, resulting in a paradoxical expansion of this progenitor subset. We propose that this occurs through the maintenance of the immature CFU-E population, generating larger numbers of mature CFU-Es.

The critical role of $p57^{Kip2}$ in CFU-Es was shown by shRNA knockdown, which resulted in an opposite phenotype and an acceleration of erythroid differentiation that was associated with a decrease in proliferation. Together with recent work that identifies a role for cell-cycle status in cell-fate decisions (48), the ensemble of these data demonstrate a clear link between cell-cycle progression and differentiation of erythroid progenitors.

Importantly, erythroid progenitors from transfusion-dependent patients with DBA harbored altered levels of $p57^{Kip2}$, and expression was not sensitive to dexamethasone treatment. Indeed, the absence of changes in $p57^{Kip2}$ levels in transfusion-dependent patients is a proof of concept for the importance of this cell-cycle regulator in the response to steroids. Notably, though, there was substantial variability in the phenotype of progenitors from transfusion-dependent patients with DBA that was likely mediated by other mechanisms. In the future, it will be important to determine whether steroid responsiveness in patients with DBA is regulated at the level of a specific subset or subsets of erythroid progenitors and, furthermore, to assess the role of $p57^{Kip2}$ levels in these subsets.

Our proteomics data revealed previously unidentified dexamethasone targets that may offer additional insights into how dexamethasone influences the cell cycle and increases erythroid proliferation. Of the identified targets, many have been shown to be involved in cell-cycle regulation including PER1 and NR4A1, indicating that these proteins may function to negatively regulate the cell cycle in association with $p57^{Kip2}$ (31, 49). In this regard, it is of interest that NR4A1 mediates TGF-β signaling, which is also aberrant in DBA and could thus be involved in corticosteroid resistance mechanisms (50). Our finding that dexamethasone globally regulates RNA processing and biosynthetic pathways may also open additional avenues for studies on the effects of dexamethasone on erythroid progenitors.

The present findings have direct relevance for the clinical use of corticosteroids for the treatment of hypoproliferative anemias, most notably DBA. Although corticosteroid use stably increases red cell mass and induces hematopoietic remission or marked improvement in many patients with DBA, other patients are not responsive or cannot continue glucocorticoid treatment because of adverse side effects. We anticipate that our insights into the mechanism of action of glucocorticoids on human erythropoiesis, and specifically on the immature CFU-E subset, will promote the development of targeted drugs and treatment strategies that will induce a sustained effect on erythroid progenitors in more patients with fewer side effects. In summary, we have identified a transitional CFU-E subset, between late BFU-E and mature CFU-E stages, that is responsive to dexamethasone. These findings contribute to our understanding of erythroid progenitor biology and will, we believe, lead to the development of new treatment strategies for erythroid disorders.

Methods

Human studies

$CD34^+$ cells were obtained from deidentified control adult PB leukoreduction filters, deidentified CB units, deidentified BM samples, or phlebotomized patients with DBA. In order to limit sample variability, blood samples from multiple control PB or CB donors were pooled.

Patients with DBA were defined as transfusion dependent or steroid responsive on the basis of their clinical need for chronic RBC transfusion or successful management with corticosteroids, respectively.

The 3 patients with DBA presented in Figure 1E were followed after diagnosis and initial treatment with prednisone. The dose of prednisone was decreased after the initial response.

Isolation and culturing of $CD34^+$ cells

Mononuclear cells from PB, CB, or BM were separated using Lymphoprep (STEMCELL Technologies), and $CD34^+$ cells were purified with anti-CD34 microbeads and MACS Columns (Miltenyi Biotec) according to manufacturer's protocol. $CD34^+$ cells were cultured at a density of 10^5 cells/mL in serum-free expansion media as previously described (26), with a base media of StemSpan SFEM (STEMCELL Technologies) initially supplemented with 100 ng/mL SCF, 10 ng/mL IL-3, 0.5 U/mL Epo, 4 μL/mL lipid mixture 1 (MilliporeSigma), 2 mM L-glutamine, and 200 μg/mL transferrin. Beginning on day 7, the dose of Epo was increased to 3 U/mL, and on day 11, the dose of transferrin was increased to 1 mg/mL. Dexamethasone (MilliporeSigma) was added to cultures at 100 nM as indicated, as this dose was found to be optimal (Supplemental Figure 2). Olomoucine (MilliporeSigma) was added at 1 μM as indicated.

Flow cytometry and cell sorting

Erythroid progenitors were examined using surface markers as previously described (18). Erythroid progenitors were analyzed on day 4 of differentiation, at which point 10^5 cells were stained for 15 minutes at room temperature with an antibody cocktail containing anti–IL-3R phycoerythrin-Cy7 (PE-Cy7), anti–GPA PE, anti–CD34 FITC, anti–CD36 allophycocyanin (APC), anti–CD71 Alexa Fluor 700, and anti–CD105 Brilliant Violet 421 (BD Biosciences; 560826, 555570, 555821, 550956, 560566, and 563920, respectively). BFU-Es were defined as $GPA^-IL\text{-}3R^-CD34^+CD36^-$, CFU-Es as $GPA^-IL\text{-}3R^-CD34^-CD36^+$, and transitional progenitors as $GPA^-IL\text{-}3R^-CD34^+CD36^+$. Dead cells were excluded from further analysis with 7-aminoactinomycin D (BD Biosciences) staining. Analysis was performed using a BD Fortessa flow cytometer with FCS Express 6 and FlowJo 10 software. BFU-Es, CFU-Es, and transitional progenitors were sorted for downstream experiments using a BD FACSAria at low pressure with a 100-μm nozzle. Fluorescence minus 1 and isotype controls were used to define the different populations of progenitor cells and resolve the continuum. Functional assays using sorted cells in colony-forming assays were performed to further confirm the identity and purity of the different cell populations.

Colony-forming assays

Sorted erythroid progenitors were seeded onto methylcellulose media H4230 (STEMCELL Technologies) supplemented with Epo alone at 0.5 U/mL or onto complete methylcellulose media H4435 (STEMCELL Technologies) at 200 cells/mL. BFU-E and CFU-E colonies were counted and measured on days 14 and 7 of culturing, respectively. Colony area was determined by modeling each colony as an ellipse and measuring its major axis a and minor axis b to calculate the area using the formula area $= \pi ab/4$. Dexamethasone (100 nM) was added to cultures as indicated.

Cell-cycle staining

For live cell-cycle staining to examine cell-cycle profile, erythroid progenitors were incubated with 5 mg/mL Hoechst 33342 for 3 hours at 37°C before staining with an antibody cocktail for surface markers.

Western blot analysis

Cells were lysed in RIPA Lysis and Extraction Buffer (Thermo Fisher Scientific) with 1:100 protease inhibitor cocktail (MilliporeSigma) on ice for 10 minutes and then centrifuged at maximum speed for 10 minutes. Supernatants were mixed at 1:1 (vol/vol) with 2× Laemmli Sample Buffer (Bio-Rad) with 0.1 M DTT and boiled for 5 minutes. Samples were then separated with SDS-PAGE for 1.5 hours at 150 V and transferred onto nitrocellulose membranes for 1 hour at 95 V. Membranes were then blocked with 4% (wt/vol) milk powder and 1% (wt/vol) BSA in 0.1% Tween-20 (vol/vol) PBST for 3 hours. Membranes were then incubated with the following primary antibodies overnight at 4°C: $p57^{Kip2}$ (BD Biosciences; 556346), $p27^{Kip1}$ (BD Biosciences; 610241), NR4A1 (BD Biosciences; 554088), GAPDH (MilliporeSigma; CB1001), and α-globin (Santa Cruz Biotechnology; sc-514378). Membranes were washed 5 times for 5 minutes with PBST and then incubated with HRP-conjugated secondary antibodies (Bio-Rad) for 2 hours at room temperature. Membranes were imaged with Pierce ECL Western Blotting Substrate (Thermo Fisher Scientific) using a Chemi-Doc MP Imaging System (Bio-Rad). Western blot images are representative of multiple experiments and were quantified with ImageJ software (NIH).

Lentivirus transduction

$p57^{Kip2}$- and $p27^{Kip1}$-knockdown experiments were each carried out with 2 lentiviral shRNA-knockdown constructs targeting CDKN1C and CDKN1B, respectively (clone IDs: NM_000076.2-1451s21c1 and NM_000076.2-1216s21c1 for CDKN1C and NM_004064.3-841s21c1 and NM_004064.3-643s21c1 for CDKN1B; MilliporeSigma). shRNA-knockdown constructs targeting luciferase were used as controls. After 2 days of culturing in serum-free expansion media, erythroid progenitors were placed in 10% FBS IMDM with 3 U/mL heparin and 8 μg/mL polybrene. Lentivirus particles were then added at a MOI of 30 and spinoculated for 2 hours at 1500 *g*. Cells were then incubated overnight and placed in serum-free expansion media. After a 24-hour recovery, lentivirus transduction was positively selected with 1 μg/mL puromycin, which was maintained until day 11 of culture.

Proteomics profiling

In-solution digestion. $CD34^+$ cell pellets were lysed for 30 minutes at 4°C in 8 M urea, 50 mM Tris-HCl, pH 8.0, 75 mM NaCl, 1 mM EDTA, 2 μg/μL aprotinin (MilliporeSigma), 10 μg/μL leupeptin (Roche), and 1 mM PMSF (MilliporeSigma). Lysates were cleared via centrifugation at 20,000 *g*, and protein concentration was determined using a bicinchoninic acid (BCA) protein assay (Pierce, Thermo Fisher Scientific). Remaining lysis buffer was used to equalize sample concentrations to the lowest measured concentration before proceeding. Protein reduction was performed with 5 mM DTT for 1 hour at room temperature, followed by alkylation with 10 mM iodoacetamide for 45 minutes at room temperature in the dark. Sample volumes were then adjusted with 50 mM Tris-HCl, pH 8.0, to reduce urea concentration to 2 M preceding enzymatic digestion. Proteins were digested first with endoproteinase LysC (Wako Laboratories) for 2 hours at 25°C and then overnight with sequencing-grade trypsin (Promega) at 25°C, both at enzyme/substrate ratios of 1:50. Following digestion, samples were acidified to a concentration of 1% with neat formic acid, and insoluble peptides and urea were removed via centrifugation at 20,000 *g*. The remaining soluble peptides were desalted using a 100-mg reverse-phase tC18 SepPak cartridge (Waters). Cartridges were conditioned with 1 mL 100% MeCN and 1 mL 50% MeCN/0.1% formic acid (FA) and then equilibrated with 4× 1 mL 0.1% trifluoroacetic acid (TFA). Samples were loaded onto the cartridge and washed 3 times with 1 mL 0.1% TFA and once with 1 mL 1% FA, and then eluted with 2× 600 μL 50% acetonitrile (MeCN) and 0.1% FA. The peptide concentration of desalted samples was again estimated with a BCA assay, such that the proper amount for TMT labeling could be removed, dried in a vacuum centrifuge, and stored at –80°C.

TMT labeling of peptides. Samples were divided into 2 groups: PB- and CB-derived cells, and each set was separately labeled with TMT plex isobaric mass tagging reagents (Thermo Fisher Scientific) as previously described (51). Each 6-plex contained triplicate samples of dexamethasone- and DMSO-treated cells. Digested peptides were resuspended in 50 mM HEPES, pH 8.5, at a concentration of 2.5 mg/mL. Dried TMT reagent was reconstituted at 20 μg/μL in 100% anhydrous MeCN and added to samples at a 1:1 TMT/peptide mass ratio (100 μg for PB samples and 70 μg for CB samples due to the limited amount of material). Labeling was performed for 1 hour at 25°C with shaking. The TMT reaction was quenched with 5% hydroxylamine to a final concentration of 0.2% and shaken for 15 minutes at 25°C. TMT-labeled samples within each plex were then combined, dried to completion via vacuum centrifugation, reconstituted in 1 mL 0.1% FA, and desalted with a 100-mg SepPak cartridge as described above.

Basic reverse-phase fractionation. TMT-labeled peptides were fractionated via offline basic reverse-phase (bRP) chromatography as previously described (52). Chromatography was performed with a Zorbax 300 Extend-C18 column (4.6 × 250 mm, 3.5 μm; Agilent Technologies) on an Agilent 1100 HPLC system. Samples were reconstituted in 900 μL bRP solvent A (5 mM ammonium formate, pH 10.0, in 2% vol/vol MeCN) and injected with this solvent at a flow rate of 1 mL/min. Peptides were separated at the same flow rate with a 96-minute gradient, beginning with an initial increase to 16% bRP solvent B (5 mM ammonium formate, pH 10.0, in 90% vol/vol MeCN), followed by a linear 60-minute gradient to 40% and stepwise ramping to 44% and finally 60% bRP solvent B. A total of 96 fractions were collected in a row-wise snaking pattern into a Whatman 2-mL 96-well plate (GE Healthcare) and were then concatenated nonsequentially into a final 24 fractions for proteomics analysis. The fractions were dried via vacuum centrifugation.

LC-MS/MS. Dried fractions were reconstituted in 3% MeCN/0.1% FA to a peptide concentration of 1 μg/μL and analyzed via coupled NanoflowLC-MS/MS using a Proxeon Easy-nLC1000 (Thermo Fisher Scientific) and a Q-Exactive Plus Series Mass Spectrometer (Thermo Fisher Scientific). A sample load of 1 μg for each fraction was separated on a capillary column (36-μm outer diameter × 75-μm inner diameter) containing an integrated emitter tip and heated to 50°C, followed by packing to a length of approximately 30 cm with ReproSil-Pur C18-AQ 1.9 μm beads (Maisch GmbH). Chromatography was performed with a 110-minute gradient consisting of solvent A (3% MeCN/0.1% FA) and solvent B (90% MeCN/0.1% FA). The gradient profile, described as minutes/percentage solvent B, was 0:2, 1:6, 85:30, 94:60, 95:90, 100:90, 101:50, and 110:50, with the first 6 steps being performed at a flow rate of 200 nL/min and the last 2 at a flow rate of 500 nL/min. Ion acquisition on the Q-Exactive Plus was performed in data-dependent mode, acquiring HCD-MS/MS scans at a resolution of

17,500 on the top-12 most abundant precursor ions in each full MS scan (70,000 resolution). The automatic gain control (AGC) target was set to 3×10^6 ions for MS1 and 5×10^4 for MS2, and the maximum ion time was set to 120 ms for MS2. The collision energy was set to 30, peptide matching was set to "preferred," isotope exclusion was enabled, and dynamic exclusion time was set to 20 seconds.

The original mass spectra and the protein sequence database used for searches have been deposited in the public proteomics repository MassIVE (http://massive.ucsd.edu) and are accessible at ftp://massive.ucsd.edu/MSV000084614.

Data analysis. Data were analyzed using Spectrum Mill, version 6.01.202 (Agilent Technologies). In extracting spectra from the raw format for MS/MS searching, spectra from the same precursor or within a retention time window of ±60 seconds and an m/z range of ±1.4 were merged. Spectra were filtered to include only those with a precursor mass range of 750 to 6000 Da and a sequence tag length greater than 0. MS/MS searching was performed against a human UniProt database (www.uniprot.org). Digestion enzyme conditions were set to "Trypsin allow P" for the search, allowing up to 4 missed cleavages within a matched peptide. Fixed modifications were carbamidomethylation of cysteine and TMT6 on the N-terminus and internal lysine. Variable modifications were oxidized methionine and acetylation of the protein N-terminus. Matching criteria included a 30% minimum matched peak intensity and a precursor and product mass tolerance of ±20 ppm. Peptide-level matches were validated if found to be below the 1.0% FDR threshold and within a precursor charge range of 2 to 6. A second round of validation was then performed for protein-level matches, requiring a minimum protein score of 0. Protein-centric information, including experimental ratios, was then summarized in a table, which was quality filtered for nonhuman contaminants, keratins, and any proteins not identified by at least 2 fully quantified peptides with 2 ratio counts.

Statistics

All statistical evaluations comparing the different experimental groups were performed using GraphPad Prism 8 software for unpaired 2-tailed Student's t test, 2-way ANOVA with Tukey's post hoc test, and Kruskal-Wallis test with Dunn's post hoc analysis with corrections for multiple comparisons. A P value of less than 0.05 was considered statistically significant. Raw data and complete, unedited blots corresponding to the additional independent experiments are presented in Supplemental Figure 7. For proteomics analyses, PB and CB plexes were analyzed separately, each using biologically paired samples to compare dexamethasone treatment with a DMSO control. Data were median normalized and subjected to a 1-sample moderated t test using an internal R-Shiny package based in the limma R library. Correction for multiple testing was performed using the Benjamini-Hochberg FDR method. ssGSEA was performed as previously described (53) using an R script (available at https://github.com/broadinstitute/ssGSEA2.0). ssGSEA was performed separately on PB and CB plexes, using the $\log_2$-transformed ratios of dexamethasone/control as input. Parameters were set as follows: sample.norm.type = "rank", weight = 0.75, statistic = "area.under.RES", output.score.type = "NES", nperm = 1e3, min.overlap = 10, correl.type = "z.score", par = T, spare.cores = 1. The heatmap in Figure 3F was generated using the average of triplicate enrichment scores, ranked to create a list of top-10 and bottom-10, eliminating redundant rows. It should be noted that the TMT plex design used limits direct quantitative comparisons between PB and CB samples, as the stochastic sampling of spectra on the mass spectrometer can lead to technical differences in the proteins identified in different plexes that are not necessarily driven by biological causes. Therefore, the observed differences between PB and CB samples were validated in follow-up experiments.

Study approval

All human studies were approved by the IRBs of Northwell Health and Stanford University. Written, informed consent was obtained from all participants prior to their inclusion in the study.

Author contributions

The co–first authors RJA and HY are listed in alphabetical order; they designed and performed most of the experiments, analyzed data, and wrote the manuscript. NW, JH, BMD, and JP performed experiments. MEO, NDU, and SAC designed, performed, and analyzed the proteomics studies and edited the manuscript. AV, JML, and LDC analyzed data related to patients with DBA. CH, SK, and NT designed and analyzed data and edited the manuscript. NM, AN, and LB designed the project, analyzed data, and wrote the manuscript.

Acknowledgments

The authors thank the patients and their families for their contributions. We thank Betsy J. Barnes, Philippe Marambaud, and Mark J. Koury for helpful discussions and critical reading of the manuscript. We also thank the Tissue Donation Program at Northwell Health for providing access to BM samples. This research was supported in part by NIH grants DK32094 (to NM), HL079571 (to JML and AV), HL134812 (to JML, AV, and LB), CA210986 and CA214125 (to SAC), CA210979 (to DRM), and HL144436 (to LB and AN); the Diamond Blackfan Anemia Foundation (to LB); and the Pediatric Cancer Foundation (to JML and LB). AN is the recipient of an American Society of Hematology (ASH) Bridge Grant and a Faculty Scholar grant from the Maternal and Child Health Research Institute at Stanford University. LB is the recipient of a St. Baldrick's Scholar award.

Address correspondence to: Lionel Blanc, Laboratory of Developmental Erythropoiesis, Feinstein Institutes for Medical Research, 350 Community Drive, Manhasset New York 11030, USA. Phone: 516.562.1507; Email: lblanc@northwell.edu.

1. Danilova N, Gazda HT. Ribosomopathies: how a common root can cause a tree of pathologies. *Dis Model Mech.* 2015;8(9):1013–1026.
2. Vlachos A, Blanc L, Lipton JM. Diamond Blackfan anemia: a model for the translational approach to understanding human disease. *Expert Rev Hematol.* 2014;7(3):359–372.
3. Khajuria RK, et al. Ribosome levels selectively regulate translation and lineage commitment in human hematopoiesis. *Cell.* 2018;173(1):90–103.e19.
4. Ludwig LS, et al. Altered translation of GATA1 in Diamond-Blackfan anemia. *Nat Med.* 2014;20(7):748–753.
5. Quarello P, et al. Diamond-Blackfan anemia: genotype-phenotype correlations in Italian patients with RPL5 and RPL11 mutations. *Haematologica.* 2010;95(2):206–213.
6. Da Costa L, Moniz H, Simansour M, Tchernia G, Mohandas N, Leblanc T. Diamond-Blackfan anemia, ribosome and erythropoiesis. *Transfus Clin Biol.* 2010;17(3):112–119.

7. Vlachos A, Muir E. How I treat Diamond-Blackfan anemia. *Blood*. 2010;116(19):3715–3723.
8. Chan HS, Saunders EF, Freedman MH. Diamond-Blackfan syndrome. II. In vitro corticosteroid effect on erythropoiesis. *Pediatr Res*. 1982;16(6):477–478.
9. Kadmiel M, Cidlowski JA. Glucocorticoid receptor signaling in health and disease. *Trends Pharmacol Sci*. 2013;34(9):518–530.
10. Hwang Y, et al. Global increase in replication fork speed during a $p57^{KIP2}$-regulated erythroid cell fate switch. *Sci Adv*. 2017;3(5):e1700298.
11. Lee HY, et al. PPAR-α and glucocorticoid receptor synergize to promote erythroid progenitor self-renewal. *Nature*. 2015;522(7557):474–477.
12. Li H, et al. Rate of progression through a continuum of transit-amplifying progenitor cell states regulates blood cell production. *Dev Cell*. 2019;49(1):118–129.e7.
13. Zhang L, et al. ZFP36L2 is required for self-renewal of early burst-forming unit erythroid progenitors. *Nature*. 2013;499(7456):92–96.
14. Gregory CJ, Eaves AC. Human marrow cells capable of erythropoietic differentiation in vitro: definition of three erythroid colony responses. *Blood*. 1977;49(6):855–864.
15. Gregory CJ, Eaves AC. Three stages of erythropoietic progenitor cell differentiation distinguished by a number of physical and biologic properties. *Blood*. 1978;51(3):527–537.
16. McLeod DL, Shreeve MM, Axelrad AA. Improved plasma culture system for production of erythrocytic colonies in vitro: quantitative assay method for CFU-E. *Blood*. 1974;44(4):517–534.
17. Stephenson JR, Axelrad AA, McLeod DL, Shreeve MM. Induction of colonies of hemoglobin-synthesizing cells by erythropoietin in vitro. *Proc Natl Acad Sci U S A*. 1971;68(7):1542–1546.
18. Li J, et al. Isolation and transcriptome analyses of human erythroid progenitors: BFU-E and CFU-E. *Blood*. 2014;124(24):3636–3645.
19. Flygare J, Rayon Estrada V, Shin C, Gupta S, Lodish HF. HIF1alpha synergizes with glucocorticoids to promote BFU-E progenitor self-renewal. *Blood*. 2011;117(12):3435–3444.
20. Lodish H, Flygare J, Chou S. From stem cell to erythroblast: regulation of red cell production at multiple levels by multiple hormones. *IUBMB Life*. 2010;62(7):492–496.
21. Gao X, et al. TGF-β inhibitors stimulate red blood cell production by enhancing self-renewal of BFU-E erythroid progenitors. *Blood*. 2016;128(23):2637–2641.
22. Freire PR, Conneely OM. NR4A1 and NR4A3 restrict HSC proliferation via reciprocal regulation of C/EBPα and inflammatory signaling. *Blood*. 2018;131(10):1081–1093.
23. Golde DW, Bersch N, Cline MJ. Potentiation of erythropoiesis in vitro by dexamethasone. *J Clin Invest*. 1976;57(1):57–62.
24. Ohene-Abuakwa Y, Orfali KA, Marius C, Ball SE. Two-phase culture in Diamond Blackfan anemia: localization of erythroid defect. *Blood*. 2005;105(2):838–846.
25. Iskander D, et al. Elucidation of the EP defect in Diamond-Blackfan anemia by characterization and prospective isolation of human EPs. *Blood*. 2015;125(16):2553–2557.
26. Dulmovits BM, et al. Pomalidomide reverses γ-globin silencing through the transcriptional reprogramming of adult hematopoietic progenitors. *Blood*. 2016;127(11):1481–1492.
27. Nathan DG, Gardner FH. Erythroid cell maturation and hemoglobin synthesis in megaloblastic anemia. *J Clin Invest*. 1962;41:1086–1093.
28. Davies SV, Cavill I, Bentley N, Fegan CD, Poynton CH, Whittaker JA. Evaluation of erythropoiesis after bone marrow transplantation: quantitative reticulocyte counting. *Br J Haematol*. 1992;81(1):12–17.
29. d'Onofrio G, Chirillo R, Zini G, Caenaro G, Tommasi M, Micciulli G. Simultaneous measurement of reticulocyte and red blood cell indices in healthy subjects and patients with microcytic and macrocytic anemia. *Blood*. 1995;85(3):818–823.
30. Yan H, et al. Developmental differences between neonatal and adult human erythropoiesis. *Am J Hematol*. 2018;93(4):494–503.
31. Reddy TE, Gertz J, Crawford GE, Garabedian MJ, Myers RM. The hypersensitive glucocorticoid response specifically regulates period 1 and expression of circadian genes. *Mol Cell Biol*. 2012;32(18):3756–3767.
32. Nagy Z, Marta A, Butz H, Liko I, Racz K, Patocs A. Modulation of the circadian clock by glucocorticoid receptor isoforms in the H295R cell line. *Steroids*. 2016;116:20–27.
33. Fassett MS, Jiang W, D'Alise AM, Mathis D, Benoist C. Nuclear receptor Nr4a1 modulates both regulatory T-cell (Treg) differentiation and clonal deletion. *Proc Natl Acad Sci U S A*. 2012;109(10):3891–3896.
34. Yoo YG, Yeo MG, Kim DK, Park H, Lee MO. Novel function of orphan nuclear receptor Nur77 in stabilizing hypoxia-inducible factor-1alpha. *J Biol Chem*. 2004;279(51):53365–53373.
35. Zhang FL, Shen GM, Liu XL, Wang F, Zhao YZ, Zhang JW. Hypoxia-inducible factor 1-mediated human GATA1 induction promotes erythroid differentiation under hypoxic conditions. *J Cell Mol Med*. 2012;16(8):1889–1899.
36. Matsumoto A, et al. p57 is required for quiescence and maintenance of adult hematopoietic stem cells. *Cell Stem Cell*. 2011;9(3):262–271.
37. Hsieh FF, et al. Cell cycle exit during terminal erythroid differentiation is associated with accumulation of p27(Kip1) and inactivation of cdk2 kinase. *Blood*. 2000;96(8):2746–2754.
38. Pateras IS, Apostolopoulou K, Niforou K, Kotsinas A, Gorgoulis VG. p57KIP2: "Kip"ing the cell under control. *Mol Cancer Res*. 2009;7(12):1902–1919.
39. Abraham RT, et al. Cellular effects of olomoucine, an inhibitor of cyclin-dependent kinases. *Biol Cell*. 1995;83(2-3):105–120.
40. Ludwig LS, et al. Transcriptional states and chromatin accessibility underlying human erythropoiesis. *Cell Rep*. 2019;27(11):3228–3240.e7.
41. Schulz VP, et al. A unique epigenomic landscape defines human erythropoiesis. *Cell Rep*. 2019;28(11):2996–3009.e7.
42. Heuston EF, et al. Establishment of regulatory elements during erythro-megakaryopoiesis identifies hematopoietic lineage-commitment points. *Epigenetics Chromatin*. 2018;11(1):22.
43. Farrar JE, et al. Altered epigenetic maturation in early erythroid cells from Diamond Blackfan anemia patients treated with transfusions, corticosteroids, or in remission. *Blood*. 2018;132(Suppl 1):752.
44. D'Arena G, Musto P, Cascavilla N, Di Giorgio G, Zendoli F, Carotenuto M. Human umbilical cord blood: immunophenotypic heterogeneity of $CD34^+$ hematopoietic progenitor cells. *Haematologica*. 1996;81(5):404–409.
45. Fauser AA, Messner HA. Fetal hemoglobin in mixed hemopoietic colonies (CFU-GEMM), erythroid bursts (BFU-E) and erythroid colonies (CFU-E): assessment by radioimmune assay and immunofluorescence. *Blood*. 1979;54(6):1384–1394.
46. Nathan DG, et al. Human erythroid burst-forming unit: T-cell requirement for proliferation in vitro. *J Exp Med*. 1978;147(2):324–339.
47. Tusi BK, et al. Population snapshots predict early haematopoietic and erythroid hierarchies. *Nature*. 2018;555(7694):54–60.
48. Pauklin S, Vallier L. The cell-cycle state of stem cells determines cell fate propensity. *Cell*. 2013;155(1):135–147.
49. Palumbo-Zerr K, et al. Orphan nuclear receptor NR4A1 regulates transforming growth factor-β signaling and fibrosis. *Nat Med*. 2015;21(2):150–158.
50. Ge J, et al. Dysregulation of the transforming growth factor β pathway in induced pluripotent stem cells generated from patients with Diamond Blackfan anemia. *PLoS ONE*. 2015;10(8):e0134878.
51. Zecha J, et al. TMT Labeling for the masses: a robust and cost-efficient, in-solution labeling approach. *Mol Cell Proteomics*. 2019;18(7):1468–1478.
52. Mertins P, et al. Reproducible workflow for multiplexed deep-scale proteome and phosphoproteome analysis of tumor tissues by liquid chromatography-mass spectrometry. *Nat Protoc*. 2018;13(7):1632–1661.
53. Barbie DA, et al. Systematic RNA interference reveals that oncogenic KRAS-driven cancers require TBK1. *Nature*. 2009;462(7269):108–112.

Supplemental materials

Steroid resistance in Diamond Blackfan anemia associates with p57Kip2 dysregulation in erythroid progenitors

Ryan J. Ashley, **Hongxia Yan**, Nan Wang, John Hale, Brian M. Dulmovits, Julien Papoin, Meagan E. Olive, Namrata D. Udeshi, Steven A. Carr, Adrianna Vlachos, Jeffrey M. Lipton, Lydie Da Costa, Christopher Hillyer, Sandrina Kinet, Naomi Taylor, Narla Mohandas, Anupama Narla, and Lionel Blanc

Supplemental Figure 1: Dexamethasone significantly delays Glycophorin A upregulation in terminal erythroblasts in both PB- and CB-derived progenitors.

Supplemental Figure 2: Alterations in BFU-E and CFU-E cells as a function of Dexamethasone treatment.

Supplemental Figure 3: Measurement of CFU-E colony area.

Supplemental Figure 4: Changes in transcripts in PB- and CB-derived progenitors as a function of erythroid differentiation.

Supplemental Figure 5: Changes in cell cycle dynamics as a function of erythroid differentiation stage and responsiveness to dexamethasone.

Supplemental Figure 6: Impact of p57Kip2 and p27Kip1 downregulation on the growth and differentiation of PB CD34+ progenitors

Supplemental Figure 7: Additional representative data related to the main figures.

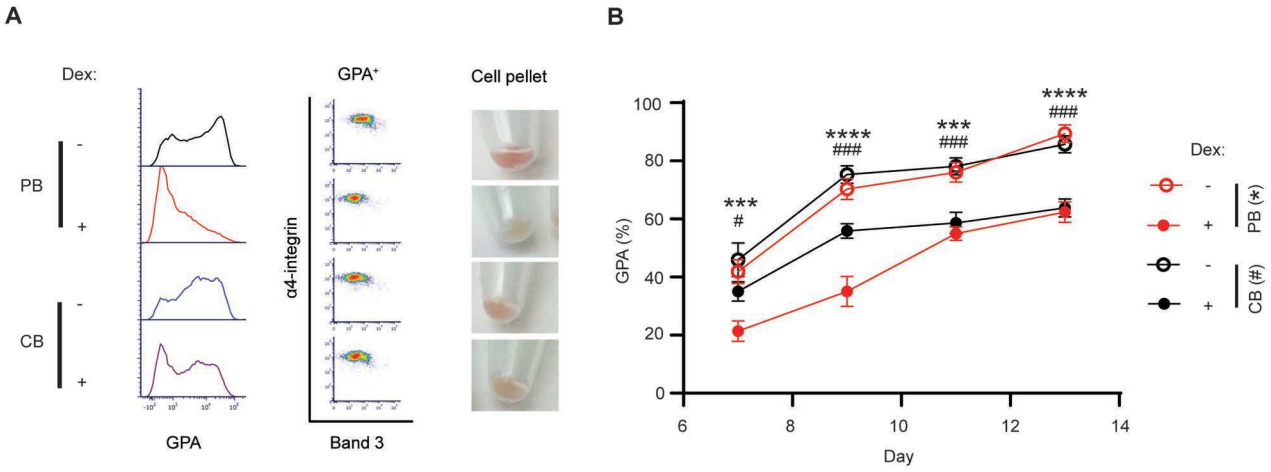

Supplemental Figure 1: Dexamethasone significantly delays Glycophorin A upregulation in terminal erythroblasts in both PB- and CB-derived progenitors.

(A) Representative histograms and cell pellets of PB- and CB-derived progenitors differentiated in the absence (-) or presence (+) of Dex (unsorted day 11). GPA expression as well as Band3 and α4-integrin expression of GPA^+ cells are shown. **(B)** Quantification of the percentages of GPA-positive cells following erythroid differentiation of PB- (n=4) and CB-derived (n=4) progenitors in the absence (solid circles) or presence (open circles) of Dex (horizontal lines present means ± SE; $^{*,\#}P < 0.05$, $^{**,\#\#}P < 0.01$, ns-non-significant, by two-way ANOVA with Tukey's post-hoc analysis with corrections for multiple comparisons to assess differences between PB-derived cells (*) and CB-derived cells (#) in the presence or absence of Dex).

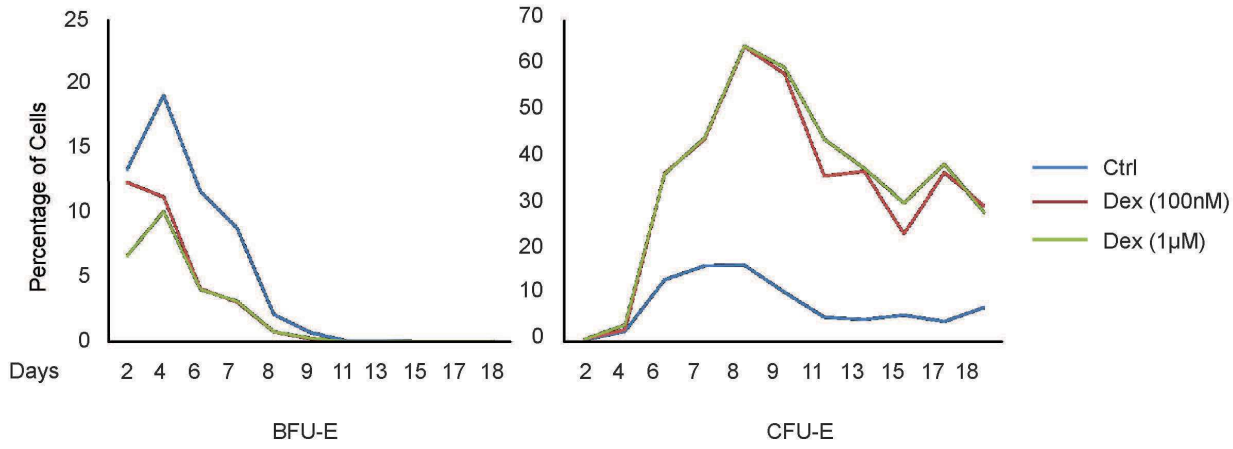

Supplemental Figure 2: Alterations in BFU-E and CFU-E cells as a function of Dexamethasone treatment.

The percentages of BFU-E and CFU-E generated from PB-derived $CD34^+$ progenitors following expansion in the absence (Ctrl) or presence of Dex (100nm and 1μm) are presented.

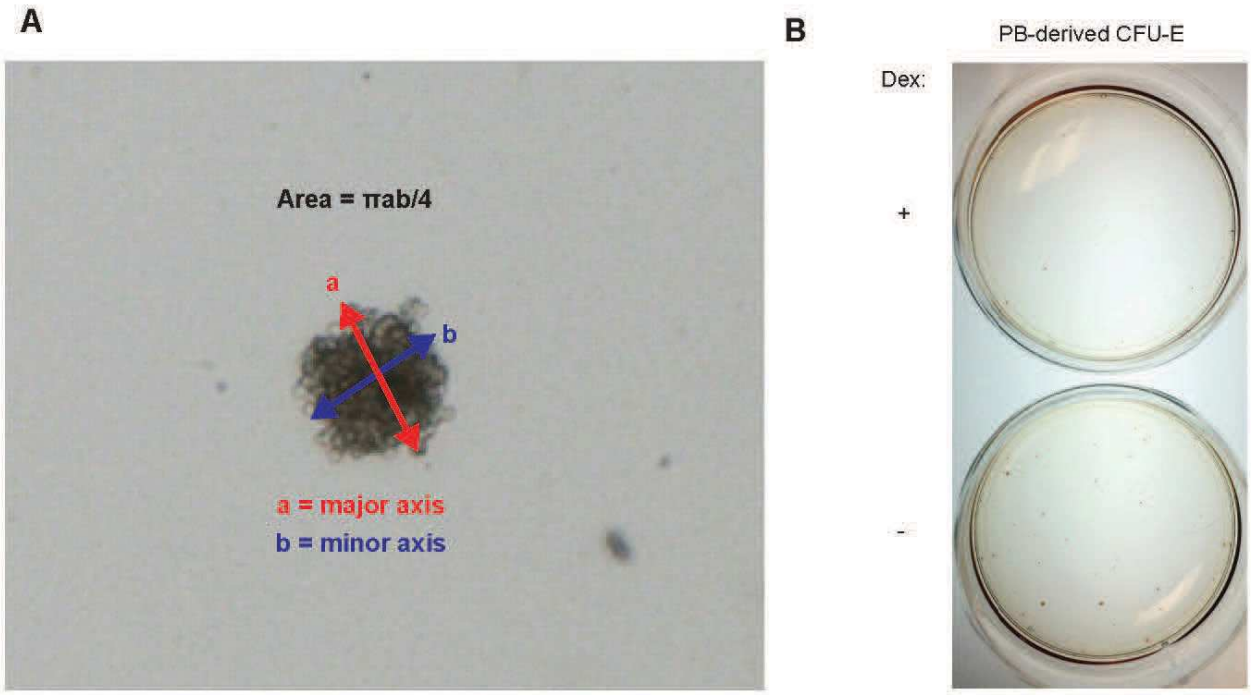

Supplemental Figure 3: Measurement of CFU-E colony area.

(A) Example of a CFU-E colony area measurement. Colony morphology was modeled as an ellipse and the area was determined by measuring the major axis "a" and minor axis "b" to calculate area by the formula A = πab/4. **(B)** Representative images of CFU-E colonies generated from PB-derived CFU-E in the absence (-) or presence (+) of dexamethasone (Dex).

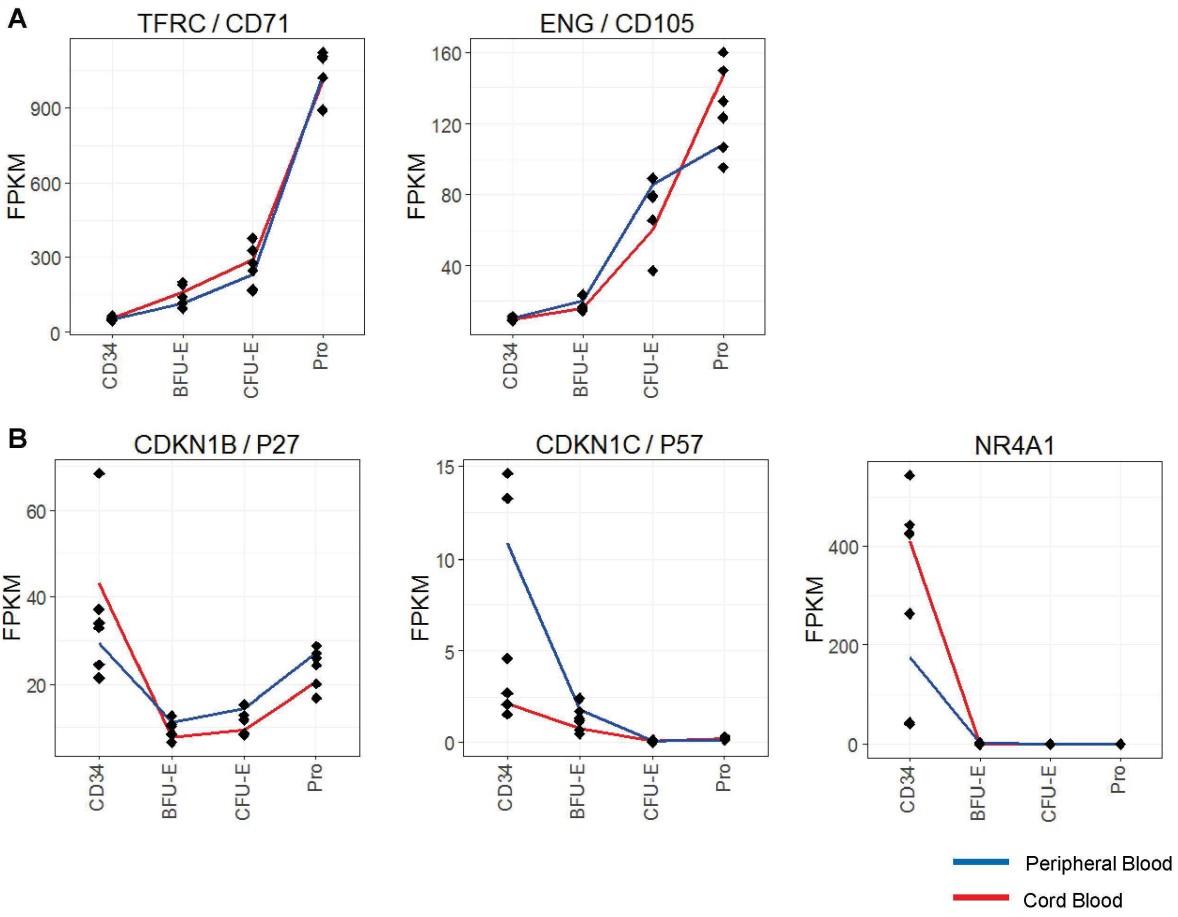

Supplemental Figure 4: Changes in transcripts in PB- and CB-derived progenitors as a function of erythroid differentiation.

Quantification of transcripts of **(A)** *TFRC* (CD71), *ENG* (CD105), and **(B)** *CDKN1B* ($p27^{Kip1}$), *CDKN1C* ($p57^{Kip2}$), and *NR4A1* in sorted erythroid subsets derived from PB (blue) and CB (red) progenitors. Data were originally published in Yan *et al*. 2018 (30).

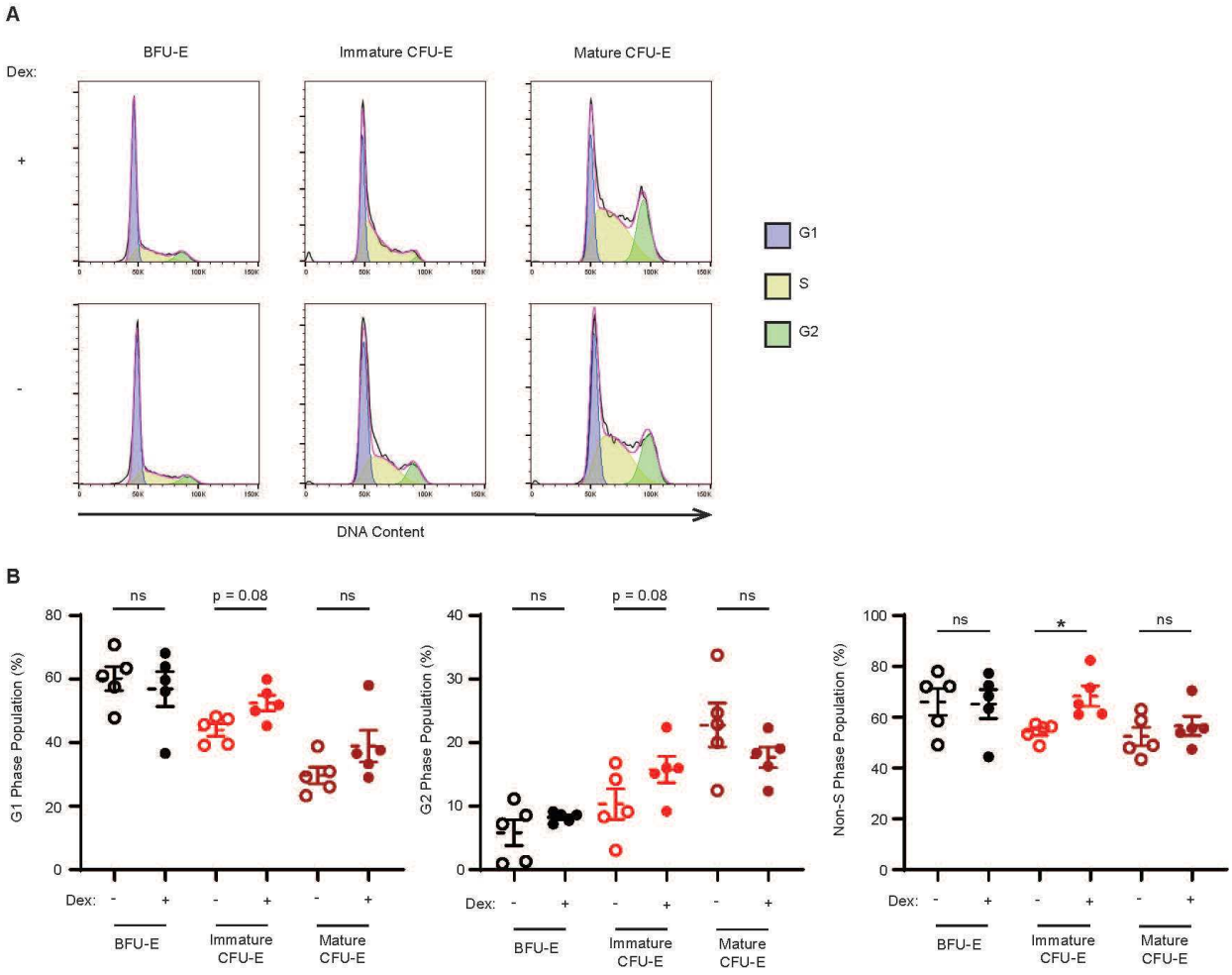

Supplemental Figure 5: Changes in cell cycle dynamics as a function of erythroid differentiation stage and responsiveness to dexamethasone.

(A) Representative cell cycle profiles of PB-derived BFU-E, immature CFU-E and mature CFU-E generated in the absence (-) or presence (+) of dexamethasone. Cells were stained with Hoechst 33342 and evaluated by flow cytometry. The G0/G1, S and G2/M phases of the cell cycle are shown in purple, yellow and green, respectively. **(B)** Quantification of the percentages of cells in G0/G1, G2/M phases and non-S phases populations of the cell cycle within PB-derived BFU-E, immature CFU-E and mature CFU-E subsets in the absence (-) or presence (+) of dexamethasone (n = 5). Means ± SE are shown; ns, non-significant, *$P < 0.05$, by 2-tailed Student's *t* test.

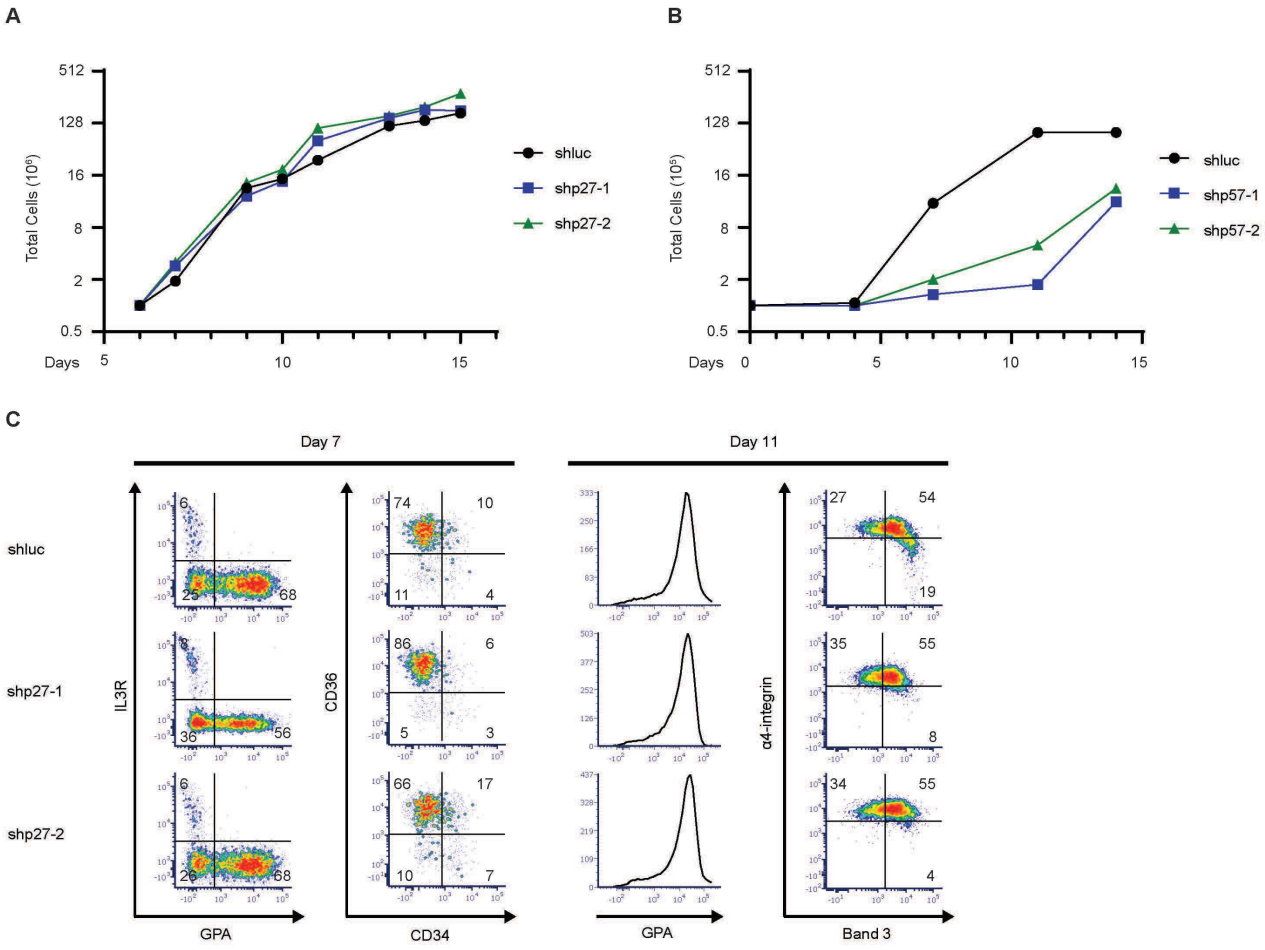

Supplemental Figure 6: Impact of $p57^{Kip2}$ and $p27^{Kip1}$ downregulation on the growth and differentiation of PB $CD34^+$ progenitors

(A) PB-derived $CD34^+$ progenitors were transduced with lentiviral vectors harboring an shRNA targeting a control gene (luciferase) or $p27^{Kip1}$ (two different shRNAs, labelled 1 and 2, are shown). The expansion of these progenitors between days 6 and 15 are presented (results represent data from 1 of 3 independent experiments). **(B)** PB-derived $CD34^+$ progenitors were transduced with lentiviral vectors harboring an shRNA targeting a control gene (luciferase) or $p57^{Kip2}$ (two different shRNAs, labelled 1 and 2, are shown). The expansion of these progenitors between days 0 and 15 are shown. **(C)** Flow cytograms of PB $CD34^+$ cells transduced with lentivirus for shRNA knockdown of $p27^{Kip1}$ and luciferase control.

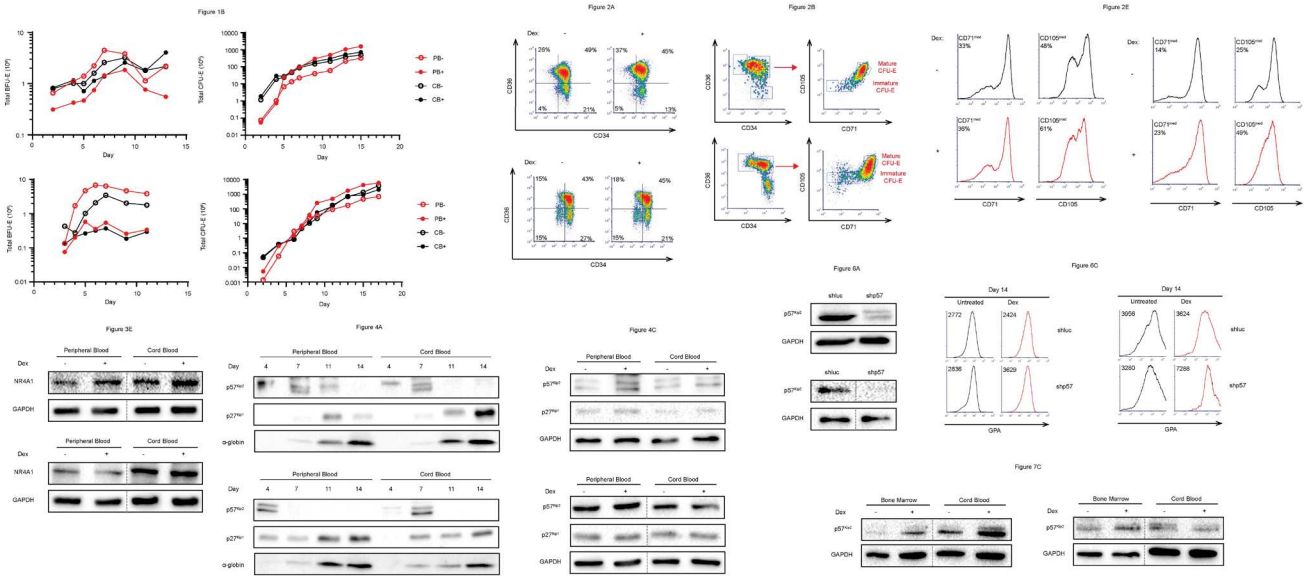

Supplemental Figure 7: Additional representative data related to the main figures.

Figure legends are identical to those in original main related figures.

Original article 2

Comprehensive phenotyping of erythropoiesis in human bone marrow: Evaluation of normal and ineffective erythropoiesis

Hongxia Yan1,2 | Abdullah Ali3 | Lionel Blanc4,5 | Anupama Narla6 | Joseph M. Lane7,8 | Erjing Gao1 | Julien Papoin4 | John Hale1 | Christopher D. Hillyer1 | Naomi Taylor2,9 | Patrick G. Gallagher10,11,12 | Azra Raza3 | Sandrina Kinet2 | Narla Mohandas1

1 New York Blood Center, New York, New York, USA. 2 Institut de Génétique Moléculaire de Montpellier, University of Montpellier, CNRS, Montpellier, France. 3 Myelodysplastic Syndromes Center, Columbia University, New York, New York, USA. 4 The Feinstein Institute for Medical Research, Manhasset, New York, USA. 5 Zucker School of Medicine at Hofstra/Northwell, Hempstead, New York, USA. 6 Stanford University School of Medicine, Stanford, California, USA. 7 Department of Orthopaedic Surgery, Hospital for Special Surgery, New York, New York, USA. 8 Department of Orthopaedic Surgery, New York-Presbyterian Hospital, Weill Cornell Medical Center, New York, New York, USA. 9 Pediatric Oncology Branch, NCI, CCR, NIH, Bethesda, Maryland, USA. 10 Department of Pediatrics, Yale University School of Medicine, New Haven, Connecticut, USA. 11 Department of Pathology, Yale University School of Medicine, New Haven, Connecticut, USA. 12 Department of Genetics, Yale University School of Medicine, New Haven, Connecticut, USA

Sandrina Kinet and Narla Mohandas are co-senior authors.

https://doi.org/10.1002/ajh.26247

Introduction of original article 2

The work reported in this article accomplished the characterization and evaluation of erythropoiesis in human bone marrow, with a focus on early erythropoiesis. Compared to the extensively studied terminal erythroid differentiation, early erythropoiesis is much less well understood. Although some progress has been made in immunophenotyping of erythroid progenitors, the heterogeneity of erythroid progenitors and the regulation of early erythropoiesis remains to be largely elucidated.

In last few years, erythroid progenitors have been identified using different surface markers. Dr. Narla's lab has defined $CD34^{+}CD36^{-}$ and $CD34^{-}CD36^{+}$ as burst forming unit-erythroid (BFU-E) and colony forming unit-erythroid (CFU-E), respectively. More recently, a transition population $CD34^{+}CD36^{+}$ between BFU-E and CFU-E was identified using *in vitro* model of PB derived $CD34^{+}$ cells. Of these defined populations, significant heterogeneity has been observed. Meanwhile, different surface markers have been used to define erythroid progenitors with BFU-E or CFU-E colony forming ability, suggesting that a comprehensive immunophenotyping on early erythropoiesis is needed to resolve the heterogeneity.

To delineate the heterogeneity, we firstly divided previously defined erythroid progenitor populations into more subsets using additional surface markers. Combining the colony forming ability of these subsets and the dynamic changes of surface expression of a specific set of surface markers, I redefined the heterogeneous continuum of erythroid progenitors into four sequentially maturing populations, EP1, EP2, EP3 and EP4.

On this basis, I developed an efficient and reproducible flow cytometry-based strategy for stage-wise detection of erythroid differentiation from BFU-E to reticulocytes. By simultaneous detection of nine consecutive developmental stages, including 4 progenitor stages and 5 stages of erythroblasts, this strategy enabled a visualized evaluation of the dynamic continuum of erythropoiesis.

To extend this strategy into the context of ineffective erythropoiesis in related disorders, I evaluated the erythroid differentiation in the bone marrow of patients with MDS. Surprisingly, I identified previously unrecognized defects at varied stages of erythroid progenitors. The findings suggested that, the previously reported apoptosis in late stage erythroblasts of MDS patients might not be the only cause of anemia in this disease. The disrupted differentiation of erythroid progenitors may also contribute to, at least partially, the ineffective erythropoiesis in MDS, which opens a new avenue for a better understanding of the mechanism of ineffective erythropoiesis in MDS.

Taken together, this work delineated the heterogeneity of erythroid progenitors by comprehensive immunophenotyping and developed a flow cytometry-based strategy for stage-wise evaluation of human erythropoiesis. This strategy enabled a precise characterization of specific stages of human erythropoiesis, which will facilitate our understanding of normal and disordered erythropoiesis.

Check for updates

Received: 17 May 2021 | Accepted: 18 May 2021

DOI: 10.1002/ajh.26247

RESEARCH ARTICLE

AJH WILEY

Comprehensive phenotyping of erythropoiesis in human bone marrow: Evaluation of normal and ineffective erythropoiesis

Hongxia Yan[1,2] | Abdullah Ali[3] | Lionel Blanc[4,5] | Anupama Narla[6] | Joseph M. Lane[7,8] | Erjing Gao[1] | Julien Papoin[4] | John Hale[1] | Christopher D. Hillyer[1] | Naomi Taylor[2,9] | Patrick G. Gallagher[10,11,12] | Azra Raza[3] | Sandrina Kinet[2] | Narla Mohandas[1]

[1]New York Blood Center, New York, New York, USA

[2]Institut de Génétique Moléculaire de Montpellier, University of Montpellier, CNRS, Montpellier, France

[3]Myelodysplastic Syndromes Center, Columbia University, New York, New York, USA

[4]The Feinstein Institute for Medical Research, Manhasset, New York, USA

[5]Zucker School of Medicine at Hofstra/Northwell, Hempstead, New York, USA

[6]Stanford University School of Medicine, Stanford, California, USA

[7]Department of Orthopaedic Surgery, Hospital for Special Surgery, New York, New York, USA

[8]Department of Orthopaedic Surgery, New York-Presbyterian Hospital, Weill Cornell Medical Center, New York, New York, USA

[9]Pediatric Oncology Branch, NCI, CCR, NIH, Bethesda, Maryland, USA

[10]Department of Pediatrics, Yale University School of Medicine, New Haven, Connecticut, USA

[11]Department of Pathology, Yale University School of Medicine, New Haven, Connecticut, USA

[12]Department of Genetics, Yale University School of Medicine, New Haven, Connecticut, USA

Correspondence
Narla Mohandas, New York Blood Center, 310 E67th street, New York, NY, USA.
Email: mnarla@nybc.org

Funding information
National Heart, Lung, and Blood Institute, Grant/Award Numbers: HL144436, HL152099; National Institute of Diabetes and Digestive and Kidney Diseases, Grant/Award Number: DK32094

Abstract

Identification of stage-specific erythroid cells is critical for studies of normal and disordered human erythropoiesis. While immunophenotypic strategies have previously been developed to identify cells at each stage of terminal erythroid differentiation, erythroid progenitors are currently defined very broadly. Refined strategies to identify and characterize BFU-E and CFU-E subsets are critically needed. To address this unmet need, a flow cytometry-based technique was developed that combines the established surface markers CD34 and CD36 with CD117, CD71, and CD105. This combination allowed for the separation of erythroid progenitor cells into four discrete populations along a continuum of progressive maturation, with increasing cell size and decreasing nuclear/cytoplasmic ratio, proliferative capacity and stem cell factor responsiveness. This strategy was validated in uncultured, primary erythroid cells isolated from bone marrow of healthy individuals. Functional colony assays of these progenitor populations revealed enrichment of BFU-E only in the earliest population, transitioning to cells yielding BFU-E and CFU-E, then CFU-E only. Utilizing CD34/CD105 and GPA/CD105 profiles, all four progenitor stages and all five stages of terminal erythroid differentiation could be identified. Applying this immunophenotyping strategy to primary bone marrow cells from patients with myelodysplastic syndrome,

Sandrina Kinet and Narla Mohandas are co-senior authors.

 © 2021 Wiley Periodicals LLC.

identified defects in erythroid progenitors and in terminal erythroid differentiation. This novel immunophenotyping technique will be a valuable tool for studies of normal and perturbed human erythropoiesis. It will allow for the discovery of stage-specific molecular and functional insights into normal erythropoiesis as well as for identification and characterization of stage-specific defects in inherited and acquired disorders of erythropoiesis.

1 | INTRODUCTION

The human bone marrow generates ~2.5 million red cells every second at steady state through a process defined as erythropoiesis.[1] In contrast to the myeloid and lymphoid lineages where high throughput immunophenotyping has allowed for the characterization of distinct development stages,[2–4] it is still not possible to comprehensively phenotype all distinct stages of erythropoiesis. This is an area of particular relevance in cases of ineffective erythropoiesis where disturbances in the normal progression of erythroid differentiation contribute to anemia (e.g., thalassemia, Diamond-Blackfan anemia and myelodysplastic syndromes [MDS]).

Since the development of single parameter flow cytometry analysis in the 1980s,[5,6] there has been progress in defining cell surface markers that allow for the identification of human erythroid progenitors and terminally differentiating erythroblasts.[7–16] Using Glycophorin A (GPA), α4-integrin and Band 3 as surface markers, we were previously able to resolve and quantify five distinct stages of terminally differentiating erythroblasts.[12] Furthermore, four different surface markers have been used to identify BFU-E as IL3R$^-$GPA$^-$CD34$^+$CD36$^-$ and CFU-E as IL3R$^-$GPA$^-$CD34$^-$CD36$^+$.[14] In addition, a transient population of IL3R$^-$GPA$^-$CD34$^+$CD36$^+$ progenitor cells were identified in an in vitro model of adult erythropoiesis.[17] However, these latter markers do not allow homogeneous subsets to be distinguished[18]; BFU-E and CFU-E progenitor populations that are defined in this manner are functionally heterogeneous, as reflected in their generation of colonies of markedly different sizes (our unpublished data).

Here, we aimed to resolve the heterogeneity of these early stages of erythropoiesis. By combining established surface markers (CD34 and CD36) with CD117 (c-kit), CD71 and CD105, we were able to isolate four distinct erythroid progenitor populations and resolve the continuum of early erythropoiesis. Furthermore, our studies reveal that the expression kinetics of CD105 allow the previously identified five stages of terminal erythroid differentiation to be distinguished.

Based on our previous and current data, we were able to use a 10-color flow cytometry panel to quantitate nine distinct erythroid stages in normal human bone marrow. To evaluate the relevance of these findings in diseases with disordered erythropoiesis, we tested this novel flow cytometry panel in a small cohort of patients with myelodysplastic syndromes (MDS). We observed that ineffective erythropoiesis in MDS patients is associated with stage-specific erythroid defects. Thus, our novel and comprehensive strategy for the phenotyping of human bone marrow erythropoiesis reveals novel aspects of the continuum in normal and disordered human erythropoiesis.

2 | MATERIALS AND METHODS

2.1 | Sources of CD34$^+$ cells and primary human bone marrow samples

Leukopaks were obtained from the New York Blood Center. Bone marrow tissues from hip surgeries were collected through the Tissue Donation Program at Northwell Heath and bone marrow aspirates from the Hospital for Special Surgery and the MDS Center at Columbia University. All studies were conducted in accordance with the declaration of Helsinki and under institutional review board (IRB) approval of the New York Blood Center, Northwell Health, the Hospital for Special Surgery and the MDS Center at Columbia University.

2.2 | Statistical analyses

Statistical evaluations between different experimental groups were performed using GraphPad Prism 9 (unpaired two-tailed Student's *t*-test) and $p < 0.05$ was considered to indicate statistical significance.

2.3 | Other methods

Additional methods are presented as supplemental materials.

3 | RESULTS

3.1 | Human erythroid progenitor populations can be divided into distinct subsets

We previously showed that erythroid progenitors capable of forming BFU-E and CFU-E in methylcellulose assays could be isolated based on their CD34/CD36 expression profiles.[14] However, the resulting

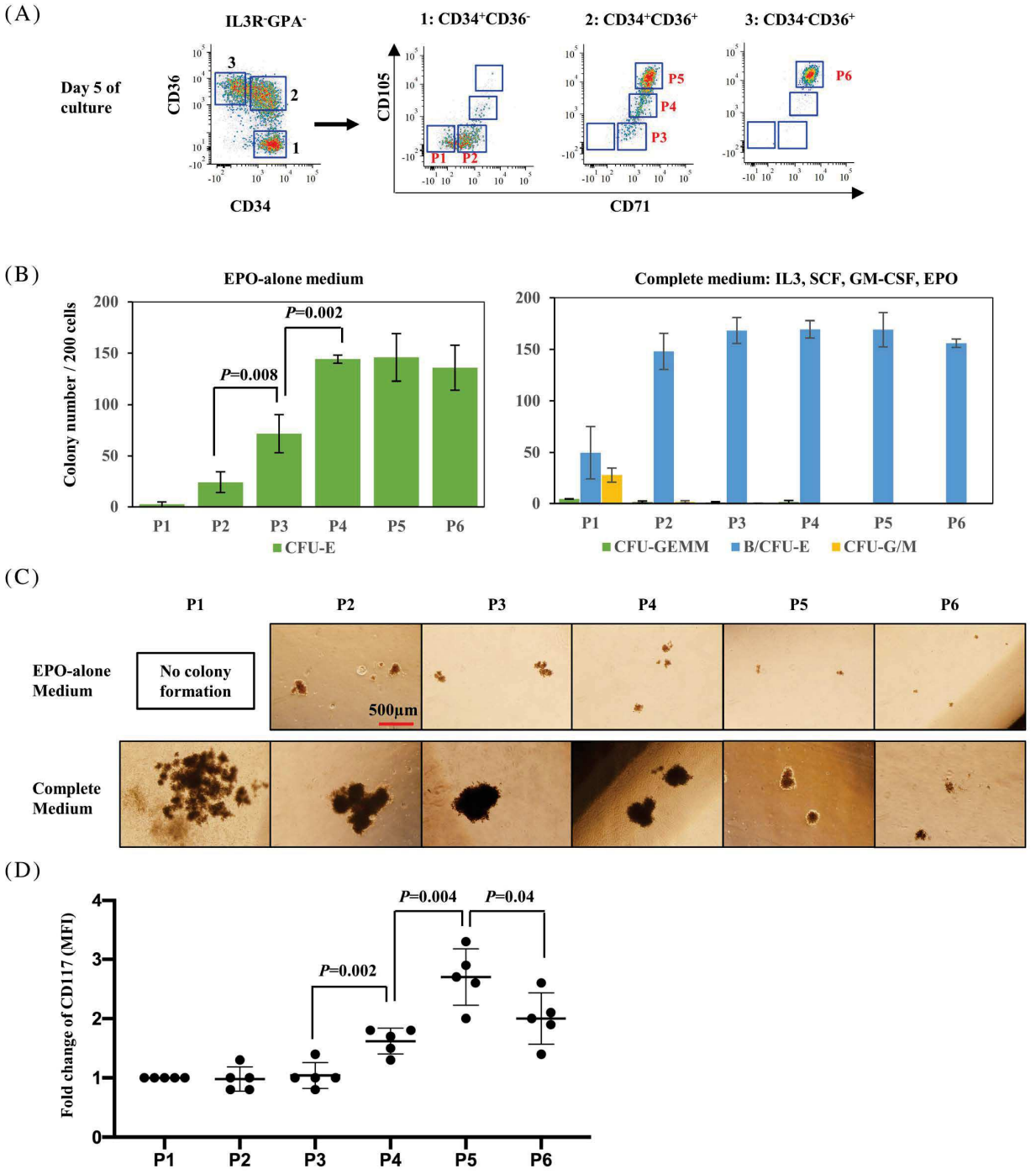

FIGURE 1 Human erythroid progenitor populations can be divided into distinct subsets. (A) Representative FACS plots illustrating expression of CD71 and CD105 in previously defined erythroid progenitor populations $CD34^{+}CD36^{-}$, $CD34^{+}CD36^{+}$ and $CD34^{-}CD36^{+}$. Based on their expression, six subsets including P1, P2, P3, P4, P5 and P6, were gated and sorted for colony forming assay. (B) Number of colonies generated from 200 FACS-sorted cells of P1-P6, separately, in EPO-alone medium (left panel) and complete medium (right panel). Error bars indicate standard deviation (SD) of the mean ($n = 4$). (C) Representative images of colonies generated by P1 to P6 cells, in EPO-alone and complete medium. The photos were taken under an inverted microscope at ×4 magnification, scale bar = 500 μm. (D) CD117 expression on surface of P1 to P6 cells. Error bars indicate standard deviation (SD) of the mean ($n = 5$)

colonies were heterogeneous in size, indicating that these BFU-E and CFU-E populations were likely mixed populations of erythroid progenitor cells. In addition, we recently demonstrated that two populations of CFU-E, immature and mature CFU-E, could be identified in adult-derived erythroid progenitors using a phenotype of $CD71^{hi}CD105^{med}$ and $CD71^{hi}CD105^{hi}$, respectively.[19] Thus, the potential of these two markers to resolve heterogeneity was further investigated in erythroid progenitor cell populations. Flow cytometric analyses of the $CD34^+CD36^-$, $CD34^+CD36^+$, and $CD34^-CD36^+$ erythroid progenitor populations ($IL3R^-GPA^-$) derived from EPO-differentiated adult $CD34^+$ cells revealed six distinct sub-populations based on CD71/CD105 expression profiles (Figure 1(A)). Specifically, $CD34^+CD36^-$ cells could be divided into P1 ($CD71^-CD105^-$) and P2 ($CD71^+CD105^-$) subpopulations while $CD34^+CD36^+$ cells were divided into three subpopulations P3 ($CD71^+CD105^-$), P4 ($CD71^+CD105^{low}$) and P5 ($CD71^+CD105^{high}$). The vast majority of $CD34^-CD36^+$ cells were phenotyped as P6 ($CD71^+CD105^{high}$).

These six cell populations were sorted and their ability to form colonies in the presence of EPO-alone or in complete medium with SCF, IL3, GM-CSF and EPO was evaluated[20] (Figure 1(B), (C)).

The EPO-alone media, a condition that only supports CFU-E colony formation,[21,22] did not result in the formation of colonies from the P1 population and only a small number of colonies (24 ± 10 per 200 plated cells) from the P2 population. The P3 population generated more colonies than P2 but colony-forming efficiency remained low (72 ± 18 per 200 plated cells). In contrast, the P4 population formed well-hemoglobinized colonies with a significantly higher colony-forming efficiency (144 ± 4 per 200 plated cells; $p = 0.002$). Both P5 and P6 populations generated typical CFU-E-like colonies (Figure 1(B) left panel and 1(C) upper panel).

In complete medium supplemented with SCF, IL3, GM-CSF and EPO, the P1 population generated both erythroid and myeloid colonies, but had a low colony-forming efficiency (4.3 ± 0.2 CFU-GEMM, 50 ± 25 BFU-E and 28 ± 7 CFU-G/M per 200 plated cells). In contrast, the P2 population exhibited a much higher colony-forming efficiency with a predominance of typical multiple-cluster BFU-Es (148 ± 18 B/CFU-E per 200 plated cells). With regards to the transition population, the P3 population showed a similar colony-forming ability as the P2 population. And in accordance with our published findings,[19] the P4 population of cells gave rise to a comparable number of erythroid colonies in both EPO-alone and complete media but the colony size was much larger in complete media, implying that this subset is sensitive to SCF-induced proliferation (Figure 1(B) right panel and 1(C) bottom panel). As opposed to the P4 population, the sensitivity of the P5 and P6 populations to SCF was decreased, as reflected by a lower augmentation in colony size in complete media. Together, these data demonstrate that the sequential maturation of erythroid progenitors is accompanied by decreased sensitivity to SCF.

Note, SCF is a critical growth factor for erythroid and myeloid progenitors. To better define the differential sensitivity of the six identified erythroid progenitor populations to SCF, the expression levels of CD117/c-Kit, the receptor for SCF ligand, was examined (Figure 1(D)). All six sub-populations expressed CD117 with lower levels of expression on the P2 and P3 populations. Expression levels increased starting with the P4 population, peaking with the P5 population and subsequently decreasing in the P6 population.

Together, these data indicate that the erythroid progenitor continuum can be immunophenotyped as $CD117^+CD71^+IL3R^-GPA^-CD34^{+/-}$ with CD105 expression levels distinguishing the transition from BFU-E to CFU-E.

3.2 | Validation of the continuum of erythroid progenitors

Following the phenotyping of human erythroid progenitors, we attempted to identify and quantitate the different stages of erythropoiesis. Adult-derived $CD34^+$ cells were differentiated for 5 days in the presence of rEPO and $CD117^+GPA^-$ cells were evaluated (gating out granulocyte-monocyte progenitors (GMPs) and megakaryocyte-committed progenitors (MkPs) as a function of CD45RA and CD41a expression, respectively). Based on the expression levels of CD34 and CD105, the erythroid progenitor compartment ($IL3R^-CD71^+$) could be sub-divided into four distinct populations. We specifically defined $CD34^+CD105^-$ as EP1 (erythroid progenitor 1), $CD34^+CD105^{low}$ as EP2, $CD34^{+/low}CD105^{high}$ as EP3 and $CD34^-CD105^{high}$ as EP4 (Figure 2(A)).

The morphology of the four sorted erythroid progenitor populations is shown in Figure 2(B). The EP1 cell population was consistently smaller than the other three cell populations and showed the highest nuclear/cytoplasmic ratio. An increase in cell size and a decrease in nuclear/cytoplasmic ratio was noted, consistent with the progressive maturation of the progenitor population from EP1 to EP4.

Functional assays on these isolated cell subsets revealed that EP1 is composed predominantly of BFU-E while EP2, EP3 and EP4 represent increasingly mature CFU-E populations with reduced proliferative responsiveness to SCF (Figure 2(C)–(E)). These four populations correspond to populations P2 to P6, defined on the basis of CD71/CD105 expression profiles (Figure 1).

To validate our hypothesis that these subsets reflected a continuum of erythroid progenitors, the isolated EPs were cultured to undergo further erythroid differentiation and their differentiation potential monitored (Figure 2(F)). Following 2 days of differentiation, flow cytometry analysis showed progressive acquisition of GPA expression ranging from 16% for EP1 to 78% for EP4. More importantly, during 2 days of culture, EPs progressed along the proposed continuum from EP1 to EP4. Specifically, EP1 progressed into EP2/EP3/EP4, EP2 progressed to EP3/EP4, and EP3 shifted to EP4 (Figure 2(F)). Finally, we observed that the EP1 population had the highest proliferative capacity with a progressive decrease in the proliferative capacities of EP2, EP3 and EP4 populations, respectively (Figure 2(G)). Together, these data support the hierarchical progression of erythroid progenitors from an EP1 to EP4 state.

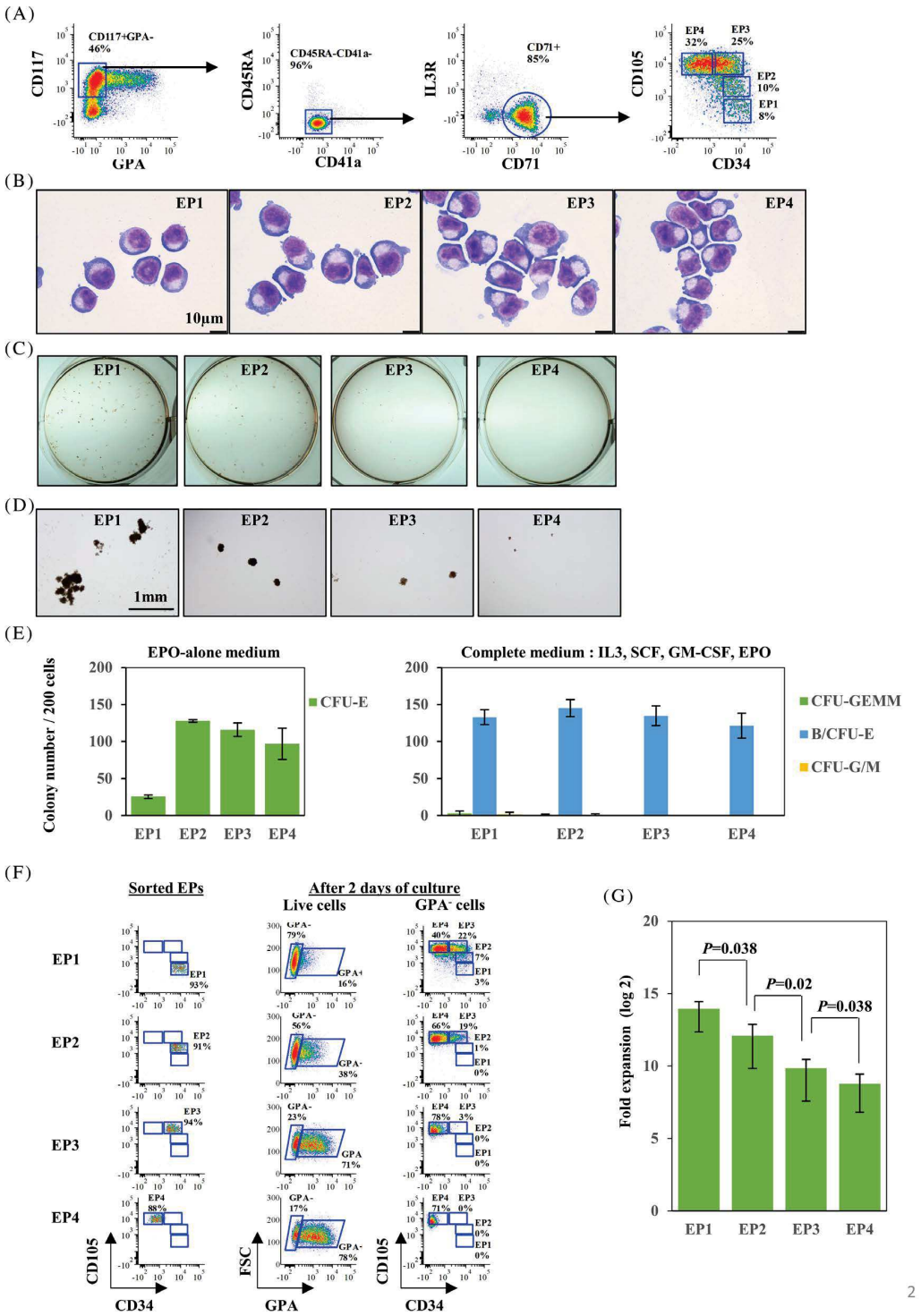

FIGURE 2 Legend on next page.

3.3 | CD34/CD105 expression profiles distinguish the *in vivo* continuum of erythroid progenitors

Based on the *in vitro* analyses presented above, it was of interest to determine whether this profiling strategy could be extended to primary, uncultured human bone marrow samples containing erythroid cells at all stages of erythropoiesis.

Representative flow cytometry plots of positively selected CD117+ cells from bone marrow mononuclear cells are shown in Figure 3(A). Following the same strategy used to identify EP1 to EP4 populations, $CD117^{+}GPA^{-}CD45RA^{-}CD41a^{-}$ cells were subsequently sub-divided into two populations, $IL3R^{-}CD71^{+}$ (erythroid lineage) and $IL3R^{+}CD71^{-}$ (non-erythroid lineage) subsets. EP1 to EP4 subsets were further gated from the $IL3R^{-}CD71^{+}$ compartment based on their CD34 and CD105 profiles (Figure 3(A)). To exclude any admixture of cells from other lineages with erythroid progenitors, a lineage cocktail was used to document that all four EP populations were Lin^{-} (Figure S1(A)).

To examine the morphology and functionality of these four populations, EP1 to EP4 were FACS sorted. $IL3R^{+}CD71^{-}$ cells were also sorted as a control for more primitive progenitors. Although erythroid progenitors in the bone marrow are not morphologically recognizable amongst the highly heterogeneous bone marrow cells, we observed morphological differences between the four groups of sorted erythroid progenitors in terms of cell size and nuclear/cytoplasmic ratio (Figure 3(B)). Consistent with our data from *in vitro* differentiated $CD34^{+}$ cells, EP1 cells were the smallest cells and had the highest nuclear/cytoplasmic ratio, similar to the more primitive $IL3R^{+}CD71^{-}$ cells. Sequential differentiation from EP1 to EP4 was accompanied by an increase in cell size and a decrease in the nuclear/cytoplasmic ratio. Furthermore, the forward scatter profiles of these cell populations are consistent with noted differences in cell size (-Figure S1(B)).

Functional assays on these isolated cells revealed that EP1 is enriched in BFU-Es (100±14 BFU-E per 200 plated cells) in complete medium (Figure 3(D)), but with fewer well-hemoglobinized CFU-E colonies in conditions of EPO alone (22±13 CFU-E per 200 plated cells) (Figure 3(E) left panel). As expected, $IL3R^{+}CD71^{-}$ cells failed to generate CFU-E colonies in EPO-alone medium but gave rise to more CFU-G and CFU-M as compared to BFU-E in complete medium (28±7 CFU-G/M, 10±5 BFU-E per 200 plated cells). In contrast, while EP2 cells generated a comparable number of erythroid colonies in both types of media (Figure 3(E)), colonies were much larger in complete media than in EPO-alone media (Figure 3(C),(D)). In contrast, for EP3 and EP4, a similar number of colonies were noted in the two types of media.

Together, these data validate our *in vitro* findings and confirm the existence of four specific and successive stages of erythroid progenitors *in vivo* in human bone marrow. They also identify the critical role of CD105 in distinguishing stages of human erythropoiesis. We find that BFU-E EP1, immature CFU-E EP2, and sequentially mature CFU-Es EP3 and EP4 constitute the continuum of early human erythropoiesis, thereby providing new insights into erythroid progenitor biology.

3.4 | Decreases in CD105 expression levels distinguish terminally differentiating erythroblasts in human bone marrow

Since CD105 (Endoglin, a member of TGF-β receptor family) is expressed in proerythoblast and basophilic erythroblasts[23,24] (Figure 4 (A)), we explored its potential to distinguish distinct stages of terminally differentiating erythroblasts. We found that the expression of CD105 decreased markedly starting with late basophilic erythroblasts; lower levels of expression were detected in polychromatic erythroblasts and little or no expression detected in orthochromatic erythroblasts (Figure 4(A)).

Representative CD105 and GPA flow cytometry profiles on positively selected $CD71^{+}$ cells from bone marrow mononuclear cells are shown in Figure 4(B). We were able to identify five distinct clusters of cells: $GPA^{low}CD105^{high}$ as proerythroblasts, $GPA^{high}CD105^{high}$ as early basophilic erythroblasts, $GPA^{high}CD105^{int}$ as late basophilic erythroblasts, $GPA^{high}CD105^{low}$ as polychromatic erythroblasts and $GPA^{high}CD105^{-}$ as orthochromatic erythroblasts. As we have previously shown that the surface expression of α4-integrin and band 3 can be used to distinguish these five distinct stages, we analyzed the overlap of these flow patterns using both strategies (Figure 4(B), (C)). Morphological Giemsa staining analyses confirmed the purity of the five populations obtained (Figure 4(D)). Notably, CD105/GPA profiles allowed for a better discrimination than α4-integrin/Band 3 profiles, especially at late stages of the terminal erythroid differentiation.

FIGURE 2 Validation of the continuum of erythroid progenitors. (A) Representative FACS plots for definition of erythroid progenitors from *in vitro* culture of human $CD34^{+}$ cells, on Day 5 of differentiation. (B) Representative cytospin images of sorted EP1, EP2, EP3 and EP4 cells from *in vitro* culture of human $CD34^{+}$ cells. The cells were sorted on Day 5 of differentiation. The images were captured under Leica DM2000 microscope at ×100 magnification, scale bar = 10 μm. (C) Representative images of colonies generated by sorted EP1, EP2, EP3 and EP4 cells from *in vitro* culture of human $CD34^{+}$ cells, in complete medium. The photos were taken using a Nikon D3500 camera. (D) Representative images of colonies generated by sorted EP1, EP2, EP3 and EP4 cells from *in vitro* culture of human $CD34^{+}$ cells, in complete medium. The photos were taken under an inverted microscope at ×4 magnification, scale bar = 1 mm. (E) Quantitative analysis of colony forming ability of sorted EP1, EP2, EP3 and EP4 cells from *in vitro* culture of human $CD34^{+}$ cells. The data are from three independent experiments. (F) Representative FACS plots for sorting purity of EP1, EP2, EP3 and EP4 (left panel) and their differentiation progress after 2 days of culture (right panel). (G) Number of cell divisions of EP1 to EP4 by the end of differentiation. The numbers were calculated based on final erythroid yield of EP1 to EP4 under same culture conditions. The data are from three independent experiments

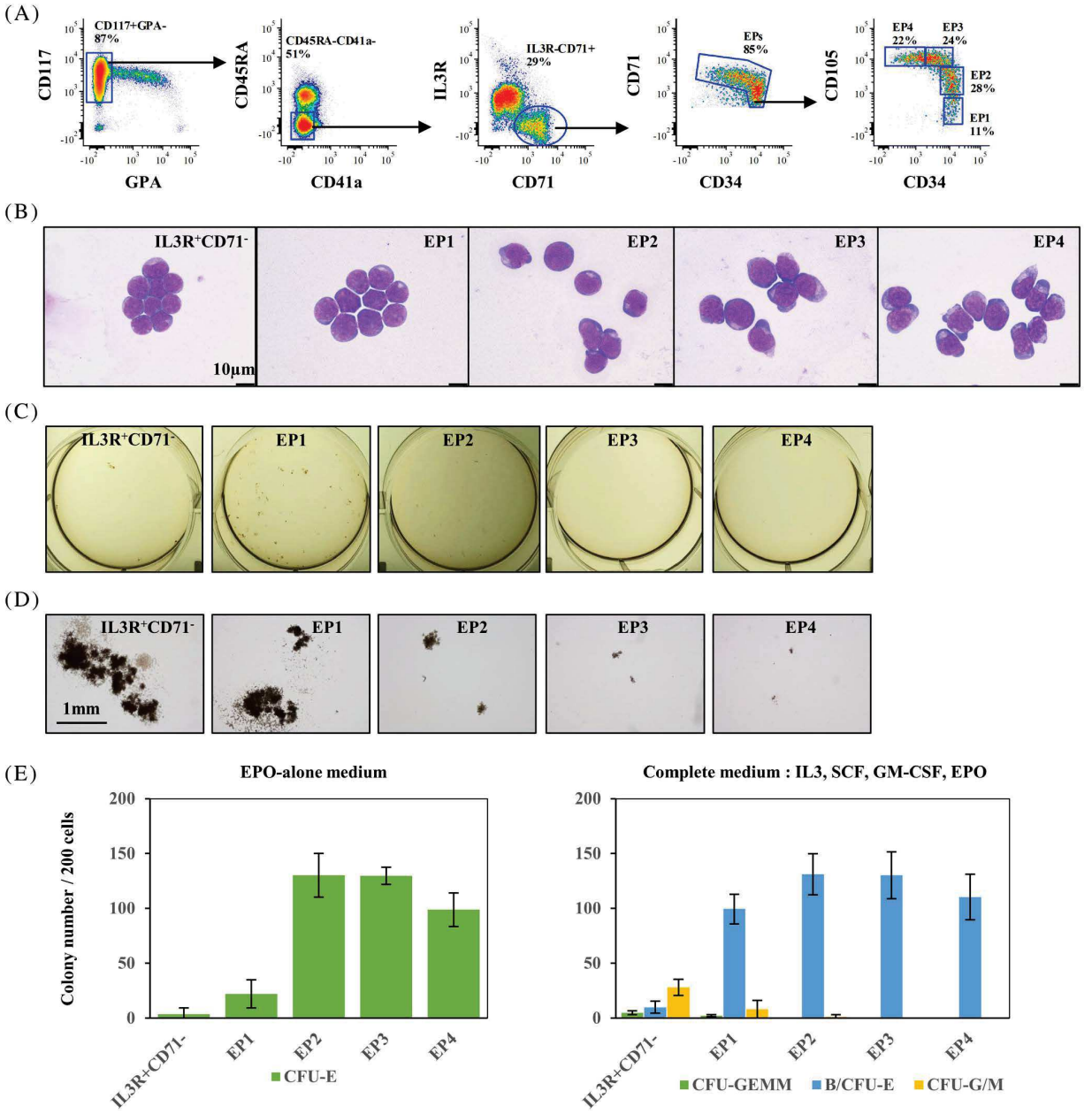

FIGURE 3 CD34/CD105 expression profiles distinguish the *in vivo* continuum of erythroid progenitors. (A) Representative FACS plots illustrating strategy for definition of erythroid progenitors using enriched CD117^{+} cells from primary bone marrow. The gates of EP1 to EP4 were made based on expression of CD34 and CD105. (B) Representative cytospin images of sorted IL3R^{+}CD71^{-}, EP1, EP2, EP3 and EP4 cells from primary bone marrow. The images were captured under Leica DM2000 microscope at ×100 magnification, scale bar = 10 μm. (C) Representative images of colonies generated by sorted IL3R^{+}CD71^{-}, EP1, EP2, EP3 and EP4 cells, in complete medium. The photos were taken using a Nikon D3500 camera. (D) Representative images of colonies generated by sorted IL3R^{+}CD71^{-}, EP1, EP2, EP3 and EP4 cells, in complete medium. The photos were taken under an inverted microscope at ×4 magnification, scale bar = 1 mm. (E) Quantitative analysis of colony forming ability of sorted IL3R^{+}CD71^{-}, EP1, EP2, EP3 and EP4 cells from six independent experiments

We then applied this strategy to evaluation of *in vitro* differentiated adult-derived CD34^{+} cells. Proerythroblasts and early basophilic erythroblasts were sorted on Day 7 and late basophilic, poly- and orthochromatic erythroblasts were sorted on Day 14 of differentiation (Figure S2(A)). All five stages of erythroblasts were successfully isolated based on their CD105/GPA profiles and the morphologies of the sorted cells confirmed the five distinct populations (Figure S2(B)). Interestingly, similar to our cultured erythroid progenitors, more intracellular vesicles were noted in *in vitro* differentiated proerythroblasts and basophilic erythroblasts,

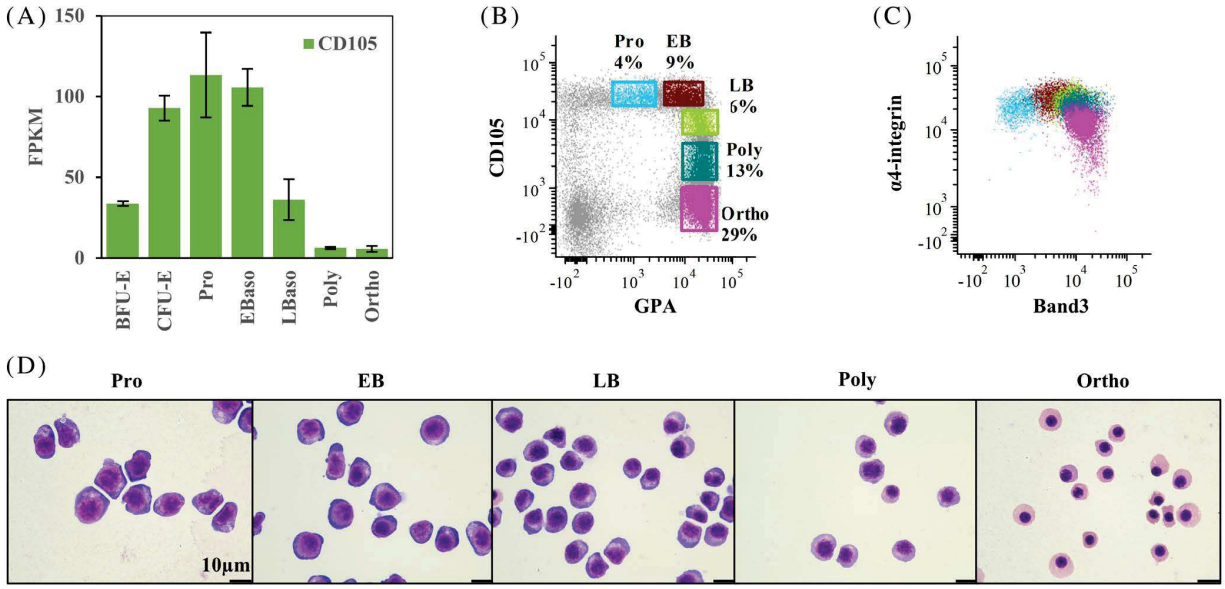

FIGURE 4 Decreases in CD105 expression levels distinguish terminally differentiating erythroblasts in human bone marrow. (A) Relative mRNA expression of CD105 at distinct stages of erythroid differentiation. The data are from RNA-seq on three biological replicates12,14. (B) Representative FACS plots for definition of erythroblasts at distinct stages. The gates were made based on expression of CD105 and GPA. (C) Dot plot overlay of gated erythroblast populations showing their expression of α4-integrin and Band3. (B) The color of each population sources from the gating plot. (D) Representative cytospin images of sorted erythroblasts at distinct stages from primary bone marrow. The images were captured under Leica DM2000 microscope at ×100 magnification, scale bar = 10 μm

compared to their bone marrow counterparts (Figure 4(D) and Figure S2(B)).

Thus, staining for CD105 in combination with GPA can be used as to resolve all five previously described stages of terminal erythropoiesis.

3.5 | An integrated FACS strategy enables stage-wise detection of human adult erythropoiesis

Having established that cell surface CD105 levels can be used in conjunction with other surface markers to resolve the continuum of erythropoiesis up to reticulocytes, we developed an optimal 10-color flow cytometry strategy using the cell surface markers CD34, CD117, IL3R, CD45RA, CD41a, CD71, CD105, GPA and nucleic acid dye syto16 as well as the cell viability dye 7AAD for a comprehensive analytical strategy to distinguish the nine distinct stages of erythropoiesis in human bone marrow.

For quantitation of erythroid progenitors, GPA^- cells were analyzed for expression of CD117 and CD34 and $CD117^+$ cells were gated. Based on expression levels of CD45RA and CD41a, the $CD45RA^-$ $CD41a^-$ cells were gated and expression levels of IL3R and CD71 monitored. Following gating of $CD71^+$ cells, the expression levels of CD34 and CD105 were analyzed and four distinct populations of erythroid progenitors, EP1 to EP4 could be quantitated (Figure 5(A)).

To quantitate terminally differentiated erythroblasts, GPA^+ cells with high levels of expression of CD71 were analyzed (Figure 5(A)). The $CD71^+GPA^+$ cells consisted of nucleated erythroblasts ($syto16^+$) and reticulocytes ($syto16^-$). Based on the expression levels of CD105 and GPA, the $syto16^+$ erythroblast population could be further divided into five distinct clusters: proerythroblasts, early and late basophilic erythroblasts, polychromatic erythroblasts and orthochromatic erythroblasts (Figure 5(A)).

By overlaying these two profiles, nine distinct populations could be easily distinguished, reflecting the continuum of stages of erythropoiesis in human bone marrow (Figure 5(B)). To further validate this continuum, FACS-purified EPs were cultured and their differentiation was monitored every 2 days by quantitating the expression of CD105 and GPA. As shown in Figure 5(C), EP1, EP2, EP3 and EP4 differentiated along the CD105/GPA axis as anticipated; EP1 and EP4 subsets required 12 and 8 days respectively to mature into orthochromatic erythroblasts.

We then examined surface expression of erythroid-associated proteins throughout erythropoiesis. As shown in Figure 5(D), the expression of CD117 increased during early erythropoiesis and reached a peak at the EP3 stage before decreasing gradually from the EP4 and proerythroblast stage with a subsequent marked reduction at later stages of differentiation. The well-defined erythroid markers, CD71 and CD36 were expressed to varying degrees at all stages of erythroid differentiation. As erythroid progenitors have been identified in the $CD34^+CD38^+$ compartment,[25] and low-level expression of CD45 was previously reported in BFU-E and CFU-E populations,[14]

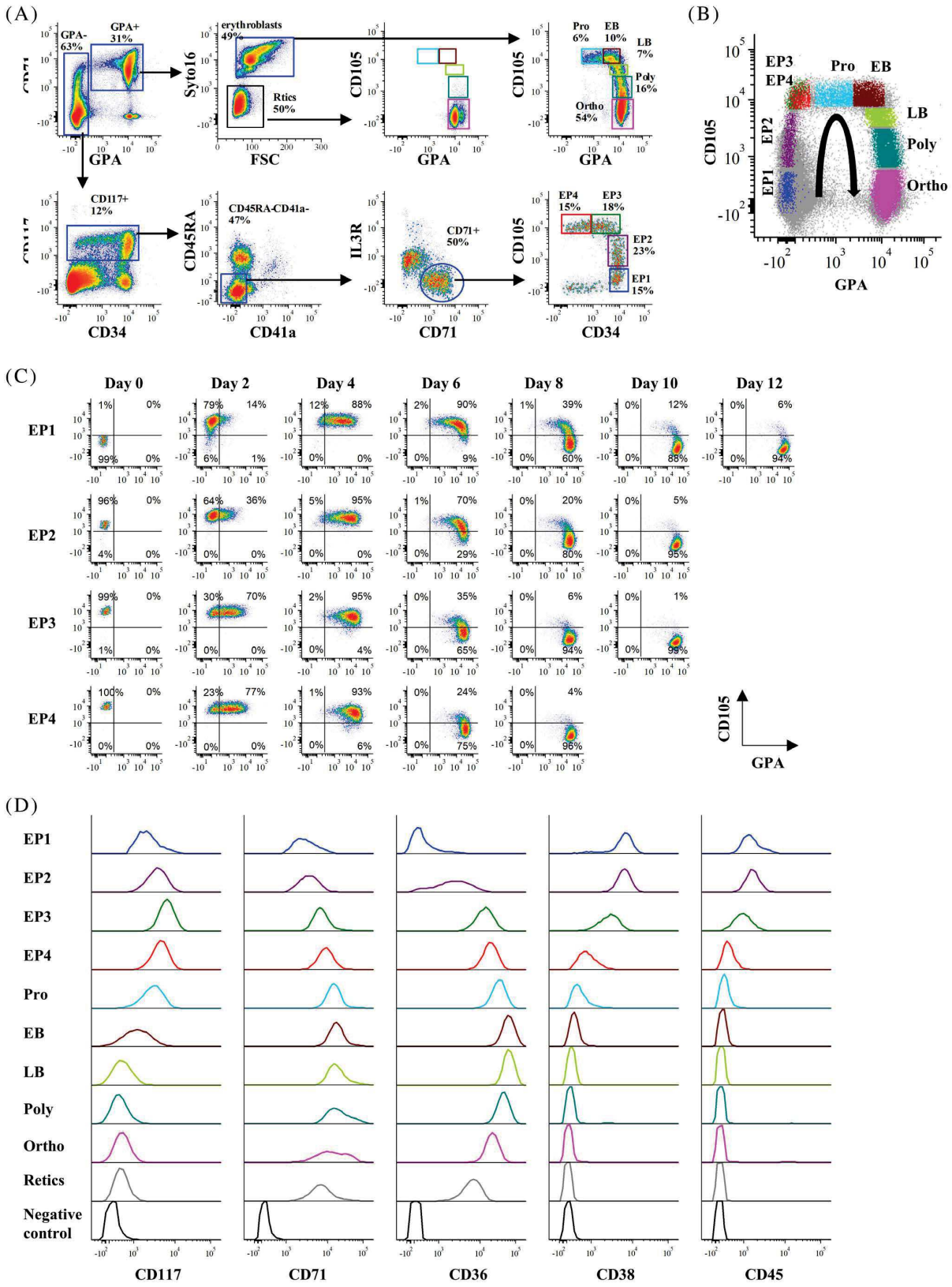

FIGURE 5 Legend on next page.

TABLE 1 The clinical features and mutational analyses of MDS patients

Patient No.	Age	Gender	Diagnosis	Transfusion	Somatic mutations in genes	Aspirate ME ratio	Hg (g/dl)	Hematocrit (%)	Risk group
1	68	M	MDS-RS-MLD	None	*SF3B1*; *SRSF2*	4:1	9.7	30.3	Intermediate
2	72	M	MDS-RS-MLD	Transfusion dependent	*SF3B1*; *DNMT3A*; *TET2*; *NF1*	3:1	8.9	25.6	High
3	80	M	MDS/MPN-Unclassifiable or CMML-2	None	*SRSF2*; *STAG2*; *JAK2*; *IDH2*; *RUNX1*	7:1	8.7	28.8	Intermediate
4	67	M	MDS-EB1	None	*U2AF1*; *BCOR*; *STAG2*; *NRAS*	1:1	7.5	24.5	Intermediate
5	62	F	MDS-EB1	None	*SF3B1*	2:1	8	24.5	High

we measured their expression levels during the entire course of erythroid development and differentiation. Both CD38 and CD45 were expressed at comparable levels in the EP1 and EP2 populations with decreased levels at the EP3 stage and little or no expression at EP4 stage. Neither of these proteins was expressed in terminally differentiated erythroblasts.

Taken together, the novel flow cytometry-based strategy we have developed enables a comprehensive characterization and quantitation of nine distinct stages of steady-state human adult erythropoiesis. This approach provides a simple, intuitive and comprehensive means to study the dynamic process of normal human erythropoiesis.

3.6 | The impaired terminal erythroid differentiation in MDS is associated with defective erythroid progenitor differentiation

Ineffective erythropoiesis leading to the sub-optimal production of red cells leads to anemia, a major clinical feature of numerous human red cell disorders including thalassemia and MDS.[26,27] The decreased production of red cells could result from a block at any of the multiple stages of erythropoiesis, Currently, there is no standardized strategy to address this important issue. We therefore explored whether our novel phenotyping strategy could provide new insights into ineffective erythropoiesis.

We assessed erythropoiesis in the bone marrow of five patients with MDS using the newly developed strategy. The clinical features and mutational analyses for these five patients are shown in Table 1. As shown in Figure 6(A), two subjects, MDS-1 and MDS-2 showed comparable terminal erythroid differentiation to that detected in healthy controls. Correspondingly, erythroid progenitor differentiation with reasonable numbers of progenitors at each stage of development were found. In the third subject, MDS-3, there were decreased numbers of mature CFU-E (EP3 and EP4) without a significant effect on terminal differentiation. Significantly impaired terminal erythroid differentiation was detected in subjects MDS-4 and MDS-5, in association with marked decreases in erythroid progenitor populations (Figure 6(A)).

Quantification of the different subsets of erythroid cells revealed that while the number of erythroblasts increased during successive development stages in healthy controls, decreases in erythroid progenitors resulted in a marked diminution of terminally differentiated erythroblasts (Figure 6(B)). These findings imply that defects in erythroid progenitor differentiation accounts, at least in part, for the impaired terminal erythroid differentiation in MDS. Our findings on a small cohort of MDS subjects begins to provide new insights into our understanding of the underlying mechanisms of ineffective erythropoiesis in MDS and highlights the potential usefulness of this newly established strategy to comprehensively study ineffective erythropoiesis in various human disorders.

4 | DISCUSSION

Erythropoiesis is a complex and tightly regulated process encompassing multiple steps from the hematopoietic stem cell to committed erythroid progenitor cells (BFU-E and CFU-E) and ultimately to mature erythrocytes. This process involves ~15 cell divisions and requires a coordinated cell division that is dependent on growth factors, specific niches and physiologic needs. A comprehensive assessment of this process is dependent on the identification of a

FIGURE 5 An integrated FACS strategy enables stage-wise detection of human adult erythropoiesis. (A) Representative FACS plots illustrating an integrated gating strategy for human erythroid continuum from BFU-E to reticulocytes from primary human bone marrow. (B) Dot plot overlay of gated erythroid progenitor and erythroblast populations showing their expression of CD105 and GPA. The color of each population sources from the gating plots in (A) and the curved arrow indicates the erythroid differentiation trajectory. (C) Representative FACS plots showing sequential maturation of sorted EP1, EP2, EP3 and EP4 in culture along the indicated trajectory in (B). (D) Representative histograms of erythroid-associated genes expression (CD117, CD71, CD36, CD38 and CD45) in primary human bone marrow cells at distinct erythroid differentiation stages

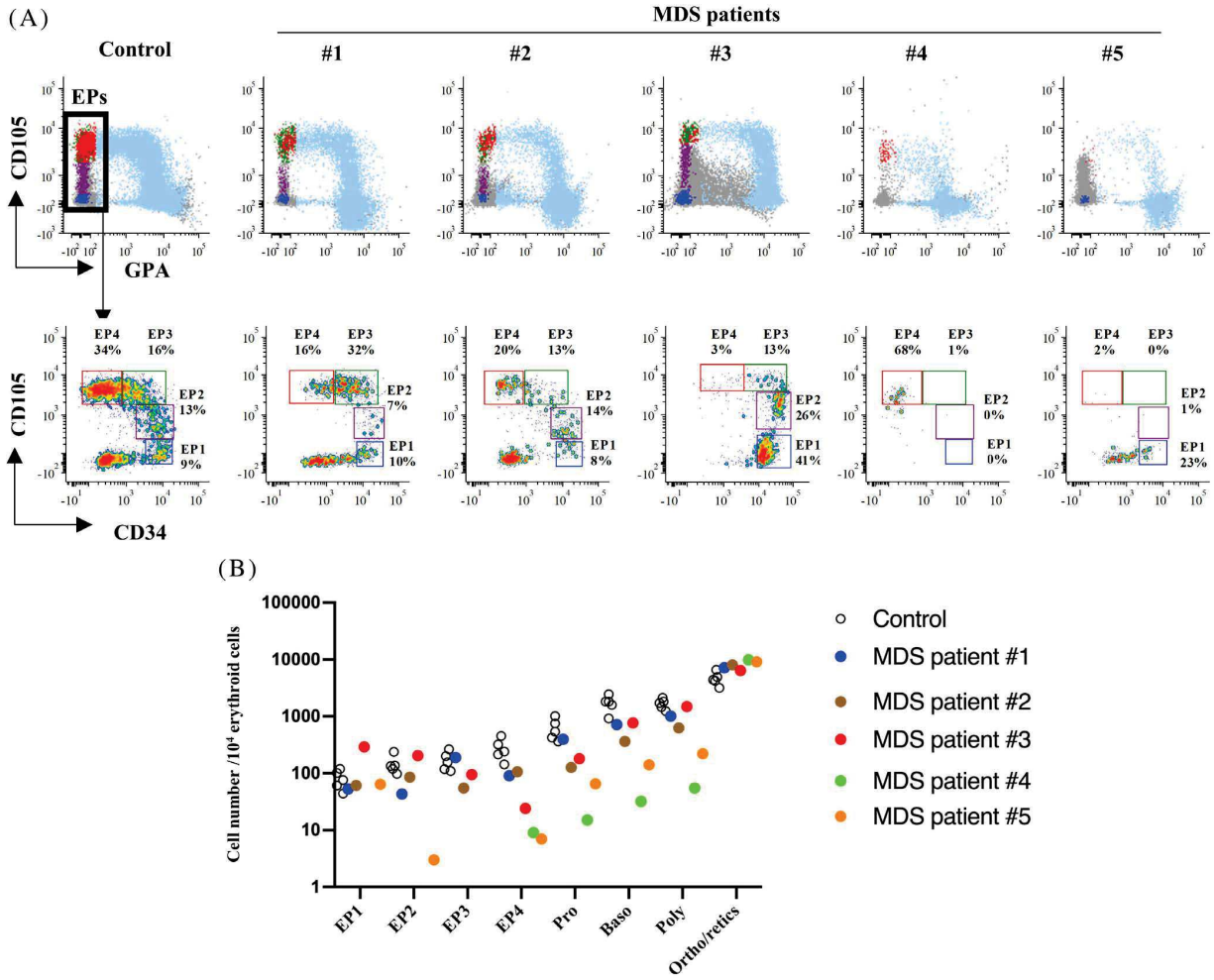

FIGURE 6 The impaired terminal erythroid differentiation in MDS is associated with defective erythroid progenitor differentiation. (A) The FACS plots showing erythroid continuum in MDS. The upper panel shows CD105/GPA overlay of erythroid populations, and the lower panel shows further analysis on erythroid progenitor differentiation. The light blue dots represent $CD71^{+}GPA^{+}$ cells. (B) Quantification of erythroid progenitors and erythroblasts showing decreased EPs in MDS patients with impaired terminal erythroid differentiation. The y-axis indicates the cell number of each population in 10^4 erythroid cells. The black circles are healthy controls and the colored dots represent the different MDS samples. Each color corresponds to a specific MDS sample

maximal number of distinct stages, which is a critical prerequisite for the development of a detailed understanding of the underlying regulatory mechanism(s). In contrast to the significant progress made in the phenotypic characterization of myeloid and lymphoid lineages, much less progress has been made in the phenotyping of distinct stages of erythropoiesis. To address this unmet need, we developed an immunophenotyping strategy to monitor human erythropoiesis using a specific set of cell surface markers.

In a previous study, we immunophenotyped $IL3R^{-}CD34^{+}CD36^{-}GPA^{-}$ as BFU-E, $IL3R^{-}CD34^{-}CD36^{+}GPA^{-}$ as CFU-E, and $CD34^{+}CD36^{+}$ progenitors as a mixture containing BFU-E and CFU-E.[14,17] However, while it appeared that these populations represented distinct stages of erythroid progenitors, the isolated cell populations were functionally heterogeneous,[18,19] indicating that further characterization was needed. Based on the expression of CD36 and CD105, in the previously defined MEP population ($Lin^{-}CD34^{+}CD38^{+}CD45RA^{-}IL3R^{-}$),[25] Iskander and colleagues identified Early Erythroid Progenitor (EEP) and Late Erythroid Progenitor (LEP) populations, generating BFU-E and CFU-E colonies, respectively.[15] Also from this population of $Lin^{-}CD34^{+}CD38^{+}CD45RA^{-}IL3R^{-}$ MEPS, Morris and colleagues documented that $CD71^{+}$ $CD105^{-}$ MEPs primarily generated large erythroid colonies while $CD71^{int/+}$ $CD105^{+}$ MEPs gave rise mostly to CFU-E colonies.[16] Both studies focused on the $CD34^{+}$ cell compartment indicating that CD105 could serve as a key marker to distinguish CFU-E from BFU-E.

By integrating CD71 and CD105 into our previously established surface marker phenotyping evaluation, we delineated the heterogeneity of previously defined populations of erythroid progenitors and

identified four successive stages of erythroid progenitors. The four populations from EP1 to EP4 constitute continuum of committed erythroid progenitors and enable the stage-specificity of early erythropoiesis to be refined. Notably, the lower erythroid colony-forming efficiency of EP1, particularly in cells isolated from primary bone marrow cells, suggest the presence of a small proportion of bipotential MEP in the EP1 population. Recent studies have indicated that CD38 and MPL can be used to identify rare MEPs[28–30] and as such further studies are warranted to study the specification of MEP to erythroid-committed progenitors, especially EP1, in the bone marrow.

Furthermore, we found that CD105 can be used to study terminal erythroid differentiation. In a previous study, we documented the importance of that the surface markers, GPA, α4-integrin and Band3 markers to distinguish between five distinct stages of terminal erythroid differentiation.[12] In the present study, we find that GPA and CD105 provide a more precise discrimination of these five distinct development stages. This finding therefore enables us to resolve the full continuum of erythropoiesis using one comprehensive set of markers.

As the availability of human bone marrow samples is limited, *in vitro* culture of $CD34^+$ HSPCs has been widely used as a model of human normal and disordered erythropoiesis.[31–36] However, differences between *in vitro* models and "true" *in vivo* erythropoiesis in human bone marrow exist. While the functional features of erythroid progenitors and erythroblasts are largely similar between these two systems, some differences exist.[12] Based on cytospin images of isolated cells at equivalent stages of development as a function of GPA/CD105 profiles, we detected a greater abundance of larger sized vesicles from the EP1 subset to polychromatic erythroblast stages in *in vitro* differentiated as compared to *in vivo* BM-differentiated subsets. These vesicles appear to be lipid droplets (our unpublished data) and our data suggest that they are likely the result of metabolic stress response occurring during *in vitro* differentiation.

Our study enables a precise characterization of specific stages of human erythropoiesis, promoting the study of specific erythroid defects in disorders with aberrant or ineffective erythropoiesis. In our cohort of MDS patients, we were able to identify defects at different stages of erythroid progenitor development. Admittedly, this is a small cohort but we believe that our novel method will be applicable to the study of MDS patients as well as patients with other anemias. We expect that future studies will advance our understanding of the mechanisms underlying these disorders and promote evaluation of specific therapies, including corticosteroids and immunomodulatory agents, in rescuing erythropoiesis in these patients.

In summary, we have developed an efficient and comprehensive immunophenotyping strategy to characterize the multiple stages of human erythropoiesis. We anticipate that this technique will serve as a valuable new tool, promoting our understanding of normal and disordered human erythropoiesis.

ACKNOWLEDGMENTS

This research was supported in part by NIH grants DK32094 (N.M, P.G.G, S.K), HL144436 and HL152099 (L.B).

CONFLICT OF INTEREST

The authors declare no conflict of interest.

AUTHOR CONTRIBUTIONS

Hongxia Yan and Narla Mohandas designed the research; Hongxia Yan and Erjing Gao performed most of the experiments; Hongxia Yan, Abdullah Ali, Lionel Blanc, Anupama Narla, Joseph M Lane, Julien Papoin, John Hale, Christopher D Hillyer, Naomi Taylor, Patrick G. Gallagher, Azra Raza, Sandrina Kinet, and Narla Mohandas analyzed and interpreted the data; Hongxia Yan and Narla Mohandas cowrote the manuscript; Abdullah Ali, Lionel Blanc, Anupama Narla, Christopher D Hillyer, Naomi Taylor, Patrick G. Gallagher, and Sandrina Kinet edited the manuscript; and all authors read and commented on the final manuscript.

DATA AVAILABILITY STATEMENT

Data available on request from the authors The data that support the findings of this study are available from the corresponding author upon reasonable request.

ORCID

Hongxia Yan https://orcid.org/0000-0002-8187-2788
Anupama Narla https://orcid.org/0000-0003-2325-3388

REFERENCES

1. Palis J. Primitive and definitive erythropoiesis in mammals. *Front Physiol*. 2014;5:3.
2. Loken M, Shah V, Dattilio K, Civin C. Flow cytometric analysis of human bone marrow. II. Normal B lymphocyte development. *Blood*. 1987;70(5):1316-1324.
3. Terstappen LWMM, Safford M, Loken MR. Flow cytometric analysis of human bone marrow III. Neutrophil maturation. *Leukemia*. 1990;4(9):657-663.
4. Terstappen LWMM, Loken MR. Myeloid cell differentia tion in normal bone marrow and acute myeloid leukemia assessed by multidimensional flow cytometry. *Anal Cell Pathol*. 1990;2:229-240.
5. Robinson J, Sieff C, Delia D, Edwards PA, Greaves M. Expression of cell-surface HLA-DR, HLA-ABC and glycophorin during erythroid differentiation. *Nature*. 1981;289(5793):68-71.
6. Sieff C, Bicknell D, Caine G, Robinson J, Lam G, Greaves MF. Changes in cell surface antigen expression during hemopoietic differentiation. *Blood*. 1982;60(3):703-713.
7. Loken MR, Shah VO, Dattilio KL, Civin CI. Flow cytometric analysis of human bone marrow: I. Normal erythroid development. *Blood*. 1987;69(1):255-263.
8. Okumura N, Tsuji K, Nakahata T. Changes in cell surface antigen expressions during proliferation and differentiation of human erythroid progenitors. *Blood*. 1992;80(3):642-650.
9. van Lochem EG, van der Velden VHJ, Wind HK, te Marvelde JG, Westerdaal NAC, van Dongen JJM. Immunophenotypic differentiation patterns of normal hematopoiesis in human bone marrow: reference patterns for age-related changes and disease-induced shifts. *Cytometry*. 2004;60B(1):1-13.
10. Terszowski G, Waskow C, Conradt P, et al. Prospective isolation and global gene expression analysis of the erythrocyte colony-forming unit (CFU-E). *Blood*. 2005;105(5):1937-1945.
11. Pronk CJH, Rossi DJ, Månsson R, et al. Elucidation of the phenotypic, functional, and molecular topography of a myeloerythroid progenitor cell hierarchy. *Cell Stem Cell*. 2007;1(4):428-442.

12. Hu J, Liu J, Xue F, et al. Isolation and functional characterization of human erythroblasts at distinct stages: implications for understanding of normal and disordered erythropoiesis in vivo. *Blood*. 2013;121(16):3246-3253.
13. Wangen JR, Eidenschink Brodersen L, Stolk TT, Wells DA, Loken MR. Assessment of normal erythropoiesis by flow cytometry: important considerations for specimen preparation. *Int J Lab Hematol*. 2014;36(2):184-196.
14. Li J, Hale J, Bhagia P, et al. Isolation and transcriptome analyses of human erythroid progenitors: BFU-E and CFU-E. *Blood*. 2014;124(24):3636-3645.
15. Iskander D, Psaila B, Gerrard G, et al. Elucidation of the EP defect in Diamond-Blackfan anemia by characterization and prospective isolation of human EPs. *Blood*. 2015;125(16):2553-2557.
16. Mori Y, Chen JY, Pluvinage JV, Seita J, Weissman IL. Prospective isolation of human erythroid lineage-committed progenitors. *Proc Natl Acad Sci U S A*. 2015;112(31):9638-9643.
17. Yan H, Hale J, Jaffray J, et al. Developmental differences between neonatal and adult human erythropoiesis. *Am J Hematol*. 2018;93:494-503.
18. Dulmovits BM, Hom J, Narla A, et al. Characterization, regulation and targeting of erythroid progenitors in normal and disordered human erythropoiesis. *Curr Opin Hematol*. 2017;24(3):159-166.
19. Ashley RJ, Yan H, Narla A, Blanc L. Steroid resistance in Diamond Blackfan anemia associates with $p57^{Kip2}$ dysregulation in erythroid progenitors. *J Clin Invest*. 2020;130(4):2097-2110.
20. Dover GJ, Chan T, Sieber F. Fetal hemoglobin production in cultures of primitive and mature human erythroid progenitors: differentiation affects the quantity of fetal hemoglobin produced per fetal-hemoglobin-containing cell. *Blood*. 1983;61(6):1242-1246.
21. Stephenson JR, Axelrad AA, Mcleod DL, Shreeve MM. Induction of colonies of hemoglobin-synthesizing cells by erythropoietin in vitro. *Proc Natl Acad Sci U S A*. 1971;68(7):1542-1546.
22. Dai CH, Krantz SB, Zsebo KM. Human burst-forming units-erythroid need direct interaction with stem cell factor for further development. *Blood*. 1991;78(10):2493-2497.
23. Bühring HJ, Müller CA, Letarte M, et al. Endoglin is expressed on a subpopulation of immature erythroid cells of normal human bone marrow. *Leukemia*. 1991;5(10):841-847.
24. Rokhlin OW, Cohen MB, Kubagawa H, Letarte M, Cooper MD. Differential expression of endoglin on fetal and adult hematopoietic cells in human bone marrow. *J Immunol*. 1995;154(9):4456-4465.
25. Manz MG, Miyamoto T, Akashi K, Weissman IL. Prospective isolation of human clonogenic common myeloid progenitors. *Proc Natl Acad Sci U S A*. 2002;99(18):11872-11877.
26. Ali AM, Huang Y, Pinheiro RF, et al. Severely impaired terminal erythroid differentiation as an independent prognostic marker in myelodysplastic syndromes. *Blood Adv*. 2018;2(12):1393-1402.
27. Taher AT, Musallam KM, Cappellini MD. β-Thalassemias. *N Engl J Med*. 2021;384(8):727-743.
28. Sanada C, Xavier-Ferrucio J, Lu Y-C, et al. Adult human megakaryocyte-erythroid progenitors are in the CD34 + CD38 mid fraction. *Blood*. 2016;128:923-933.
29. Xavier-Ferrucio J, Krause DS. Concise review: bipotent megakaryocytic-erythroid progenitors: concepts and controversies. *Stem Cells*. 2018;36(8):1138-1145.
30. Lu Y-C, Sanada C, Xavier-Ferrucio J, et al. The molecular signature of megakaryocyte-erythroid progenitors reveals a role for the cell cycle in fate specification HHS public access. *Cell Rep*. 2018;25(8):2083-2093.
31. Fibach E, Manor D, Oppenheim A, Rachmilewitz EA. Proliferation and maturation of human erythroid progenitors in liquid culture. *Blood*. 1989;73(1):100-103.
32. Panzenbö B, Bartunek P, Mapara MY, Zenke M. Growth and differentiation of human stem cell factor/erythropoietin-dependent erythroid progenitor cells in vitro. *Blood*. 1998;92(10):3658-3668.
33. Giarratana M-C, Kobari L, Lapillonne H, et al. Ex vivo generation of fully mature human red blood cells from hematopoietic stem cells. *Nat Biotechnol*. 2005;23(1):69-74.
34. Bouhassira EE. Concise review: production of cultured red blood cells from stem cells. *Stem Cells Transl Med*. 2012;1(12):927-933.
35. Fibach E. Erythropoiesis in vitro—a research and therapeutic tool in thalassemia. *J Clin Med*. 2019;8(12):2124.
36. Deleschaux C, Moras M, Lefevre SD, Ostuni MA. An overview of different strategies to recreate the physiological environment in experimental erythropoiesis. *Int J Mol Sci*. 2020;21(15):1-15.

SUPPORTING INFORMATION

Additional supporting information may be found online in the Supporting Information section at the end of this article.

How to cite this article: Yan H, Ali A, Blanc L, et al. Comprehensive phenotyping of erythropoiesis in human bone marrow: Evaluation of normal and ineffective erythropoiesis. *Am J Hematol*. 2021;1–13. https://doi.org/10.1002/ajh.26247

Supplemental materials

Comprehensive phenotyping of erythropoiesis in human bone marrow: Evaluation of normal and ineffective erythropoiesis

Hongxia Yan | Abdullah Ali | Lionel Blanc | Anupama Narla | Joseph M. Lane | Erjing Gao | Julien Papoin | John Hale | Christopher D. Hillyer | Naomi Taylor | Patrick G. Gallagher | Azra Raza | Sandrina Kinet | Narla Mohandas

Supplemental Figure 1. EP1, EP2, EP3 and EP4 cells from primary bone marrow are lineage negative and their cell sizes change along the erythroid progenitor maturation.

Supplemental Figure 2. CD105 enables isolation of erythroblasts from In Vitro culture of CD34+ cells.

Supplemental methods

Supplemental Figure 1.

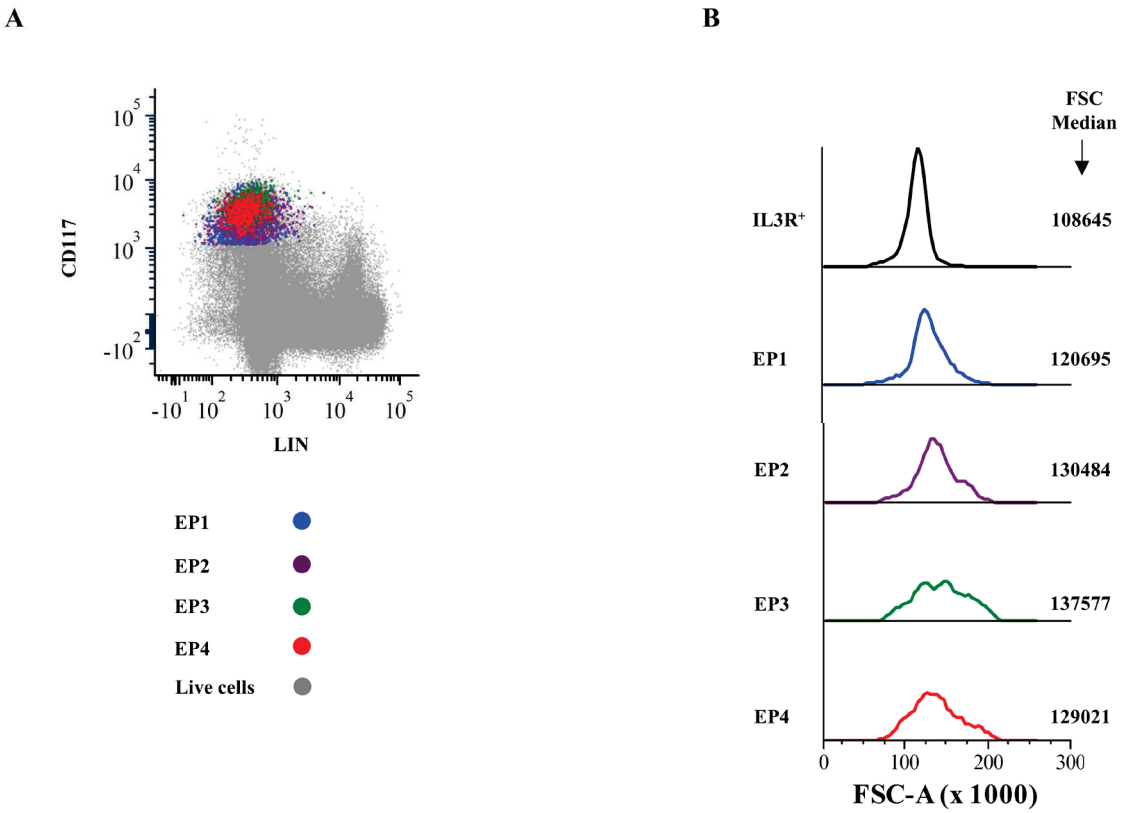

Supplemental Figure 1. EP1, EP2, EP3 and EP4 cells from primary bone marrow are lineage negative and their cell sizes change along the erythroid progenitor maturation. (A) Dot plot overlay of gated EP1 to EP4 from primary bone marrow showing their expression of CD117 and Lineage cocktail. (B) Histogram overlay of gated EP1 to EP4 showing their FSC changes along the erythroid progenitor maturation. FSC medians of each population were indicated at the right side of the histogram.

Supplemental Figure 2.

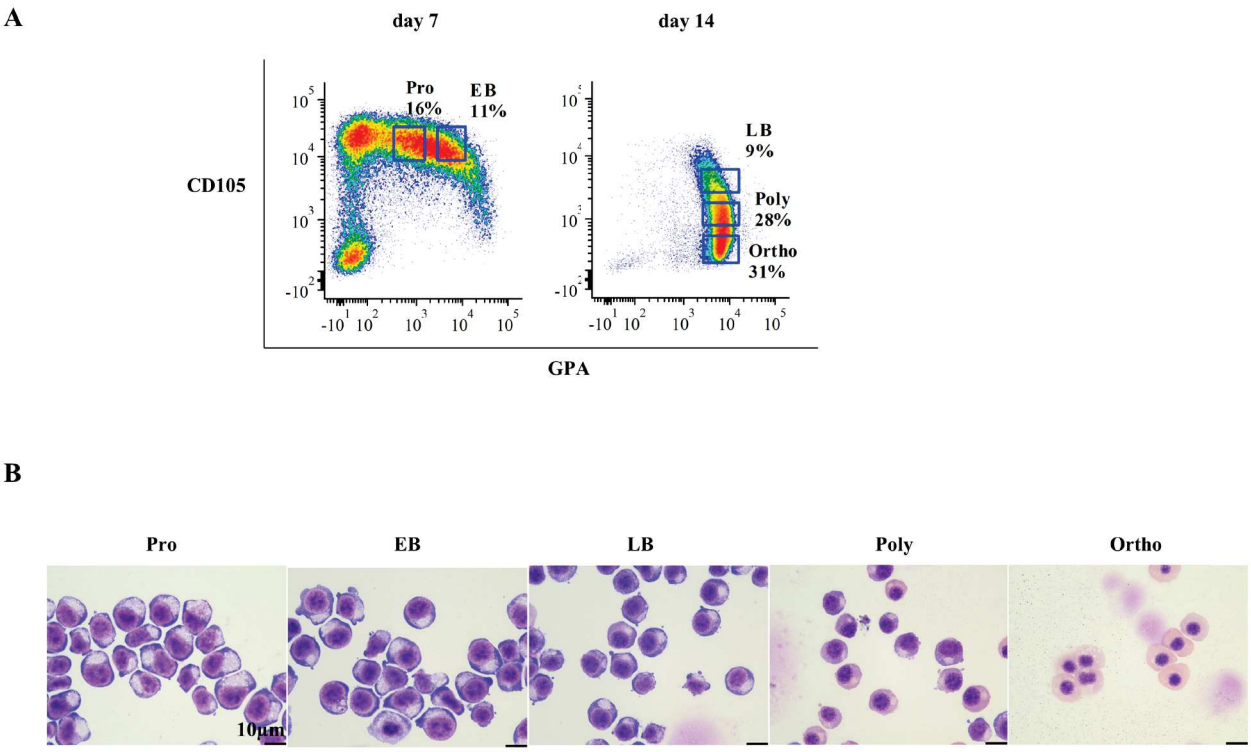

Supplemental Figure 2. CD105 enables isolation of erythroblasts from *In Vitro* culture of CD34⁺ cells. (A) Representative FACS plots for gating erythroblasts at distinct stages from *in vitro* culture of human CD34⁺ cells. Pro-erythroblasts, early basophilic erythroblasts were sorted on day 7 of culture (left panel), late basophilic erythroblasts, polychromatic and orthochromatic erythroblasts were sorted on day 14 of culture (right panel). (B) Representative cytospin images of sorted erythroblasts at distinct stages from *in vitro* culture of human CD34⁺ cells. The images were captured under Leica DM2000 microscope at ×100 magnification, scale bar=10μm.

Supplemental methods

Isolation and culture of CD34$^+$ cells

CD34$^+$ cells were isolated from non-mobilized leukopaks by magnetic positive selection using the CD34$^+$ MicroBead Kit UltraPure from Miltenyi Biotec, according to the manufacturer's instructions. Purified CD34$^+$ cells (purity between (90-98%) were differentiated toward erythrocytes using an *in vitro* three-phase culture system, as described previously(J. Hu et al., 2013).

Antibodies

Anti-Band3 FITC was prepared in our lab. Anti-IL3R PE-Cy7 was from eBioscience. Anti-CD117 PE and anti-α4 integrin APC were purchased from Miltenyi Biotec. All other antibodies were purchased from BD Biosciences.

Flow cytometry and cell sorting

Erythroid differentiation of cultured CD34$^+$ cells and bone marrow mononuclear cells were assessed on a BD LSR Fortessa (Becton Dickinson), and data were analyzed using FCS express 7 software (De Novo, Inc). Erythroid cells at distinct stages of differentiation were sorted by a BD FACSAria Fusion Cell Sorter with a 100 µm nozzle.

To sort erythroid progenitors from *in vitro* culture of CD34$^+$ cells, cells were collected after 5 days of culture and following antibodies were used to isolate erythroid progenitors at distinct stages: anti-IL3R PE-Cy7, anti-glycophorin A (GPA) BV421, anti-CD34 APC, anti-CD36 FITC, anti-CD71 APC-H7, and anti-CD105 PE-CF594, anti-CD117 PE, anti-CD45RA AF700, anti-CD41a BV510. Erythroblasts were sorted on day 7 of culture for proerythroblasts and early basophilic erythroblasts, and on day 14 of culture for late basophilic, polychromatic, and orthochromatic erythroblasts, using

anti-glycophorin A (GPA) PE, anti-CD105 APC and syto-16 to exclude reticulocytes on day 14.

To sort erythroid progenitors from bone marrow aspirates, mononuclear cells were separated using Ficoll-Hypaque density gradient centrifugation, followed by enrichment of $CD117^+$ cells using a CD117 MicroBead kit from Miltenyi Biotec, according to the manufacturer's instructions. Afterwards, the same antibodies as described above were used for isolation of erythroid progenitors at distinct stages. For erythroblast isolation from bone marrow aspirates, $CD71^+$ cells were enriched from mononuclear cells using CD71 MicroBead kit from Miltenyi Biotec and stained with anti-glycophorin A (GPA) PE, anti-CD105 APC and syto-16.

Human lineage cocktail, anti-CD45 AF700, anti-CD38 v450, anti-α4 integrin APC and anti-Band3 FITC antibodies were used to examine expression of corresponding surface markers in bone marrow mononuclear cells.

Colony forming assay

Cells were diluted to a density of 200 cells in 1ml of MethoCult® H4434 classic medium for BFU-E colony assay with SCF, IL-3, GM-CSF and EPO and 1ml of MethoCult® H4330 medium for CFU-E colony assay with EPO only (Stem Cell Technologies). BFU-E and CFU-E colonies were defined according to the criteria described by Dover et al(Dover, Chan, & Sieber, 1983). CFU-E colonies were counted on day 7 and BFU-E colonies were counted on day 15. Images were obtained using an Olympus IX71 or a Nikon ECLIPSE TS100 inverted microscope under 4X objective magnification.

Cytospin preparation

Cytospins were prepared by the Thermo Scientific Shandon 4 Cytospin, using $1x10^5$ cells in 200 μl of PBS. Slides were stained with May-Grünwald solution (Sigma)

for 5 minutes, rinsed in 40 mM Tris buffer for 90 seconds, and subsequently stained with Giemsa solution (Sigma) for 15 minutes. After staining, the slides were rinsed briefly in double distilled water and allowed to dry at room temperature. Images were taken using a Leica DM2000 inverted microscope under 100X objective magnification.

Reference

1. Hu J, Liu J, Xue F, et al. Isolation and functional characterization of human erythroblasts at distinct stages: implications for understanding of normal and disordered erythropoiesis in vivo. *Blood*. 2013;121(16):3246-3253. doi:10.1182/blood-2013-01-476390
2. Dover GJ, Chan T, Sieber F. Fetal hemoglobin production in cultures of primitive and mature human erythroid progenitors: differentiation affects the quantity of fetal hemoglobin produced per fetal-hemoglobin-containing cell. *Blood*. 1983;61(6):1242-1246. http://www.ncbi.nlm.nih.gov/pubmed/6188507. Accessed August 19, 2016.

DISCUSSION &

PERSPECTIVES

- **Erythroid progenitors: the continuum and the heterogeneity**

Over last decades, significant variations have been observed in erythroid progenitors, from their proliferation capacity, differentiation potential, to their sensitivity and dependence to various growth factors such as IL-3, SCF and EPO (C. H. Dai et al., 1991; Chun Hua Dai et al., 1991; Muta, Krantz, Bondurant, & Wickrema, 1994; Sawada, Krantz, Dessypris, Koury, & Sawyer, 1989), indicating that early erythropoiesis is a continuum composed of successively differentiating progenitors with heterogeneous potentials. To improve our understanding of early erythropoiesis, prospective isolation and characterization of erythroid progenitors with different potentials is required.

Conventionally, erythroid progenitors are defined as either BFU-E or CFU-E by their ability to form erythroid colonies in colony-forming assays. Since it was established in the 1970s, colony-forming assays have been used in numerous studies and laid the foundation of our current understanding in erythroid progenitors' biology (Dulmovits et al., 2017). However, colony-forming assays are endpoint assessment, which do not allow the prospective isolation of erythroid progenitors for further studies.

In 2014, Dr. Narla's lab developed a FACS based method for the isolation of BFU-E and CFU-E. According to the expression of a set of surface antigens, they identified BFU-E and CFU-E as $IL3R^{-}GPA^{-}CD34^{+}CD36^{-}$ and $IL3R^{-}GPA^{-}CD34^{-}CD36^{+}$, respectively (J. Li et al., 2014). This method has been widely used in the field and cited 140 times so far. Indeed, derived data from this method including transcriptomic analysis on isolated BFU-E and CFU-E provided important database for the field. However, these two immunophenotypically-defined populations did not present the entire continuum of early erythropoiesis, as indicated by identification of the transition population of $CD34^{+}CD36^{+}$ in a follow-up study (Yan et al., 2018). Noteworthy, the transition population is a heterogeneous population composed of BFU-E and CFU-E.

In addition, we observed greatly varied sizes of colonies generated by the defined BFU-E $CD34^{+}CD36^{-}$, indicating that there is still heterogeneity in this population. Adding to the complexity, we noticed that the continuum is different depending on the developmental source of human HSPCs. Using different surface markers such as CD71, CD105 and CD110 (Thrombopoietin Receptor, TPO-R), several groups have also identified erythroid progenitor populations (Iskander et al., 2015; Mori et al., 2015; Chad Sanada et al., 2016), but these works didn't uncover the entire continuum of early erythropoiesis as well, since they only focus on the $CD34^{+}$ HSPCs.

Although some advances have been made in the phenotyping and identification of erythroid progenitors, our current understanding of early erythropoiesis is not sufficiently detailed to dissect the remarkable heterogeneity of erythroid progenitors. The unresolved heterogeneity and incomplete phenotyping of erythroid progenitors not only hinders our understanding of normal erythroid differentiation, it also impedes identification of erythroid defects and cellular targets of therapeutic drugs in associated disorders, such as DBA and MDS. DBA is an inherited bone marrow failure with defects at the erythroid progenitor stages. Most patients respond firstly to steroids but then some of them develop a resistance. The mechanism of action and resistance to steroids has remained elusive, partly due to the lack of efficient immunophenotyping on the whole continuum of early erythropoiesis.

The findings of my thesis project offered new insights into erythroid biology by dissecting the heterogeneous erythroid progenitors into four successively differentiating and functionally distinct populations, with EP1 as BFU-E, EP2 as immature CFU-E, EP3 and EP4 as sequentially mature CFU-Es (Results original article 2, Figure 3). The dissection of erythroid progenitor heterogeneity enables us to begin to define the entire continuum of erythroid progenitors at a stage-wise resolution. Importantly, it led to the identification of specific population of immature CFU-Es that

respond to glucocorticoids in the treatment of DBA. It's also possible to use it to identify other cell populations that responsive to other drugs or growth factors in different disease contexts. Moreover, it could also enable us to identify stage-wise defects of erythroid disorders such as MDS and DBA.

Indeed, using the novel FACS strategy developed in this thesis, I evaluated erythropoiesis in the bone marrow of patients with MDS and identified defects at various erythroid progenitor stages (Results original article 2, Figure 6). Although MDS is a highly heterogeneous disease, a recent study suggested that impaired TED could serve as a prognostic marker regardless the various gene mutations. Still, the cause(s) of impaired TED remain(s) to be fully elucidated. Early studies have indicated that increased apoptosis during TED is associated with the decreased number of early erythroblasts. Herein, our findings of erythroid defects at progenitor stage in MDS opened a new avenue for understanding the ineffective erythropoiesis in this disease.

Given the high heterogeneity of MDS in gene mutations and clinical manifestations, more samples from patients with MDS and long-term fellow-up study are required. So far, we have completed analysis of 46 samples. Although current data from these samples is still not sufficient enough to tell the correlation between gene mutations and phenotype of erythroid differentiation, we observed erythroid progenitor defects in 26 of them, accompanied with apoptosis in associated defective stages in most of these patients. Presently, more samples analysis and fellow-up study is still in progress. Completion of this work will uncover the potential correlation between erythroid progenitor defects, gene mutations and disease outcomes, provide cellular and molecular insights into mechanism of ineffective erythropoiesis in MDS, eventually improve treatment of anemia in MDS and increase the quality of life of patients.

Very recently, using this strategy, I was also able to assess erythropoiesis from bone marrow sample of a patient with DBA harboring a *RPS19* mutation (**Figure 16**).

As described in the introduction, DBA patients with *RPS19* mutation appear to have milder clinical manifestations. Unsurprisingly, I observed close to normal TED in this patient. However, it's not the case for early erythropoiesis. In the bone marrow from a healthy donor, erythroid progenitors exhibited progressively increased cell numbers from immature EP1 to sequentially more mature EP2, EP3 and EP4. Notably, a significant decline in the number of EP4 cells, the mature CFU-E, was observed in the DBA patient. **Further analysis on more samples from patients with DBA may help to identify possible correlation between ribosomal protein gene mutation and erythroid defect at specific stages**.

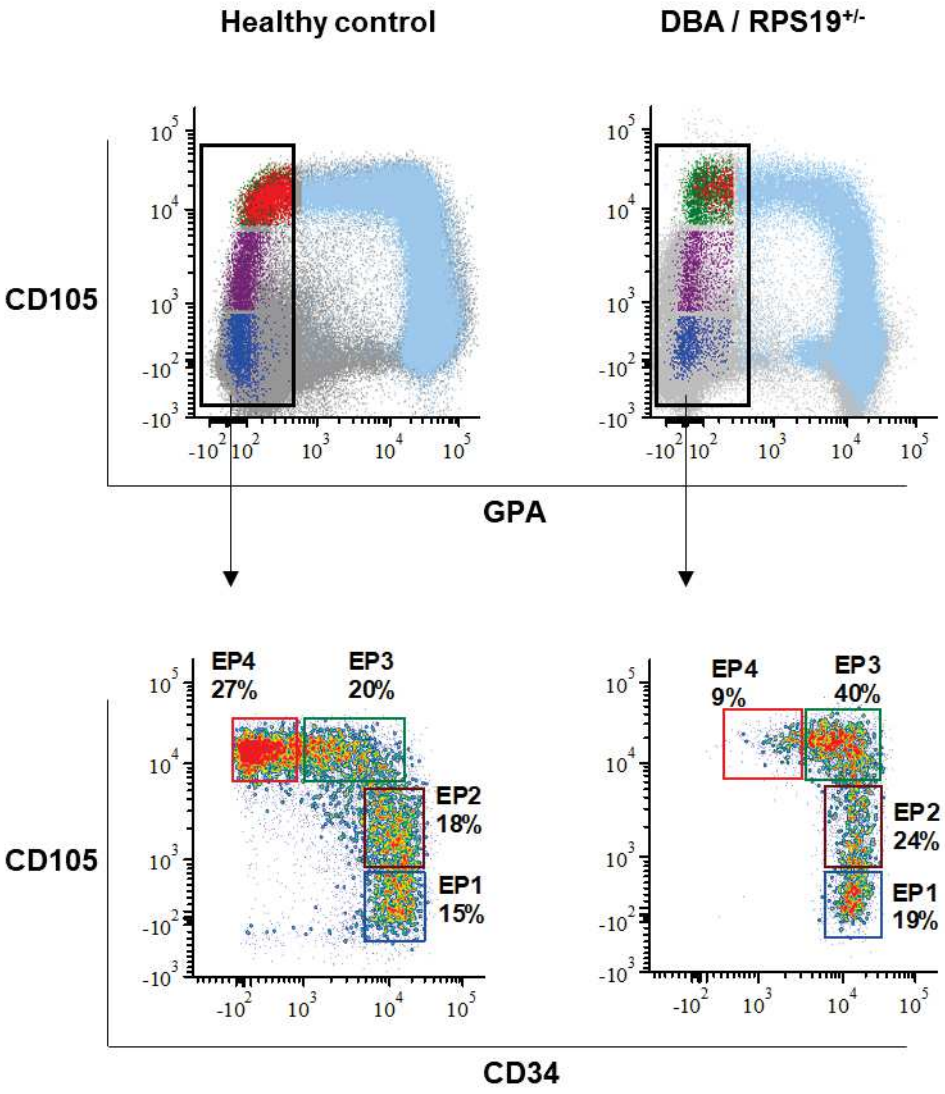

Figure 16. Disturbed differentiation of erythroid progenitors in a DBA patient with RPS19 haploinsufficiency. Flow cytometry analysis of erythropoiesis in the bone marrow of a DBA patient / RPS19$^{+/-}$ (right) and bone marrow cells from a healthy donor (left) was also analyzed as a control. Upper panel displayed the entire continuum of erythropoiesis from EP1 (blue dots), EP2 (purple dots), EP3 (green dots), EP4 (red dots), to erythroblasts (light blue dots). The differentiation of erythroid progenitors was further analyzed using CD34 and CD105 (Lower panel), which revealed the defective progression from EP3 (green) to EP4 (red) (unpublished data).

Together, the immunophenotyping strategy developed in this thesis takes into account both the continuum and the heterogeneity of erythroid progenitors, depicted a clearer profile of early erythropoiesis. Importantly, the stage-wise evaluation of erythropoiesis allows identification of stage specific defects in pathological conditions and responsive cell targets of potential therapeutic regents. Combing insights form these two aspects will not only improve our understanding of dyserythropoiesis, but also facilitate individualized treatment of heterogeneous erythroid disorders such as MDS and DBA.

Currently, further investigations on isolated populations of EP1 to EP4, such as RNA-sequencing, CHIP-sequencing, ATAC-sequencing and proteomics analysis, are ongoing. The successful accomplishment of above studies will offer a more comprehensively characterization of these defined populations, provide novel insights into the regulatory mechanism of early erythropoiesis, and promote our understanding in the complexity of erythroid progenitors in the contexts of normal and disordered erythropoiesis.

- **Steroid resistance and cell cycle regulation in erythropoiesis**

Glucocorticoid such as dexamethasone is one of the main therapeutic treatments for DBA, in addition to red cells transfusion. While around 80% DBA patients respond

initially to glucocorticoids, half of them became refractory after a period of treatment. Moreover, another 20% of patients with DBA never respond to glucocorticoids(Narla et al., 2011). In other words, more than half of these patients have a resistance to glucocorticoids and have to rely on chronic red cells transfusion. Therefore, more investigations into the mechanisms of action of glucocorticoid are needed to reveal the molecular basis of glucocorticoid response in erythropoiesis and glucocorticoid resistance in patients with DBA.

Glucocorticoids resistance is a well-known aspect of many chronic diseases, e.g., asthma, depression, cancer, and several autoimmune diseases (Timmermans, Souffriau, & Libert, 2019). Glucocorticoids principally act through GR signaling, and multiple alterations along the pathway may contribute to glucocorticoids resistance. In the context of anti-inflammatory treatment, activation of MAPK pathway has been identified as a common mechanism of glucocorticoids resistance (Sevilla et al., 2021). However, the mechanisms of the glucocorticoid resistance in patients with DBA are poorly understood. No correlation has been identified between the gene mutated in DBA and response to glucocorticoids. In families who all carry the same gene mutation, some patients respond to glucocorticoids while others never respond, or initially respond and later become refractory to treatment (Narla et al., 2011).

A study suggested that differences in GR polymorphisms and variable expression of GR isoforms might contribute to the variability in patient responses (Varricchio & Migliaccio, 2014). Interestingly, different DNA methylation and chromatin accessibility patterns were identified in glucocorticoid responsive and unresponsive patients, suggesting that glucocorticoid resistance may have an epigenetic basis (Farrar et al., 2018). In addition, defects in GR expression, ligand binding, nuclear translocation or DNA binding may also involve in glucocorticoid resistance, as presented in non-erythroid disorders treatment with glucocorticoids (Ito, Chung, & Adcock, 2006).

In the present thesis project, we demonstrated the role of cell cycle regulation in the mechanism of action of dexamethasone and mechanisms of glucocorticoid resistance in patients with DBA. This work initiated from an earlier observation that only PB-derived $CD34^+$ cells responded to dexamethasone with an enhanced expansion of CFU-E, but not CB derived $CD34^+$ cells. As described in the original article 1, an immature CFU-E population characterized by $CD71^{hi}CD105^{med}$ was identified as the principal responsive cells to dexamethasone from the previous transition population $CD34^+CD36^+$ that specifically predominate in adult erythropoiesis but not neonatal erythropoiesis.

Importantly, our findings confirmed the critical role of $p57^{Kip2}$ mediated cell cycle regulation during early erythropoiesis, which explained, at least partially, the mechanism of action of dexamethasone in erythroid lineage and the glucocorticoids resistance in DBA patients.

The critical role of the cell cycle is well-established in hematopoiesis, notably its regulatory function for maintenance of the stemness of long-term HSCs. In differentiating MPP cells, the cell cycle was maintained at a slow cycling rate and cell fate of a MPP can be predicted by the cell cycle speed or the expression of regulatory proteins (X. Hu, Eastman, & Guo, 2019; Passegué, Wagers, Giuriato, Anderson, & Weissman, 2005). Moreover, cell fate can be modulated towards a specified lineage by altering the cell cycle rate (X. Hu et al., 2019; Passegué et al., 2005).

Upon commitment towards the erythroid lineage, the cell cycle still retains a slow cycling rate in BFU-E, which begins to accelerate and allow for extensive cell expansion in the later progenitor and erythroblast stages (Kumkhaek et al., 2013). A recent study in the mouse model revealed that the self-renewal of murine erythroid progenitors rely on a slow replication fork speed, and cell fate switch from self-renewal to differentiation was associated with a global increase in replication fork speed and

consequently a shorter S-phase (Hwang et al., 2017). Consistently, I observed dynamic changes of cell cycle throughout the erythroid differentiation process, as shown by the percentage of S-phase cells. The percentage of S-phase cells is relatively low level in EP1, the BFU-E cells, then gradually increase from EP2 to EP4 the sequentially more mature CFU-E cells. Afterwards, high ratio of S-phase was retained until polychromatic erythroblasts and abruptly dipped in orthochromatic erythroblasts (**Figure 17**), which exit cell cycle prior to enucleation.

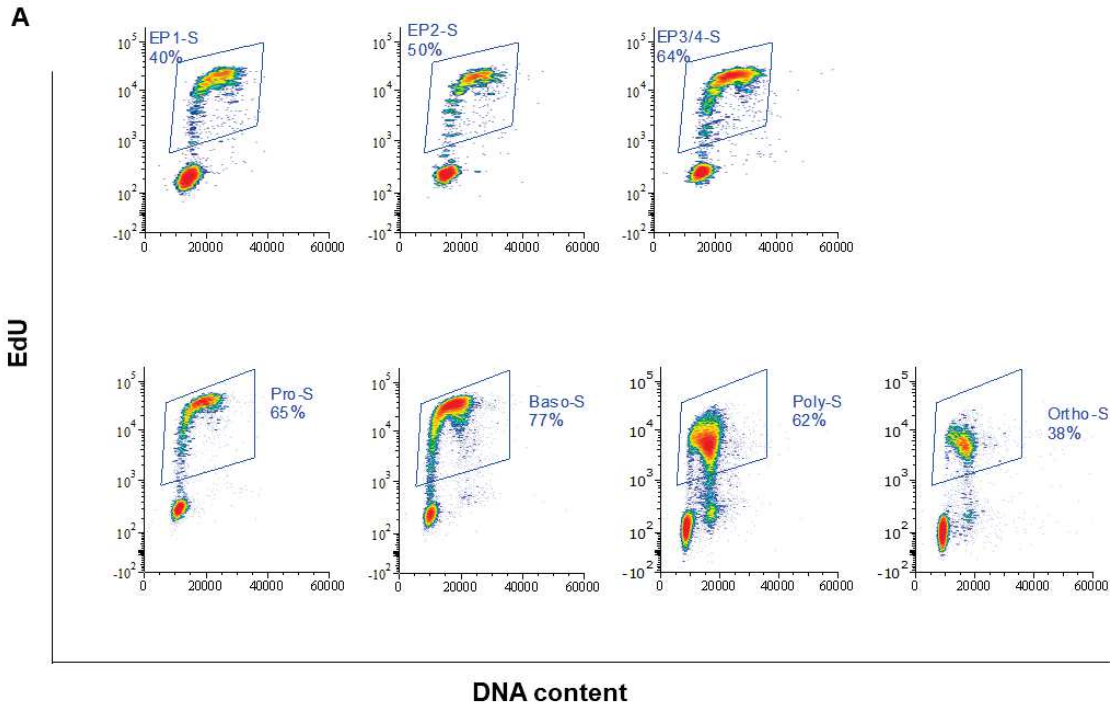

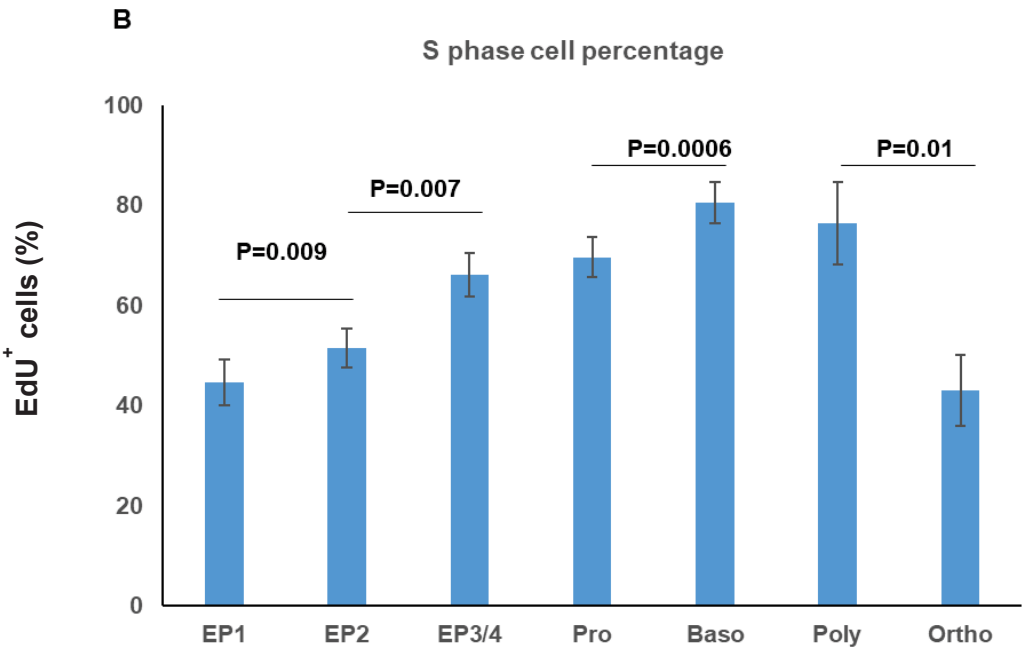

Figure 17. Cell cycle dynamics during human erythropoiesis. PB derived CD34⁺ cells were differentiated *in vitro* for erythroid differentiation and 5-ethynyl-2′-deoxyuridine (EdU) incorporation was performed on day 5 for analysis of EP1, EP2 and EP3/4, day 11 for analysis of proerythroblasts and basophilic erythroblasts and day 14 for analysis of poly and orthochromatic erythroblasts. Cells were firstly incubated with EdU for 2 hours and followed by surface antigen staining, erythroid progenitors and precursors of different stages were gated as described in original article 2. **(A)** Representative plots of S-phase cells ratio in erythroid progenitors and precursors at different stages. **(B)** Statistical analysis of S-phase cells at distinct stages of erythroid differentiation (n=4).

The dynamic changes of the cell cycle state during erythropoiesis are tightly regulated by extrinsic regulators including THPO, Wnt, SCF and TGFβ, and numerous intrinsic regulators such as members of the Cip/Kip family of proteins (Yamada & Kawauchi, 2013). Our findings indicated that $p57^{Kip2}$, a CDK inhibitor belonging to the Cip/Kip family, has differential expression kinetics between CB and PB derived erythroid progenitors, and the difference in expression baseline may account for their different responses to dexamethasone treatment.

As a negative cell cycle regulator, $p57^{Kip2}$ is involved in maintaining the quiescence state of HSC, critical for stemness maintenance (Matsumoto et al., 2011; Zou et al., 2011). Notably, the induction of dexamethasone on $p57^{Kip2}$ expression was documented in several type of mammalian cells including rat placentas, human endometrial stromal cells and HeLa cells (E. H et al., 2015; S. T. Kim, Lee, & Gye, 2011; Samuelsson, Pazirandeh, Davani, & Okret, 1999). Moreover, dexamethasone induced $p57^{Kip2}$ expression inhibited cell cycle progression of HeLa cells (Samuelsson et al., 1999). More recently, Socolovsky et al found that $p57^{Kip2}$ negatively regulated the replication fork speed and the resulted slow cell cycle is required for murine erythroid progenitor self-renewal. Importantly, the expression of $p57^{Kip2}$ is also essential for dexamethasone mediated CFU-E self-renewal (Hwang et al., 2017; Pop et al., 2010).

In the human system, we found that $p57^{Kip2}$ is expressed at early stages of human erythropoiesis and lost in TED in both sources of $CD34^+$ cells, but CB-derived cells maintained its expression for a longer period. Upon dexamethasone treatment, PB-derived CFU-Es demonstrated increased expression of $p57^{Kip2}$, but its expression in CB-derived CFU-Es was largely unchanged with a relative higher basal level than its PB counterparts. Furthermore, the expression of $p57^{Kip2}$ was upregulated by dexamethasone in $CD34^+$ cells from steroid-responsive patients, but not transfusion-dependent patients with DBA. Conversely, inhibition of $p57^{Kip2}$ by lentiviral mediated RNA interference abrogated the effect of dexamethasone in PB derived $CD34^+$ cells. These results confirmed the role of $p57^{Kip2}$ mediated cell cycle regulation in murine erythropoiesis and reconcile the field with regards to the erythroid progenitor stage responding to dexamethasone. Indeed, glucocorticoids specifically induce the maintenance and expansion of an immature CFU-E progenitor population in humans mediated through negative cell cycle regulation by $p57^{Kip2}$, and the dysregulated

expression of $p57^{Kip2}$ in steroid-resistant patients account, at least partially, for the resistance.

In addition to $p57^{Kip2}$, our proteomics studies identified other cell cycle regulators such as NR4A1, implying a general negative regulation on cell cycle induced by dexamethasone. Indeed, olomoucine, a specific inhibitor of CDK1 and CDK2, led to the similar maintenance of the immature CFU-E population as we observed with dexamethasone treatment, suggesting a more generalizable role of CDK inhibition. Interestingly, NR4A1 was recently identified as previously unrecognized downstream targets of *c-Myc* and was critical for maintenance of HSCs functions (Chen et al., 2019; Sheng et al., 2021). Notably, both $p57^{Kip2}$ and NR4A1 are negative regulators of cell cycle progression and are closely associated with HSCs quiescence and maintenance of HSCs self-renewal. NR4A1 was also expressed in human MEP bipotent progenitors (Y.-C. Lu et al., 2018), but its role in more restricted erythroid lineage was not clear. Further investigations on NR4A1 may provide additional insights in molecular basis for a more detailed understanding of mechanisms of action of glucocorticoids in human erythropoiesis and facilitate the exploration of using CDK inhibitors as potential therapeutic drugs for DBA patients with steroid resistance.

Our findings in this study provided novel insights in understanding the mechanism of action of dexamethasone and glucocorticoids resistance in DBA patients. Moreover, dexamethasone-induced cell cycle regulation mediated by $p57^{Kip2}$ highlighted the tight link between the cell cycle and maintenance of specific cell state during early erythropoiesis, suggesting the potential opportunities to modulate erythropoiesis by intervening cell cycle regulation in treatment of erythroid disorders with defective erythroid progenitors.

- **Metabolic regulation of human erythropoiesis**

The importance of cell metabolism has been increasingly recognized in the regulation of erythropoiesis. Recent findings showed that diverse metabolic networks function in concert with transcription factors, growth facotrs and epigenetic regulators to regulate erythroid differentiation, including but not limit to iron and heme metabolism, amino acid and glucose metabolism, energy production and redox homeostasis (Oburoglu et al., 2016).

As shown in the recently published article (ANNEX original article 2), we have described the impaired erythroblasts maturation and enucleation caused by disturbed redox homeostasis and identified IDH1 as a critical regulator of redox homeostasis during TED. Using an *in vitro* model of human erythropoiesis, we observed that OXPHOS levels dynamically change during erythroid differentiation, increasing at the early stages and decreasing at the late stages of TED. Consistently, we observed a progressive decrease in mitochondria biomass and activity during TED, as assessed by Mito Tracker staining and Seahorse Mito Stress Test (ANNEX original article 2, Figure 1 D and E). Interestingly, Liang et al demonstrated a critical but unanticipated role of mitochondria in erythroblast enucleation (Liang et al., 2021). They observed that mitochondria migrate and aggregate near the nucleus before nuclear expulsion. More interestingly, they found that low activity of mitochondria during late stage of TED is fueled by pyruvate but not *in situ* glycolysis, which is critical for erythroblast enucleation. Consistently, Sen et al recently demonstrated that PGC1β, a critical coactivator of mitochondrial biogenesis, is required for erythroblast maturation. Reduced levels of PGC1β directly affected iron and heme homeostasis and eventually hemoglobin production (Sen, Chen, & Singbrant, 2021).

As discussed above, mitochondria play an essential role in energy production and heme biogenesis. However, the activity of mitochondria during human erythropoiesis remains to be fully defined. Herein, using our refined FACS strategy, I examined at

higher resolution the stage specific dynamics of mitochondria biomass and polarization throughout human erythropoiesis in the bone marrow, from the most immature erythroid progenitor BFU-E to orthochromatic erythroblasts and reticulocytes.

I first observed that the elevation of mitochondria polarization predates the increase of mitochondria biomass during early erythropoiesis. Both mitochondria biomass and polarization plateaued at mature CFU-E (EP3/EP4) to proerythroblast stage, which is in accord to the active proliferation activities during this phase. Afterwards, mitochondria polarization declined followed by the decrease of mitochondria biomass but eventually both dropped down to a significant lower level at orthochromatic erythroblast stage (**Figure 18**). Consistently, Moras et al observed a progressive decrease in mitochondria biomass during erythroblast maturation (Moras et al., 2021). Our results revealed dynamic changes of mitochondria activity during human adult erythropoiesis in the bone marrow. Especially, the low level of mitochondria activity in BFU-E followed by a marked increase in CFU-E are in line with the previous recognition on the negative correlation of OXPHOS level and cell self-renewal capacity. In contrast, decrease of mitochondria biomass and polarization at late stage of TED, in line with the decrease of OXPHOS level (ANNEX original article 2), is essential for erythroblast maturation and enucleation.

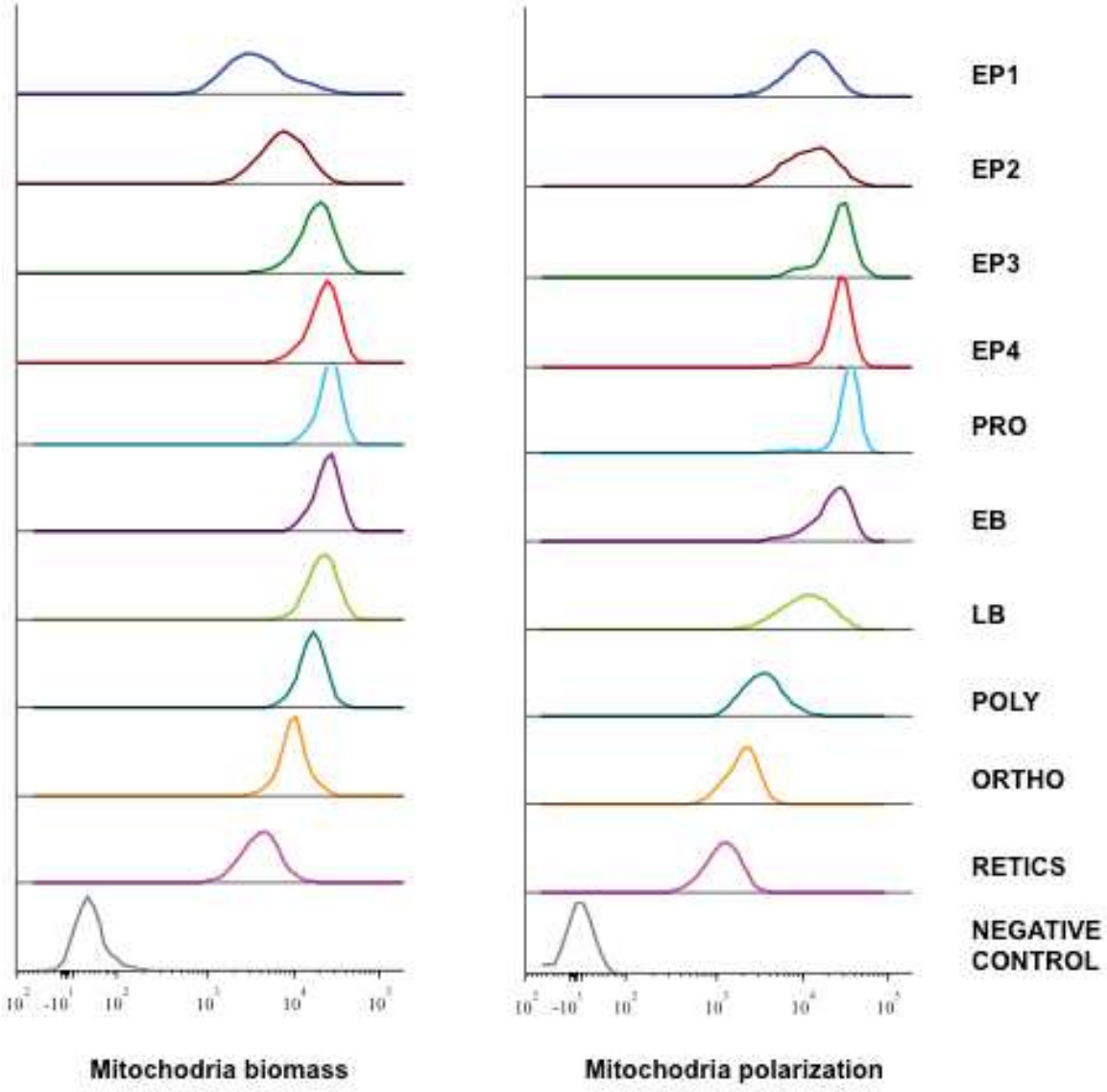

Figure 18. Dynamic changes of mitochondria biomass and polarization during human erythropoiesis. Representative flow analysis of mitochondria biomass (left) and polarization (right) in primary bone marrow cells from a non-anemic donor. Bone marrow mononuclear cells were isolated by Ficoll density gradient centrifugation for Mitotracker dye staining, then surface antigens staining was performed for stage specific analysis by flow cytometry.

To fuel mitochondria-centered metabolic pathways, numerous nutrients are needed to be transported into the cells, and bioavailability of these nutrients will impact cellular signaling and gene expression during erythropoiesis. Therefore, specific transporters for these nutrients are required to be expressed on the surface of cells.

To obtain an overview of the metabolic changes during erythropoiesis, we measured the surface expression levels of a set of nutrients transporters of erythroid cells at distinct differentiating stages by using receptor binding domain (RBD), derived from envelope glycoproteins evolved across a range of retroviruses that use these transporters to interact with host cells (H. Liu, Bi, Wang, Lu, & Jiang, 2015). Combining this unique tool with the FACS strategy described in RESULTS original article 2, we documented the distinct expression pattern of 9 transporters, including riboflavin importers (RFVT1 and RFVT2, SLC52A1 and SLC52A2), phosphate importers (PiT1 and PiT2, SLC20A1 and SLC20A2) and exporter (XPR1, SLC53A1), heme exporter (FLVCR1, SLC49A1), cationic amino acid importer (CAT1, SLC7A1), multivitamin transporters (SMVT, SLC5A6), neutral amino acid transporter (ASCT2, SLC1A5) and glucose importer (GLUT1, SLC2A1) (**Figure 19**). These distinct expression patterns of transporters throughout the continuum of erythropoiesis, from BFU-E to orthochromatic erythroblast, may reflect the dynamic change in nutrient requirement at specific stages of human erythropoiesis.

Indeed, Oburoglu et al have demonstrated the importance of ASCT2 and GLUT1 for erythroid lineage commitment (Oburoglu, Tardito, Fritz, De Barros, et al., 2014). The role of FLVCR1 in regulating heme/globin balance at BFU was also known (Quigley et al., 2004). Consistently, we observed that FLVCR1 was highly expressed on BFU-E and CFU-E and declined upon entering TED where globin production catches up to heme biosynthesis.

Interestingly, RFVT1/2 exhibited a similar expression pattern as FLVCR1 with a specific high level of expression only on erythroid progenitors followed by an immediate decrease in TED (**Figure 19**).

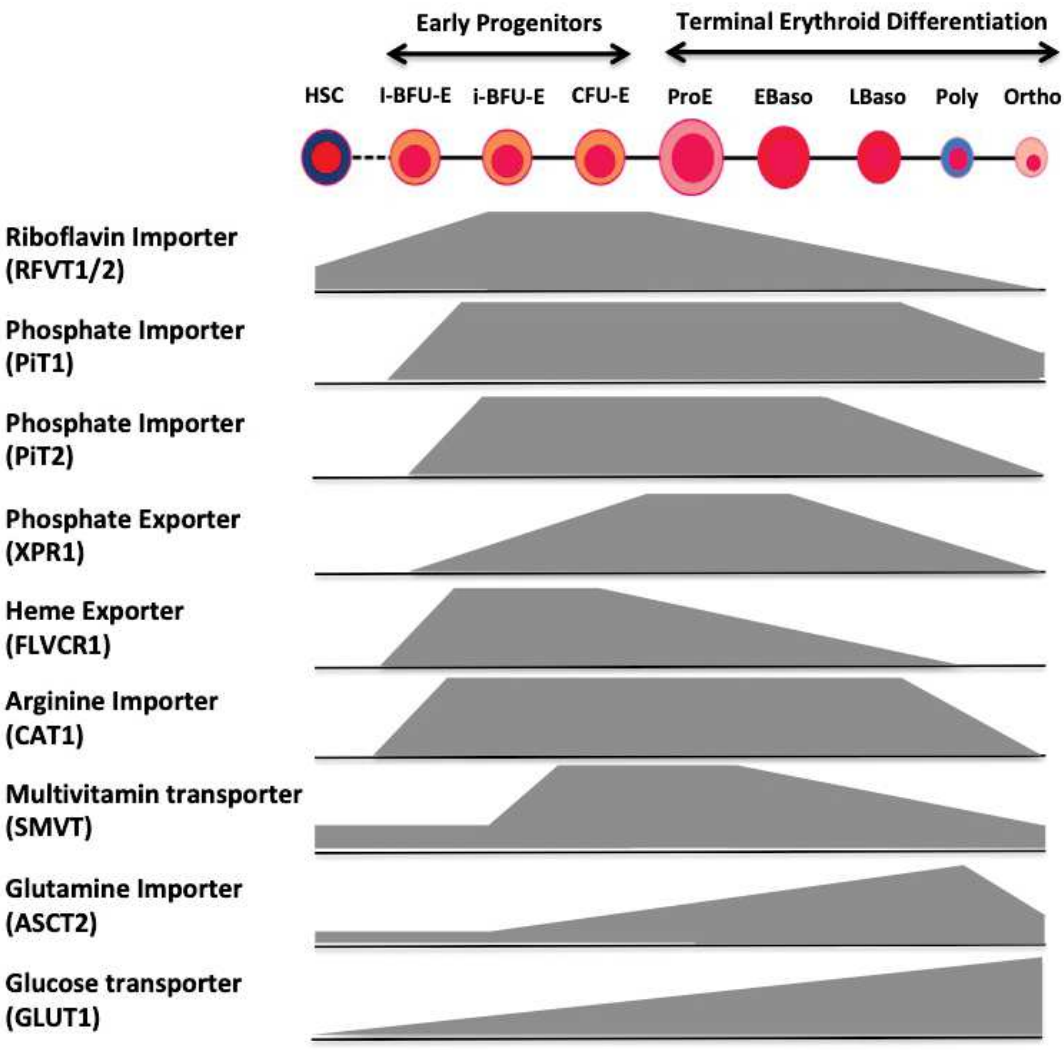

Figure 19. Dynamic changes in the expression of nutrient transporters during human erythropoiesis. Nine nutrient transporters, including riboflavin importers (RFVT1/2), phosphate importers (PiT1 and PiT2) and exporter (XPR1), heme exporter (FLVCR1), arginine importer (CAT1), multivitamin transporters (SMVT), glutamine importer (ASCT2) and glucose importer (GLUT1), have distinct expression patterns during human erythroid differentiation (Justus et al., 2019).

Riboflavin, also known as vitamin B2, is one of the thirteen essential vitamins for the human body. Riboflavin and its derivatives, flavin mononucleotide or riboflavin phosphate (FMN) and flavin adenine dinucleotide (FAD), play a critical role in mitochondria energy metabolism and are also involved in lipid and amino acid metabolism (Xin et al., 2017). However, riboflavin cannot be synthesized or stored in

the human body, and has to be provided through daily diets. Riboflavin deficiency is rarely life threatening, but it is fairly common especially in developing countries. Combined with other conditions, such as in patients with diabetes mellitus, infections, pregnancy, or genetic disorders of flavin transport and function, riboflavin deficiency can lead to various clinical abnormalities including impaired nerve functions and anemia (Hassan & Thurnham, 1977; Mosegaard et al., 2020; Xin et al., 2017). Therefore, high expression levels of the riboflavin transporter in erythroid progenitors are in line with the rapid increase in energy supply required by active proliferation of CFU-E, as reflected by the peak of mitochondria biomass and polarization (**Figure 18**) and the increase of S-phase cells from EP1 BFU-E to CFU-E EP2-4 (**Figure 17**).

Phosphate is critical for a variety of cellular processes including ATP production, signal transduction, nucleic acid and lipid synthesis and cell membrane composition, (Chande et al., 2020; Forand et al., 2016; Justus et al., 2019; Koumakis et al., 2019). The constant expression of phosphate importers and temporal expression of phosphate exporters on early erythroblasts suggest coordinated effects of these transporters in maintaining the phosphate homeostasis and its importance for erythroid differentiation (Z. Q. Wang et al., 1995)(Festing, Speer, Yang, & Giachelli, n.d.; L. Liu, Sánchez-Bonilla, Crouthamel, Giachelli, & Keel, 2013).

Hence, further investigation on the function of these transporters and associated nutrients/metabolites will advance our understanding in the metabolic regulation of erythropoiesis, thus improve a more comprehensive understanding of the complex regulatory machinery of human erythropoiesis. Moreover, provide insights into the pathologies of erythroid diseases with metablic alterations.

- **Closing words**

Through two interrelated studies centered on early erythropoiesis, I explored the nature of erythroid progenitor biology in both physiological and pathological contexts. The findings from this research depicted a clearer concept of the continuum of early erythropoiesis and provided novel insights into the regulation and modulation of erythroid progenitors in normal and disordered erythropoiesis.

With extending techniques and knowledge gained from this project into the contexts of heterogeneous erythroid disorders such as DBA and MDS, I hope that combination of precise evaluation of stage specific defects of erythropoiesis and identification of targeting cells of potential therapeutic regents could facilitate individualized treatment for patients with heterogeneous gene mutations and clinical manifestations. Eventually, thorough understanding of erythroid progenitor biology could possibly enable us to treat the diseases by “nurturing” defective erythroid progenitors toward effective erythropoiesis.

ANNEXES

Original article 1

Developmental differences between neonatal and adult human erythropoiesis

Hongxia Yan1[#] | John Hale1[#] | Julie Jaffray1 | Jie Li2 | Yaomei Wang2 | Yumin Huang2 | Xiuli An2 | Christopher Hillyer1 | Nan Wang3 | Sandrina Kinet4 | Naomi Taylor4 | Narla Mohandas1* | Anupama Narla3* | Lionel Blanc5,6 *

1 Red Cell Physiology Laboratory, New York Blood Center, New York, New York 10065;

2 Membrane Biology Laboratory, New York Blood Center, New York, New York 10065;

3 Stanford University School of Medicine, Palo Alto, California 94304;

4 GREx, Institut de Génétique Moléculaire de Montpellier, University of Montpellier, CNRS, Montpellier 34095, France;

5 Laboratory of Developmental Erythropoiesis, Center for Autoimmune, Musculoskeletal, and Hematopoietic Diseases, The Feinstein Institute for Medical Research, Manhasset, New York 11030;

6 Department of Molecular Medicine and Pediatrics, Donald and Barbara Zucker School of Medicine at Hofstra Northwell, Hempstead, New York 11549.

# **Hongxia Yan** and John Hale contributed equally to this work.

* Narla Mohandas, Anupama Narla and Lionel Blanc are co-senior authors

https://doi.org/10.1002/ajh.25015

Received: 18 December 2017 | Accepted: 20 December 2017

DOI: 10.1002/ajh.25015

RESEARCH ARTICLE

WILEY AJH

Developmental differences between neonatal and adult human erythropoiesis

Hongxia Yan[1#] | John Hale[1#] | Julie Jaffray[1] | Jie Li[2] | Yaomei Wang[2] | Yumin Huang[2] | Xiuli An[2] | Christopher Hillyer[1] | Nan Wang[3] | Sandrina Kinet[4] | Naomi Taylor[4] | Narla Mohandas[1*] | Anupama Narla[3*] | Lionel Blanc[5,6]*

[1]Red Cell Physiology Laboratory, New York Blood Center, New York, New York 10065; [2]Membrane Biology Laboratory, New York Blood Center, New York, New York 10065; [3]Stanford University School of Medicine, Palo Alto, California 94304; [4]GREx, Institut de Génétique Moléculaire de Montpellier, University of Montpellier, CNRS, Montpellier 34095, France; [5]Laboratory of Developmental Erythropoiesis, Center for Autoimmune, Musculoskeletal, and Hematopoietic Diseases, The Feinstein Institute for Medical Research, Manhasset, New York 11030; [6]Department of Molecular Medicine and Pediatrics, Donald and Barbara Zucker School of Medicine at Hofstra Northwell, Hempstead, New York 11549

Correspondence
Lionel Blanc, Laboratory of Developmental Erythropoiesis, The Feinstein Institute for Medical Research, 350 Community Drive, Manhasset NY 11030.
Email: Lblanc@northwell.edu
and
Anupama Narla, Department of Pediatrics,, Division of Hematology/Oncology,, Stanford University School of Medicine and Lucile Packard Children's Hospital, Palo Alto, CA 94304.
Email: Anunarla@stanford.edu

Funding information
National Institutes of Health, Grant/Award Numbers: DK26263 (to N.M.) and DK32094 (to N.M. and N.T.), DK090145 (to A.N.), HL134043 (subcontract to L.B); Agence Nationale pour la Recherche (to N. T); St. Baldrick's Foundation (to L.B); Pediatric Cancer Foundation (to L.B.)

Abstract

Studies of human erythropoiesis have relied, for the most part, on the in vitro differentiation of hematopoietic stem and progenitor cells (HSPC) from different sources. Here, we report that despite the common core erythroid program that exists between cord blood (CB)- and peripheral blood (PB)-HSPC induced toward erythroid differentiation in vitro, significant functional differences exist. We undertook a comparative analysis of human erythropoiesis using these two different sources of HSPC. Upon in vitro erythroid differentiation, CB-derived cells proliferated 4-fold more than PB-derived cells. However, CB-derived cells exhibited a delayed kinetics of differentiation, resulting in an increased number of progenitors, notably colony-forming unit (CFU-E). The phenotypes of early erythroid differentiation stages also differed between the two sources with a significantly higher percentage of $IL3R^{-}GPA^{-}CD34^{+}CD36^{+}$ cells generated from PB- than CB-HSPCs. This subset was found to generate both burst-forming unit (BFU-E) and CFU-E colonies in colony-forming assays. To further understand the differences between CB- and PB-HSPC, cells at eight stages of erythroid differentiation were sorted from each of the two sources and their transcriptional profiles were compared. We document differences at the CD34, BFU-E, poly- and orthochromatic stages. Genes exhibiting the most significant differences in expression between HSPC sources clustered into cell cycle- and autophagy-related pathways. Altogether, our studies provide a qualitative and quantitative comparative analysis of human erythropoiesis, highlighting the impact of the developmental origin of HSPCs on erythroid differentiation.

1 | INTRODUCTION

Erythropoiesis is the biological process that regulates the formation of red blood cells. This process is highly coordinated and involves a series of differentiation stages that are initiated in hematopoietic stem and progenitor cells (HSPCs), cell types that possess self-renewing and multi-potential differentiation potential, respectively. HSPCs give rise to more committed hematopoietic progenitors including myeloid progenitors, megakaryocytes, and erythroid progenitor.[1] Recent data have demonstrated that, in humans, red cells can originate directly from HSPCs or from a more committed progenitor.[2] The erythroid burst-forming unit (BFU-E) is the most primitive single-lineage committed erythroid progenitor that can be functionally defined. This BFU-E then differentiates into a more committed erythroid colony-forming unit (CFU-E) that ultimately differentiates into proerythroblasts, the first

*Co-senior authors.

#Hongxia Yan and John Hale contributed equally to this work.

 © 2018 Wiley Periodicals, Inc.

morphologically recognizable erythroid precursor in the bone marrow.[3] Four to five divisions, occurring over the course of four to five days, lead to the orthochromatic stage, followed by enucleation and subsequent formation of the nascent reticulocyte. Reticulocyte maturation is the final stage of erythropoiesis and is characterized by extensive membrane remodeling and the loss of all internal organelles.[4,5]

Studies of erythropoiesis have historically relied, in large part, on mouse models. However, these models have failed to recapitulate various physiologic and pathological aspects of human erythroid differentiation. Indeed, recent studies from our groups and others have highlighted divergent epigenetic, transcriptional, and proteomic landscapes between murine and human erythropoiesis.[6–13] To better study human erythropoiesis, in vitro culture systems have been developed. Since the original method reported by Fibach,[14] these culture systems have been continually adapted and modified[15–19] and we are now able to use CD34$^+$ cells to recapitulate all stages of erythropoiesis, from the HSPC through the reticulocyte stage. These culture systems have promoted the study of normal and disordered erythropoiesis, providing important insights into the mechanisms regulating human erythroid differentiation. However, the majority of these studies used a single source of CD34$^+$ progenitor cells with the broad assumption that differentiation data obtained from fetal liver (FL), cord blood (CB), bone marrow (BM), and peripheral blood (PB) are roughly equivalent.[6,8,20–24] In addition, comparisons from previous studies were complicated by the inability to isolate pure populations of cells at distinct erythroid stages, a bottleneck that has recently been alleviated by the immunophenotypic characterization of each distinct stage of erythropoiesis.[18,21]

Here, we undertook a comparative analysis of the erythroid differentiation potential of human CB and PB CD34$^+$ cells, from the BFU-E to the orthochromatic erythroblast. We found that CB-derived CD34$^+$ cells differentiate at a slower rate than their adult counterparts but exhibit an increased reticulocyte differentiation potential. Furthermore, our studies reveal the existence and maintenance of a population of progenitors that is specific to PB, giving rise to both BFU-E and CFU-E. To better understand the functional differences between CB- and PB-HSPCs, we isolated individual stages of erythropoiesis and performed global gene expression profiles. These data significantly contribute to our understanding of the impact of the developmental origin of HSPCs on erythroid differentiation and provide an important resource for future studies of normal and disordered human erythropoiesis.

2 | MATERIAL AND METHODS

2.1 | CD34$^+$ cell culture, flow cytometry analysis, and fluorescence-activated cell sorting of erythroid progenitors and precursors

CB was obtained from the New York Blood Center and PB from the New York Blood Center and the Stanford Blood Center. The present study was conducted in accordance with the declaration of Helsinki and was exempt from institutional review board approval since none of the human samples had identifiable personal information. CD34$^+$ cells were purified from CB or nonmobilized PB leukoreduction filters by magnetic positive selection (Miltenyi Biotec). Erythroid differentiation of isolated CD34$^+$ cells (Figure 1A) was monitored as a function of surface marker expression on a BD LSR Fortessa (Becton Dickinson) and data subsequently analyzed using FCS express 6 software (De Novo, Inc) as previously described.[18,21] Pure populations of erythroid cells at distinct stages of differentiation were sorted using a MoFlo high-speed cell sorter (Beckman-Coulter) as previously described.[18,21]

2.2 | Antibodies

APC-conjugated CD235a (GPA), PE-conjugated-CD34, FITC-conjugated-CD36 and cell viability marker 7-AAD were purchased from BD Biosciences, PE-conjugated α4 integrin from Miltenyi Biotec, PE-Cyanine7-conjugated-IL-3R (CD123) from eBioscience, and a mouse mAb against human Band3 was used as previously described.[18]

2.3 | Colony assay

Cells were diluted to a density of 200 cells in 1 mL of MethoCult® H4434 classic medium for BFU-E colony assay with SCF, IL-3, GM-CSF and Epo and 1 mL of MethoCult® H4330 medium for CFU-E colony assay with Epo only (Stem Cell Technologies) and incubated at 37°C in a humidified atmosphere with 5% CO_2. BFU-E and CFU-E colonies were defined according to the criteria described by Dover et al.[25] CFU-E colonies were counted on day 7 and BFU-E colonies were counted on day 15 by investigators blinded to the experimental conditions.

2.4 | Cytospin preparation

Cytospins were prepared on slides (5×10^4 cells in 200 μl of PBS), using the Thermo Scientific Shandon 4 Cytospin. Slides were stained with May-Grünwald solution (Sigma) for 5 minutes, rinsed in 40 mM Tris buffer for 90 seconds, and subsequently stained with Giemsa solution (Sigma) for 15 minutes. Cells were imaged using a Leica DM2000 inverted microscope under 100× objective magnifications.

2.5 | RNA-seq and bioinformatics analysis

RNA was extracted from FACS-sorted cells at 8 distinct stages of erythropoiesis, derived from CB- and PB-CD34$^+$ cells. cDNA libraries were prepared using the Illumina TruSeq kit and sequenced on the Illumina HiSeq 2500 (Epigenomics Core of Weill Cornell Medical College, New York). This sequencing strategy produced ~15–80 million 50 bp single end reads per sample. For each distinct stage of erythropoiesis, 3 biological replicates were obtained from independently cultured and sorted samples from different donations. Quality control of reads was performed and low-quality reads removed. Reads were aligned to the hg19 reference genome using HISAT2.[26] Raw read counts were extracted from the aligned reads using the featureCounts program.[27] Differential expression analysis was assessed at each stage by comparing the two original sources of CD34$^+$ cells using the DESeq2 bioconductor package.[28] Using gene expression data from each stage, the subset of genes differentially expressed as a function of HSPC source

was split into 10 clusters using divisive hierarchical clustering. Gene ontology enrichment analysis of the gene sets was then performed on each cluster using the cluster Profiler R package[29] with the gene background of all genes expressed across all stages in both sources.

2.6 | Statistical analysis

Statistical evaluations between different experimental groups were performed using GraphPad Prism 7 (unpaired *t*-test) and $P < .05$ was considered to indicate statistical significance.

3 | RESULTS

3.1 | CB-HSPCs lead to more erythroid cells than PB-HSPCs

We first monitored the proliferative capacities of the two different sources of $CD34^+$ cells during in vitro erythroid differentiation. $CD34^+$ cells were isolated from CB or adult PB and then cultured for 15 days as described in the Material and Methods to induce their differentiation toward reticulocytes (Figure 1A). While a decrease in cell numbers was observed at Day 2 of culture of both CB and PB $CD34^+$ cells, the cells recovered thereafter and started growing exponentially. From Day 3 to Day 6, there was no noticeable difference in the growth rates between the two sources of cells. However, while cells from CB continued to grow exponentially from Day 6 until Day 12, the growth of PB-derived cells was slower with significantly fewer cells by Day 9. By the end of culture, cell growth in both cultures plateaued, suggesting a terminal erythroid differentiation with decreased division (Figure 1G). CB-HSPCs yielded 4-fold more erythroid cells than PB-HSPCs under our culture conditions (Figure 1B, $45\,085 \pm 14\,103$ vs. $10\,988 \pm 1218$; $P < .05$), suggesting that the former have an increased proliferation potential under conditions of erythroid differentiation.

3.2 | CB-HSPCs exhibit a slower kinetics of EPO-induced differentiation than PB-HSPCs

The finding that CB-HSPCs proliferated to a significantly greater extent than their adult counterpart led us to investigate the differentiation capacities of the two sources of $CD34^+$ cells. Using our recently published methods of immuno-phenotyping which allow for the characterization of each stage of human erythroid differentiation, from BFU-E to orthochromatic erythroblasts, we first monitored terminal erythroid differentiation using the expression of three surface markers, namely Glycophorin A (GPA), Band3 and α4-integrin.[18] Low, but detectable GPA expression was first observed in both cultures at Day 3. From Day 4 to Day 8, the levels of GPA increased in both cultures; however, the percentages of GPA-positive cells in adult PB-derived culture were significantly higher than that of their CB counterpart (Figure 1C). At Day 6, a mean of $42.4 \pm 3.2\%$ of PB precursors were already GPA-positive as compared to $27.2 \pm 5.8\%$ for CB precursors ($P < .01$). Similar differences were detected at Day 8, with percentages of GPA-positive cells of $80.1 \pm 3.6\%$ vs. $65.4 \pm 4.6\%$ for PB and CB precursors, respectively ($P < .05$). This difference in GPA expression was associated with a delayed terminal erythroid differentiation in the CB-derived cultures, as documented by lower levels of Band3 expression at Day 6 and Day 8 (Figure 1D,E). After Day 10, differentiation was more similar for the two progenitors as reflected by expression patterns of GPA, Band3 and α4-integrin with completion of terminal erythroid differentiation (Figure 1C-F). Furthermore, Giemsa staining reflected the differentiation delay in CB-derived cultures; pro- and basophilic erythroblasts were still detected at Day 12 (Figure 1G, arrows). These data further suggest a slower kinetics of erythroid differentiation of CB-derived $CD34^+$ HSPCs as compared to their adult PB-derived counterpart.

3.3 | Increased persistence of CD34 expression in EPO-differentiated PB-HSPCs as compared to CB-HSPCs

Since major differences were observed between Day 5 and Day 8 of culture, at a stage corresponding to the transition from CFU-E to proerythroblast, we further investigated the differentiation of erythroid progenitors and precursors based on the initial source of $CD34^+$ cells. Proerythroblasts were sorted on the basis of their expression levels of GPA, Band3, and α4-integrin and their proliferation and differentiation toward orthochromatic erythroblasts were monitored. Although it is well documented that proerythroblasts undergo 4 to 5 cell divisions to generate orthochromatic erythroblasts, no comparative studies using highly pure populations of proerythroblasts have been performed. Interestingly, the growth patterns of proerythroblasts from both CB and adult PB were very similar (Figure 2A), suggesting that the growth differences observed between CB- and PB-HSPC sources are the result of a program initiated at the earlier progenitor levels.

We therefore elected to focus on erythroid progenitors, and used the surface markers IL-3R, GPA, CD34, and CD36, to monitor differentiation of CB- or PB-HSPCs from Day 0 to Day 6. A similar pattern of expression of IL-3R and GPA was detected for both CB and PB-derived HSPCs, with a progressive loss of IL-3R and the acquisition of GPA (Figure 2B). Nevertheless, quantitatively, there were major differences between the two sources. Cells from both sources expressed comparative levels of IL-3R in the first two days of culture, but following that time point, cells derived from PB lost IL-3R at a faster rate than CB-derived progenitors (Figure 2B,C). Since erythroid colony-forming cells are enriched in the IL-3R-negative population, we further compared the differentiation potential of gated $IL\text{-}3R^-GPA^-$ cells derived from both CB and PB (Figure 2D-F).

We previously showed that erythroid differentiation is characterized by an increased expression of CD36 and a loss of CD34. While the $IL\text{-}3R^-GPA^-CD34^+CD36^-$ population predominantly generates more primitive BFU-E colonies, the $IL\text{-}3R^-GPA^-CD34^-CD36^+$ population contains CFU-E colony-forming cells. Using this gating strategy, we found that there was no difference in the relative percentages of immunophenotypically defined BFU-E ($IL\text{-}3R^-GPA^-CD34^+CD36^-$) between CB and PB throughout the culture process (Figure 2E). However, there were significantly more immunophenotypically defined CFU-E ($IL\text{-}3R^-GPA^-CD34^-CD36^+$) generated in CB in comparison to PB. Indeed, CFU-E represented 20% of the total cell population in CB-

A

	D0-7	D7-11	D11-15	D15-20
Cell conc.(10^6/ml)	0.1	0.1	1	5
Human AB Serum	3%	3%	3%	3%
Human Plasma	2%	2%	2%	2%
Insulin	10ug/ml	10ug/ml	10ug/ml	10ug/ml
Heparin	3 IU/ml	3 IU/ml	3 IU/ml	3 IU/ml
Holo-transferrin	200 ug/ml	200 ug/ml	1mg/ml	1mg/ml
EPO	3 IU/ml	1 IU/ml	1 IU/ml	
SCF	10 ng/ml	10 ng/ml		
IL-3	1ng/ml			

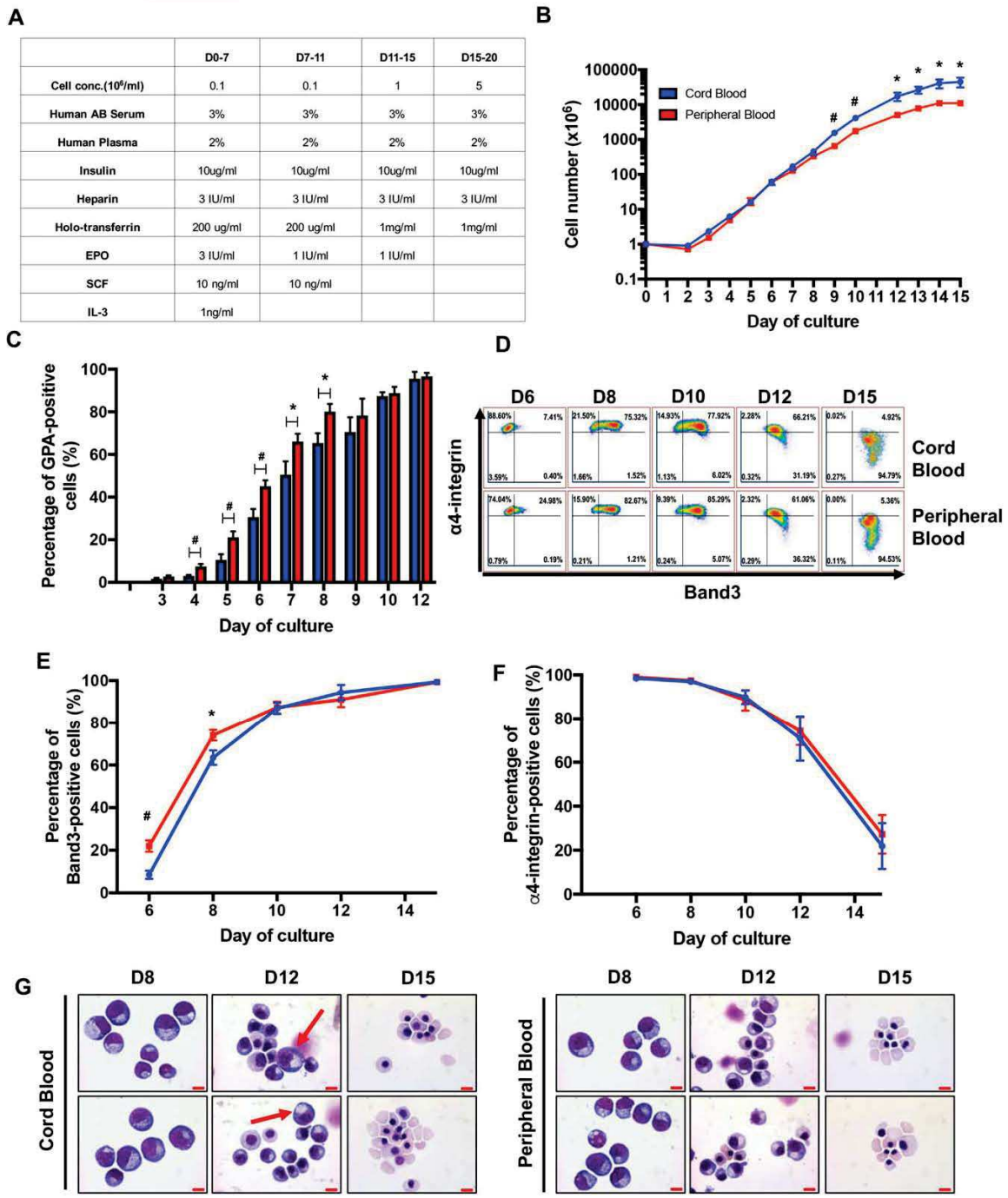

FIGURE 1 Distinct kinetics and erythroid maturation potential of CB- and PB-derived $CD34^+$ cells. (A) Description of the erythroid differentiation culture system. (B) Growth curves of CB- and PB-derived $CD34^+$ cells in erythroid culture medium ($N = 6$). (C) Quantification of GPA expression, monitored by flow cytometry, on the indicated days of culture. Means ± SEM are presented ($N = 9$). (D) Terminal erythroid differentiation was monitored on the indicated days by flow cytometry and representative plots of α4-integrin versus Band3 within the GPA^+ subset are shown ($N = 6$). (E-F) Quantitative analysis of Band3 (E) and α4-integrin (F) expression on indicated days of culture ($N = 6$). (G) Representative cytospin images of differentiated erythroblasts derived from CB and PB $CD34^+$ cells. Arrows indicate the presence of more immature precursors in CB cultures; scale bar = 10 μm. $^*P < .05$, $^{**}P < .01$, $^{\#}P < .005$ [Color figure can be viewed at wileyonlinelibrary.com]

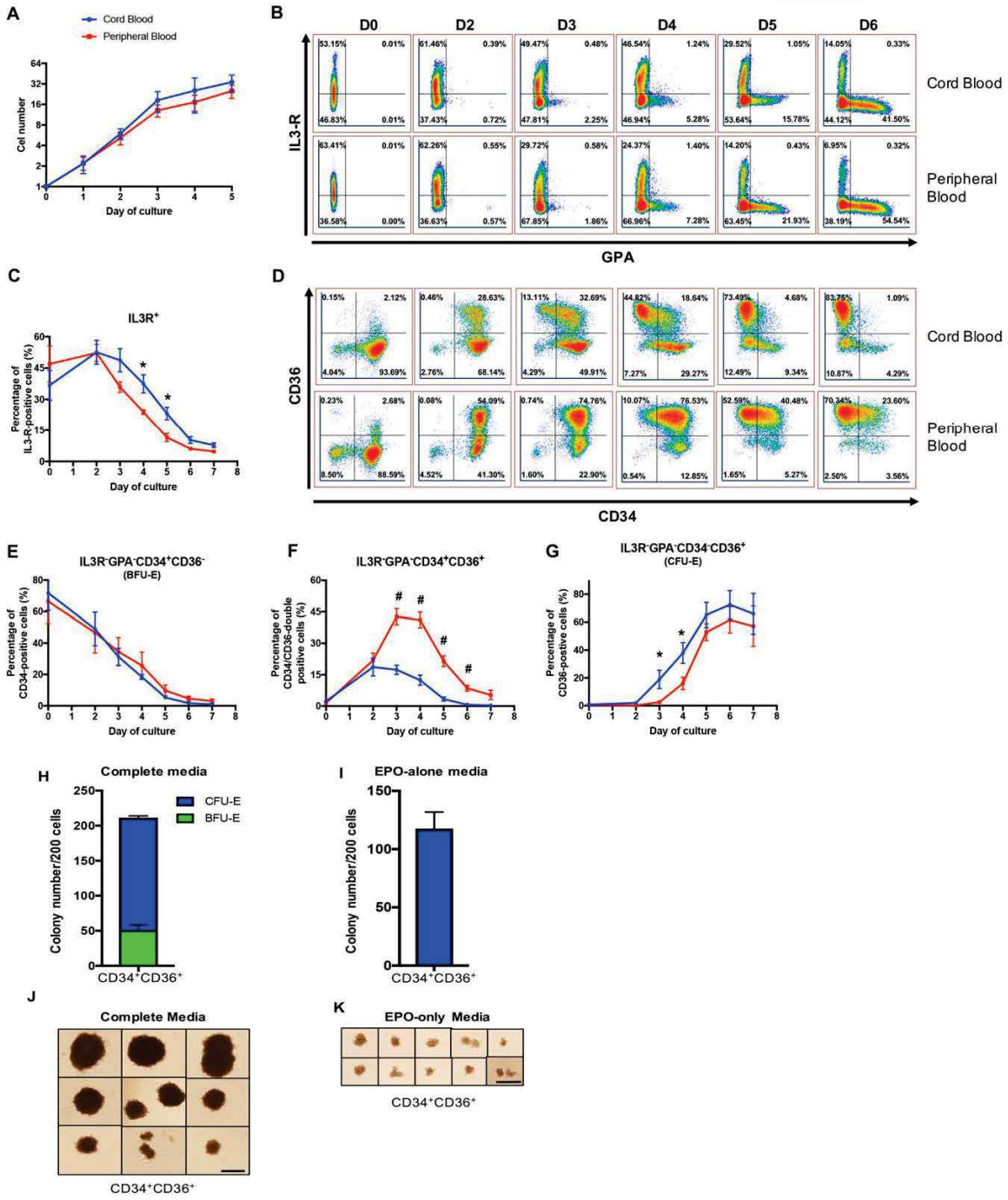

FIGURE 2 CB-HSPCs exhibit a significantly higher CFU-E differentiation potential than PB-HSPCs. **(A)** Growth curves of sorted proerythroblasts derived from CB (blue) and PB (red) $CD34^+$ cells at the indicated time points ($N = 4$). **(B)** Representative dot plots of GPA versus IL-3R expression at the indicated time points of erythroid differentiation. **(C)** Quantification of IL-3R expression at the indicated days of differentiation ($N = 6$). **(D)** Representative dot plots of CD36 versus CD34 expression within the gated $IL\text{-}3R^-/GPA^-$ population. BFU-E and CFU-E are identified as $IL\text{-}3R^-GPA^-CD34^+CD36^-$ and $IL\text{-}3R^-GPA^-CD34^-CD36^+$, respectively. **(E-G)** Quantification of the percentages of $IL\text{-}3R^-GPA^-CD34^+CD36^-$ **(E)**, $IL\text{-}3R^-GPA^-CD34^+CD36^+$ **(F)**, and $IL\text{-}3R^-GPA^-CD34^-CD36^+$ **(G)** cells at the indicated days of in vitro erythroid differentiation ($N = 6$). **(H-K)** The erythroid colony forming ability of sorted $IL\text{-}3R^-GPA^-CD34^+CD36^+$ cells derived from PB was assessed in a colony-forming assay in complete medium supporting multiple lineage colony formation **(H)** and in the presence of EPO-alone **(I)**, ($N = 3$) and representative images of erythroid colonies generated from PB-derived $IL\text{-}3R^-GPA^-CD34^+CD36^+$ cells in complete media **(J)** or EPO-alone **(K)**. Scale bar = 1 mm. $^*P < .05$, $^{**}P < .01$ [Color figure can be viewed at wileyonlinelibrary.com]

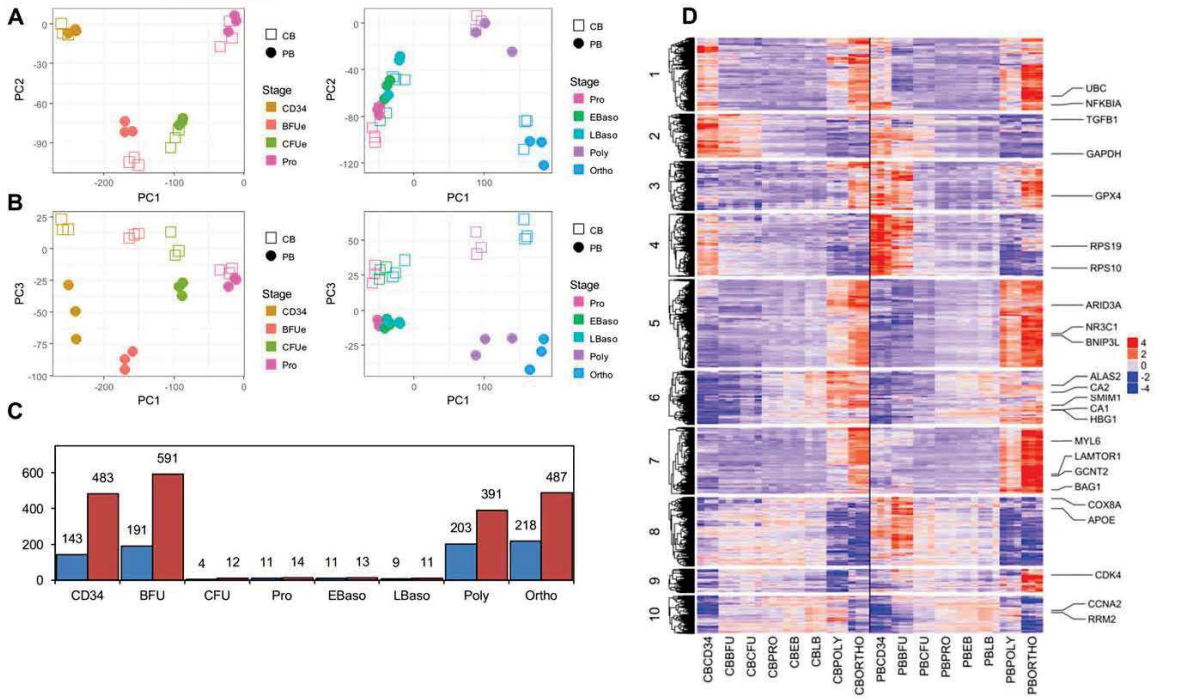

FIGURE 3 Principal Component Analysis (PCA), frequency and cluster analysis of differentially expressed genes as a function of erythroid stage and HSPC source. **(A-B)** PCA plot of 3 biological replicates of CB- and PB-derived cells at 8 different stages of erythroid differentiation. **(A)** Cells were sorted according to the PC1 and PC2 principle components; $CD34^+$ progenitors to proerythroblasts (Pro) are presented in the left panel and proerythroblasts to orthochromatic erythroblasts (Ortho) are presented in the right panel. **(B)** The same samples were sorted according to PC1 and PC3 principle components with progenitors and terminal differentiation stages presented in the left and right panels, respectively. **(C)** The number of differentially expressed genes between CB and PB at each stage of erythroid differentiation are presented. Blue bars indicate genes that are downregulated in PB as compared to CB while red bars indicate upregulated genes. **(D)** Expression values of differentially expressed genes between CB and PB, at each of 8 stages of erythroid differentiation, are shown as a heat map. In each row, the color code is used to distinguish expression levels of a particular gene as indicated in the legend. Rows are organized by divisive hierarchical clustering and split into 10 clusters for CB (left panel) and PB (right panel). Enriched GO terms for Cluster 1: unfolded proteins, Cluster 2: leukocyte migration and activation, Cluster 3: oxidative phosphorylation, Cluster 4: ribosomal proteins, Cluster 5: autophagy, Cluster 6: gas transport-related, Cluster 7: autophagy, Cluster 8: mitochondrial respiratory chain complexes and assembly, Cluster 9: RNA splicing and mitochondrial translation, and Cluster 10: cell cycle [Color figure can be viewed at wileyonlinelibrary.com]

derived cultures at Day 3 while no CFU-E were found in PB. CFU-E appeared rapidly in PB-derived cultures thereafter and by Day 5, the percentages of CFU-E in CB- and PB-derived cultures were not statistically different (Figure 2G). However, it is important to note that a subset of $CD34^+CD36^+$ cells, phenotypically located in the transition between BFU-E and CFU-E, were present at significant numbers in PB- but not CB-derived cultures, from Days 3 to 6 of culture (Figures 2D,F).

These surprising findings led us to investigate the status and overall potential of the PB-derived $CD34^+CD36^+$ population. Indeed, these cells, potentially sharing characteristics with either BFU-E and/or CFU-E, have not been previously described. We sorted cells from this population and plated 200 cells to perform functional colony-forming assays. As one would expect, these cells respond to complete medium with SCF, IL-3, GM-CSF, and EPO supporting multiple lineage colony formation (Figure 2H,J). In addition, we observed that these cells already have the ability to respond to EPO alone (Figure 2I,K), suggesting that they are already engaged in erythroid differentiation beyond the BFU-E stage. Taken together this data suggests that the $CD34^+CD36^+$ population, specific to PB-HSPCs, contains cells transitioning from a BFU-E to a CFU-E stage, with the ability to form both colonies.

3.4 | Differences in the transcriptomes of CB-derived and PB-derived HSPC

Using our defined surface markers, cells at each stage of erythroid differentiation were sorted to >95% purity and transcriptomes were compared as a function of the $CD34^+$ cell source. The principle component analysis is shown in Figure 3A and demonstrates that cells at each distinct stage of development formed distinct clusters in the first two principle components (PC1 and PC2). However, all stages from CB and PB completely separated from each other into their own clusters when viewed using the 3rd principle component (PC1 versus PC3, Figure 3B). From this analysis, we can conclude that the differences between the two sources are smaller than the differences between stages.

The principle component analysis also showed that the gene expression pattern significantly differed during the very early development stages (ie, at the CD34 and BFU-E stages) and at the very late differentiation stages (ie, Polychromatophilic and Orthochromatic erythroblasts). This is in agreement with the significant differences in differentially expressed genes between the two sources at each stage (Figure 3C).

We then undertook an in depth comparative analysis of the transcriptome of human erythropoiesis. Many of the differentially expressed genes corresponded to well characterized differences between fetal and adult erythropoiesis, and were used as internal controls for our analysis.[30] These included those responsible for hemoglobin synthesis with fetal globin genes (*HBG1*, *HBG2*, and *HBE1*) significantly upregulated in CB while adult globin genes (*HBB*, and *HBD*) were upregulated in PB. Additionally, the gene encoding the I-branching enzyme, responsible for the conversion of fetal i antigen to adult I blood group antigen GCNT2,[31–33] as well as the CA1 and CA2 genes, encoding carbonic anhydrases 1 and 2,[34,35] were upregulated in PB as compared to CB (Supporting Information Figure S1).

To gain further insights into the overall observed changes in the biological processes between CB and PB, the differentially expressed genes at all stages were clustered. Divisive hierarchical clustering was used on the gene expression profile across all stages for both sources and the dendrogram partitioned into 10 clusters as shown graphically in Figure 3D. Gene ontology (GO) enrichment analysis of the biological process gene sets was performed on each cluster (Supporting Information Table S1). Clusters 2,3,4, and 8 had gene expression patterns showing differences in expression at the CD34 and BFU-E stages between CB and PB. Of note, Cluster 2 genes showed higher expression at the CD34 and BFU-E stages in CB over PB and enriched GO terms ($P.adj < 10^{-6}$) corresponding to leukocyte migration and activation, consistent with CB being less committed to the erythroid lineage than PB which is in agreement with our earlier findings (Figure 2). Clusters 1,5,7, and 9 exhibited patterns with differences in expression at the late stages, Polychromatophilic and Orthochromatic erythroblasts. Among those, Clusters 5 and 7 presented genes with increased expression in PB compared to CB, and these genes are associated with autophagy ($P.adj < 10^{-6}$). Cluster 10 genes exhibited a general increase in expression across many stages from BFU-E to Polychromatophilic erythroblasts in CB-derived cultures and was enriched in GO terms related to cell cycle, mitosis and DNA replication ($P.adj < 10^{-6}$).

Within these clusters, we analyzed our transcriptome data on the basis of several genes critical for erythropoiesis or its regulation. The master regulators of erythropoiesis, defined as members of the core erythroid network,[36] did not differ between CB and PB (Figure 4A), highlighting the similarities between the core differentiating programs. Recently, others have suggested that regulators of globin switching differ between CB and PB. In our study however, these did not significantly change (Figure 4B), except for *MYB*, which was described as unchanged in the Merryweather-Clarke study.[23] Consistent with the flow cytometry data, genes involved in lineage commitment were upregulated in CB, at the CD34 and BFU-E stages (Figure 4C), supporting our data that CB-HSPCs have increased proliferative potential as compared to adult PB-HSPCs. This upregulation was however transient and expression levels rapidly decreased as erythroid differentiation progresses to the CFU-E stage. We also observed that genes involved in cell cycle regulation were expressed at higher levels in CB than in PB (Figure 4D). Finally, we document that genes involved in the autophagy pathway were upregulated in PB, specifically at the late stages (Figure 4E), consistent with a role for autophagy in late stages of erythropoiesis.[37,38] Altogether, these data highlight the specificity in the developmental regulation of erythropoiesis and the differences between neonatal and adult erythropoiesis.

4 | DISCUSSION

Erythropoiesis has been extensively studied with much research focusing on terminal erythroid differentiation. As such we have a better understanding of the molecular events leading to the formation of the reticulocyte from the pro-erythroblastic stage.[39] However, much less is known regarding the differentiation of human HSPCs to the precursor stages, and the events leading from the BFU-E to CFU-E progenitor stages have remained largely unexplored, mainly due to the difficulty of obtaining highly enriched populations of human erythroid progenitors. Different models have been used to study erythropoiesis, and all present their own unique advantages as well as challenges. Differences between species have been highlighted, notably with regards to changes in their transcriptomes during erythroid differentiation.[36] In the present study, we present evidence that even within the same species, the transcriptomes of erythroid progenitors differ as a function of the developmental source of HSPCs.

One of the main strengths of our study is that we used only one variable, the origin of the $CD34^+$ cells. We induced differentiation of $CD34^+$ cells from either CB or adult PB using the same culture conditions. We report that these cells exhibit distinct kinetics of differentiation and proliferation. CB-HSPCs lead to the generation of a significantly higher number of reticulocytes than adult PB-HSPC (4-fold) but their kinetics of differentiation is slower. Since the kinetics of growth from sorted pro-erythroblasts to orthochromatic erythroblasts are similar (Figure 2A), one can rule out terminal differentiation as potential mechanism for the differences observed. However, we document that CB-HSPCs retain IL-3R on their surface for a longer period time. In this context, and in accordance with our data, one may suggest that these cells can generate more immunophenotypically-defined CFU-E, which in turn will lead to a higher number of reticulocytes than PB-HSPCs.

In addition to the immunophenotypically defined $IL3R^-GPA^-CD34^-CD36^+$ that we previously characterized as a population leading to CFU-E in colony-forming assays, we observe the presence of a population specific to PB-HSPC, immunophenotypically defined as $IL3R^-GPA^-CD34^+CD36^+$. Using functional assays, we show that this population represents a transitory state during erythroid differentiation, able to give rise to both BFU-E and CFU-E in vitro. BFU-E generated from this population are heterogeneous in size, which, according to the empirical definition of a BFU-E,[40] suggests that they represent both

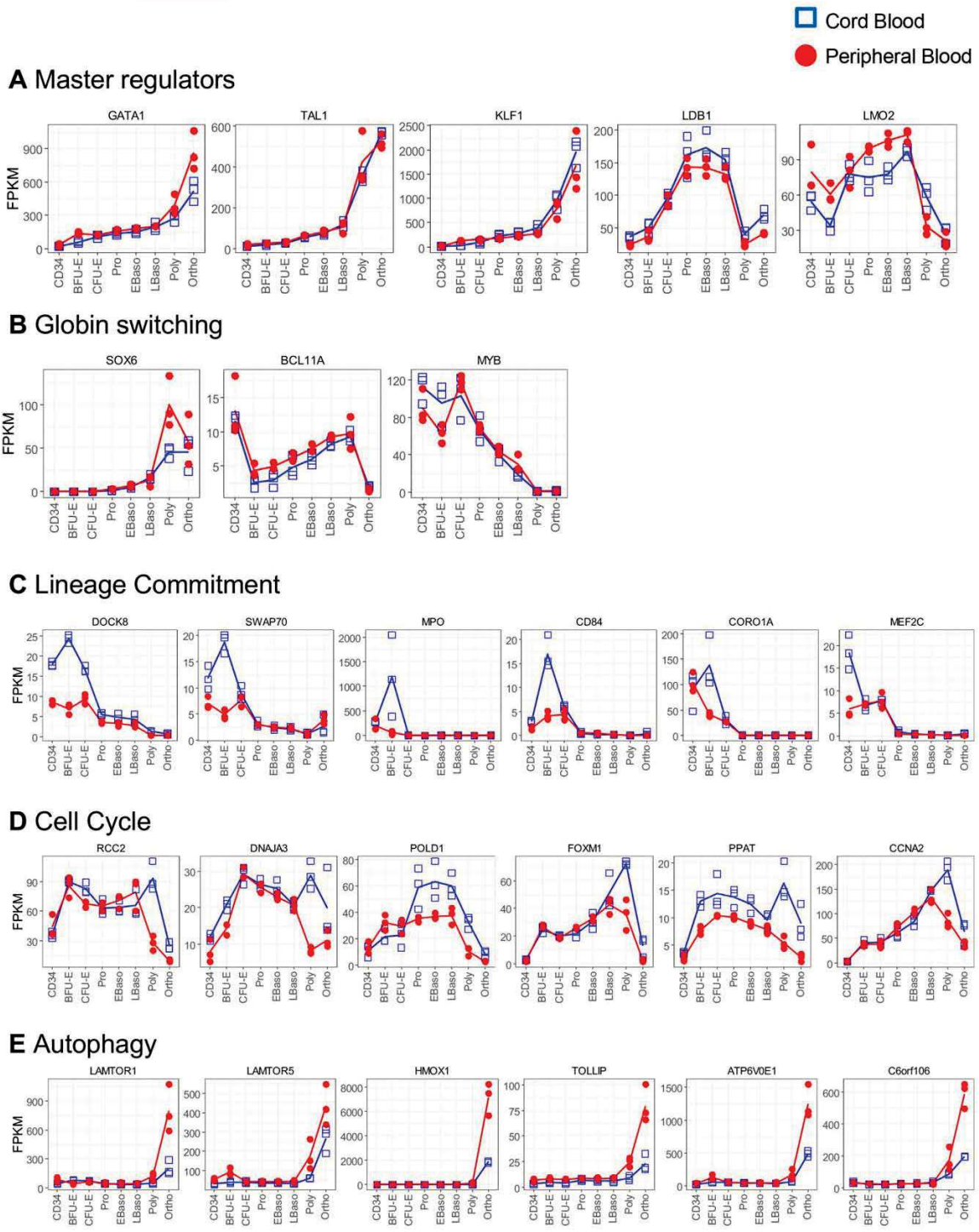

FIGURE 4 Expression profiles of specific genes that are critical for erythroid differentiation in CB- and PB-derived progenitors. **(A)** Expression profiles of master regulators of erythropoiesis are presented as a function of differentiation stage and HSPC source (CB, blue; PB, red), with 3 samples per stage. **(B)** Expression profiles of genes involved in hemoglobin switching are presented as in (A). **(C)** Presentation of the top differentially expressed genes in cluster 2, enriched in GO terms related to lineage commitment. **(D)** Presentation of the top differentially expressed genes in cluster 10, enriched in GO terms related to cell cycle. **(E)** Presentation of the top differentially expressed genes in clusters 5 and 7, enriched in GO terms related to autophagy [Color figure can be viewed at wileyonlinelibrary.com]

early and late BFU-E. It will be of interest to determine why this population is only very transient detected during the erythroid differentiation of CB-HSPCs.

This study is the first to compare the transcriptomes of sorted erythroid populations derived from PB and CB, allowing for a direct comparison of stage-specific gene expression during human erythropoiesis. One elegant study published in 2016 compared the transcriptome of human erythropoiesis using $CD34^+$ cells from CB and adult PB and highlighted a similarity between the erythroid gene expression dynamics of adult and neonatal erythropoiesis.[23] In our study, we found similar data regarding the genes encoding the core erythroid program; however, we also found significant differences. In their study, Merryweather-Clarke et al. concluded that the transcriptomes of erythroid progenitors and precursors derived from CB- and adult PB-HSPCs were not different. The apparent discrepancies may be due to differences in the in vitro culture systems used in the two studies as well as differences in the analyzed subsets. To control for changes between progenitor populations, all our subsets were sorted, fostering high-resolution transcriptomics analyses.

The culture system utilized here together with the data sets for CB- and PB-derived erythroid progenitors will allow for a more robust evaluation of changes in pathological contexts. Our comparative analysis will undoubtedly foster research of multiple diseases where differentiation is being performed on PB-HSPCs but the majority of comparative data have been obtained using CB-HSPCs.

In summary, our data demonstrate that the source of $CD34^+$ cells is critical for the study of erythropoiesis, in normal and disordered conditions. It also provides a qualitative and quantitative comparative analysis of human erythropoiesis from CB and adult PB. All of the transcriptome data are deposited on Gene Expression Omnibus (GSE107218). These data will provide a framework for studies of disordered human erythropoiesis and will foster the ex vivo evaluation of new therapeutic strategies for patients with bone marrow failure syndromes.

ACKNOWLEDGMENTS

This research was supported in part by National Institutes of Health grants DK26263 (to N.M.) and DK32094 (to N.M. and N.T.), DK090145 (to A.N.), HL134043 (subcontract to L.B), and by the Pediatric Cancer Foundation (to L.B.). A.N is the recipient of an ASH Bridge award. L.B. is the recipient of a St. Baldrick's Scholar award. N.T. and S.K are supported by a French national (ANR) research grant and the French Laboratory of excellence (Labex) GR-Ex.

CONFLICT OF INTEREST

The authors declare no competing financial interests.

AUTHOR CONTRIBUTIONS

H.Y. and J.H. designed and performed research, analyzed data, and edited the manuscript; J.J., J.L., Y.W., Y.H., and N.W. performed research, analyzed data, and edited the manuscript; X.A., and C.H. analyzed data and edited the manuscript; and S.K., N.T, N.M., A.N. and L.B designed research, analyzed data, and wrote the manuscript.

ORCID

Lionel Blanc http://orcid.org/0000-0002-0185-6260

REFERENCES

[1] Orkin SH, Zon LI. Hematopoiesis: an evolving paradigm for stem cell biology. *Cell*. 2008;132(4):631–644.

[2] Notta F, Zandi S, Takayama N, et al. Distinct routes of lineage development reshape the human blood hierarchy across ontogeny. *Science*. 2016;351(6269):aab2116.

[3] Koury MJ, Haase VH. Anaemia in kidney disease: harnessing hypoxia responses for therapy. *Nat Rev Nephrol*. 2015;11(7):394–410.

[4] Blanc L, Vidal M. Reticulocyte membrane remodeling: contribution of the exosome pathway. *Curr Opin Hematol*. 2010;17:177–183.

[5] Ney PA. Normal and disordered reticulocyte maturation. *Curr Opin Hematol*. 2011;18(3):152–157.

[6] An X, Schulz VP, Li J, et al. Global transcriptome analyses of human and murine terminal erythroid differentiation. *Blood*. 2014;123(22):3466–3477.

[7] An X, Schulz VP, Mohandas N, et al. Human and murine erythropoiesis. *Curr Opin Hematol*. 2015;22(3):206–211.

[8] Pishesha N, Thiru P, Shi J, et al. Transcriptional divergence and conservation of human and mouse erythropoiesis. *Proc Natl Acad Sci UsaU S A*. 2014;111(11):4103–4108.

[9] Ulirsch JC, Lacy JN, An X, et al. Altered chromatin occupancy of master regulators underlies evolutionary divergence in the transcriptional landscape of erythroid differentiation. *PLoS Genet*. 2014;10(12):e1004890.

[10] Brand M, Ranish JA, Kummer NT, et al. Dynamic changes in transcription factor complexes during erythroid differentiation revealed by quantitative proteomics. *Nat Struct Mol Biol*. 2004;11(1):73–80.

[11] Hricik T, Federici G, Zeuner A, et al. Transcriptomic and phosphoproteomic analyzes of erythroblasts expanded in vitro from normal donors and from patients with polycythemia vera. *Am J Hematol*. 2013;88(9):723–729.

[12] Montel-Hagen A, Blanc L, Boyer-Clavel M, et al. The Glut1 and Glut4 glucose transporters are differentially expressed during perinatal and postnatal erythropoiesis. *Blood*. 2008;112(12):4729–4738.

[13] Richardson BM, Heesom KJ, Parsons SF, et al. Analysis of the differential proteome of human erythroblasts during in vitro erythropoiesis by 2-D DIGE. *Prot Clin Appl*. 2009;3(9):1123–1134.

[14] Fibach E, Manor D, Oppenheim A, et al. Proliferation and maturation of human erythroid progenitors in liquid culture. *Blood*. 1989;73(1):100–103.

[15] Dulmovits BM, Appiah-Kubi AO, Papoin J, et al. Pomalidomide reverses gamma-globin silencing through the transcriptional reprogramming of adult hematopoietic progenitors. *Blood*. 2016;127(11):1481–1492.

[16] Giarratana MC, Kobari L, Lapillonne H, et al. Ex vivo generation of fully mature human red blood cells from hematopoietic stem cells. *Nat Biotechnol*. 2005;23(1):69–74.

[17] Giarratana MC, Rouard H, Dumont A, et al. Proof of principle for transfusion of in vitro-generated red blood cells. *Blood*. 2011;118(19):5071–5079.

[18] Hu J, Liu J, Xue F, et al. Isolation and functional characterization of human erythroblasts at distinct stages: implications for understanding of normal and disordered erythropoiesis in vivo. *Blood*. 2013;121(16):3246–3253.

[19] Oburoglu L, Tardito S, Fritz V, et al. Glucose and glutamine metabolism regulate human hematopoietic stem cell lineage specification. *Cell Stem Cell*. 2014;15(2):169–184.

[20] Gautier EF, Ducamp S, Leduc M, et al. Comprehensive proteomic analysis of human erythropoiesis. *Cell Rep*. 2016;16(5):1470–1484.

[21] Li J, Hale J, Bhagia P, et al. Isolation and transcriptome analyses of human erythroid progenitors: BFU-E and CFU-E. *Blood*. 2014;124(24):3636–3645.

[22] Merryweather-Clarke AT, Atzberger A, Soneji S, et al. Global gene expression analysis of human erythroid progenitors. *Blood*. 2011;117(13):e96–108.

[23] Merryweather-Clarke AT, Tipping AJ, Lamikanra AA, et al. Distinct gene expression program dynamics during erythropoiesis from human induced pluripotent stem cells compared with adult and cord blood progenitors. *BMC Genomics*. 2016;17(1):817.

[24] Xu J, Shao Z, Glass K, et al. Combinatorial assembly of developmental stage-specific enhancers controls gene expression programs during human erythropoiesis. Dev. *Cell*. 2012;23(4):796–811.

[25] Dover GJ, Chan T, Sieber F. Fetal hemoglobin production in cultures of primitive and mature human erythroid progenitors: differentiation affects the quantity of fetal hemoglobin produced per fetal-hemoglobin-containing cell. *Blood*. 1983;61(6):1242–1246.

[26] Kim D, Langmead B, Salzberg SL. HISAT: a fast spliced aligner with low memory requirements. *Nat Methods*. 2015;12(4):357–360.

[27] Liao Y, Smyth GK, Shi W. featureCounts: an efficient general purpose program for assigning sequence reads to genomic features. *Bioinformatics*. 2014;30(7):923–930.

[28] Love MI, Huber W, Anders S. Moderated estimation of fold change and dispersion for RNA-seq data with DESeq2. *Genome Biol*. 2014;15(12):550

[29] Yu G, Wang LG, Han Y, et al. clusterProfiler: an R package for comparing biological themes among gene clusters. *OMICS*. 2012;16(5):284–287.

[30] Sankaran VG, Xu J, Orkin SH. Advances in the understanding of haemoglobin switching. *Br J Haematol*. 2010;149(2):181–194.

[31] Marsh WL. Anti-i: a cold antibody defining the Ii relationship in human red cells. *Br J Haematol*. 1961;7:200–209.

[32] Marsh WL, Nichols ME, Reid ME. The definition of two I antigen components. *Vox Sang*. 1971;20(3):209–217.

[33] Yu LC, Twu YC, Chang CY, et al. Molecular basis of the adult i phenotype and the gene responsible for the expression of the human blood group I antigen. *Blood*. 2001;98(13):3840–3845.

[34] Boyer SH, Siegel S, Noyes AN. Developmental changes in human erythrocyte carbonic anhydrase levels: coordinate expression with adult hemoglobin. Dev. *Biol*. 1983;97(1):250–253.

[35] Weil SC, Walloch J, Frankel SR, et al. Expression of carbonic anhydrase and globin during erythropoiesis in vitro. *Ann N Y Acad Sci*. 1984;429:335–337.

[36] Nandakumar SK, Ulirsch JC, Sankaran VG. Advances in understanding erythropoiesis: evolving perspectives. *Br J Haematol*. 2016;173(2):206–218.

[37] Betin VM, Singleton BK, Parsons SF, et al. Autophagy facilitates organelle clearance during differentiation of human erythroblasts: evidence for a role for ATG4 paralogs during autophagosome maturation. *Autophagy*. 2013;9(6):881–893.

[38] Griffiths RE, Kupzig S, Cogan N, et al. The ins and outs of human reticulocyte maturation: autophagy and the endosome/exosome pathway. *Autophagy*. 2012;8(7):1150–1151.

[39] Ji P. New insights into the mechanisms of mammalian erythroid chromatin condensation and enucleation. *Int Rev Cell Mol Biol*. 2015;316:159–182.

[40] Axelrad A, McLeod D, Shreeve M, Heath D. Properties of cells that produce erythropoietic colonies in vitro. In: Robinson W, ed. *Hemopoiesis in Culture, US Government Printing Office*. Bethesda, MD; 1974:226–237.

SUPPORTING INFORMATION

Additional Supporting Information may be found online in the supporting information tab for this article.

How to cite this article: Yan H, Hale J, Jaffray J, et al. Developmental differences between neonatal and adult human erythropoiesis. *Am J Hematol*. 2018;00:1–10. https://doi.org/10.1002/ajh.25015

Original article 2

An IDH1-vitamin C crosstalk drives human erythroid development by inhibiting pro-oxidant mitochondrial metabolism

Pedro Gonzalez-Menendez,1,2,10,* Manuela Romano,1,2,10 **Hongxia Yan**,1,3 Ruhi Deshmukh,4 Julien Papoin,5 Leal Oburoglu,1,2 Marie Daumur,1,2 Anne-Sophie Dume´ ,1,2 Ira Phadke,1,2,6 Ce´ dric Mongellaz,1,2 Xiaoli Qu,3 Phuong-Nhi Bories,7 Michaela Fontenay,2,7 Xiuli An,3 Vale´ rie Dardalhon,1,2 Marc Sitbon,1,2 Vale´ rie S. Zimmermann,1,2 Patrick G. Gallagher,8 Saverio Tardito,4,9 Lionel Blanc,6 Narla Mohandas,3 Naomi Taylor,1,2,7,11,* and Sandrina Kinet1,2,*

1Institut de Ge´ ne´ tique Mole´ culaire de Montpellier, Univ. Montpellier, CNRS, Montpellier, France. 2 Laboratory of Excellence GR-Ex, Paris 75015, France. 3 New York Blood Center, New York, NY, USA. 4 Cancer Research UK Beatson Institute, Glasgow G61 1BD, UK. 5 The Feinstein Institute for Medical Research, Manhasset, NY, USA. 6 Pediatric Oncology Branch, NCI, CCR, NIH, Bethesda, MD, USA. 7 Service d'He´ matologie Biologique, Assistance Publique-H^opitaux de Paris, Institut Cochin, Paris, France. 8 Departments of Pediatrics and Genetics, Yale University School of Medicine, New Haven, CT, USA. 9 Institute of Cancer Sciences, University of Glasgow, Glasgow G61 1QH, UK.

10 These authors contributed equally

*Correspondence: pedro.gonzalez-menendez@igmm.cnrs.fr (P.G.-M.), taylorn4@mail.nih.gov (N.T.), kinet@igmm.cnrs.fr (S.K.)

https://doi.org/10.1016/j.celrep.2021.108723

Cell Reports

Article

An IDH1-vitamin C crosstalk drives human erythroid development by inhibiting pro-oxidant mitochondrial metabolism

Graphical Abstract

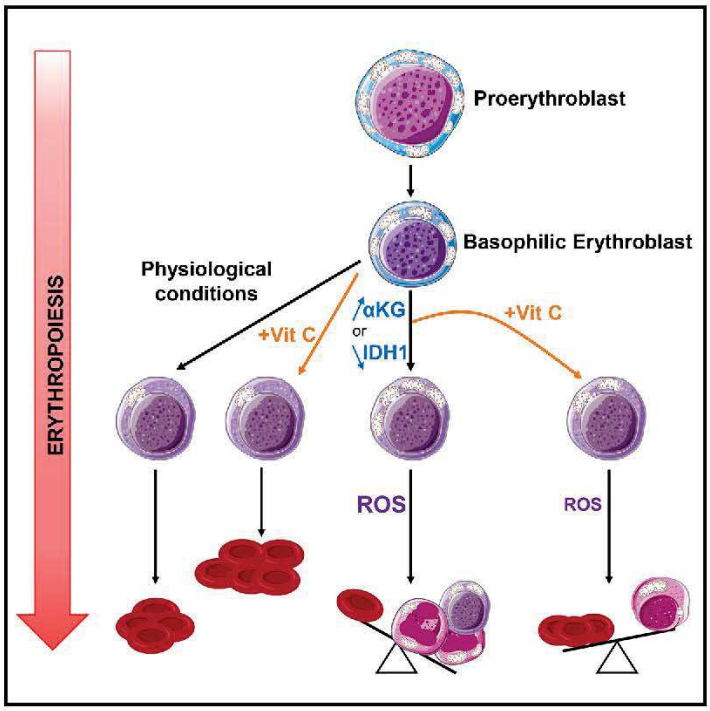

Highlights

- Glutamine-dependent OXPHOS drives early erythroid differentiation
- OXPHOS-induced ROS inhibit erythroblast enucleation
- IDH1 downregulation augments ROS, leading to pathological erythroid differentiation
- Vitamin C rescues erythroid differentiation under conditions of oxidative stress

Authors

Pedro Gonzalez-Menendez, Manuela Romano, Hongxia Yan, ..., Narla Mohandas, Naomi Taylor, Sandrina Kinet

Correspondence

pedro.gonzalez-menendez@igmm.cnrs.fr (P.G.-M.), taylorn4@mail.nih.gov (N.T.), kinet@igmm.cnrs.fr (S.K.)

In Brief

Gonzalez-Menendez et al. show that terminal erythroid differentiation is dependent on the suppression of mitochondrial metabolism. Disturbances in levels of the α-ketoglutarate and IDH1 TCA-cycle regulators result in ineffective erythropoiesis, with generation of morphologically abnormal erythroblasts. Vitamin C restores redox homeostasis and rescues late-stage erythropoiesis by scavenging reactive oxygen species.

Gonzalez-Menendez et al., 2021, Cell Reports *34*, 108723
February 2, 2021
https://doi.org/10.1016/j.celrep.2021.108723

Cell Reports

CellPress
OPEN ACCESS

Article

An IDH1-vitamin C crosstalk drives human erythroid development by inhibiting pro-oxidant mitochondrial metabolism

Pedro Gonzalez-Menendez,[1,2,10,*] Manuela Romano,[1,2,10] Hongxia Yan,[1,3] Ruhi Deshmukh,[4] Julien Papoin,[5] Leal Oburoglu,[1,2] Marie Daumur,[1,2] Anne-Sophie Dumé,[1,2] Ira Phadke,[1,2,6] Cédric Mongellaz,[1,2] Xiaoli Qu,[3] Phuong-Nhi Bories,[7] Michaela Fontenay,[2,7] Xiuli An,[3] Valérie Dardalhon,[1,2] Marc Sitbon,[1,2] Valérie S. Zimmermann,[1,2] Patrick G. Gallagher,[8] Saverio Tardito,[4,9] Lionel Blanc,[6] Narla Mohandas,[3] Naomi Taylor,[1,2,7,11,*] and Sandrina Kinet[1,2,*]

[1]Institut de Génétique Moléculaire de Montpellier, Univ. Montpellier, CNRS, Montpellier, France
[2]Laboratory of Excellence GR-Ex, Paris 75015, France
[3]New York Blood Center, New York, NY, USA
[4]Cancer Research UK Beatson Institute, Glasgow G61 1BD, UK
[5]The Feinstein Institute for Medical Research, Manhasset, NY, USA
[6]Pediatric Oncology Branch, NCI, CCR, NIH, Bethesda, MD, USA
[7]Service d'Hématologie Biologique, Assistance Publique-Hôpitaux de Paris, Institut Cochin, Paris, France
[8]Departments of Pediatrics and Genetics, Yale University School of Medicine, New Haven, CT, USA
[9]Institute of Cancer Sciences, University of Glasgow, Glasgow G61 1QH, UK
[10]These authors contributed equally
[11]Lead contact
*Correspondence: pedro.gonzalez-menendez@igmm.cnrs.fr (P.G.-M.), taylorn4@mail.nih.gov (N.T.), kinet@igmm.cnrs.fr (S.K.)
https://doi.org/10.1016/j.celrep.2021.108723

SUMMARY

The metabolic changes controlling the stepwise differentiation of hematopoietic stem and progenitor cells (HSPCs) to mature erythrocytes are poorly understood. Here, we show that HSPC development to an erythroid-committed proerythroblast results in augmented glutaminolysis, generating alpha-ketoglutarate (αKG) and driving mitochondrial oxidative phosphorylation (OXPHOS). However, sequential late-stage erythropoiesis is dependent on decreasing αKG-driven OXPHOS, and we find that isocitrate dehydrogenase 1 (IDH1) plays a central role in this process. IDH1 downregulation augments mitochondrial oxidation of αKG and inhibits reticulocyte generation. Furthermore, IDH1 knockdown results in the generation of multinucleated erythroblasts, a morphological abnormality characteristic of myelodysplastic syndrome and congenital dyserythropoietic anemia. We identify vitamin C homeostasis as a critical regulator of ineffective erythropoiesis; oxidized ascorbate increases mitochondrial superoxide and significantly exacerbates the abnormal erythroblast phenotype of IDH1-downregulated progenitors, whereas vitamin C, scavenging reactive oxygen species (ROS) and reprogramming mitochondrial metabolism, rescues erythropoiesis. Thus, an IDH1-vitamin C crosstalk controls terminal steps of human erythroid differentiation.

INTRODUCTION

Hematopoietic stem cell (HSC) numbers as well as their differentiation state are tightly regulated throughout the lifetime of an individual, allowing the sustained production of all mature blood lineages under physiological conditions. Circulating mature erythrocytes are a terminally differentiated product of HSCs that have undergone a series of lineage-fate engagements that gradually restrict their potential, resulting in a commitment to the erythroid lineage. Commitment defines the beginning of erythropoiesis; a three-stage process characterized by early erythropoiesis, terminal erythroid differentiation, and reticulocyte maturation. Early erythropoiesis is characterized by commitment of multilineage progenitor cells into erythroid progenitor cells, with proliferation and development into erythroid burst-forming unit cells, followed by erythroid colony-forming unit cells and proerythroblasts. Terminal erythroid differentiation begins with proerythroblasts differentiating in a stepwise manner to early then late basophilic erythroblasts, polychromatic erythroblasts, and orthochromatic erythroblasts that enucleate to become reticulocytes.

Erythropoiesis is a metabolically daunting process when evaluated at the level of cell numbers. In healthy adults, committed erythroid progenitors support the production of 2.4 million erythrocytes per second via a synchronized regulation of iron, glucose, fatty acid, and amino acid metabolism. Iron is indispensable for heme biosynthesis in erythroblasts (Oburoglu et al., 2016). The utilization of both glutamine and glucose in *de novo* nucleotide biosynthesis is a *sine qua non* for erythroid differentiation (Oburoglu et al., 2014), and glutamine-derived

This is an open access article under the CC BY-NC-ND license (http://creativecommons.org/licenses/by-nc-nd/4.0/).

production of succinyl-coenzyme A (succinyl-CoA) is also required for the production of heme (Burch et al., 2018). Furthermore, amino acids regulate mTOR signaling (Chung et al., 2015) as well as lipid metabolism (Huang et al., 2018) during erythropoiesis. The critical nature of metabolism in erythroid differentiation is further highlighted by the recent identification of "metabolic regulators" as an erythropoietin (EPO)-induced phosphorylation target set (Held et al., 2020).

It is important though to note that terminal erythroid differentiation is a distinctive process; each mitosis results in the production of daughter cells that differ, morphologically and functionally, from their parent cells. This sequential maturation is tightly regulated at each stage of erythroid differentiation, associated with decreased cell size, enhanced chromatin condensation, progressive hemoglobinization, and changes in membrane organization and transcriptome specificities (An et al., 2014; Hu et al., 2013; Li et al., 2014; Ludwig et al., 2019; Schulz et al., 2019). Moreover, during the late stages of mammalian terminal erythroid differentiation, erythroblasts expel their nuclei and lose all organelles, including mitochondria (Moras et al., 2017). Thus, the constraints of a late-stage terminally differentiating erythroblast differ significantly from that of an erythroid-committed progenitor early in erythroid development. Indeed, in mice, early-stage erythroid progenitors have been found to require mTORC1-mediated mitochondrial biogenesis and reactive oxygen species (ROS) production (Liu et al., 2017; Luo et al., 2017; Zhao et al., 2016), while terminal erythropoiesis requires that cells be protected from oxidative stress (Case et al., 2013; Filippi and Ghaffari, 2019; Hyde et al., 2012; Xu et al., 2019; Zhao et al., 2016).

Significant differences in murine versus human erythroid development have been documented, especially as relates to the diversity of erythroid progenitor subpopulations in human bone marrow (BM) (Gautier et al., 2020; Schulz et al., 2019; Yan et al., 2018). Furthermore, regarding oxidative stress, it is important to note that murine and human erythropoiesis differ dramatically as a function of vitamin C/ascorbate plasma concentrations and expression of the SLC2A1/GLUT1 transporter, shuttling dehydroascorbic acid (DHA) across the membrane and rapidly reducing it to ascorbate (reviewed by May et al., 2001). Indeed, humans exhibit a deficiency in vitamin C production, due to inactivation of L-gulono-γ-lactone oxidase (GLO), the enzyme that catalyzes the terminal step of L-ascorbic acid (AA) biosynthesis (Burns, 1957). While human erythrocytes express the highest level of the GLUT1 transporter, harboring greater than 200,000 molecules per cell (Helgerson and Carruthers, 1987; Mueckler, 1994), we found that erythroid GLUT1 expression is a specific feature of mammals that have lost the ability to synthesize AA from glucose (Montel-Hagen et al., 2008a, 2008b). This potential evolutionary compensation, and subsequent alterations in the ability of plasma vitamin C to scavenge ROS/reactive nitrogen species (RNS), make it critical to evaluate the stepwise changes that regulate the progression of human erythropoiesis.

Here, we demonstrate that during the early stages of human red blood cell development, erythroid progenitors exhibit increased oxidative phosphorylation (OXPHOS) activity. This correlated with the increased generation of the alpha-ketoglutarate (αKG) TCA-cycle intermediate, generated by the anaplerotic utilization of glutamine, and a directly augmented OXPHOS. However, upon terminal differentiation of erythroblasts, mitochondrial biomass, OXPHOS, mitochondrial ROS, and superoxide production were all markedly decreased. Supraphysiological levels of αKG markedly attenuated terminal erythroid differentiation and enucleation. The impact of αKG was directly coupled to its role in mitochondrial metabolism, as enucleation was similarly inhibited by mitochondrial ROS and superoxide, induced by MitoParaquat (MitoPQ) or DHA. Moreover, enucleation was rescued by ROS scavengers, including vitamin C, glutathione (GSH), N-acetylcysteine (NAC), and vitamin E.

We identified the cytoplasmic isocitrate dehydrogenase 1 (IDH1) enzyme, catalyzing the interconversion between αKG and isocitrate, as a critical enzyme in this process. Lentiviral-mediated downregulation of IDH1, by significantly increasing mitochondrial metabolism and mitochondrial superoxide production, dramatically inhibited enucleation and resulted in the generation of abnormal multinucleated erythroblasts. Notably, both αKG and DHA markedly exacerbated the negative impact of IDH1 downregulation, while the vitamin C antioxidant rescued erythroid differentiation. Indeed, the vitamin-C-mediated quenching of ROS in erythroblasts accelerated human erythroid differentiation. This effect was specific to an IDH1-vitamin C axis; inhibition of TET2 in late-stage erythroblasts did not attenuate enucleation. Thus, our data identify IDH1 as a critical regulator of redox homeostasis, promoting late-stage erythropoiesis. Furthermore, these results highlight the therapeutic potential of vitamin C in human erythropoiesis, especially under pathological conditions where ROS are increased and vitamin C levels are not sufficient to combat oxidative damage.

RESULTS

Early erythropoiesis is associated with augmented glutamine utilization and OXPHOS

As glutaminolysis is required for erythroid lineage specification (Oburoglu et al., 2014), we evaluated the utilization of glutamine during early stages of human erythropoiesis at day 4 following recombinant erythropoietin (rEPO) stimulation, a time point at which the erythroid markers CD36, CD71 (transferrin receptor), and glycophorin A (GlyA) are upregulated (Figure S1A). The anaplerotic contribution of glutamine can be evaluated by tracing glutamine labeled with heavy stable carbons and nitrogens ($^{13}C_5{}^{15}N_2$). As shown in Figure 1A, the portion of glutamate derived from $^{13}C_5{}^{15}N_2$ glutamine, a measure of glutaminase activity, increased significantly following erythropoietin-induced erythroid differentiation of human $CD34^+$ progenitors ($p < 0.05$; Figure 1A). Additionally, the contribution of labeled glutamine to the pool of glutamate ($^{13}C_5{}^{15}N_1$ glutamate/$^{13}C_0$ glutamate) as well as the portion of $^{13}C_5$ labeled αKG increased significantly upon erythroid differentiation. This glutamate-derived generation of αKG was critical for OXPHOS in erythroid progenitors, as the oxygen consumption rate (OCR) was abrogated by the aminooxyacetic acid (AOA) transaminase inhibitor, blocking conversion of glutamate to αKG, and was completely restored by αKG supplementation (Figure 1B).

These data show that glutamine supports the tricarboxylic acid (TCA) cycle and downstream OXPHOS via the cataplerotic

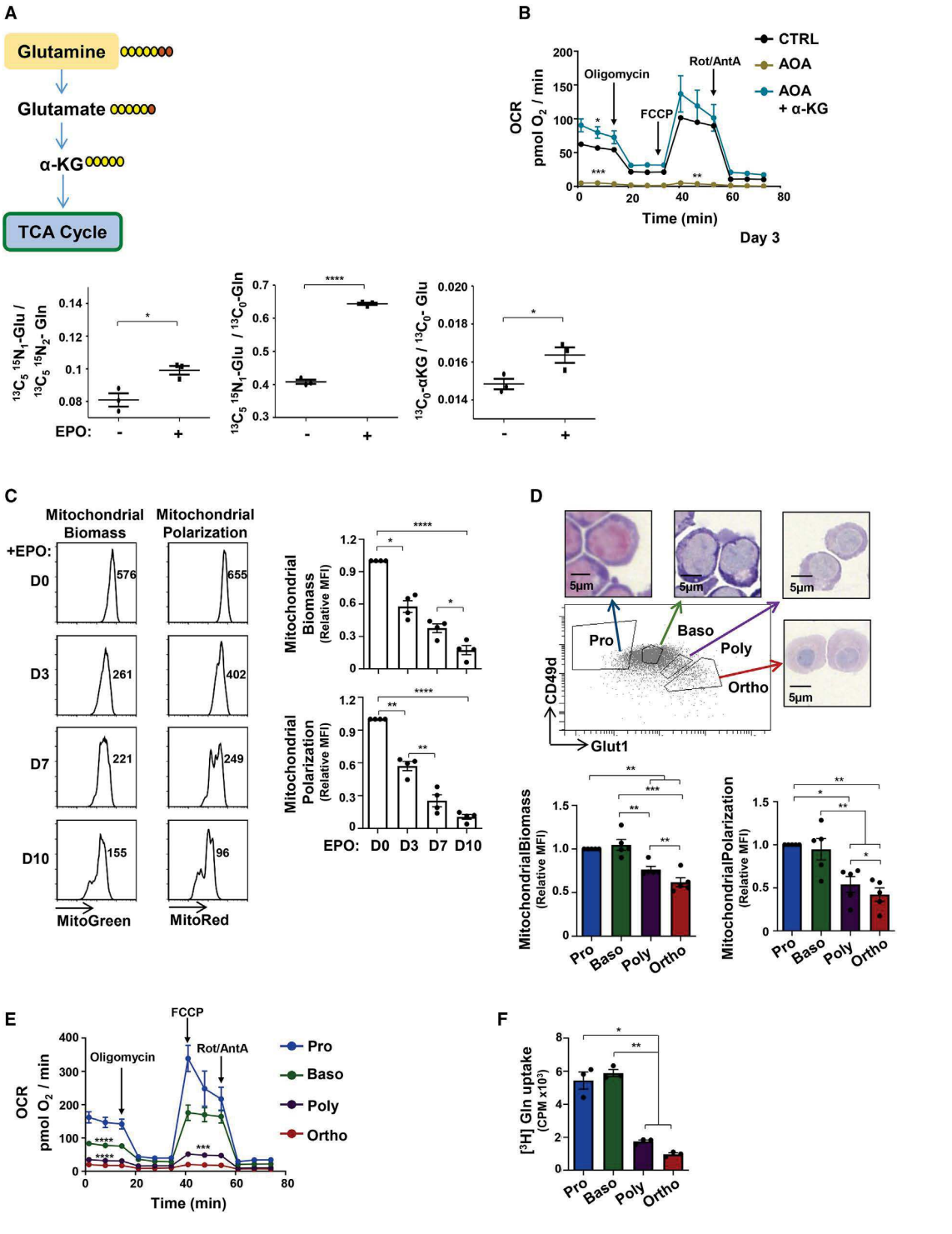

(legend on next page)

utilization of αKG. As each stage of terminal erythroid differentiation is defined by a decreased cell size with the final stage of erythropoiesis resulting in enucleation and reticulocyte maturation, we assessed whether mitochondrial biomass and transmembrane polarization decrease following commitment of progenitors to an erythroid lineage fate. Indeed, both mitochondrial biomass and polarization, evaluated by MitoGreen and MitoRed staining, respectively, decreased massively upon erythroid differentiation, monitored as a function of day of differentiation (days 0–10) as well as on erythroblast subsets fluorescence-activated cell sorting (FACS) sorted on the basis of their CD49d/GLUT1 staining profiles ($p < 0.05$ to $p < 0.0001$; Figures 1C, 1D, and S1B).

These changes in mitochondrial biomass and polarization had functional consequences on terminal erythroid differentiation (Figure 1D). Erythroblasts at distinct stages of differentiation exhibited significant differences in their levels of OXPHOS, as estimated by their OCRs; basal OCR decreased from 146.9 ± 15.5 to 17.5 ± 0.6 pmol O_2/min between the proerythroblast and orthochromatic erythroblast stages of differentiation ($p < 0.0001$; Figure 1E). Notably, the respiratory capacities of both polychromatic and orthochromatic subsets were minimal; neither of these terminal subsets exhibited a spare respiratory capacity, as measured by the ability of the cell to increase its respiration in response to an Carbonyl cyanide-4-(trifluoromethoxy)phenylhydrazone (FCCP)-mediated disruption of mitochondrial membrane potential (Figure 1E). Similarly, these differences were also detected with increasing time after EPO induction (Figure S1C). Consistent with a critical role for glutamine in the oxidative potential of the erythroblast, glutamine uptake was significantly higher in proerythroblasts and basophilic erythroblasts than in polychromatic/orthochromatic erythroblasts ($p < 0.01$; Figure 1F). Thus, in marked contrast with the high-energy state of early erythroid progenitors, terminal maturation results in a significant attenuation of glutamine uptake and an associated decrease in OXPHOS.

αKG increases mitochondrial function while negatively regulating terminal erythroid differentiation and enucleation

As decreased mitochondrial function of terminally differentiated erythroblasts was associated with decreased glutamine uptake, we evaluated whether αKG, the anaplerotic product of glutamine that enters into the TCA cycle, directly contributed to the erythroblast's respiratory capacity. Importantly, we found that αKG directly regulates the metabolic state of progenitors, as the injection of a cell-permeable αKG immediately augmented the maximal respiratory capacity of erythroblasts at both day 3 and day 7 of EPO induction ($p < 0.001$ and $p < 0.0001$; Figure 2A). This increase in OXPHOS did not alter the generation of CD34$^+$ CD36$^+$ committed erythroid colony-forming unit (CFU-E) progenitors or GlyA$^+$ erythroblasts or the upregulation of CD36 or CD71 erythroid markers (Figures 2B and S2A). While αKG did not alter mitochondrial biomass or polarization at early stages of development (day 3; Figure S2B), it substantially affected these parameters when it was added only at later stages (from days 7 to 10). Mitochondrial biomass and polarization were significantly higher in αKG-supplemented late-stage erythroblasts than in control erythroblasts ($p < 0.01$ and $p < 0.001$; Figure 2C). Furthermore, progression from the CD49d$^+$GLUT1$^+$ basophilic erythroblast to the CD49d Glut1$^+$ orthochromatic stage was significantly inhibited by αKG ($p < 0.05$ and $p < 0.01$; Figure 2D). This phenomenon was also associated with a significantly attenuated level of enucleation, decreasing by 32% ± 7% and 52% ± 7% in the presence of αKG at days 10 and 14 of erythroid differentiation, respectively ($p < 0.001$ and $p < 0.01$; Figure 2D). Notably, this effect was specific to αKG and was not recapitulated by other TCA-cycle intermediates such as succinate or citrate (Figure S2C).

Augmented mitochondrial superoxide generation at the basophilic erythroblast stage abrogates terminal erythroid differentiation and enucleation

Generation of ROS within mitochondria is associated with the oxidative function of these organelles (Adam-Vizi and Tretter, 2013; Murphy, 2009), and αKG can directly contribute to ROS generation through the catalytic activity of αKG dehydrogenase (αKGDH) (Starkov et al., 2004; Tretter and Adam-Vizi, 2004). NADH produced by αKGDH also stimulates superoxide production by complex I of the electron transport chain (ETC; Figure 3A) (Adam-Vizi and Tretter, 2013; Murphy, 2009). We therefore evaluated whether addition of αKG, the substrate of αKGDH, alters

Figure 1. Early erythropoiesis results in increased metabolism followed by decreased mitochondrial activity during terminal erythroid differentiation

(A) Schematic representation of glutamine conversion to α-ketoglutarate (αKG), showing the metabolism of [$^{13}C_5{}^{15}N_2$] heavy-labeled glutamine (Gln) carbons (yellow) and nitrogens (orange; top). Peak area ratios of heavy atoms from [$^{13}C_5{}^{15}N_2$]Gln into glutamate ([$^{13}C_5{}^{15}N_1$]Glu), the relative level of [$^{13}C_5{}^{15}N_1$]Glu, and the portion of [$^{13}C_5$]αKG at day 4 of differentiation in the absence or presence of rEPO are shown (±SEM). Horizontal lines represent mean levels. Each dot represents an individual technical replicate, representative of one of two independent experiments.

(B) Oxygen consumption rates (OCRs), a measure of OXPHOS, were monitored by sequential injection of oligomycin, FCCP, and rotenone/antimycin A (Rot/AntA) as indicated. Mean basal oxygen consumption, maximal consumption following FCCP, and minimal levels following inhibition of the electron transport chain (ETC) Rot/AntA (bottom panel) are presented at day 3 of erythroid differentiation in control conditions (CTRL), in the presence of the AOA transaminase inhibitor (1 mM) or AOA + αKG (3.5mM). Means ± SEM are presented (n = 3).

(C) Mitochondrial biomass and polarization were evaluated by MitoTracker Green and MitoTracker Red staining, respectively, at days 0, 3, 7, and 10 of differentiation (n = 4).

(D) Pro-erythroblasts (Pro) and basophilic (Baso), polychromatic (Poly), and orthochromatic (Ortho) erythroblasts were sorted as a function of their GLUT1/CD49d profile (top panel). H&E staining of sorted erythroblasts is shown. Mitochondrial biomass and polarization were evaluated as in (C), and means ± SEM are presented (n = 5).

(E) OCR was monitored 15 h post-sorting and means ± SEM are presented (n = 6).

(F) Glutamine uptake was monitored 18 h following sorting using L-[3,4-^{3}H (N)]glutamine (0.5 μCi) for 10 min at room temperature (RT). Uptake is expressed as mean counts per minute (CPM) for triplicate samples ± SEM.

Statistical significance was determined by a one-way ANOVA with Tukey's post hoc test (*$p < 0.05$; **$p < 0.01$; ***$p < 0.001$; ****$p < 0.0001$).

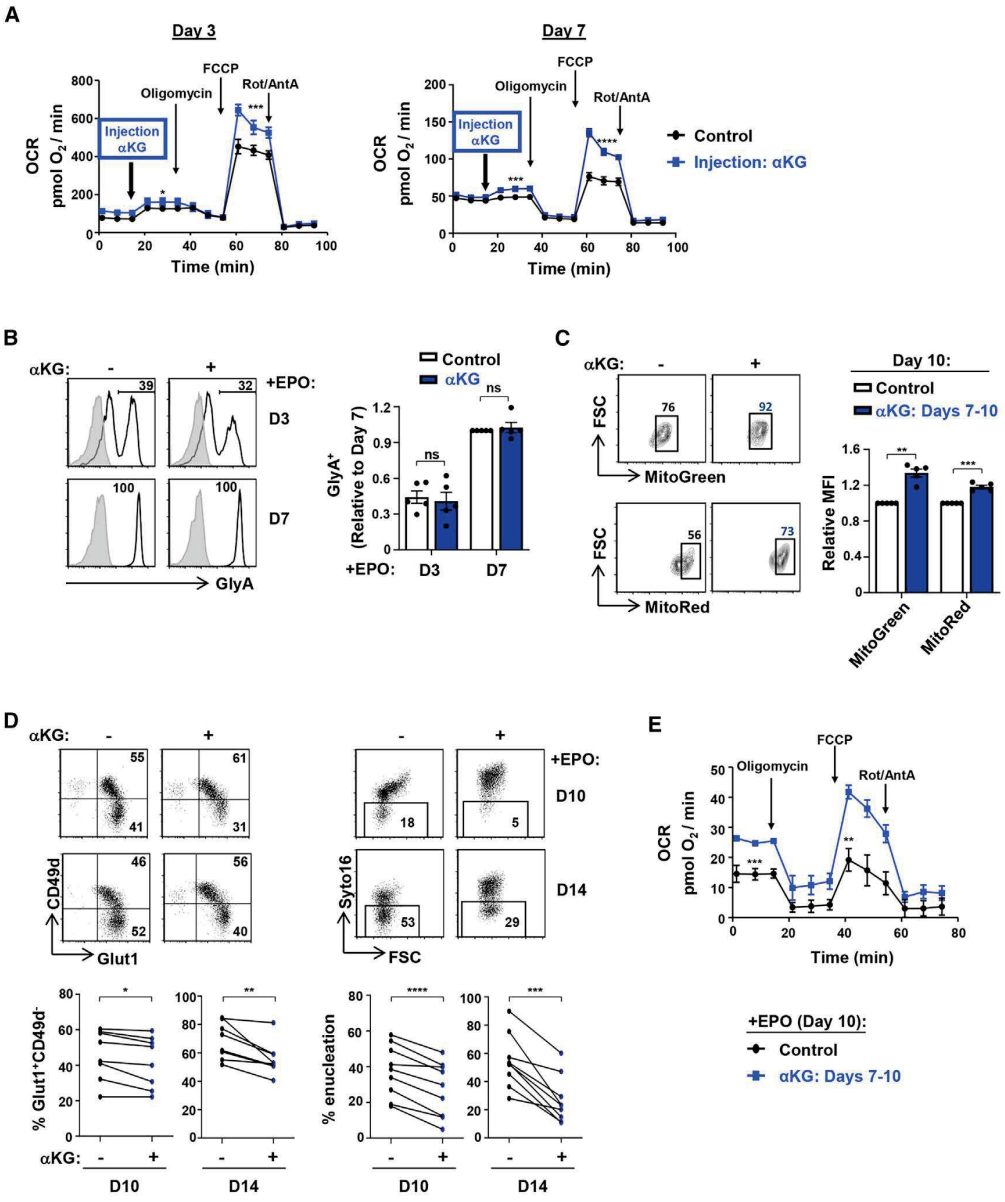

Figure 2. αKG increases mitochondrial function while significantly inhibiting terminal erythroid differentiation and enucleation

(A) CD34$^+$ HSPCs were differentiated with EPO, and OXPHOS was evaluated at days 3 (left) and 7 (right) directly following injection of cell-permeable αKG (3.5 mM, blue line) into the Seahorse analyzer. Mean OCR ± SEM are presented for the indicated conditions (n = 5–6 per time point).

(B) Progenitors were stimulated with rEPO in the absence (−) or presence (+) of αKG. Expression of GlyA was monitored at days 3 and 7, and representative histograms (left) are shown (gray histograms, isotype controls; black lines, specific staining). Mean levels of GlyA$^+$ cells were quantified in the different conditions (right), with levels at day 7 arbitrarily set at 1 (means ± SEM of five independent experiments; ns, nonsignificant).

(C) Mitochondrial biomass and mitochondrial membrane potential (MMP) were monitored following erythroid differentiation in the absence (−) or presence (+) of αKG (between days 7 and 10). Representative dot plots showing the percentages of cells with high mitochondrial biomass and MMP at day 10 are presented (left). Mean biomass and MMP (±SEM) are presented (right; n = 5).

(D) CD49d/Glut1 profiles of GlyA$^+$ erythroblasts differentiated in the absence or presence of αKG (starting at day 7) were monitored at days 10 and 14 of differentiation, and representative dot plots are shown (top left). Percentages of Glut1$^+$CD49d$^-$ orthochromatic erythroblasts are shown for eight individual donors (bottom left). Erythroblast enucleation was evaluated as a function of Syto16 nucleic acid staining, and representative dot plots indicating the percentages of Syto16$^-$ enucleated cells are presented (top right). Percentage enucleation in nine individual donors is presented (bottom right).

(legend continued on next page)

the redox state of the cell. Direct measurement of mitochondrial superoxide with the fluorescent MitoSOX indicator showed that αKG induced a 1.3-fold increase in superoxide ($p < 0.01$) as well as an overall increase of 1.3-fold in all mitochondrial ROS ($p < 0.001$), monitored as a function of DHR123 fluorescence (MitoROS) (Figure 3B).

These data suggested that the negative impact of αKG on erythroid maturation was linked to its role in altering the erythroblast redox state. We therefore assessed whether directly increasing mitochondrial superoxide would inhibit erythroid maturation. Erythroblasts were treated with MitoPQ, a newly synthesized paraquat compound that is targeted to the mitochondria by conjugation to the lipophilic tri-phenylphosphonium cation (Robb et al., 2015). This compound selectively increases superoxide production within mitochondria at 1,000-fold higher efficiency than untargeted paraquat (PQ) (Robb et al., 2015); within the mitochondria, $mitoPQ^{2+}$ is reduced to the radical monocation at the flavin site of complex I and the monocation then reacts with O_2 to generate superoxide ($O_2^{\cdot-}$) (Figure 3C). MitoPQ dramatically increased mitochondrial superoxide (MitoSOX), MitoROS, and mitochondrial biomass (MitoGreen) in differentiating erythroblasts ($p < 0.01$ and $p < 0.05$; Figure 3D). The impact of both MitoPQ and αKG was specific to mitochondrial ROS, as total intracellular ROS levels were not significantly changed (Figures S3A and S3B). Notably, short-term MitoPQ treatment significantly altered late erythropoiesis, with a 25% ± 5% decrease in erythroblast enucleation ($p < 0.01$; Figure 3E).

To assess whether mitochondrial superoxide production has similar effects on erythroblasts at different stages of differentiation, we FACS-sorted early basophilic and late orthochromatic erythroblasts on the basis of their GLUT1/CD49d profiles. Representative cytospins are shown in Figure 3F. Notably, MitoPQ dramatically decreased the ability of basophilic erythroblasts to differentiate to reticulocytes, attenuating enucleation by 94% ± 3% ($p < 0.001$; Figure 3F). In contrast, the maturation of orthochromatic erythroblasts was not affected by MitoPQ treatment (Figure 3F). These data show that a cell type that exhibits only very minimal OXPHOS potential, such as an orthochromatic erythroblast (Figure 1E), is not sensitive to a drug whose impact is dependent on mitochondrial function. In contrast, selectively increasing superoxide production in the mitochondrial matrix of an early erythroblast significantly inhibits erythroid maturation, revealing the critical role of this pathway in the proper progression of erythroid differentiation.

DHA and vitamin C have opposing effects on erythroid maturation

As we found that oxidative stress, monitored as a function of mitochondrial superoxide production and OXPHOS, was associated with attenuated late-stage erythroid differentiation and enucleation, it was of interest to determine whether these parameters were directly responsible for these observed effects. Vitamin C has the potential to promote a redox environment, but its activity is countered by the oxidized form of vitamin C, DHA. The rapid reduction of intracellular DHA to vitamin C (Figure 4A) results in concomitant increases in endogenous ROS in tumor cell lines (Kc et al., 2005; Yun et al., 2015), but its role in erythroid cells is not known. Of note, DHA is transported via the GLUT1 glucose transporter, the most highly expressed transporter on human erythrocytes (Bianchi and Rose, 1986; Helgerson and Carruthers, 1987; May, 1998; Montel-Hagen et al., 2008b, 2009). We found that the addition of DHA significantly increased mitochondrial biomass and superoxide production in differentiating erythroblasts (Figure 4B). The DHA-induced increase in superoxide production was associated with a significant decrease in the enucleation of late-stage erythroblasts (from a mean of 40% ± 3% to 24% ± 3%; $p < 0.0001$; Figure 4C). Thus, under all tested conditions of superoxide production, enucleation of late-stage erythroblasts was severely attenuated.

Based on these data, it was important to evaluate whether vitamin C would have opposing effects on the redox state of erythroblasts and, subsequently, on erythroid maturation. As vitamin C is extremely labile, undergoing oxidation to DHA in culture media with a half-life of ~70 min (Yun et al., 2015), we evaluated the effect of AA-2-phosphate, which is resistant to spontaneous oxidation (Frikke-Schmidt and Lykkesfeldt, 2010; Hata and Senoo, 1989; Manning et al., 2013). This phosphorylated vitamin C molecule significantly enhanced the antioxidant capacity of the developing erythroblast, with a 23% ± 3% decrease in mitochondrial superoxide production ($p < 0.0001$; Figures 4D and S3C). To evaluate whether vitamin C can alter an imbalanced high oxidative state in erythroblasts, we tested its impact on αKG-induced metabolic changes in differentiating erythroblasts. Vitamin C significantly diminished mitochondrial superoxide production as well as mitochondrial biomass and polarization ($p < 0.0001$, $p < 0.01$, and $p < 0.05$; Figures 4E and S3D). Moreover, we found that while both αKG and MitoPQ significantly increased the percentages of erythroblasts in the S-G2/M phases of the cell cycle (with cell death remaining <15%), vitamin C decreased cell-cycle progression to control levels ($p < 0.05$ and $p < 0.01$; Figures 4F, S3E, and S3F).

Most importantly, vitamin C rescued the enucleation defect observed in these erythroblasts ($p < 0.0001$; Figure 4G). This effect was due to the reduced form of vitamin C; as only the long-acting derivative and not the labile form of vitamin C promoted enucleation (Figure S3G). Moreover, other ROS scavengers, including NAC (a thiol-containing antioxidant), GSH (the most abundant antioxidant), and Trolox (a water-soluble analog of vitamin E lacking the phytyl chain), recapitulated the actions of vitamin C, significantly augmenting terminal enucleation in the presence of αKG (Figure S4A). Similarly to the data shown above, highlighting the regulation of erythroid differentiation by mitochondrial metabolism at early erythroblast stages (Figure 3F), vitamin C significantly increased enucleation of sorted basophilic erythroblasts, but not orthochromatic erythroblasts (Figure S4B).

(E) OCR was evaluated on day 10 erythroid progenitors in control conditions (black line) and following addition of αKG at day 7 (blue line). Mean levels ± SEM are presented (n = 5–6).
ns, nonsignificant; *$p < 0.05$; **$p < 0.01$; ***$p < 0.001$; ****$p < 0.0001$.

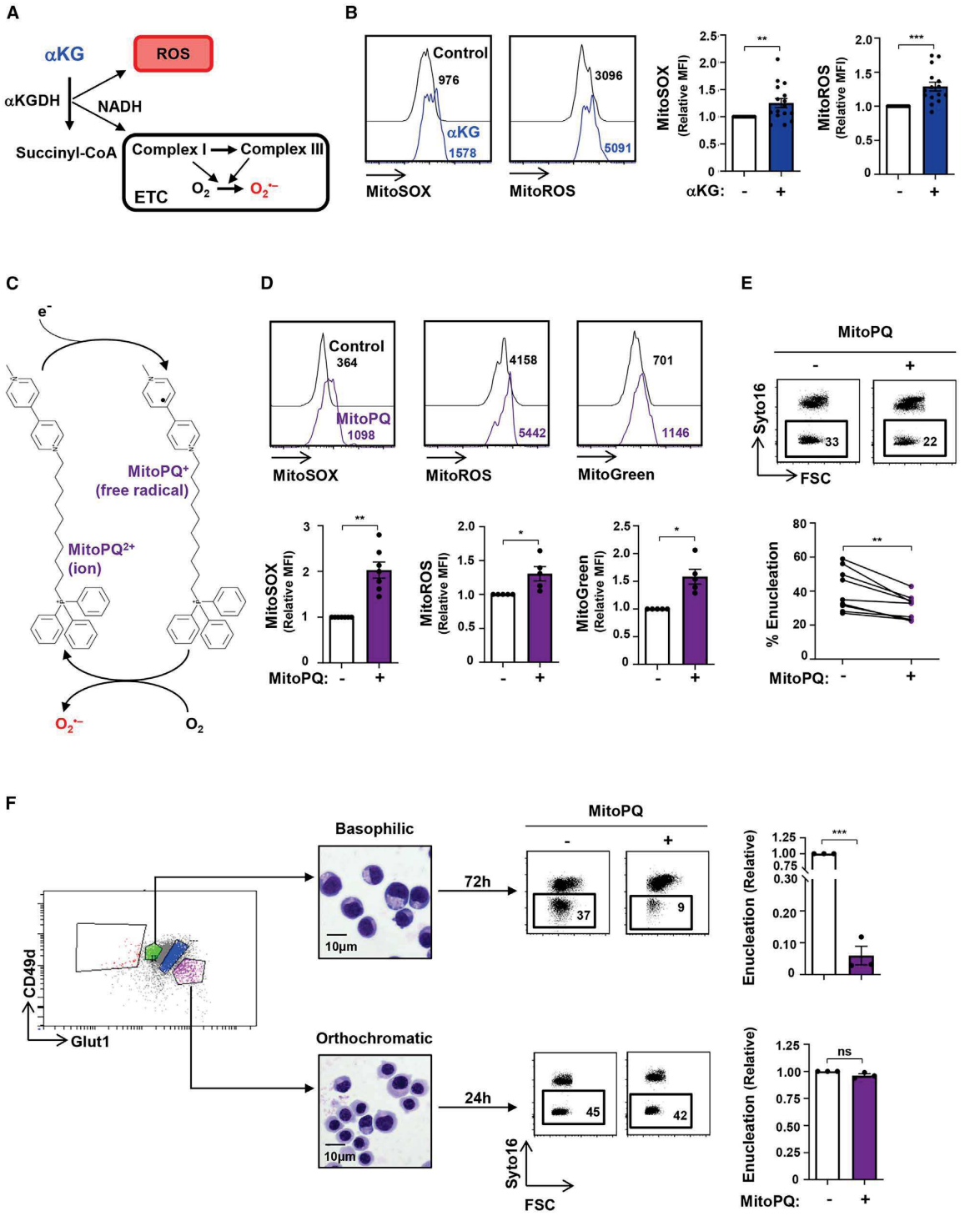

(legend on next page)

The ensemble of these data strongly suggests that the impact of vitamin C is due to its alteration of the redox state of the erythroblast. However, as autophagy is also a critical regulator of enucleation (Keerthivasan et al., 2011), we evaluated the impact of vitamin C following Spautin1-mediated inhibition of autophagy (Liu et al., 2011). As expected, Spautin significantly inhibited enucleation ($p < 0.01$), but vitamin C did not rescue this defect (Figure S5A), highlighting an autophagy-independent role of vitamin C in erythroid differentiation. Iron and its uptake as diferric transferrin by the transferrin receptor CD71 are also critical for erythroid differentiation (Kautz and Nemeth, 2014), and we therefore evaluated a potential crosstalk between iron and vitamin C. Interestingly, in the absence of transferrin, vitamin C did not increase enucleation in αKG-treated erythroblasts, but its presence (50 or 200 μg/mL) positively affected enucleation (Figure S5B). Thus, vitamin C and other ROS scavengers decrease the redox state of erythroblasts, promoting enucleation under conditions of αKG-induced oxidative stress in a transferrin-dependent manner.

Vitamin C accelerates the erythroid differentiation of cord blood, peripheral blood, and BM progenitor cells

The ability of vitamin C to rescue erythroid differentiation under conditions of augmented oxidative stress led us to evaluate its potential to directly modulate erythroid differentiation of $CD34^+$ hematopoietic stem and progenitor cells (HSPCs) from different sources. $CD34^+$ progenitors from cord blood (CB), adult peripheral blood (PB), and BM were directly differentiated with rEPO. While BM-derived progenitors differentiated much more rapidly than CB- and PB-derived progenitors to an erythroid-committed CFU-E ($CD34^-$ $CD36^+$), vitamin C did not alter the erythroid progenitor continuum (Figure S5C). In agreement with previous data (Yan et al., 2018), CB progenitors exhibited a delayed generation of $GlyA^+$ erythroblasts compared to PB and BM progenitors (Figure 5A). Notably, vitamin C significantly increased the percentages of $GlyA^+$ cells ($p < 0.05$) and increased maturation to a $GlyA^+CD105^-$ state by 2.1- ± 0.5-fold ($p < 0.01$, Figure 5A), without altering cell growth (Figure S5D). Furthermore, vitamin C resulted in an enhanced enucleation of erythroid progenitors generated from these three sources (Figure 5B). Thus, vitamin C significantly accelerates erythroid differentiation and enucleation of human $CD34^+$ progenitors, irrespective of their source of origin.

IDH1 activity regulates mitochondrial activity in differentiating erythroblasts

The data presented above demonstrated that conditions that increase mitochondrial activity in human erythroblasts, including ectopic αKG and MitoPQ, inhibit terminal erythroid differentiation. Under physiological conditions, αKG is mobilized in the mitochondria, where it can be converted to succinyl-CoA by αKGDH, producing ROS and the NADH that provides electrons for the ETC (Figure 6A). αKG can be generated from isocitrate in the mitochondria by IDH2/IDH3 and interconverted in the cytoplasm by IDH1. Interestingly, transcripts of all three enzymes are significantly reduced during erythroid differentiation, potentially suggesting a negative role for these pathways in late-stage erythroblasts (Figure S6A). As mitochondrial biomass is markedly decreased during erythroid differentiation, we evaluated the role of the cytoplasmic IDH enzyme, IDH1, in erythroid differentiation by an shIDH1-mediated approach. Using two independent short hairpin RNAs (shRNAs), shIDH1-1 and shIDH1-2, we detected a 36% ± 7% and 54% ± 5% reduction, respectively, and as such used shIDH1-2 in the differentiation experiments (Figure S6B).

Importantly, *IDH1* knockdown did not inhibit erythroid differentiation, as monitored by the generation of CFU-E, $GlyA^+$ erythroblasts or upregulation of the CD36 or CD71 erythroid markers (Figures 6B, S6C, and S6D). However, downregulating IDH1 resulted in a decreased expansion (Figure S6E) and significantly increased mitochondrial superoxide production, mitochondrial biomass, and polarization ($p < 0.01$; Figures 6C and S6F). In accord with these data, *IDH1* knockdown augmented the OXPHOS capacity of the cells, with a 3.0- and 3.7-fold increase in basal and maximal OCR levels, respectively (shIDH1-2 construct) (Figure 6D). Notably, the function of IDH1 appears to be substantially more critical for the differentiation of erythroid as compared to non-erythroid progenitors. The percentages of progenitors transduced with an scramble shRNA (shControl) or shIDH1 lentiviral vector harboring the GFP reporter gene remained approximately stable over a 6-day period, with 47%–57% GFP^+ cells, in the absence of rEPO. These cells had a myeloid phenotype as shown by a $CD11b^+$, $CD33^+$, $CD13^+$ phenotype (Figure S6G). However, following rEPO-mediated erythroid induction, the percentages of shControl cells decreased by 24%, while the percentages of shIDH1-transduced cells decreased by 56% (Figure 6E).

Figure 3. Mitochondrial superoxide production impedes erythroid enucleation

(A) Schematic of the generation of mitochondrial reactive oxygen species (ROS) via the conversion of αKG to succinate, of which superoxide is a major source.

(B) The impact of αKG (3.5 mM) on mitochondrial superoxide and mitochondrial ROS production in erythroblasts was evaluated at day 10 of erythroid differentiation as a function of MitoSOX and MitoROS, respectively. Representative histograms are shown (left). Staining in the presence of αKG was normalized to control conditions, and relative median fluorescence intensities (MFIs) are presented ($n = 15–16$, right).

(C) Schematic of MitoParaquat (MitoPQ) cycling within the mitochondria; $mitoPQ^{2+}$ is reduced to the radical monocation at the flavin site of complex I, and the monocation then reacts with O_2 to generate superoxide ($O_2^{\cdot-}$) (Robb et al., 2015).

(D) Differentiating erythroblasts were treated with MitoPQ (50 μM) at day 7 of differentiation, and representative histograms of mitochondrial superoxide, ROS, and biomass at day 10 are presented (top). MFIs are presented relative to control conditions ($n = 5–6$, bottom).

(E) The impact of MitoPQ on enucleation was evaluated at day 10 by Syto16 staining, and representative dot plots are presented (top). Percent enucleation in nine independent experiments is shown (bottom).

(F) The impact of MitoPQ on early basophilic erythroblasts as compared to late orthochromatic erythroblasts was determined by FACS sorting erythroblast populations as a function of their GLUT1/CD49d profiles (left), and representative cytospins of the sorted subsets are shown (middle). Early basophilic and late orthochromatic subsets were then cultured for 72 h or 24 h, respectively, in the absence (–) or presence (+) of MitoPQ, and enucleation was evaluated (right). Enucleation was quantified relative to control conditions ($n = 3$).

ns, nonsignificant; $^*p < 0.05$; $^{**}p < 0.01$; $^{***}p < 0.001$.

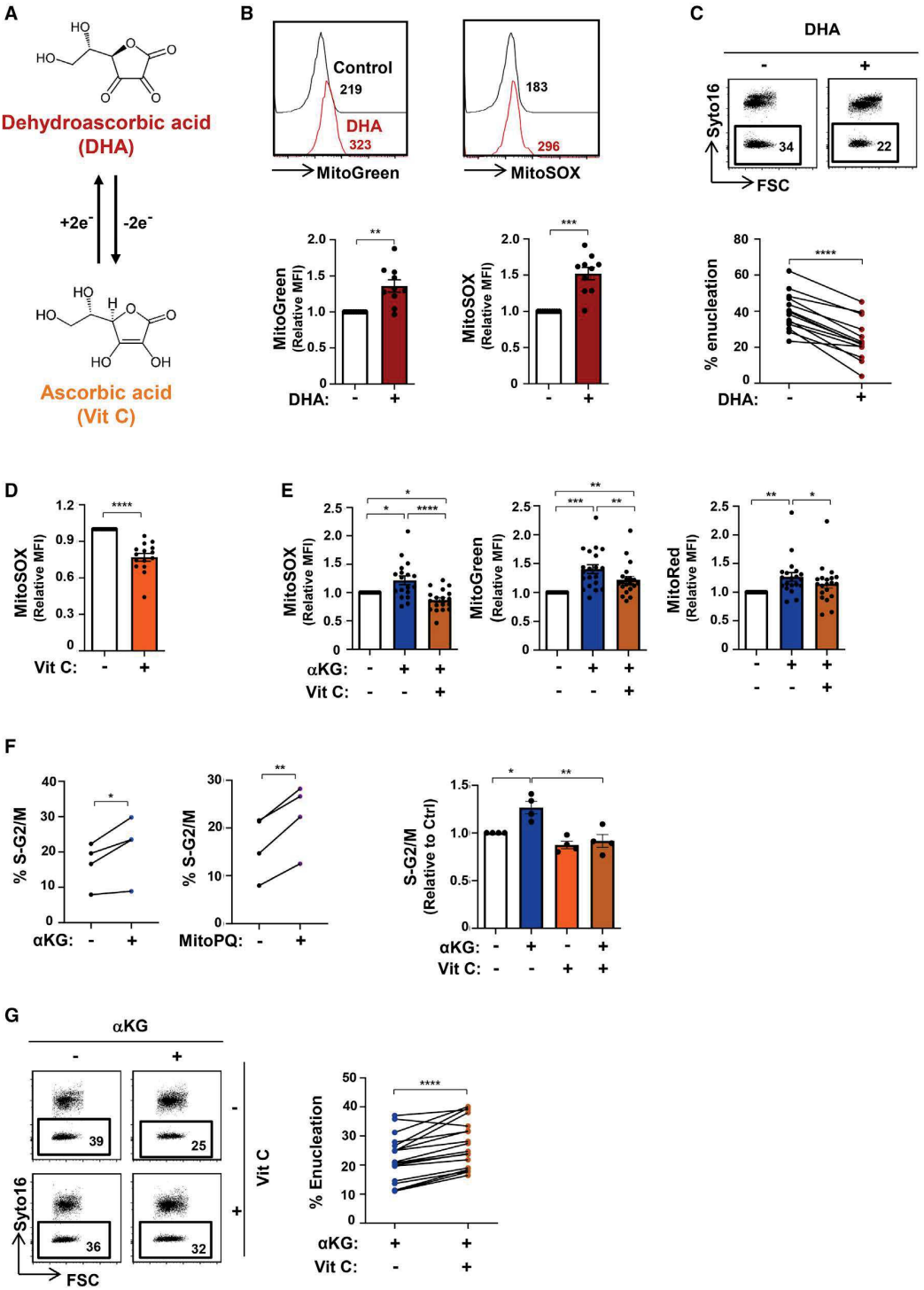

(legend on next page)

To better understand the negative selection of erythroid progenitors with downregulated IDH1, we performed metabolomic and flux experiments following IDH1 knockdown. First, we found that at day 4 of IDH1 downregulation (~50%; Figure S6B), there was a mean decrease of αKG and citrate of 43% and 21%, respectively (Figure 6F). These data highlight the importance of the IDH1 enzyme in the generation of αKG and its interconversion to citrate. Furthermore, they demonstrate the role of glutamine metabolism in the generation of these intermediates in early erythroid progenitors (day 4); a mean of 75.1% and 69.0% of αKG and citrate harbored ^{13}C carbons from glutamine, respectively (Figure 6G). Several groups have also found that the relative ratio of αKG to citrate regulates differentiation, either by inhibiting (Carey et al., 2015; Vardhana et al., 2019) or priming (TeSlaa et al., 2016; Tischler et al., 2019) stem cell differentiation. In this regard, it is interesting to note that erythroid differentiation resulted in the loss of both αKG and citrate between days 4 and 7 of differentiation, with a mean loss of 87% and 68%, respectively (n = 2 biological experiments performed in triplicate; Figure 6G). These data point to a greater loss of αKG than citrate, consistent with a negative role of high αKG levels in late erythroid differentiation (Figure 2). Furthermore, following IDH1 downregulation, TCA intermediates were maintained at a higher level, with decreases in αKG and citrate of only 31% and 36%, respectively (Figure 6G). Thus, the premature inhibition of IDH1 alters the physiological loss of TCA-cycle intermediates upon erythroid differentiation.

Vitamin C rescues terminal erythroid differentiation in the absence of IDH1

Under conditions of IDH1 downregulation, mitochondrial metabolism was augmented, as shown by increased superoxide production and OXPHOS (Figures 6C and 6D). On the basis of these data, we hypothesized that *IDH1* knockdown would attenuate late-stage erythroid differentiation and enucleation, and this was indeed the case. Following transduction of $CD34^+$ HSPCs with a vector harboring an shIDH1 RNA, the emergence of $Glut1^+CD49$ orthochromatic erythroblasts was significantly decreased (shIDH1-2 construct, $p < 0.01$; Figure 7A). Furthermore, enucleation was decreased by 59% ± 2% (shIDH1-2 construct, $p < 0.0001$; Figure 7B), and this effect was detected even when IDH1 was downregulated at day 4 post-rEPO-induced differentiation (Figure S7A). Consistent with an impact of IDH1 on the redox state of the cell, both αKG and DHA exacerbated the effect of *IDH1* knockdown on erythroblast enucleation, from 47% ± 8% to 27% ± 8% and 24% ± 4%, respectively ($p < 0.01$ and $p < 0.05$; Figure 7C). Most importantly, vitamin C significantly increased enucleation under these conditions by 35% ± 13% ($p < 0.05$, Figure 7D). Intriguingly, other ROS scavengers, including NAC, GSH, and Trolox, did not increase enucleation, even though they were present throughout the differentiation period (Figure S7B). Importantly, vitamin C, but not NAC, GSH, or Trolox, decreased mitochondrial superoxide generation ($p < 0.05$; Figure S7C). Thus, collectively, these data show that IDH1-induced decreases in mitochondrial OXPHOS are required for the later stages of terminal erythroid differentiation and enucleation. However, under conditions of decreased IDH1 expression, this negative effect can be counteracted by a vitamin-C-mediated modulation of the intracellular redox balance.

As αKG and vitamin C act as cofactors in supporting the dioxygenase activity of TET2, it was important to assess whether the effects that we detected here were coupled to their impact on TET2 activation (Inoue et al., 2016). However, if αKG served only to support the dioxygenase activity of TET2, then its presence would be expected to augment erythroid differentiation, while our data showed the opposite effect (Figure 2). To directly address this point and evaluate the role of an αKG/TET2 as compared to an αKG/IDH1 axis, we downregulated TET2 by an shRNA approach (Yan et al., 2017). TET2 levels decrease with differentiation ($p < 0.0001$; Figure S7D), but mRNA levels were further diminished by a mean of 55% by shRNA-mediated knockdown (Figure S7E). While this downregulation resulted in a significant delay in the generation of $GlyA^+$ terminal erythroblasts ($p < 0.0001$; Figure S7F), it did not delay enucleation when the shRNA-mediated knockdown of TET2 was performed at day 4 of differentiation (Figure 7E). Moreover, enucleation in shTET2-treated erythroid progenitors was not augmented by vitamin C (Figure 7E). These data strongly imply distinct roles for IDH1 and TET2 in regulating enucleation of late-stage erythroid progenitors.

Mutations in IDH1/IDH2 are strongly associated with myelodysplastic syndromes (MDSs) that are characterized by

Figure 4. Antagonistic roles of dehydroascorbic acid and vitamin C on mitochondrial oxidative stress and erythroblast enucleation

(A) Schematic of the interconversion between dehydroascorbic acid (DHA) and ascorbic acid (vitamin C) via a two-electron reduction/oxidation process, respectively.

(B) The impact of DHA (1 mM) on mitochondrial superoxide production and biomass in late erythroblasts was evaluated between days 7 and 10 after EPO induction, and representative histograms of MitoGreen and MitoSOX staining, respectively, are shown (top). Quantification relative to control conditions is shown (n = 10, bottom).

(C) Enucleation was evaluated at day 10 after EPO induction in the absence (−) or presence (+) of DHA (days 7–10), and representative dot plots are shown (top). Percent enucleation in 14 independent experiments is presented (bottom).

(D) The impact of the stable L-ascorbic acid (AA) 2-phosphate derivative of vitamin C (100 μM) was evaluated on mitochondrial superoxide generation (days 7–10), and MFIs were quantified relative to control conditions (n = 15, bottom).

(E) The impact of vitamin C on αKG-mediated increases in MitoSOX, MitoGreen, and MitoRed staining was evaluated by flow cytometry, and relative MFIs are presented (n = 18–20).

(F) The percentages of cells in S-G2/M of the cell cycle were evaluated in the indicated conditions by phosphatidylinositol (PI) staining (n = 4, left). The percentages of erythroid progenitors in S-G2/M were evaluated relative to control conditions, and means ± SEM are presented (right).

(G) Enucleation was evaluated in the presence or absence of vitamin C and αKG. Representative histograms (left) as well as changes in percent enucleation are presented (n = 18, right).

*$p < 0.05$; **$p < 0.01$; ***$p < 0.001$;****$p < 0.0001$.

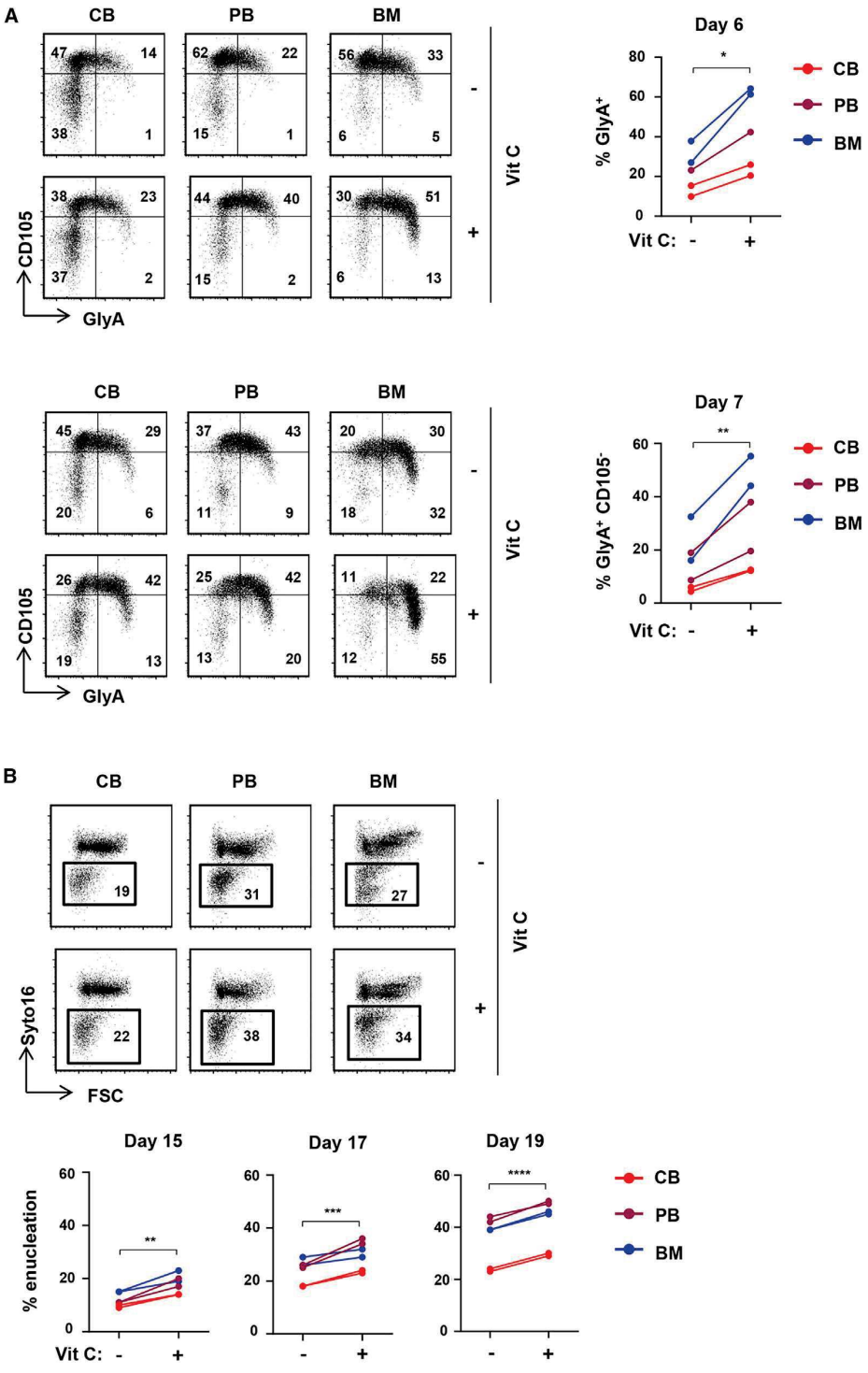

(legend on next page)

ineffective erythropoiesis (reviewed by Bejar and Steensma, 2014; Fenaux et al., 2014). The anemia that dominates the early course of MDS is associated with an aberrant erythroid differentiation marked by the generation of multinucleated erythroblasts (Abdel-Wahab and Levine, 2013). Notably, we found that *IDH1* knockdown increased the percentages of erythroblasts with abnormal multinucleated erythroblasts from 10% ± 1% to 23% ± 2% ($p < 0.05$; Figure 7F). Moreover, vitamin C markedly decreased the generation of these abnormal erythroblasts, not only in *IDH1*-knockdown erythroblasts but also in normal erythroblasts, to 4% ± 0.4% and 4% ± 0.2%, respectively ($p < 0.05$ and $p < 0.01$; Figure 7F). These data suggest that the multinucleated erythroblasts detected in MDS patients may be associated with an increased mitochondrial metabolism. Vitamin C, a redox scavenger, significantly attenuated the generation of these abnormal cells.

DISCUSSION

The generation of ROS and its intricate relationship with cellular redox homeostasis is a critical regulator of stem cell homeostasis. Notably, low ROS levels, associated with low mitochondrial biogenesis and activity, are necessary for HSC quiescence and self-renewal (Filippi and Ghaffari, 2019; Jang and Sharkis, 2007; Qian et al., 2016; Suda et al., 2011; Takubo et al., 2013; Tan and Suda, 2018; Vannini et al., 2016; Yu et al., 2013). Conversely, HSC division and differentiation occur under conditions that promote mitochondrial biogenesis and OXPHOS (Chen et al., 2008; Mantel et al., 2010; Maryanovich et al., 2015; Yu et al., 2013). In the context of erythropoiesis, it has been shown that early erythroid development requires induction of mitochondrial ROS, a consequence of OXPHOS (Liu et al., 2017; Zhao et al., 2016). Here, we show that glutamine metabolism, via the anaplerotic contribution of αKG into the TCA cycle, directly increases OXPHOS in human erythroid precursors. This increased OXPHOS promoted erythroid commitment and early erythropoiesis, but terminal erythroid differentiation was dependent on the suppression of TCA-cycle-linked mitochondrial networks. Elevated intracellular αKG levels, with associated increased OXPHOS and ROS, inhibited late-stage erythroid maturation and enucleation.

Mechanistically, we identify the catalysis of αKG by the cytoplasmic IDH1 enzyme as a critical step in erythropoiesis; the negative repercussions of IDH1 downregulation in terminal erythroid differentiation was further exacerbated by elevated αKG levels. Furthermore, the impact of a mitochondria-targeted redox cycler, MitoPQ (Robb et al., 2015), highlights the importance of mitochondrial superoxide as a specific inhibitor of erythroblast maturation and enucleation. Interestingly, all tested ROS scavengers, including NAC, GSH, vitamin E, and vitamin C, rescued the αKG-mediated decrease in enucleation, but only vitamin C rescued enucleation following IDH1 downregulation. This is critical in the context of human erythroid differentiation, where the absence of ascorbate synthesis, resulting in 1 mg/kg recommended exogenous supplements for humans (Pauling, 1970), is significantly lower than the hepatic production rate of 200 mg/kg/day in vitamin-C-synthesizing animals (Chatterjee, 1973; Stone, 1979). Thus, scavenging by vitamin C is likely to be suboptimal. Indeed, we found that a stable vitamin C analog rescued human terminal erythroid differentiation and enucleation in all tested conditions of oxidative stress.

Ascorbate, transported by the SVCT1/SLC23A1 and SVCT2/SLC23A2 solute carriers, regulates whole-body homeostasis of vitamin C and protection to oxidative stress, respectively (Savini et al., 2008; Tsukaguchi et al., 1999; Wilson, 2005). While vitamin C has been shown to enhance erythropoiesis in hemodialysis patients with refractory anemia (Attallah et al., 2006; Gastaldello et al., 1995; Seibert et al., 2017; Sirover et al., 2008), other studies have found that ascorbate induces hemolysis of mature erythrocytes (Zhang et al., 2016). These apparent discrepancies are likely due to the oxidation state of vitamin C. The loss of a single electron from ascorbate results in the generation of an unstable ascorbate radical, which can then lose a second electron to generate DHA (Padayatty and Levine, 2016). Unlike vitamin C, the two-electron oxidized DHA intermediate is transported by the GLUT1 glucose transporter (Bianchi and Rose, 1986; McNulty et al., 2005; Rumsey et al., 1997, 2000; Vera et al., 1993). Thus, cellular uptake of the reduced and oxidized forms of vitamin C is regulated, at least in part, by the expression of their specific transporters. SVCT2 is expressed at very high levels on HSCs, with levels decreasing as a function of erythroid development and differentiation (Agathocleous et al., 2017). Conversely, GLUT1 is upregulated during human terminal erythroid differentiation (Montel-Hagen et al., 2008b; Mueckler, 1994), promoting DHA transport (May, 1998; Montel-Hagen et al., 2008b, 2009). Thus, during intermediate steps of HSPC development, both ascorbate and DHA can potentially be transported into the cell.

One of the difficulties in studying ascorbate function is its stability. Previous research showed that freshly prepared minimum essential medium α (αMEM) culture media, but not liquid αMEM, supported T cell differentiation from hematopoietic progenitors; the difference between these formulations was due to the lability of vitamin C in the latter (Manning et al., 2013). Furthermore, several groups found that the negative impact of vitamin C on the growth of cancer cells was actually due to the GLUT1-mediated uptake of DHA, resulting in the accumulation of ROS and subsequent cell death (Yun et al., 2015; Zhang et al., 2016).

Figure 5. Vitamin C promotes erythroid commitment of EPO-stimulated progenitors from CB, BM, and PB and significantly accelerates erythroid maturation

(A) $CD34^+$ HSPCs were isolated from CB, PB, and BM. Progenitors were differentiated with EPO in the absence or presence of vitamin C (100 μM) and erythropoiesis monitored as a function of CD105/GlyA profiles. Representative profiles at days 6 (top left) and 7 (bottom left) of differentiation are presented. Quantification of $GlyA^+$ cells at day 6 (n = 5, top right) and $GlyA^+CD105^-$ cells at day 7 (n = 5, bottom right) is presented.

(B) The impact of vitamin C on enucleation was evaluated in CB, PB, and BM HSPCs, and representative plots at day 17 are presented (top). Quantification of enucleation at days 15, 17, and 19 is presented (n = 6, bottom).

*$p < 0.05$; **$p < 0.01$; ***$p < 0.001$; ****$p < 0.0001$.

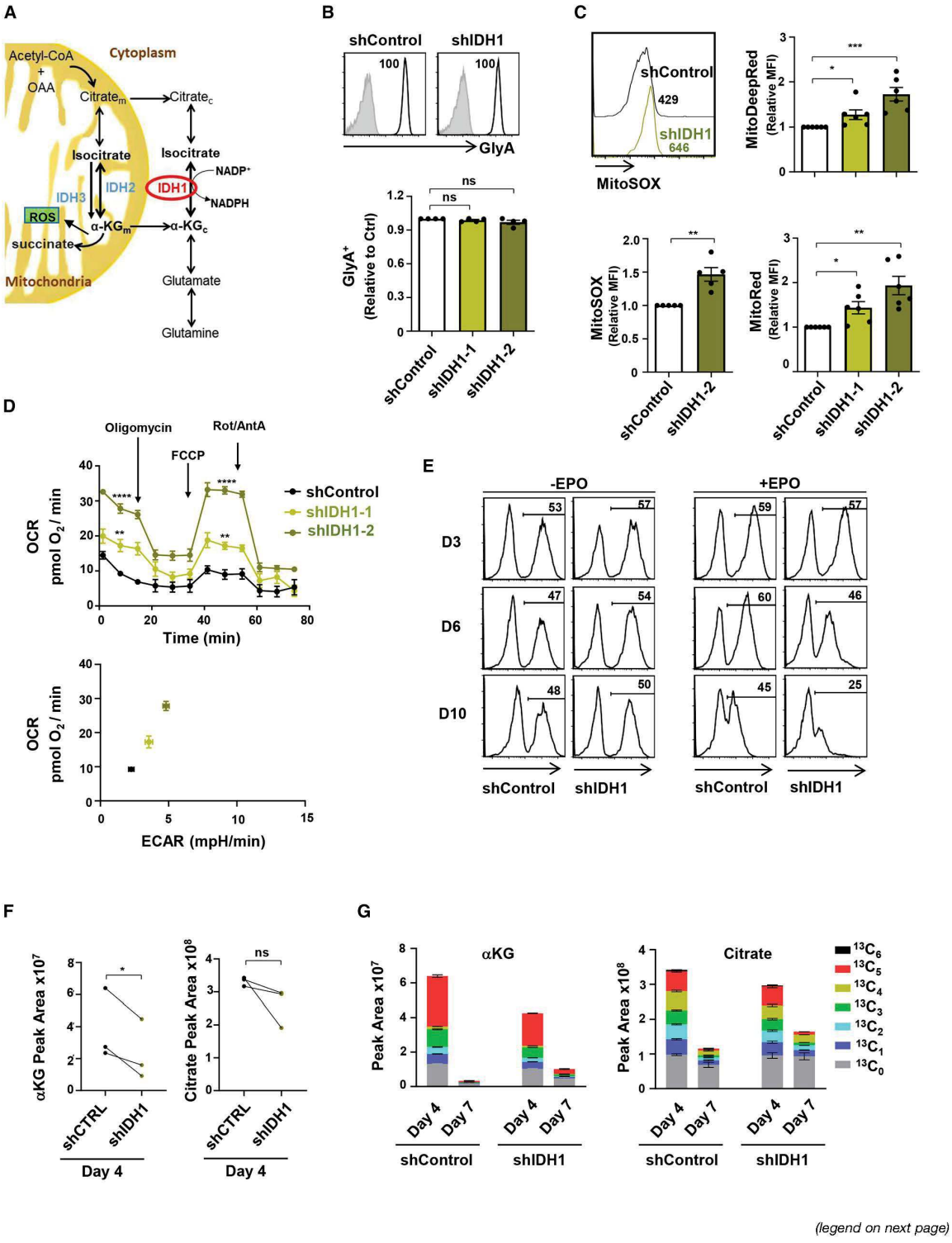

(legend on next page)

Indeed, we similarly found that the standard labile form of L-ascorbate markedly decreased erythroblast maturation and enucleation, even in the absence of ascorbate oxidase. However, under conditions where erythroid differentiation was performed in the presence of the stable ascorbate 2-phosphate analog (Hata and Senoo, 1989; Frikke-Schmidt and Lykkesfeldt, 2010; Takamizawa et al., 2004), erythroid differentiation was enhanced. Thus, care must be taken in evaluating studies using the conventional labile ascorbate, as it may not be maintained in a reduced state.

Ascorbic acid has also gained prominence as an anti-cancer therapeutic modality because of its ability to alter the activity of the Tet2 demethylase (Shenoy et al., 2018). Loss of function mutations in *TET2* are one of the most frequent events in myeloid dysplasia and leukemias (Bejar et al., 2011; Busque et al., 2012; Delhommeau et al., 2009; Kosmider et al., 2011). The initiation of demethylation by the TET family of dioxygenases occurs via the introduction of the intermediate mark 5-hydroxymethylcytosine (5hmC), and this function is dependent on several cofactors, including ascorbate, αKG, ferrous iron, and oxygen (Chen et al., 2013; Dang et al., 2009). Indeed, recent studies have shown that ascorbate is able to compensate for TET2 deficiency and suppress leukemogenesis, albeit via both TET2-dependent and TET2-independent mechanisms (Agathocleous et al., 2017; Cimmino et al., 2017). A crosstalk between ascorbate and TET2 in the metabolic status of a hematopoietic progenitor is suggested by the finding that wild-type TET2 protects murine erythroblasts from oxidative stress (Guo et al., 2017). Moreover, downregulation of TET2 in human erythroid progenitors negatively regulated human erythropoiesis in a manner that was independent of any detectable alterations in 5-methylcytosine (5mC) levels (Qu et al., 2018; Yan et al., 2017). These data are in agreement with independent studies showing that terminal erythroid differentiation requires that erythroblasts be protected from oxidative stress (Case et al., 2013; Filippi and Ghaffari, 2019; Hyde et al., 2012; Xu et al., 2019; Zhao et al., 2016).

Our study highlights the importance of ascorbate in regulating the redox state of human erythroid progenitors, especially under conditions of altered oxidative metabolism. Increases in intracellular αKG and decreases in cytoplasmic IDH1 both augmented oxidative stress and diminished erythroid maturation. IDH1, like Tet2, is mutated in a high percentage of MDS patients (Kosmider et al., 2010; Wang et al., 2017), with anemia dominating the early course of disease. Moreover, recent studies have highlighted the potential for vitamin C to promote the differentiation of IDH1-mutated AML progenitors (Mingay et al., 2018). Our data show that even in the absence of mutation, low levels of wild-type IDH1 suppress late erythroid differentiation. While the specific role of IDH1 in OXPHOS has not yet been fully delineated, it is interesting to note that IDH1 downregulation in neuronal cells resulted in an increase in ROS (Calvert et al., 2017). Furthermore, mutation of IDH1, but not IDH2, has been found to increase OXPHOS in transformed cells (Grassian et al., 2014), and wild-type IDH1 regulates the reductive carboxylation of αKG for *de novo* lipogenesis (Calvert et al., 2017; Metallo et al., 2011).

IDH-regulated αKG production has also been shown to regulate cell fate and differentiation by modulating epigenetic marks via Tet2-induced changes in global histone and DNA demethylation (Carey et al., 2015; TeSlaa et al., 2016; Tischler et al., 2019; Xiao et al., 2012). Notably, under the conditions of erythroid differentiation studied here, αKG levels attenuated terminal erythroid differentiation and late-stage erythropoiesis, while a second TET2 cofactor, ascorbate, exhibited an opposing effect, enhancing and accelerating terminal differentiation. Other agents, such as oxidized ascorbate and MitoPQ, attenuated erythroid differentiation by inducing oxidative stress. Furthermore, while TET2 downregulation delayed early erythroblast differentiation, it did not negatively impact terminal differentiation and enucleation. Together, these data strongly suggest complementary roles for TET2 and IDH1, with the latter playing a critical role in late-stage human erythropoiesis via its impact on redox homeostasis.

These data may promote mechanistic insights into inherited hematologic disease. Like MDS patients, a feature that characterizes patients with congenital dyserythropoietic anemia is the presence of multinucleated or multi-lobulated erythroblasts

Figure 6. IDH activity regulates mitochondrial superoxide production and OXPHOS in differentiation erythroblasts

(A) Schematic representation of the catalytic reactions regulating glutamine catabolism. Glutamine is interconverted to glutamate and cytosolic αKG (αKG_c). Isocitrate dehydrogenase 1 (IDH1), a cytosolic enzyme, catalyzes the production of isocitrate from αKG, promoting both forward and reverse reactions. Conversion of mitochondrial αKG (αKG_m) to succinate results in the generation of ROS.

(B) The expression of GlyA was monitored in shControl- and shIDH1-transduced cells at day 7 day of differentiation, and representative histograms (gray, isotype control; black, specific staining) are shown (top). GlyA expression in cells transduced with one of two different shIDH1 clones (shIDH1-1 and shIDH1-2) was evaluated, and relative levels are presented (n = 4, bottom).

(C) The impact of IDH1 downregulation on MitoSOX was evaluated at day 10. Representative histograms (top left) and quantification of relative MFIs (n = 5) are presented (bottom left). MitoTracker Deep Red (top right) and MitoTracker Red (bottom right) staining in shIDH1-transduced erythroblasts relative to control conditions, are presented (n = 6).

(D) OCR was determined in FACS-sorted shControl- as well as shIDH1-transduced erythroblasts at day 10 of differentiation as indicated (n = 6, top). An OCR/extracellular acidification rate (ECAR) energy map is presented (bottom).

(E) The evolution of shControl- and sh-IDH1-transduced progenitors was monitored as a function of GFP expression at days 3, 6, and 10 of differentiation in the absence (–) or presence (+) of EPO (n = 3).

(F) Total levels of αKG and citrate were evaluated by high-performance liquid chromatography-mass spectrometry (HPLC-MS) at day 4 of erythroid differentiation in shControl- and shIDH1-transduced progenitors, and mean levels are shown (n = 3 independent experiments, with statistical difference evaluated by a one-tailed t test).

(G) The isotopologues of αKG and citrate derived from [$^{13}C_5{}^{15}N_2$]Gln are presented from one experiment with three replicates for day 4 and two replicates for day 7.

ns, not significant; *p < 0.05; **p < 0.01; ***p < 0.001; ****p < 0.0001.

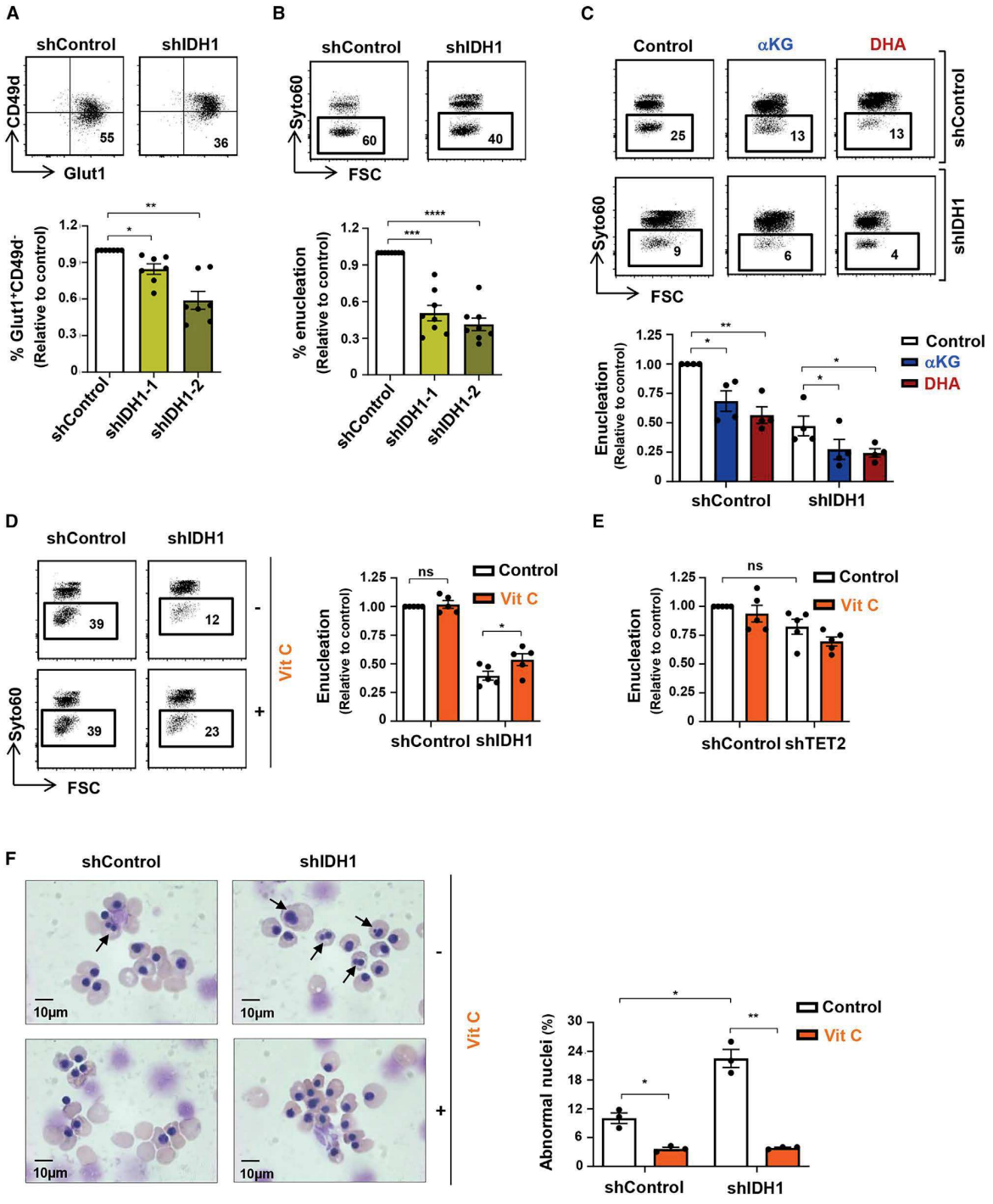

Figure 7. Vitamin C rescues dyserythropoiesis due to IDH1 downregulation

(A) Late-stage erythroblast differentiation was monitored as a GLUT1^{+}CD49d^{-} phenotype, and representative dot plots are presented (top). The percentages of GLUT1^{+}CD49d^{-} erythroblasts were evaluated following transduction with shIDH1-1 or shIDH1-2 vectors, and mean levels ± SEM relative to control cells are presented (n = 7, bottom).

(legend continued on next page)

(Crookston et al., 1969; Goasguen et al., 2018; Iolascon et al., 1996). IDH1 knockdown resulted in a significant augmentation in the percentage of abnormal multinucleated orthochromatic erythroblasts, and even more importantly, ascorbate reduced these levels back to baseline. Thus, these data provide the first evidence that the abnormal erythroblast morphology observed in diverse dyserythropoietic diseases may be coupled to oxidative stress. Furthermore, our data suggest that antioxidant treatment of these disorders in humans, a species with suboptimal redox capacity (Johnson et al., 2008), with stable ascorbate analogs could potentially restore redox homeostasis, quenching ROS and subsequently rescuing defective late-stage erythropoiesis.

STAR★METHODS

Detailed methods are provided in the online version of this paper and include the following:

- KEY RESOURCES TABLE
- RESOURCE AVAILABILITY
  - Lead contact
  - Materials availability
  - Data and code availability
- EXPERIMENTAL MODELS AND SUBJECT DETAILS
  - CD34$^+$ cell isolation and *ex vivo* differentiation assays.
- METHODS DETAIL
  - Cytospin preparation
  - Flow cytometry
  - Virus production and transduction of CD34$^+$ progenitor cells
  - Quantitative real time PCR
  - Mass spectrometry (LC-MS)
  - Seahorse analysis
  - Glutamine uptake assays
- QUANTIFICATION AND STATISTICAL ANALYSIS

SUPPLEMENTAL INFORMATION

Supplemental Information can be found online at https://doi.org/10.1016/j.celrep.2021.108723.

ACKNOWLEDGMENTS

We thank all members of our laboratories for discussions and scientific critique. We are grateful to Myriam Boyer of Montpellier Rio Imaging for support in cytometry experiments. We are indebted to the Tissue Donation Program at Northwell Health for providing access to BM samples. We thank the Unité of Thérapie Cellulaire and the hospital clinics of Clémentville and Saint-Roch (Montpellier, France) for their generous efforts in providing access to CB samples. We also thank Catherine Winchester for critical reading of the manuscript. P.G.-M. was supported by a fellowship from the Clarin-COFUND EU Program (Principado de Asturias, Spain), M.R. was supported by a fellowship from GR-Ex, and L.O. was supported by Ligue and ARC fellowships. S.T. is supported by funding from Cancer Research UK (C596/A17196 and A23982). This work was supported by generous funding from the NIH (grant DK32094 to P.G.G., N.M., S.K., and N.T. and grants HL144436 and HL152099 to L.B.); FRM, ARC, and French national (ANR) research grants (NutriDiff); and the French laboratory consortiums (Labex) EpiGenMed and GR-Ex. N.T. is presently supported by the NCI Intramural Program.

AUTHOR CONTRIBUTIONS

P.G.-M., M.R., S.K., and N.T. conceived the study; P.G.-M., M.R., H.Y., R.D., J.P., L.O., S.T., V.D., C.M., M.S., V.S.Z., L.B., N.M., S.K., and N.T. were involved in study design; and P.G.-M., M.R., H.Y., R.D., J.P., L.O., S.T., C.M., M.D., A.-S.D., I.P., X.Q., P.-N.B., and S.K. performed experiments. All authors participated in data analysis. P.-G.M., S.K., and N.T. wrote the manuscript with important critical input from M.R., H.Y., L.O., S.T., X.A., V.D., M.S., V.S.Z., P.G.G., L.B., and N.M.

DECLARATION OF INTERESTS

M.S. and S.K. are inventors on a patent describing the use of a ligand for evaluation of GLUT1 expression (N.T. gave up her rights). M.S. is a co-founder of METAFORA Biosystems, focusing on metabolite transporters under physiological and pathological conditions, and is head of the scientific board.

Received: June 10, 2020
Revised: November 26, 2020
Accepted: January 12, 2021
Published: February 2, 2021

REFERENCES

Abdel-Wahab, O., and Levine, R.L. (2013). Mutations in epigenetic modifiers in the pathogenesis and therapy of acute myeloid leukemia. Blood *121*, 3563–3572.

Adam-Vizi, V., and Tretter, L. (2013). The role of mitochondrial dehydrogenases in the generation of oxidative stress. Neurochem. Int. *62*, 757–763.

Agathocleous, M., Meacham, C.E., Burgess, R.J., Piskounova, E., Zhao, Z., Crane, G.M., Cowin, B.L., Bruner, E., Murphy, M.M., Chen, W., et al. (2017). Ascorbate regulates haematopoietic stem cell function and leukaemogenesis. Nature *549*, 476–481.

An, X., Schulz, V.P., Li, J., Wu, K., Liu, J., Xue, F., Hu, J., Mohandas, N., and Gallagher, P.G. (2014). Global transcriptome analyses of human and murine terminal erythroid differentiation. Blood *123*, 3466–3477.

Ashley, R.J., Yan, H., Wang, N., Hale, J., Dulmovits, B.M., Papoin, J., Olive, M.E., Udeshi, N.D., Carr, S.A., Vlachos, A., et al. (2020). Steroid resistance in

(B) Enucleation of shControl- and shIDH1-transduced erythroblasts was assessed on GFP$^+$ cells at day 14, and representative histograms are presented (top). Enucleation levels, relative to control cells, were quantified (n = 8, bottom).
(C) The impact of αKG and DHA on erythroblast enucleation following IDH1 knockdown was evaluated between days 7 and 10, and representative histograms are presented (top). Enucleation relative to control conditions was quantified (n = 4, bottom).
(D) The impact of vitamin C on enucleation of control and IDH1-downregulated erythroblasts was evaluated between days 7 and 10. Representative histograms (top) and quantifications (bottom) are presented (n = 5). Changes in mitochondrial superoxide were evaluated by MitoSOX staining, and MFIs are presented (n = 4).
(E) TET2 was downregulated in erythroid progenitors by shTET2 lentivirus (day 4), and enucleation was monitored at day 10 in the presence or absence of vitamin C. Means ± SEM are presented (n = 5, one-way ANOVA with Tukey's post hoc test).
(F) Nuclear morphology of orthochromatic erythroblasts differentiated from shControl- and shIDH1-transduced progenitors in the absence or presence of vitamin C was monitored. Representative cytospins are shown (left), and the quantification of orthochromatic erythroblasts with abnormal nuclei was determined by counting 500–1,000 cells (n = 3, right).
ns, not significant; *p < 0.05; **p < 0.01; ***p < 0.001; ****p < 0.0001.

Diamond Blackfan anemia associates with p57Kip2 dysregulation in erythroid progenitors. J. Clin. Invest. *130*, 2097–2110.

Attallah, N., Osman-Malik, Y., Frinak, S., and Besarab, A. (2006). Effect of intravenous ascorbic acid in hemodialysis patients with EPO-hyporesponsive anemia and hyperferritinemia. Am. J. Kidney Dis. *47*, 644–654.

Bejar, R., and Steensma, D.P. (2014). Recent developments in myelodysplastic syndromes. Blood *124*, 2793–2803.

Bejar, R., Stevenson, K., Abdel-Wahab, O., Galili, N., Nilsson, B., Garcia-Manero, G., Kantarjian, H., Raza, A., Levine, R.L., Neuberg, D., and Ebert, B.L. (2011). Clinical effect of point mutations in myelodysplastic syndromes. N. Engl. J. Med. *364*, 2496–2506.

Bianchi, J., and Rose, R.C. (1986). Glucose-independent transport of dehydroascorbic acid in human erythrocytes. Proc. Soc. Exp. Biol. Med. *181*, 333–337.

Burch, J.S., Marcero, J.R., Maschek, J.A., Cox, J.E., Jackson, L.K., Medlock, A.E., Phillips, J.D., and Dailey, H.A., Jr. (2018). Glutamine via α-ketoglutarate dehydrogenase provides succinyl-CoA for heme synthesis during erythropoiesis. Blood *132*, 987–998.

Burns, J.J. (1957). Missing step in man, monkey and guinea pig required for the biosynthesis of L-ascorbic acid. Nature *180*, 553.

Busque, L., Patel, J.P., Figueroa, M.E., Vasanthakumar, A., Provost, S., Hamilou, Z., Mollica, L., Li, J., Viale, A., Heguy, A., et al. (2012). Recurrent somatic TET2 mutations in normal elderly individuals with clonal hematopoiesis. Nat. Genet. *44*, 1179–1181.

Calvert, A.E., Chalastanis, A., Wu, Y., Hurley, L.A., Kouri, F.M., Bi, Y., Kachman, M., May, J.L., Bartom, E., Hua, Y., et al. (2017). Cancer-associated IDH1 promotes growth and resistance to targeted therapies in the absence of mutation. Cell Rep. *19*, 1858–1873.

Carey, B.W., Finley, L.W., Cross, J.R., Allis, C.D., and Thompson, C.B. (2015). Intracellular alpha-ketoglutarate maintains the pluripotency of embryonic stem cells. Nature *518*, 413–416.

Case, A.J., Madsen, J.M., Motto, D.G., Meyerholz, D.K., and Domann, F.E. (2013). Manganese superoxide dismutase depletion in murine hematopoietic stem cells perturbs iron homeostasis, globin switching, and epigenetic control in erythrocyte precursor cells. Free Radic. Biol. Med. *56*, 17–27.

Chatterjee, I.B. (1973). Evolution and the biosynthesis of ascorbic acid. Science *182*, 1271–1272.

Chen, C., Liu, Y., Liu, R., Ikenoue, T., Guan, K.L., Liu, Y., and Zheng, P. (2008). TSC-mTOR maintains quiescence and function of hematopoietic stem cells by repressing mitochondrial biogenesis and reactive oxygen species. J. Exp. Med. *205*, 2397–2408.

Chen, Q., Chen, Y., Bian, C., Fujiki, R., and Yu, X. (2013). TET2 promotes histone O-GlcNAcylation during gene transcription. Nature *493*, 561–564.

Chung, J., Bauer, D.E., Ghamari, A., Nizzi, C.P., Deck, K.M., Kingsley, P.D., Yien, Y.Y., Huston, N.C., Chen, C., Schultz, I.J., et al. (2015). The mTORC1/4E-BP pathway coordinates hemoglobin production with L-leucine availability. Sci. Signal. *8*, ra34.

Cimmino, L., Dolgalev, I., Wang, Y., Yoshimi, A., Martin, G.H., Wang, J., Ng, V., Xia, B., Witkowski, M.T., Mitchell-Flack, M., et al. (2017). Restoration of TET2 function blocks aberrant self-renewal and leukemia progression. Cell *170*, 1079–1095.e20.

Crookston, J.H., Crookston, M.C., Burnie, K.L., Francombe, W.H., Dacie, J.V., Davis, J.A., and Lewis, S.M. (1969). Hereditary erythroblastic multinuclearity associated with a positive acidified-serum test: a type of congenital dyserythropoietic anaemia. Br. J. Haematol. *17*, 11–26.

Dang, L., White, D.W., Gross, S., Bennett, B.D., Bittinger, M.A., Driggers, E.M., Fantin, V.R., Jang, H.G., Jin, S., Keenan, M.C., et al. (2009). Cancer-associated IDH1 mutations produce 2-hydroxyglutarate. Nature *462*, 739–744.

Delhommeau, F., Dupont, S., Della Valle, V., James, C., Trannoy, S., Massé, A., Kosmider, O., Le Couedic, J.P., Robert, F., Alberdi, A., et al. (2009). Mutation in TET2 in myeloid cancers. N. Engl. J. Med. *360*, 2289–2301.

Fenaux, P., Haase, D., Sanz, G.F., Santini, V., Buske, C., and Group, E.G.W. (2014). Myelodysplastic syndromes: ESMO Clinical Practice Guidelines for diagnosis, treatment and follow-up. Ann. Oncol. *25*, 57–69.

Filippi, M.D., and Ghaffari, S. (2019). Mitochondria in the maintenance of hematopoietic stem cells: new perspectives and opportunities. Blood *133*, 1943–1952.

Frikke-Schmidt, H., and Lykkesfeldt, J. (2010). Keeping the intracellular vitamin C at a physiologically relevant level in endothelial cell culture. Anal. Biochem. *397*, 135–137.

Gastaldello, K., Vereerstraeten, A., Nzame-Nze, T., Vanherweghem, J.L., and Tielemans, C. (1995). Resistance to erythropoietin in iron-overloaded haemodialysis patients can be overcome by ascorbic acid administration. Nephrol. Dial. Transplant. *10* (*Suppl 6*), 44–47.

Gautier, E.F., Leduc, M., Ladli, M., Schulz, V.P., Lefèvre, C., Boussaid, I., Fontenay, M., Lacombe, C., Verdier, F., Guillonneau, F., et al. (2020). Comprehensive proteomic analysis of murine terminal erythroid differentiation. Blood Adv. *4*, 1464–1477.

Goasguen, J.E., Bennett, J.M., Bain, B.J., Brunning, R., Vallespi, M.T., Tomonaga, M., Zini, G., and Renault, A.; The International Working Group on Morphology of MDS (2018). Dyserythropoiesis in the diagnosis of the myelodysplastic syndromes and other myeloid neoplasms: problem areas. Br. J. Haematol. *182*, 526–533.

Grassian, A.R., Parker, S.J., Davidson, S.M., Divakaruni, A.S., Green, C.R., Zhang, X., Slocum, K.L., Pu, M., Lin, F., Vickers, C., et al. (2014). IDH1 mutations alter citric acid cycle metabolism and increase dependence on oxidative mitochondrial metabolism. Cancer Res. *74*, 3317–3331.

Guo, S., Jiang, X., Wang, Y., Chen, L., Li, H., Li, X., and Jia, Y. (2017). The protective role of TET2 in erythroid iron homeostasis against oxidative stress and erythropoiesis. Cell. Signal. *38*, 106–115.

Hata, R., and Senoo, H. (1989). L-ascorbic acid 2-phosphate stimulates collagen accumulation, cell proliferation, and formation of a three-dimensional tissuelike substance by skin fibroblasts. J. Cell. Physiol. *138*, 8–16.

Held, M.A., Greenfest-Allen, E., Jachimowicz, E., Stoeckert, C.J., Stokes, M.P., Wood, A.W., and Wojchowski, D.M. (2020). Phospho-proteomic discovery of novel EPO signal transducers including thioredoxin-interacting protein as a mediator of EPO-dependent human erythropoiesis. Exp. Hematol. *84*, 29–44.

Helgerson, A.L., and Carruthers, A. (1987). Equilibrium ligand binding to the human erythrocyte sugar transporter. Evidence for two sugar-binding sites per carrier. J. Biol. Chem. *262*, 5464–5475.

Hu, J., Liu, J., Xue, F., Halverson, G., Reid, M., Guo, A., Chen, L., Raza, A., Galili, N., Jaffray, J., et al. (2013). Isolation and functional characterization of human erythroblasts at distinct stages: implications for understanding of normal and disordered erythropoiesis in vivo. Blood *121*, 3246–3253.

Huang, N.J., Lin, Y.C., Lin, C.Y., Pishesha, N., Lewis, C.A., Freinkman, E., Farquharson, C., Millán, J.L., and Lodish, H. (2018). Enhanced phosphocholine metabolism is essential for terminal erythropoiesis. Blood *131*, 2955–2966.

Hyde, B.B., Liesa, M., Elorza, A.A., Qiu, W., Haigh, S.E., Richey, L., Mikkola, H.K., Schlaeger, T.M., and Shirihai, O.S. (2012). The mitochondrial transporter ABC-me (ABCB10), a downstream target of GATA-1, is essential for erythropoiesis in vivo. Cell Death Differ. *19*, 1117–1126.

Inoue, S., Lemonnier, F., and Mak, T.W. (2016). Roles of IDH1/2 and TET2 mutations in myeloid disorders. Int. J. Hematol. *103*, 627–633.

Iolascon, A., D'Agostaro, G., Perrotta, S., Izzo, P., Tavano, R., and Miraglia del Giudice, B. (1996). Congenital dyserythropoietic anemia type II: molecular basis and clinical aspects. Haematologica *81*, 543–559.

Jang, Y.Y., and Sharkis, S.J. (2007). A low level of reactive oxygen species selects for primitive hematopoietic stem cells that may reside in the low-oxygenic niche. Blood *110*, 3056–3063.

Johnson, R.J., Gaucher, E.A., Sautin, Y.Y., Henderson, G.N., Angerhofer, A.J., and Benner, S.A. (2008). The planetary biology of ascorbate and uric acid and their relationship with the epidemic of obesity and cardiovascular disease. Med. Hypotheses *71*, 22–31.

Kautz, L., and Nemeth, E. (2014). Molecular liaisons between erythropoiesis and iron metabolism. Blood *124*, 479–482.

Kc, S., Cárcamo, J.M., and Golde, D.W. (2005). Vitamin C enters mitochondria via facilitative glucose transporter 1 (Glut1) and confers mitochondrial protection against oxidative injury. FASEB J. *19*, 1657–1667.

Keerthivasan, G., Wickrema, A., and Crispino, J.D. (2011). Erythroblast enucleation. Stem Cells Int. *2011*, 139851.

Kim, F.J., Manel, N., Garrido, E.N., Valle, C., Sitbon, M., and Battini, J.L. (2004). HTLV-1 and -2 envelope SU subdomains and critical determinants in receptor binding. Retrovirology *1*, 41.

Kinet, S., Swainson, L., Lavanya, M., Mongellaz, C., Montel-Hagen, A., Craveiro, M., Manel, N., Battini, J.L., Sitbon, M., and Taylor, N. (2007). Isolated receptor binding domains of HTLV-1 and HTLV-2 envelopes bind Glut-1 on activated CD4+ and CD8+ T cells. Retrovirology *4*, 31.

Kosmider, O., Gelsi-Boyer, V., Slama, L., Dreyfus, F., Beyne-Rauzy, O., Quesnel, B., Hunault-Berger, M., Slama, B., Vey, N., Lacombe, C., et al. (2010). Mutations of IDH1 and IDH2 genes in early and accelerated phases of myelodysplastic syndromes and MDS/myeloproliferative neoplasms. Leukemia *24*, 1094–1096.

Kosmider, O., Delabesse, E., de Mas, V.M., Cornillet-Lefebvre, P., Blanchet, O., Delmer, A., Recher, C., Raynaud, S., Bouscary, D., Viguié, F., et al.; GOELAMS Investigators (2011). TET2 mutations in secondary acute myeloid leukemias: a French retrospective study. Haematologica *96*, 1059–1063.

Li, J., Hale, J., Bhagia, P., Xue, F., Chen, L., Jaffray, J., Yan, H., Lane, J., Gallagher, P.G., Mohandas, N., et al. (2014). Isolation and transcriptome analyses of human erythroid progenitors: BFU-E and CFU-E. Blood *124*, 3636–3645.

Liu, J., Xia, H., Kim, M., Xu, L., Li, Y., Zhang, L., Cai, Y., Norberg, H.V., Zhang, T., Furuya, T., et al. (2011). Beclin1 controls the levels of p53 by regulating the deubiquitination activity of USP10 and USP13. Cell *147*, 223–234.

Liu, X., Zhang, Y., Ni, M., Cao, H., Signer, R.A.J., Li, D., Li, M., Gu, Z., Hu, Z., Dickerson, K.E., et al. (2017). Regulation of mitochondrial biogenesis in erythropoiesis by mTORC1-mediated protein translation. Nat. Cell Biol. *19*, 626–638.

Loisel-Meyer, S., Swainson, L., Craveiro, M., Oburoglu, L., Mongellaz, C., Costa, C., Martinez, M., Cosset, F.L., Battini, J.L., Herzenberg, L.A., et al. (2012). Glut1-mediated glucose transport regulates HIV infection. Proc. Natl. Acad. Sci. USA *109*, 2549–2554.

Ludwig, L.S., Lareau, C.A., Bao, E.L., Nandakumar, S.K., Muus, C., Ulirsch, J.C., Chowdhary, K., Buenrostro, J.D., Mohandas, N., An, X., et al. (2019). Transcriptional states and chromatin accessibility underlying human erythropoiesis. Cell Rep. *27*, 3228–3240.e7.

Luo, S.T., Zhang, D.M., Qin, Q., Lu, L., Luo, M., Guo, F.C., Shi, H.S., Jiang, L., Shao, B., Li, M., et al. (2017). The promotion of erythropoiesis via the regulation of reactive oxygen species by lactic acid. Sci. Rep. *7*, 38105.

Manel, N., Kim, F.J., Kinet, S., Taylor, N., Sitbon, M., and Battini, J.L. (2003). The ubiquitous glucose transporter GLUT-1 is a receptor for HTLV. Cell *115*, 449–459.

Manning, J., Mitchell, B., Appadurai, D.A., Shakya, A., Pierce, L.J., Wang, H., Nganga, V., Swanson, P.C., May, J.M., Tantin, D., and Spangrude, G.J. (2013). Vitamin C promotes maturation of T-cells. Antioxid. Redox Signal. *19*, 2054–2067.

Mantel, C., Messina-Graham, S., and Broxmeyer, H.E. (2010). Upregulation of nascent mitochondrial biogenesis in mouse hematopoietic stem cells parallels upregulation of CD34 and loss of pluripotency: a potential strategy for reducing oxidative risk in stem cells. Cell Cycle *9*, 2008–2017.

Maryanovich, M., Zaltsman, Y., Ruggiero, A., Goldman, A., Shachnai, L., Zaidman, S.L., Porat, Z., Golan, K., Lapidot, T., and Gross, A. (2015). An MTCH2 pathway repressing mitochondria metabolism regulates haematopoietic stem cell fate. Nat. Commun. *6*, 7901.

May, J.M. (1998). Ascorbate function and metabolism in the human erythrocyte. Front. Biosci. *3*, d1–d10.

May, J.M., Qu, Z., and Morrow, J.D. (2001). Mechanisms of ascorbic acid recycling in human erythrocytes. Biochim. Biophys. Acta *1528*, 159–166.

McNulty, A.L., Stabler, T.V., Vail, T.P., McDaniel, G.E., and Kraus, V.B. (2005). Dehydroascorbate transport in human chondrocytes is regulated by hypoxia and is a physiologically relevant source of ascorbic acid in the joint. Arthritis Rheum. *52*, 2676–2685.

Metallo, C.M., Gameiro, P.A., Bell, E.L., Mattaini, K.R., Yang, J., Hiller, K., Jewell, C.M., Johnson, Z.R., Irvine, D.J., Guarente, L., et al. (2011). Reductive glutamine metabolism by IDH1 mediates lipogenesis under hypoxia. Nature *481*, 380–384.

Mingay, M., Chaturvedi, A., Bilenky, M., Cao, Q., Jackson, L., Hui, T., Moksa, M., Heravi-Moussavi, A., Humphries, R.K., Heuser, M., and Hirst, M. (2018). Vitamin C-induced epigenomic remodelling in IDH1 mutant acute myeloid leukaemia. Leukemia *32*, 11–20.

Montel-Hagen, A., Blanc, L., Boyer-Clavel, M., Jacquet, C., Vidal, M., Sitbon, M., and Taylor, N. (2008a). The Glut1 and Glut4 glucose transporters are differentially expressed during perinatal and postnatal erythropoiesis. Blood *112*, 4729–4738.

Montel-Hagen, A., Kinet, S., Manel, N., Mongellaz, C., Prohaska, R., Battini, J.L., Delaunay, J., Sitbon, M., and Taylor, N. (2008b). Erythrocyte Glut1 triggers dehydroascorbic acid uptake in mammals unable to synthesize vitamin C. Cell *132*, 1039–1048.

Montel-Hagen, A., Sitbon, M., and Taylor, N. (2009). Erythroid glucose transporters. Curr. Opin. Hematol. *16*, 165–172.

Moras, M., Lefevre, S.D., and Ostuni, M.A. (2017). From erythroblasts to mature red blood cells: organelle clearance in mammals. Front. Physiol. *8*, 1076.

Mueckler, M. (1994). Facilitative glucose transporters. Eur. J. Biochem. *219*, 713–725.

Murphy, M.P. (2009). How mitochondria produce reactive oxygen species. Biochem. J. *417*, 1–13.

Oburoglu, L., Tardito, S., Fritz, V., de Barros, S.C., Merida, P., Craveiro, M., Mamede, J., Cretenet, G., Mongellaz, C., An, X., et al. (2014). Glucose and glutamine metabolism regulate human hematopoietic stem cell lineage specification. Cell Stem Cell *15*, 169–184.

Oburoglu, L., Romano, M., Taylor, N., and Kinet, S. (2016). Metabolic regulation of hematopoietic stem cell commitment and erythroid differentiation. Curr. Opin. Hematol. *23*, 198–205.

Padayatty, S.J., and Levine, M. (2016). Vitamin C: the known and the unknown and Goldilocks. Oral Dis. *22*, 463–493.

Pauling, L. (1970). Evolution and the need for ascorbic acid. Proc. Natl. Acad. Sci. USA *67*, 1643–1648.

Qian, P., He, X.C., Paulson, A., Li, Z., Tao, F., Perry, J.M., Guo, F., Zhao, M., Zhi, L., Venkatraman, A., et al. (2016). The Dlk1-Gtl2 locus preserves LT-HSC function by inhibiting the PI3K-mTOR pathway to restrict mitochondrial metabolism. Cell Stem Cell *18*, 214–228.

Qu, X., Zhang, S., Wang, S., Wang, Y., Li, W., Huang, Y., Zhao, H., Wu, X., An, C., Guo, X., et al. (2018). TET2 deficiency leads to stem cell factor-dependent clonal expansion of dysfunctional erythroid progenitors. Blood *132*, 2406–2417.

Robb, E.L., Gawel, J.M., Aksentijević, D., Cochemé, H.M., Stewart, T.S., Shchepinova, M.M., Qiang, H., Prime, T.A., Bright, T.P., James, A.M., et al. (2015). Selective superoxide generation within mitochondria by the targeted redox cycler MitoParaquat. Free Radic. Biol. Med. *89*, 883–894.

Rumsey, S.C., Kwon, O., Xu, G.W., Burant, C.F., Simpson, I., and Levine, M. (1997). Glucose transporter isoforms GLUT1 and GLUT3 transport dehydroascorbic acid. J. Biol. Chem. *272*, 18982–18989.

Rumsey, S.C., Daruwala, R., Al-Hasani, H., Zarnowski, M.J., Simpson, I.A., and Levine, M. (2000). Dehydroascorbic acid transport by GLUT4 in Xenopus oocytes and isolated rat adipocytes. J. Biol. Chem. *275*, 28246–28253.

Savini, I., Rossi, A., Pierro, C., Avigliano, L., and Catani, M.V. (2008). SVCT1 and SVCT2: key proteins for vitamin C uptake. Amino Acids *34*, 347–355.

Schulz, V.P., Yan, H., Lezon-Geyda, K., An, X., Hale, J., Hillyer, C.D., Mohandas, N., and Gallagher, P.G. (2019). A unique epigenomic landscape defines human erythropoiesis. Cell Rep. *28*, 2996–3009.e7.

Seibert, E., Richter, A., Kuhlmann, M.K., Wang, S., Levin, N.W., Kotanko, P., and Handelman, G.J. (2017). Plasma vitamin C levels in ESRD patients and occurrence of hypochromic erythrocytes. Hemodial. Int. *21*, 250–255.

Shenoy, N., Creagan, E., Witzig, T., and Levine, M. (2018). Ascorbic acid in cancer treatment: let the phoenix fly. Cancer Cell *34*, 700–706.

Sirover, W.D., Siddiqui, A.A., and Benz, R.L. (2008). Beneficial hematologic effects of daily oral ascorbic acid therapy in ESRD patients with anemia and abnormal iron homeostasis: a preliminary study. Ren. Fail. *30*, 884–889.

Starkov, A.A., Fiskum, G., Chinopoulos, C., Lorenzo, B.J., Browne, S.E., Patel, M.S., and Beal, M.F. (2004). Mitochondrial alpha-ketoglutarate dehydrogenase complex generates reactive oxygen species. J. Neurosci. *24*, 7779–7788.

Stone, I. (1979). Eight decades of scurvy. Australas. Nurses J. *8*, 28–30.

Suda, T., Takubo, K., and Semenza, G.L. (2011). Metabolic regulation of hematopoietic stem cells in the hypoxic niche. Cell Stem Cell *9*, 298–310.

Swainson, L., Kinet, S., Manel, N., Battini, J.L., Sitbon, M., and Taylor, N. (2005). Glucose transporter 1 expression identifies a population of cycling CD4+ CD8+ human thymocytes with high CXCR4-induced chemotaxis. Proc. Natl. Acad. Sci. USA *102*, 12867–12872.

Takamizawa, S., Maehata, Y., Imai, K., Senoo, H., Sato, S., and Hata, R. (2004). Effects of ascorbic acid and ascorbic acid 2-phosphate, a long-acting vitamin C derivative, on the proliferation and differentiation of human osteoblast-like cells. Cell Biol. Int. *28*, 255–265.

Takubo, K., Nagamatsu, G., Kobayashi, C.I., Nakamura-Ishizu, A., Kobayashi, H., Ikeda, E., Goda, N., Rahimi, Y., Johnson, R.S., Soga, T., et al. (2013). Regulation of glycolysis by Pdk functions as a metabolic checkpoint for cell cycle quiescence in hematopoietic stem cells. Cell Stem Cell *12*, 49–61.

Tan, D.Q., and Suda, T. (2018). Reactive oxygen species and mitochondrial homeostasis as regulators of stem cell fate and function. Antioxid. Redox Signal. *29*, 149–168.

TeSlaa, T., Chaikovsky, A.C., Lipchina, I., Escobar, S.L., Hochedlinger, K., Huang, J., Graeber, T.G., Braas, D., and Teitell, M.A. (2016). α-Ketoglutarate accelerates the initial differentiation of primed human pluripotent stem cells. Cell Metab. *24*, 485–493.

Tischler, J., Gruhn, W.H., Reid, J., Allgeyer, E., Buettner, F., Marr, C., Theis, F., Simons, B.D., Wernisch, L., and Surani, M.A. (2019). Metabolic regulation of pluripotency and germ cell fate through α-ketoglutarate. EMBO J. *38*, 38.

Tretter, L., and Adam-Vizi, V. (2004). Generation of reactive oxygen species in the reaction catalyzed by alpha-ketoglutarate dehydrogenase. J. Neurosci. *24*, 7771–7778.

Tsukaguchi, H., Tokui, T., Mackenzie, B., Berger, U.V., Chen, X.Z., Wang, Y., Brubaker, R.F., and Hediger, M.A. (1999). A family of mammalian Na+-dependent L-ascorbic acid transporters. Nature *399*, 70–75.

Vande Voorde, J., Ackermann, T., Pfetzer, N., Sumpton, D., Mackay, G., Kalna, G., Nixon, C., Blyth, K., Gottlieb, E., and Tardito, S. (2019). Improving the metabolic fidelity of cancer models with a physiological cell culture medium. Sci. Adv. *5*, eaau7314.

Vannini, N., Girotra, M., Naveiras, O., Nikitin, G., Campos, V., Giger, S., Roch, A., Auwerx, J., and Lutolf, M.P. (2016). Specification of haematopoietic stem cell fate via modulation of mitochondrial activity. Nat. Commun. *7*, 13125.

Vardhana, S.A., Arnold, P.K., Rosen, B.P., Chen, Y., Carey, B.W., Huangfu, D., Carmona Fontaine, C., Thompson, C.B., and Finley, L.W.S. (2019). Glutamine independence is a selectable feature of pluripotent stem cells. Nat. Metab. *1*, 676–687.

Vera, J.C., Rivas, C.I., Fischbarg, J., and Golde, D.W. (1993). Mammalian facilitative hexose transporters mediate the transport of dehydroascorbic acid. Nature *364*, 79–82.

Wang, N., Wang, F., Shan, N., Sui, X., and Xu, H. (2017). IDH1 mutation is an independent inferior prognostic indicator for patients with myelodysplastic syndromes. Acta Haematol. *138*, 143–151.

Wilson, J.X. (2005). Regulation of vitamin C transport. Annu. Rev. Nutr. *25*, 105–125.

Xiao, M., Yang, H., Xu, W., Ma, S., Lin, H., Zhu, H., Liu, L., Liu, Y., Yang, C., Xu, Y., et al. (2012). Inhibition of α-KG-dependent histone and DNA demethylases by fumarate and succinate that are accumulated in mutations of FH and SDH tumor suppressors. Genes Dev. *26*, 1326–1338.

Xu, P., Palmer, L.E., Lechauve, C., Zhao, G., Yao, Y., Luan, J., Vourekas, A., Tan, H., Peng, J., Schuetz, J.D., et al. (2019). Regulation of gene expression by miR-144/451 during mouse erythropoiesis. Blood *133*, 2518–2528.

Yan, H., Wang, Y., Qu, X., Li, J., Hale, J., Huang, Y., An, C., Papoin, J., Guo, X., Chen, L., et al. (2017). Distinct roles for TET family proteins in regulating human erythropoiesis. Blood *129*, 2002–2012.

Yan, H., Hale, J., Jaffray, J., Li, J., Wang, Y., Huang, Y., An, X., Hillyer, C., Wang, N., Kinet, S., et al. (2018). Developmental differences between neonatal and adult human erythropoiesis. Am. J. Hematol. *93*, 494–503.

Yu, W.M., Liu, X., Shen, J., Jovanovic, O., Pohl, E.E., Gerson, S.L., Finkel, T., Broxmeyer, H.E., and Qu, C.K. (2013). Metabolic regulation by the mitochondrial phosphatase PTPMT1 is required for hematopoietic stem cell differentiation. Cell Stem Cell *12*, 62–74.

Yun, J., Mullarky, E., Lu, C., Bosch, K.N., Kavalier, A., Rivera, K., Roper, J., Chio, I.I., Giannopoulou, E.G., Rago, C., et al. (2015). Vitamin C selectively kills KRAS and BRAF mutant colorectal cancer cells by targeting GAPDH. Science *350*, 1391–1396.

Zhang, Z.Z., Lee, E.E., Sudderth, J., Yue, Y., Zia, A., Glass, D., Deberardinis, R.J., and Wang, R.C. (2016). Glutathione depletion, pentose phosphate pathway activation, and hemolysis in erythrocytes protecting cancer cells from vitamin C-induced oxidative stress. J. Biol. Chem. *291*, 22861–22867.

Zhao, B., Mei, Y., Yang, J., and Ji, P. (2016). Erythropoietin-regulated oxidative stress negatively affects enucleation during terminal erythropoiesis. Exp. Hematol. *44*, 975–981.

STAR★METHODS

KEY RESOURCES TABLE

REAGENT or RESOURCE	SOURCE	IDENTIFIER
Antibodies		
Anti-hCD11b-PE (clone Bear1)	Beckman Coulter	Cat#IM2581U; RRID: AB_131334
Anti-hCD13-PC7 (clone Immuno103.44)	Beckman Coulter	Cat#A46528
Anti-hCD33 (clone D3HL60.251)	Beckman Coulter	Cat#A07775
Anti-hCD34-FITC (clone 581)	Becton Dickinson	Cat#55582; RRID:AB_396150
Anti-hCD34-APC (clone 581)	Becton Dickinson	Cat#555824; RRID:AB_398614
Anti-hCD34-PE (clone 81)	Beckman Coulter	Cat#A07776
Anti-hCD36-APC (clone FA6.152)	Beckman Coulter	Cat#A87786
Anti-hCD36-FITC (clone FA6.152)	Beckman Coulter	Cat#B49201; RRID:AB_2848117
Anti-hCD36-PB (clone FA6.152)	Beckman Coulter	Cat#B43302
Anti-hCD49d-APC (clone HP2/1)	Beckman Coulter	Cat#B01682
Anti-hCD71-APC (clone MA-A712)	Becton Dickinson	Cat#551374; RRID:AB_398500
Anti-hCD71-APC-AF750 (clone MA-A712)	Beckman Coulter	Cat#A89313; RRID:AB_2800452
Anti-hCD105- PECF594 (clone 266)	Becton Dickinson	Cat#562380; RRID:AB_11154054
Anti-hGlyA-PC7 (clone 11E4B-7-6)	Beckman Coulter	Cat#A71564; RRID:AB_2800449
Anti-hGlyA-APC (clone GA-R2 (HIR2))	eBioscience/ThermoFisher	Cat#17-9987-42; RRID:AB_2043823
Anti-hGlyA- BV421 (clone GA-R2 (HIR2))	Becton Dickinson	Cat#562938
Anti-hIL3R-PC7 (clone 6H6)	eBioscience/ThermoFisher	Cat#25-1239-42; RRID:AB_1257136
Goat anti-Rabbit IgG Alexa Fluor 405	Molecular Probes/ThermoFisher	Cat#A-31556; RRID:AB_221605
GLUT1 RBD-GFP	Metafora Biosystems	Cat#GLUT1_G100
GLUT1 RBD-rFc	Metafora Biosystems	Cat#GLUT1_R100
Bacterial and virus strains		
Top 10 Competent cells	ThermoFisher	Cat#C404010
Biological samples		
Human umbilical cord blood	Unité De Thérapie Cellulaire de Montpellier	N/A
Human peripheral blood	New York Blood Center	N/A
Human bone marrow	Northwell Health	N/A
Chemicals, peptides, and recombinant proteins		
2-Phospho-L-ascorbic acid	Sigma-Aldrich	Cat#A8960
tetramethylchromane-2-carboxylic acid (TROLOX)	Sigma-Aldrich	Cat#238813
N-Acetylcysteine	Sigma-Aldrich	Cat#A9165
Ascorbate Oxidase from Cucurbita sp.	Sigma-Aldrich	Cat#A0157
L-Ascorbic acid	Sigma-Aldrich	Cat#A92902
O-(Carboxymethyl)hydroxylamine hemihydrochloride (AOA)	Sigma-Aldrich	Cat#C13408
Diethylsuccinate	Sigma-Aldrich	Cat#112402
Dimethyl α-ketoglutarate	Sigma-Aldrich	Cat#349631
L-Glutathione reduced	Sigma-Aldrich	Cat#G4251
MitoParaquat	Abcam	Cat#ab146819
Spautin-1	Sigma-Aldrich	Cat#SML0440
Tri-sodium Citrate dihydrate	Sigma-Aldrich	Cat#S4641
C13-GlutamineL-Glutamine (13C5,15N2)	Cambridge Isotope Laboratories	Cat#CNLM-1275-H-PK

(Continued on next page)

Continued

REAGENT or RESOURCE	SOURCE	IDENTIFIER
L-[3,4-3H(N)]-Glutamine	Perkin Elmer	Cat#NET551250UC
Oligomycin	Sigma-Aldrich	Cat#O4876
FCCP	Sigma-Aldrich	Cat#C2920
Rotenone	Sigma-Aldrich	Cat#R8875
Antimycin A	Sigma-Aldrich	Cat#A8674
DMSO	Sigma-Aldrich	Cat#D2650
Human recombinant IL-3	R&D Systems	Cat#203-IL-010
Human recombinant IL-6	R&D Systems	Cat#206-IL-010
rhuSCF	Amgen	N/A
Stem Spam CC100	Stem Cell	Cat#02690
EPREX	Janssen	Cat#3400936992368
Human holo-transferrin	Sigma-Aldrich	Cat#T0665
Human insulin solution	Sigma-Aldrich	Cat#9278
Heparin	Sanofi	Cat#3400930484500
Bovine serum albumin	Sigma-Aldrich	Cat#A8806
IMDM	Life Technologies/ThermoFisher	Cat#21980032
StemSpam SFEM	Stem Cell	Cat#09650
StemSpam H3000	Stem Cell	Cat#09850
RPMI w/o glutamine and glucose	Pan Biotech	Cat#P04-17550
Seahorse XF Assay Medium	Agilent Technologies	102365-100
Seahorse XF Calibrant Solution	Agilent Technologies	100840-000
Ultima Gold liquid scintillation cocktail	Perkin Elmer	Cat#6013329
Critical commercial assays		
Anti-hCD34 MicroBead kit	Miltenyi Biotec	Cat#130-046-702; RRID:AB_2848167
RNeasy Mini kit	QIAGEN	Cat# 74104
QuantiTect™ Reverse Transcription Kit	QIAGEN	Cat# 205311
Experimental models: cell lines		
Jurkat E6-1	ATCC	TIB-152
293 T cells	ATCC	CRL-3216
Oligonucleotides		
IDH1 forward: 5′-GGGTTGGCCTTTGTATCTGA-3′	IDT	Custom order
IDH1 reverse: 5′-TTTACAGGCCCAGATGAAGC-3′	IDT	Custom order
IDH2 forward: 5′-TGGCTCAGGTCCTCAAGTCT-3′	IDT	Custom order
IDH2 reverse: 5′-CTCAGCCTCAATCGTCTTCC-3′	IDT	Custom order
IDH3a forward: 5′-GCGCAAAACATTTGACCTTT-3′	IDT	Custom order
IDH3a reverse: 5′-TGCACGACTCCATCAACAAT-3′	IDT	Custom order
TET2 forward: 5′-AGCAGCAGCCAATAGGACAT-3′	IDT	Custom order
TET2 reverse: 5′-AGGTTCTGTCTGGCAAATGG-3′	IDT	Custom order
βactin forward: 5′-GTCTTCCCCTCCATCGTG-3′	IDT	Custom order
βactin reverse: 5′-TTCTCCATGTCGTCCCAG-3′	IDT	Custom order

(*Continued on next page*)

Continued		
REAGENT or RESOURCE	SOURCE	IDENTIFIER
Recombinant DNA		
TRC2pLKO sh Tet2	Sigma Aldrich	Cat# TRCN0000418976
TRC2pLKO sh IDH1	Sigma Aldrich	Cat# TRCN0000312463
TRC1pLKO sh IDH1	Sigma Aldrich	Cat# TRCN0000027284
TRC1pLKO sh non-mammalian control	Sigma Aldrich	Cat# SHC002
Software and algorithms		
FlowJo (version 10)	BD Biosciences	https://www.flowjo.com/
Prism (version 8)	GraphPad Software	https://www.graphpad.com/scientific-software/prism/
Wave (version 2)	Agilent Technologies	https://www.agilent.com/en/product/cell-analysis/real-time-cell-metabolic-analysis/xf-software/seahorse-wave-desktop-software-740897
Xcalibur 2.2	ThermoFisher	http://www.casco-documentation.com/content/dam/tfs/ATG/CMD/cmd-documents/oper/oper/ms/lc-ms/soft/Man-XCALI-97209-Xcalibur-22-Acquisition-ManXCALI97209-D-EN.pdf
LCquan 2.7	ThermoFisher	https://assets.thermofisher.com/TFS-Assets/CMD/manuals/LCquan-Admin-2-7.pdf
TraceFinder 4.1	ThermoFisher	https://www.thermofisher.com/us/en/home/industrial/mass-spectrometry/liquid-chromatography-mass-spectrometry-lc-ms/lc-ms-software/lc-ms-data-acquisition-software/tracefinder-software.html
Other		
CM-H2DCFDA	Molecular Probes/Thermofisher	Cat#C6827
Dihydrorhodamine 123	Molecular Probes/Thermofisher	Cat#D23806
Mitotracker Deep Red FM	Molecular Probes/Thermofisher	Cat#M22426
MitoTracker Green FM	Molecular Probes/Thermofisher	Cat#M7514
MitoTracker Red CMXRos	Molecular Probes/Thermofisher	Cat#M7512
MitoSox Red	Molecular Probes/Thermofisher	Cat#M36008
Propidium Iodide	Sigma-Aldrich	Cat#P4170
Syto16	Molecular Probes/Thermofisher	Cat#S7578
Syto60	Molecular Probes/Thermofisher	Cat#S11342

RESOURCE AVAILABILITY

Lead contact

Further information and requests for resources and reagents should be directed to and will be fulfilled by the Lead Contact, Naomi Taylor (taylorn4@mail.nih.gov).

Materials availability

This study did not generate new unique reagents. All lentiviral vectors generated in this study are available on request.

Data and code availability

This study did not generate datasets or code.

EXPERIMENTAL MODELS AND SUBJECT DETAILS

CD34+ cell isolation and *ex vivo* differentiation assays.

All studies involving human samples were conducted in accordance with the declaration of Helsinki. CD34+ cells were isolated from umbilical cord blood within 24h of vaginal delivery of full-term infants after informed consent and approval by the "Committee for the Protection of Persons" (IRB) of the University Hospital of Montpellier. Peripheral blood from leukoreduction filters and bone marrow were obtained from deidentified donors at the New York Blood Center and the North Shore-LIJ Health System, respectively, after informed consent and approval from the respective IRBs. Approximately 60 UCB, 10 PB and 6 BM samples were used in this study. Samples did not contain any identifiers including sex, race, or ethnic origin. All samples were split such that they were used in all experimental groups. As such, there was no need to use any specific criteria to allocate biological samples to experimental groups. For the vast majority of experiments, at least 3 biological samples were used. For experiments presented in Figures 1A, 6F, and 6G, 2 biological samples were employed and technical triplicates were evaluated for both samples.

CD34+ cells (1 × 10^5 cells/ml) were expanded in StemSpan H3000 media (StemCell Technologies Inc) supplemented with StemSpam CC100 (StemCell Technologies Inc) at 37°C with a humidified 5% CO_2 atmosphere. Cells were plated in 24-well *Nunclon Delta surface plates (Nunc, Thermo Fisher Scientific).* After 4 days of expansion, cells were differentiated in IMDM medium (Invitrogen) supplemented with human holo-transferrin (200 mg/L, Sigma-Aldrich), human insulin (10 mg/L, Sigma-Aldrich), rhuSCF (10 ng/ml, Amgen), rhuIL-3 (1 ng/ml, R&D Systems). Erythropoiesis was induced by addition of 3 U/ml recombinant human erythropoietin (rEPO; Eprex, Janssen-Cilag). In some experiments, CD34+ cells were not expanded and erythropoiesis was directly induced after selection (data in Figure 5). Cytokines were supplemented every 3-4 days at the same time that media was renewed. Cells were centrifuged at 300 g for 10min at RT and then resuspended in fresh media to maintain cell concentrations between 0.1 and 1.5 × 10^6 cells/ml. In some experiments, progenitors were differentiated in the presence of 3.5 mM cell permeable dimethyl α-ketoglutarate (DMK, Sigma-Aldrich), 5 mM diethylsuccinate (Sigma Aldrich), 8 mM citrate (Sigma-Aldrich), 1 mM aminooxyacetate (AOA, Sigma-Aldrich), 50 μM MitoParaquat (MitoPQ, Abcam), 1 mM L-ascorbic acid (AA, Sigma-Aldrich), 100 μM 2-phospho-L-ascorbic acid (Vit C, Sigma-Aldrich), 100 μM N-acetylcysteine (NAC, Sigma-Aldrich), 100 μM reduced glutathione (GSH, Sigma-Aldrich), 100 μM of the water-soluble analog of vitamin E (TROLOX, Sigma Aldrich), or 10 μM of specific and potent autophagy inhibitor-1 (Spautin-1, Sigma-Aldrich). Ascorbate oxidase (1 U/mL, Sigma-Aldrich) was used to completely oxidize L-ascorbic acid to DHA in culture medium before treating the cells. Drugs were freshly added after every media change. In experiments where cells were co-cultured with α-KG (DMK, 3.5 mM) in the presence of antioxidants, α-KG was administered 2 hours after the addition of the corresponding antioxidant. As MitoPQ and TROLOX were dissolved in DMSO, control conditions included cultures using the same concentration of DMSO (0.05 and 0.1%, respectively).

METHODS DETAIL

Cytospin preparation

Cytospins were prepared on glass slides (5x10^4 cells in 200 μL of PBS), using the Thermo Scientific Shandon 4 Cytospin (300 g for 5 min). Slides were stained with May-Grünwald solution (Sigma-Aldrich) for 5 min, rinsed in 40 mM Tris buffer for 90 s, and subsequently stained with Giemsa solution (Sigma-Aldrich) for 15 minutes. Cells were imaged using a Leica DM2000 inverted microscope under 100 × objective magnification.

Flow cytometry

Expression of the CD34, CD36, CD49d, CD71, CD105 (Ashley et al., 2020), Glycophorin A, IL3R, CD11b, CD13, and CD33 surface markers was monitored on 1-2x10^5 cells using the appropriate fluorochrome-conjugated monoclonal antibodies at a 1:100 dilution (mAb), except for CD36-APC and CD71-AF750 mAbs that were used at a 1:200 and 1:500 dilution, respectively (Beckman Coulter, Becton Dickinson, eBiosciences), in a total volume of 100 μls as previously described (Hu et al., 2013; Schulz et al., 2019). Cells were incubated in the dark for 20 minutes in PBS containing 2% FBS at 4°C and then washed once in the same medium at 300 g for 10 min prior to evaluation. GLUT1 expression was monitored by binding to its retroviral envelope ligand (RBD) fused to eGFP (1:25 dilution in 50 μls; Metafora biosystems) or to the RBD-rFc fusion protein (1:25 dilution in 50 μls) for 30 minutes in PBS containing 2% FBS at 37°C followed by staining with an Alexa Fluor 405-coupled anti-rabbit IgG antibody (1:100 dilution in 100 μls) at 4°C as previously reported (Kim et al., 2004; Kinet et al., 2007; Manel et al., 2003; Swainson et al., 2005). Mitochondrial biomass was assessed in a total volume of 50 μls by MitoTrackerGreen or MitoTrackerDeepRed staining (20 nM; Invitrogen, Molecular Probes), while mitochondrial transmembrane potential levels were monitored by staining with MitoTrackerRed (50 nM; Invitrogen, Molecular Probes). Mitochondrial superoxide production, mitochondrial ROS levels and total ROS levels were assessed by staining with MitoSOX, Dihydrorodamine 123 and CM-H2DCFDA, respectively (5 μM; Invitrogen, Molecular Probes). Incubations were performed in the dark for 20 minutes in PBS + 2% FBS at RT. Enucleation was evaluated by staining with the SYTO16 or SYTO60 nucleic acid stain (1 μM and 0.5 μM, Invitrogen, Molecular Probes) for 15 minutes in PBS + 2% FBS at RT. Cell cycle analysis was performed by staining for DNA using 50 μg/mL propidium iodide (PI; Sigma-Aldrich) following permeabilization in 100 μls of 0.1% Triton X-100. To assess cell death, cells were incubated with PI (10 μg/ml). Cell sorting was performed on a FACSARIA high-speed cell sorter (BD

Biosciences) and analyses were performed on a FACS-Canto II (BD Biosciences) cytometers. A minimum of 10,000 events were recorded for each staining. Data analyses were performed using FlowJo software (Tree Star, Ashland, OR).

Virus production and transduction of CD34$^+$ progenitor cells

Lentiviral pLKO.1 plasmids harboring shRNAs directed against *IDH1* (shRNA IDH1-1: Clone ID: TRCN0000027284 and shRNA IDH1-2: ID: TRCN0000312463) and lentiviral TRC2-pLKO plasmid harboring shRNA against TET2 (ID: TRCN0000418976) (Yan et al., 2017) were obtained from Sigma-Aldrich. Cells were transduced with the shRNA IDH1-1 lentiviral plasmid, the shRNA IDH1-2 plasmid or the shRNA TET2 plasmid where the 714bp sequence encoding for EGFP was inserted in place of the puromycin gene at the unique BamHI and KpnI restriction sites. Virions were generated by transient transfection of 293T cells (2-3x10^6 cells/100mm plate in 7 mL DMEM) with these vectors (10 mg) together with the Gag-Pol packaging construct PsPax2 (5 mg) and a plasmid encoding the VSV-G envelope, pCMV-VSV-G (2.5 mg), as described previously (Loisel-Meyer et al., 2012). Cells were transfected for at least 18 hours, and transfection efficiency was verified by monitoring GFP fluorescence by microscopy. Viral supernatant was harvested 24 hours post-transfection and virions were concentrated by overnight centrifugation at 4°C at 1,500 g (with no break). Virions were resuspended in approximately 20 µl of RPMI with 10% FBS (per plate of cells), aliquoted and stored at −80°C. Titers were determined by serial dilutions of virus preparations on Jurkat cells and are expressed as Jurkat transducing units (TU/ml).

Prior to transduction of CD34$^+$ hematopoietic stem and progenitor cells (HSPCs), cells were expanded for 3 days in StemSpan medium (Stem cell Technologies Inc) supplemented with 5% fetal bovine serum (FBS), 25 ng/ml rhuSCF (Amgen), 10 ng/ml rhuIL-3 and 10 ng/ml rhuIL-6 (R&D) at 37°C with a humidified 5% CO_2 atmosphere. 5 × 10^5 cells were then exposed to viral supernatants containing 4.8 × 10^5 TU to 9.9 × 10^5 TU (representing a multiplicity of infection of 1-2). After 72h of transduction, CD34$^+$ cells (1 × 10^5 cells/ml) were cultured in presence of rEPO (3 U/ml) to induce erythropoiesis. Transduction efficiency was monitored as a function of GFP expression or after puromycin selection at 72h post-transduction, as per the lentiviral vector. In some experiments, cells were transduced at day 4 of erythroid differentiation (i.e., at day 4 following addition of EPO) under the same conditions as described above, and transduction efficiency was monitored at day 7 of differentiation.

Quantitative real time PCR

Total RNA was isolated at the indicated time points and cDNA was synthetized using the RNeasy Mini kit and the QuantiTect™ Reverse Transcription Kit (QIAGEN) as per the manufacturer's instructions. Quantitative PCR of cDNAs was performed using the Quantitect SYBR green PCR Master mix (Roche) with 10 ng of cDNA (by NanoDrop) and 0.5 µM primers in a final volume of 10µl. Primer sequences are as follows: *IDH1*: 5′-GGGTTGGCCTTTGTATCTGA-3′ (forward) / 5′- TTTACAGGCCCAGATGAAGC −3′ (reverse); IDH2: 5′-TGGCTCAGGTCCTCAAGTCT-3′ (forward) / 5′-CTCAGCCTCAATCGTCTTCC-3′ (reverse); IDH3a: 5′-GCGCAAAA CATTTGACCTTT-3′ (forward) / 5′-TGCACGACTCCATCAACAAT-3′ (reverse); TET2: 5′-AGCAGCAGCCAATAGGACAT-3′ (forward) / 5′-AGGTTCTGTCTGGCAAATGG-3′ (reverse); and β-actin: 5′-GTCTTCCCCTCCATCGTG-3′ (forward) / 5′-TTCTCCATGTCGTCCC AG-3′ (reverse). Amplification of cDNAs was performed using the LightCycler 480 (Roche). Cycling conditions included a denaturation step for 5 min at 95°C, followed by 40 cycles of denaturation (95°C for 10 s), annealing (63°C for 10 s) and extension (72°C for 10 s). After amplification, melting curve analysis was performed with denaturation at 95°C for 5 s and continuous fluorescence measurement from 65°C to 97°C at 0.1°C/s. Each sample was amplified in triplicate. Data were analyzed by LightCycler® 480 Software (Version 1.5) and Microsoft Excel. Relative expression was calculated by normalization to β-actin as indicated (delta-Ct). Real-time PCR CT values were analyzed using the 2(-Delta Delta C(T)) method to calculate fold expression (ddCt).

Mass spectrometry (LC-MS)

For profiling of intracellular metabolites, 10^6 cells were incubated in IMDM medium without glutamine and were supplemented with 2mM uniformly labeled $^{13}C_5$-$^{15}N_2$ glutamine (Cambridge Isotope Laboratories) for 6 hours (Figure 1A) or 18 hours (Figures 6F and 6G). Cells were rapidly washed in ice-cold PBS, centrifuged twice (400 g for 4 min), and metabolites were extracted in a solution of 50% methanol, 30% acetonitrile, 20% water after shaking for 20 min at 4°C. The solutions were then recentrifuged for 10 min at 16,000 g at 4°C. The volume of the extraction solution was adjusted to achieve a constant ratio of 2 x10^6 cells/ml. Alternatively, the peak areas resulting from the intracellular samples were normalized to the number of cells obtained at the end of the incubation period in parallel wells. Supernatants were stored at −20°C until analysis. Samples were analyzed by HPLC-MS as described previously (Vande Voorde et al., 2019). Data were analyzed with Xcalibur 2.2, LCquan 2.7 and TraceFinder 4.1 software (Thermo scientific). Samples were performed in triplicate, and at least 2 different biological samples were evaluated for each condition.

Seahorse analysis

Oxygen consumption rates (OCR) and extracellular acidification rates (ECAR) were measured using the XFe-96 Extracellular Flux Analyzer (Seahorse Bioscience, Agilent). The calibration plate was filled with 200 µL Milli-Q water per well and kept at 37°C overnight. At least 2 hours prior to the assay, water was replaced by 200 µL XF calibrant (Agilent)/ well. Culture plates were treated with 20 µl/well of 0.1mg/mL of Poly-D-Lysine for at least 1 hour at RT. Poly-D-Lysine (Sigma-Aldrich) solution was then removed and plates was washed twice with 200 µL Milli-Q water/well, dried, and kept at 4°C until the assay was performed. Cells (2.5 × 10^5) were placed in 50 µL XF medium (non-buffered DMEM containing 10 mM glucose and 2 mM GlutaMax, pH 7.3-7.4, Agilent), centrifuged in a carrier tray (300 g for 3min with no break), and incubated for 30 min at 37°C. An additional 130 µL XF medium was added during the

calibration time (20-30 min at 37°C). Cells were monitored in basal conditions and in response to oligomycin (1 μM; Sigma-Aldrich), FCCP (1 μM; Sigma-Aldrich), rotenone (100 nM, Sigma-Aldrich) and antimycin A (1 μM; Sigma-Aldrich). In some experiments, αKG (DMK, final concentration of 3.5 mm) was injected directly into the well before the sequential addition of oligomycin, FCCP, rotenone and antimycin A during the Mito Stress Test. Wave software (Agilent) was employed for running the Seahorse assay and analysis. Samples were performed at least in triplicate and generally 5-6 points per experiment and at least 3 independent experiments.

Glutamine uptake assays

Cells (5×10^5) were washed twice in 1.5 mL of PBS containing 2%FBS at 400 g for 4 min at RT, and starved for glutamine by incubation at 37°C in 30 μl glutamine-free RPMI for 30 min. Radiolabeled glutamine-L-[3,4-^{3}H(N)] (Perkin Elmer) was added to a final concentration of 0.5 μM (0.5 μCi/mL in a total volume of 50 μL). Cells were incubated for 10 min at room temperature, washed twice in cold PBS containing 2%FBS (1000 g, 3 min), and solubilized in 500 μL of a 0.1% SDS solution. Radioactivity was measured in 4.5 mL liquid scintillation (Perkin Elmer) using a Hidex 300 SL counter. Each independent experiment was performed in triplicate.

QUANTIFICATION AND STATISTICAL ANALYSIS

Data are represented as individual values or means. Error bars represent the standard error of the mean (SEM). Data were analyzed with GraphPad Software (GraphPad Prism), and *P*- values were determined by one-way ANOVA (Tukey's post hoc test) or t tests, as indicated in the corresponding text and figure legends. Two-tailed t tests were used in all figures except for Figure 6F where a one-tailed t test was used. Tests were paired or unpaired as indicated and a normal distribution was used in all experiments. All statistical details of experiments can be found in the figure legends. Significance is indicated as * $p < 0.05$, ** $p < 0.01$, *** $p < 0.001$ and **** $p < 0.0001$ as evaluated by GraphPad. The graphical abstract was created using BioRender and Servier Medical Art.

Cell Reports, Volume *34*

Supplemental Information

An IDH1-vitamin C crosstalk drives human erythroid development by inhibiting pro-oxidant mitochondrial metabolism

Pedro Gonzalez-Menendez, Manuela Romano, Hongxia Yan, Ruhi Deshmukh, Julien Papoin, Leal Oburoglu, Marie Daumur, Anne-Sophie Dumé, Ira Phadke, Cédric Mongellaz, Xiaoli Qu, Phuong-Nhi Bories, Michaela Fontenay, Xiuli An, Valérie Dardalhon, Marc Sitbon, Valérie S. Zimmermann, Patrick G. Gallagher, Saverio Tardito, Lionel Blanc, Narla Mohandas, Naomi Taylor, and Sandrina Kinet

Supplemental Information

An IDH1-vitamin C crosstalk drives human erythroid development by inhibiting pro-oxidant mitochondrial metabolism

Pedro Gonzalez-Menendez, Manuela Romano, Hongxia Yan, Ruhi Deshmukh, Julien Papoin, Leal Oburoglu, Marie Daumur, Anne-Sophie Dumé, Ira Phadke, Cédric Mongellaz, Xiaoli Qu, Phuong-Nhi Bories, Michaela Fontenay, Xiuli An, Valérie Dardalhon, Marc Sitbon, Valérie S. Zimmermann, Patrick G. Gallagher, Saverio Tardito, Lionel Blanc, Narla Mohandas, Naomi Taylor and Sandrina Kinet

Supplemental Information Titles

Supplemental Figure 1. ***Ex vivo*** **erythroid differentiation of human CD34$^+$ progenitors is associated with a loss in oxidative phosphorylation.** Related to Figure 1.

Supplemental Figure 2. **αKG does not alter mitochondrial function during early stages of erythropoiesis and other TCA cycle metabolites do not inhibit enucleation.** Related to Figure 2.

Supplemental Figure 3. **Impact of vitamin C on αKG- and MitoPQ-induced oxidative stress in erythroid progenitors.** Related to Figures 3 and 4.

Supplemental Figure 4. **Ascorbic acid as well as other ROS scavengers rescue erythroid progenitors from oxidative stress**. Related to Figure 4.

Supplemental Figure 5. **The impact of Vitamin C on enucleation is independent of autophagy but is dependent on transferrin uptake.** Related to Figures 4 and 5.

Supplemental Figure 6. **Downregulation of IDH1 does not alter erythroid commitment or early erythroblast generation.** Related to Figure 6.

Supplemental Figure 7. **Vitamin C but no other ROS scavengers rescues enucleation and decreases mitochondrial stress in IDH1-downregulated progenitors.** Related to Figure 7.

Supplemental Information

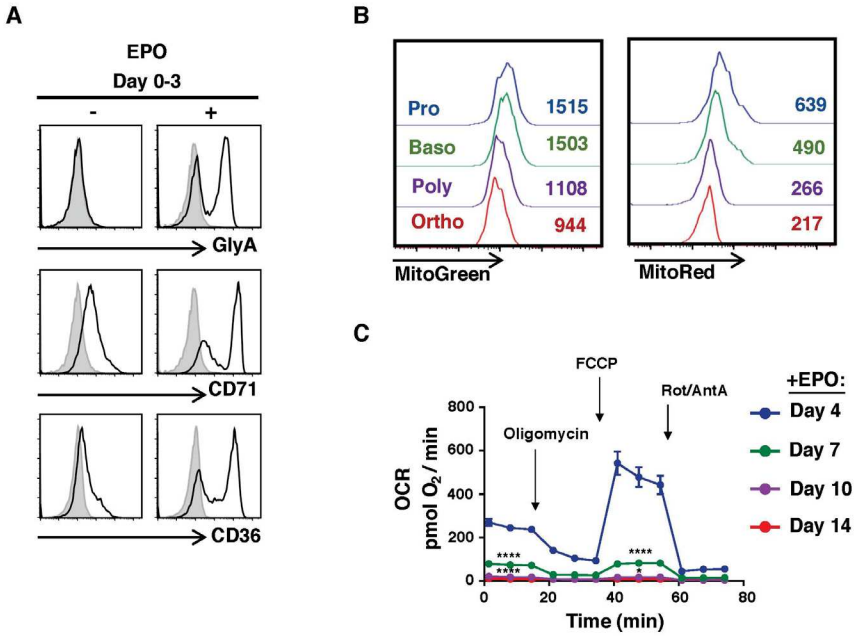

Figure S1. ***Ex vivo*** **erythroid differentiation of human CD34$^+$ progenitors is associated with a loss in oxidative phosphorylation. Related to Figure 1.** (**A**) The phenotype of CD34$^+$ progenitors differentiated in the absence (-) or presence (+) of recombinant erythropoietin (EPO). Representative histograms showing expression of GlyA, CD71, and CD36 are presented (data are representative of 1 of 10 independent experiments). (**B**) Representative histograms of mitochondrial biomass and polarization are shown for pro, basophilic, polychromatic, and orthochromatic erythroblasts, and mean levels are presented in Figure 1D. (**C**) CD34$^+$ progenitors were differentiated in the presence of recombinant erythropoietin (EPO) and OCR, a measure of oxidative phosphorylation, was monitored at the indicated days of erythroid differentiation. Basal oxygen consumption, maximal consumption following FCCP, and minimal levels following inhibition of the electron transport chain with rotenone/antimycin A (Rot/AntA) are presented as means ±SEM (n=6). ****p<0.0001

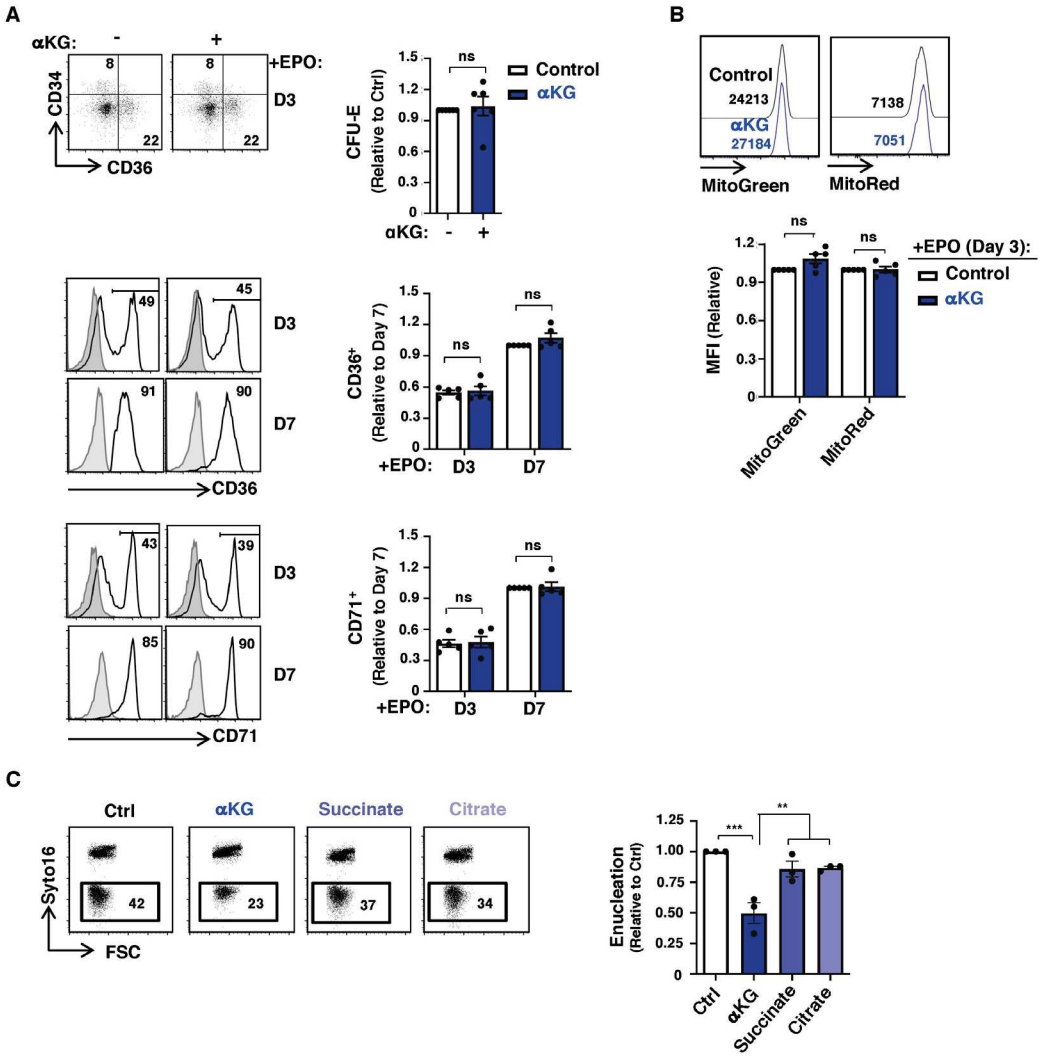

Figure S2. αKG does not alter mitochondrial function during early stages of erythropoiesis and other TCA cycle metabolites do not inhibit enucleation. Related to Figure 2. (**A**) The impact of αKG (3.5 mM) on early stages of erythropoiesis was evaluated at days 3 and 7 of EPO-induced differentiation. The induction of $CD36^{+}CD34^{-}$ CFU-E was monitored at day 3 and representative CD34/CD36 profiles as well as a quantification of the percentages of CFU-E relative to control are shown (top; n=6, non-significant, ns). Induction of CD36 (middle) and CD71 (bottom) during erythroid differentiation were monitored and representative histograms and quantifications (n=4-5) are presented (right). (**B**) Mitochondrial biomass and polarization were evaluated by flow cytometry and representative histograms as well as a quantification of MFI relative to control conditions are presented (n=5, bottom). (**C**) Differentiated erythroblasts were treated with αKG, succinate (5 mM) or citrate (8 mM) at day 7 and enucleation was evaluated at day 10 by Syto16 staining. Representative histograms (left) as well as means ±SEM (n=3 independent experiments) are shown. ** $p<0.01$, *** $p<0.001$, ns, non-significant

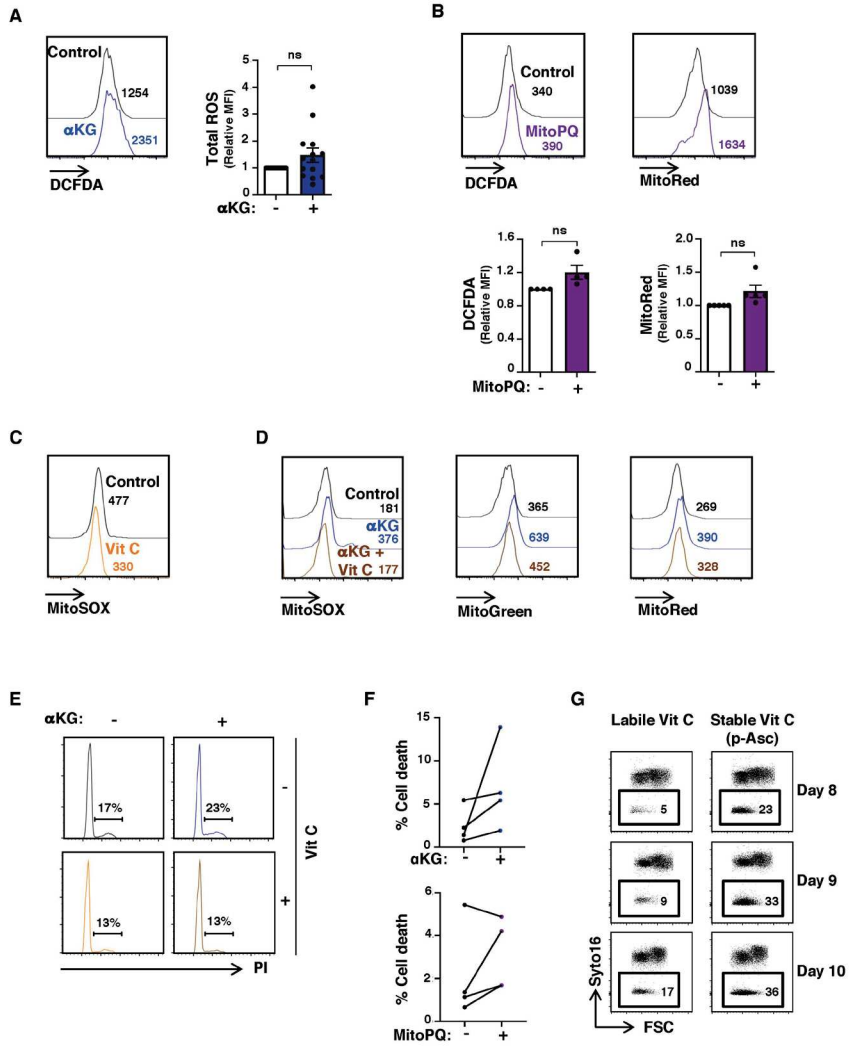

Figure S3. Impact of vitamin C on αKG- and MitoPQ-induced oxidative stress in erythroid progenitors. Related to Figures 3 and 4. (**A**) Total intracellular ROS levels were evaluated on erythroblasts differentiated from day 7-10 in the absence (control) or presence of αKG, as a function of CM-H2DCFDA staining. Representative histograms (left) and quantifications in 12 independent experiments (right) are shown. (**B**) Total ROS levels and mitochondrial polarization were evaluated in the absence or presence of MitoPQ and representative histograms (top) and MFI quantifications (bottom) are presented (n=4). (**C**) The impact of L-ascorbic acid 2-phosphate (100μM) was evaluated on the generation of mitochondrial superoxide between days 7 and 10 after EPO induction and representative histograms are shown with quantification provided in panel 4E. (**D**) The ability of Vit C to alter αKG-mediated increases in mitochondrial superoxide, biomass and membrane potential was evaluated by flow cytometry and representative histograms are shown. (**E**) Representative histograms of PI staining show the percentages of cells in S-G2/M of the cell cycle with quantifications provided in panel 4F. (**F**) Cell death was evaluated in the absence or presence of αKG (3.5mM, top) and MitoPQ (50μM, bottom) and data from 4 independent experiments are presented. (**G**) CD34^{+} HSPCs were differentiated to the erythroid lineage by treatment with rEPO for 7 days. At day 7, erythroid cells were cultured in the presence of L-ascorbate and ascorbate 2-phosphate (100μM), presenting labile and stable vitamin C, respectively (Hata and Senoo, 1989). Enucleation was evaluated 24, 48 and 72h later; at days 8, 9, and 10 of differentiation, respectively. Representative dot plots of Syto16 staining are shown and the percentages of enucleated cells are indicated.

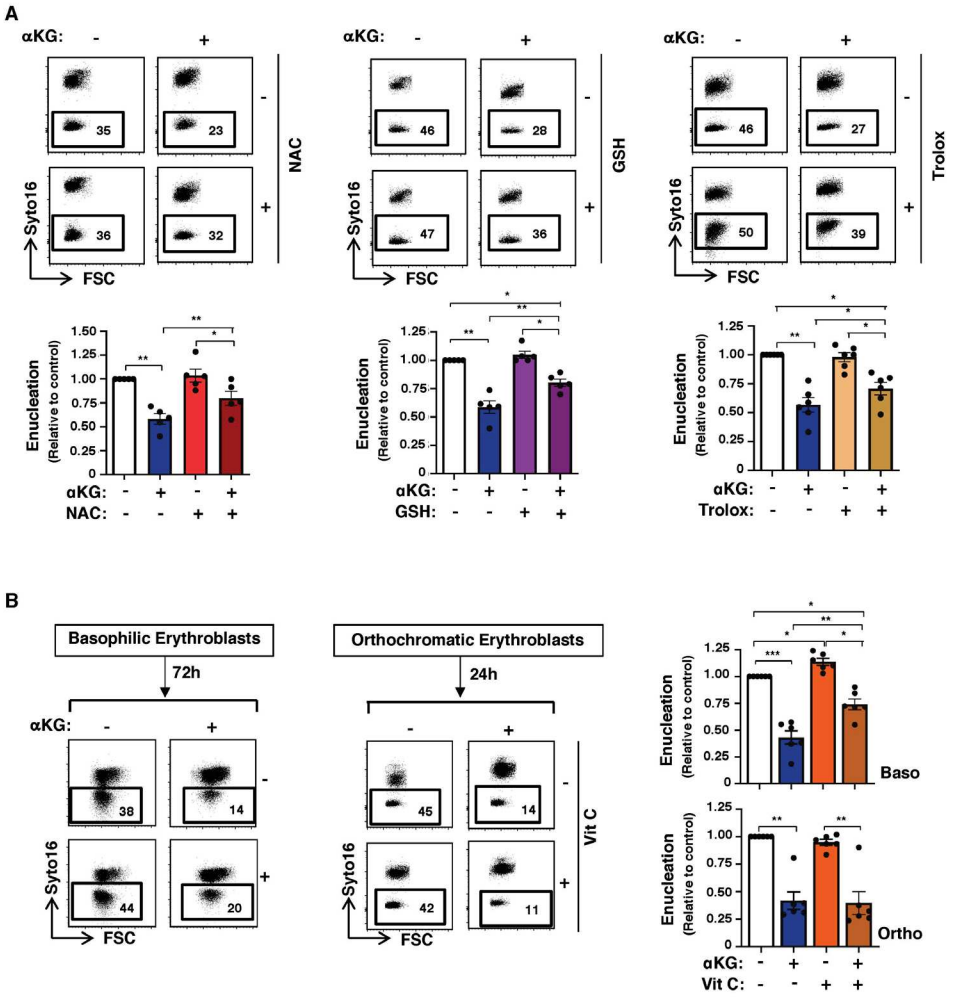

Figure S4. Ascorbic acid as well as other ROS scavengers rescue erythroid progenitors from oxidative stress. Related to Figure 4. (**A**) The impact of ROS scavengers on the αKG-mediated decrease in enucleation was evaluated for NAC (100μM, left), GSH (100μM, middle) and Trolox (100μM, right). Representative plots (top) and means ± SEM of 5-6 independent experiments (bottom) are presented. (**B**) Early basophilic (left) and late orthochromatic (right) subsets were FACS-sorted and then differentiated for 72h or 24h, respectively, in the absence (-) or presence (+) of αKG and/or Vit C as indicated. Enucleation was evaluated by Syto16 staining and representative plots are presented (left). Enucleation in experimental groups was calculated relative to control conditions and mean levels are presented (right, n=6). ns, not significant; *p<0.05, ** p<0.01, ***p<0.001

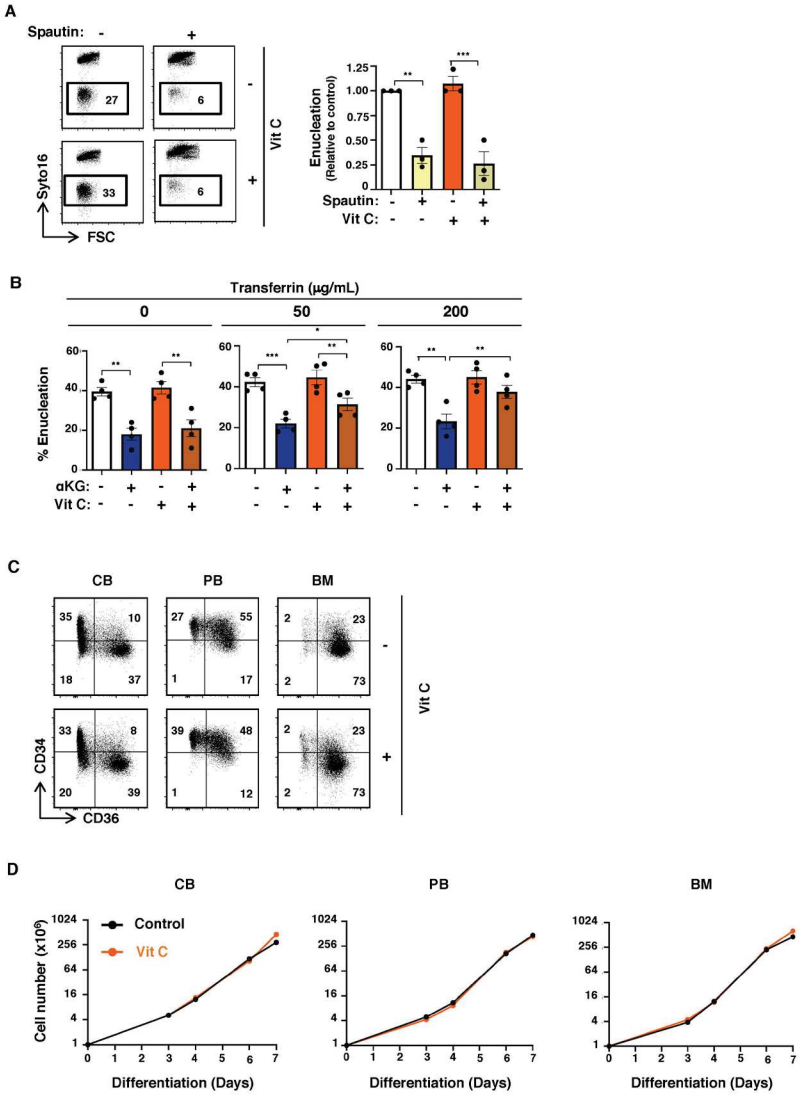

Figure S5. The impact of Vitamin C on enucleation is independent of autophagy but is dependent on transferrin uptake. Related to Figures 4 and 5. (**A**) The impact of Vit C on erythroid enucleation under conditions of a Spautin (10 µM)-mediated inhibition of autophagy was evaluated at day 10 of erythroid differentiation. Representative plots (left) and means ± SEM of 3 independent experiments (right) are shown. (**B**) Erythroblasts were differentiated in the absence or presence of transferrin (50 or 200 µg/ml), αKG (3.5mM) and Vit C (100µM) between days 7 and 10 of differentiation and enucleation was monitored by Syto16 staining. Means ± SEM of 4 independent experiments are presented. (**C**) CD34 HSPCs isolated from CB, PB, and BM were differentiated with EPO (+) in the absence (-) or presence of vitamin C (Vit C) for 4 days. The differentiation of CFU-E ($CD34^{-}CD36^{+}$) was monitored as a function of CD34/CD36 staining and representative plots are shown. (**D**) Growth of EPO-differentiated CB-, PB- and BM-derived progenitors was evaluated in the absence (-) or presence of vitamin C. Fold-increase at days 3, 4, 6 and 7 differentiation is shown for one representative experiment (n=2). *p<0.05, ** p<0.01, ***p<0.001

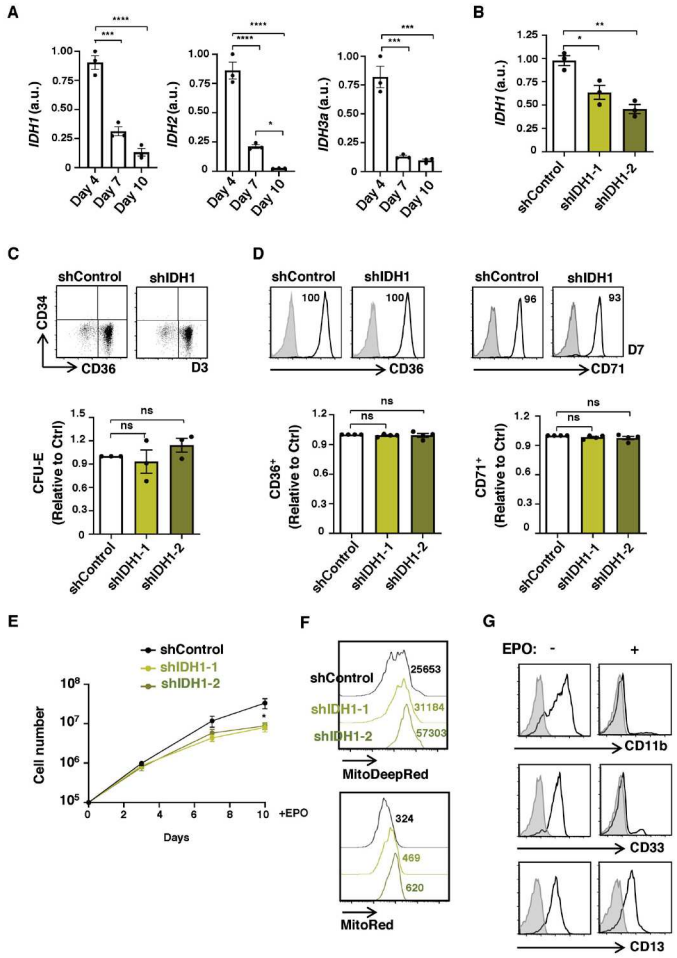

Figure S6. Downregulation of IDH1 does not alter erythroid commitment or early erythroblast generation. Related to Figure 6. (**A**) mRNA levels of IDH1, IDH2 and IDH3 were evaluated by qRT-PCR and means ± SEM relative to β-actin are shown (technical triplicates, representative of 1 of 2 independent experiments). (**B**) The efficacy of the two shIDH1 vectors was evaluated by monitoring IDH1 mRNA levels by qRT-PCR. Mean levels ±SEM relative to β-actin following transduction with shIDH1-1 and shIDH1-2 are presented. (**C**) Generation of CFU-E, defined as $CD34^{-}CD36^{+}$, were evaluated in shControl- and shIDH1-transduced progenitors at day 3 of differentiation. Representative dot plots (top) and quantification of the relative induction of CFU-E (bottom) are shown (n=3). (**D**) Differentiation of erythroblasts was evaluated by induction of the CD36 and CD71 markers and representative histograms (top) and quantifications (bottom) are shown (n=4). (**E**) The expansion of control and IDH1-downregulated progenitors was evaluated at the indicated day and means ± SEM of 5 independent experiments are shown. (**F**) Representative histograms of MitoDeepRed (top) and MitoRed (bottom) staining in shControl- and shIDH1-transduced progenitors at day 10 of differentiation. (**G**) The phenotype of $CD34^{+}$ progenitors expanded in the absence (-) or presence (+) of EPO is shown at day 7 of differentiation as a function of CD11b, CD33 and CD13 staining. Solid line and shaded histograms represent specific and non-specific staining, respectively. ns, non-significant; * p<0.05, **p<0.01, ***p<0.001, ****p<0.0001.

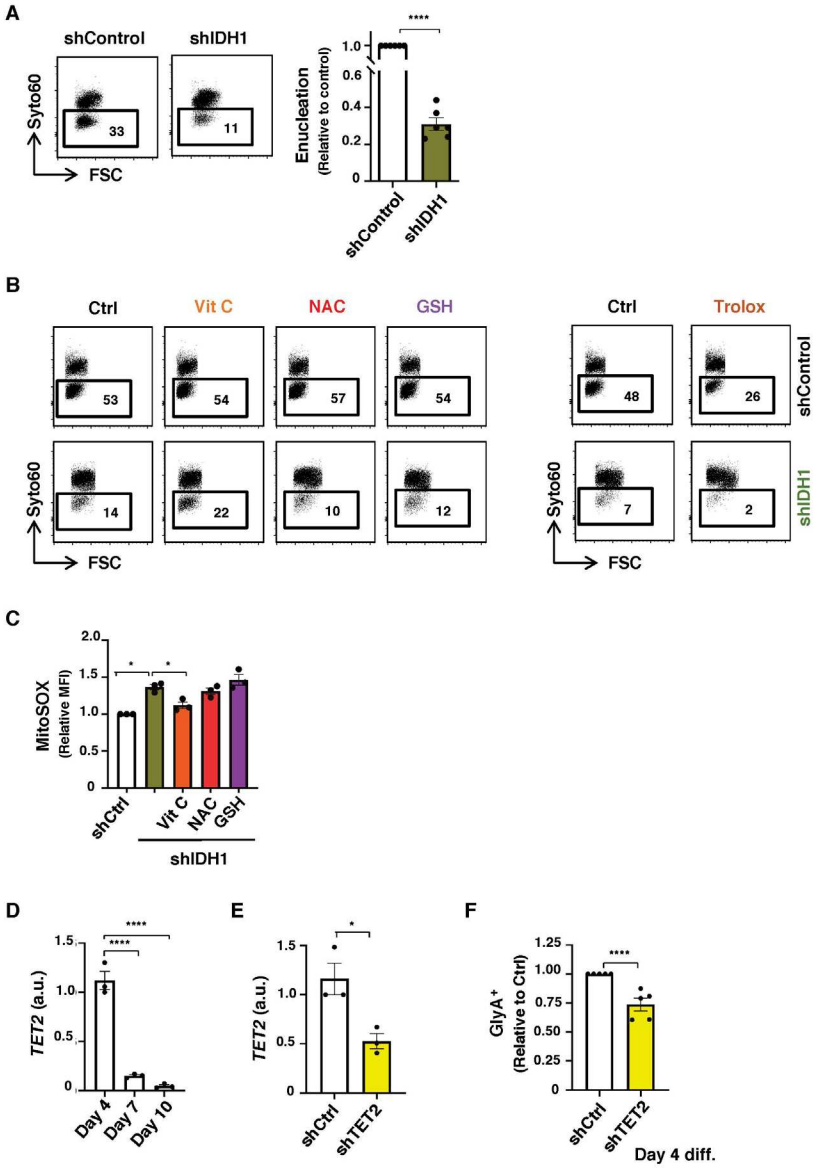

Figure S7. Vitamin C but no other ROS scavengers rescues enucleation and decreases mitochondrial stress in IDH1-downregulated progenitors. Related to Figure 7. (**A**) IDH1 was downregulated in erythroid progenitors (day 4) by transduction with shIDH1-encoding lentiviral particles and enucleation was monitored at day 10 of differentiation. Representative plots (left) and means ± SEM (right) are presented (n=6, 1-way ANOVA with Tukey's post-hoc test). (**B**) The impact of ROS scavengers (Vit C, NAC, GSH and Trolox; 100 µM) on the shIDH1-mediated decrease in enucleation was evaluated at day 10 of differentiation. Representative plots are presented (n=2). (**C**) The impact of Vit C, NAC, GSH and Trolox (with DMSO as a control) was evaluated on the shIDH1-mediated increase in MitoSOX at day 10. Means ± SEM of 3 independent experiments are shown. (**D**) TET2 mRNA levels were evaluated at days 4, 7 and 10 of differentiation and means ± SEM of 3 independent experiments are shown. (**E**) The shTET2-mediated downregulation of TET2 was evaluated by qRT-PCR and means ± SEM relative to β-actin are shown. (**F**) The impact of shTET2 on erythroid development was evaluated at day 4 of differentiation as a function of GlyA staining. The relative levels of GlyA in 5 independent experiments were normalized to control progenitors. ns, not significant; *p<0.05, ****p<0.0001

REFERENCES

Adlung, L., Stapor, P., Tönsing, C., Schmiester, L., Schwarzmüller, L. E., Postawa, L., … Schilling, M. (2021). Cell-to-cell variability in JAK2/STAT5 pathway components and cytoplasmic volumes defines survival threshold in erythroid progenitor cells. *Cell Reports*, *36*(6). https://doi.org/10.1016/j.celrep.2021.109507

Ali, A. M., Huang, Y., Pinheiro, R. F., Xue, F., Hu, J., Iverson, N., … Raza, A. (2018). Severely impaired terminal erythroid differentiation as an independent prognostic marker in myelodysplastic syndromes. *Blood Advances*, *2*(12), 1393–1402. https://doi.org/10.1182/bloodadvances.2018018440

Allen, D. M., & Diamond, L. K. (1961). Congenital (Erythroid) Hypoplastic Anemia: Cortisone Treated. *American Journal of Diseases of Children*, *102*(3), 416–423. https://doi.org/10.1001/ARCHPEDI.1961.02080010418021

An, C., Huang, Y., Li, M., Xue, F., Nie, D., Zhao, H., … An, X. (2021). Vesicular formation regulated by ERK / MAPK pathway mediates human erythroblast enucleation. *Blood Advances*.

An, X., Schulz, V. P., Li, J., Wu, K., Liu, J., Xue, F., … Gallagher, P. G. (2014). Global transcriptome analyses of human and murine terminal erythroid differentiation. *Blood*, *123*(22), 3466–3477. https://doi.org/10.1182/blood-2014-01-548305

Anna Rita Migliaccio, L. V. (2018). The challenges and opportunities provided by advanced cell culture models for human erythropoiesis to study Diamond Blackfan Anemia and other erythroid disorders. *Stem Cells*, *36*, 172–179. https://doi.org/10.1002/stem.2735.The

Antunes, A. T., Goos, Y. J., Pereboom, T. C., Hermkens, D., Wlodarski, M. W., Da Costa, L., & MacInnes, A. W. (2015). Ribosomal Protein Mutations Result in Constitutive p53 Protein Degradation through Impairment of the AKT Pathway. *PLoS Genetics*, *11*(7), 1–19. https://doi.org/10.1371/journal.pgen.1005326

Appelhoffl, R. J., Tian, Y. M., Raval, R. R., Turley, H., Harris, A. L., Pugh, C. W., … Gleadle, J. M. (2004). Differential function of the prolyl hydroxylases PHD1, PHD2, and PHD3 in the regulation of hypoxia-inducible factor. *Journal of Biological Chemistry*, *279*(37), 38458–38465. https://doi.org/10.1074/jbc.M406026200

Ashley, R. J., Yan, H., Wang, N., Hale, J., Dulmovits, B. M., Papoin, J., … Blanc, L. (2020). Steroid resistance in Diamond Blackfan anemia associates with p57Kip2 dysregulation in erythroid progenitors. *Journal of Clinical Investigation*, *130*(4), 2097–2110. https://doi.org/10.1172/JCI132284

Axelrad, A. A., Mcleod, D. L., Shreeve, M. M., & Heath, D. S. (1973). Properties of cells that produce erythrocytic colonies in vitro. *Hemopoiesis in Culture, Second International Workshop. U.S. Government Printing*, *XXX*, 226–237.

Barminko, J., Reinholt, B., & Baron, M. H. (2016). Development and differentiation of the erythroid lineage in mammals. *Dev Comp Immunol*. https://doi.org/10.1016/j.dci.2015.12.012

Barth, B., Wang, W., Sullivan, E., Papakotsi, V., Cote, A., Toran, P., … Loughran, T. P. (2019). GDF1 Regulation of Ceramide Metabolism Restores Effective Hematopoiesis in Myelodysplastic Syndrome. *Blood*, *134*(Supplement_1), 1700–1700. https://doi.org/10.1182/blood-2019-131623

Berra, E., Benizri, E., Ginouvès, A., Volmat, V., Roux, D., & Pouysségur, J. (2003). HIF prolyl-hydroxylase 2 is the key oxygen sensor setting low steady-state levels of HIF-1α in normoxia. *EMBO Journal*, *22*(16), 4082–4090. https://doi.org/10.1093/emboj/cdg392

Bessis, M. (1958). Erythroblastic island, functional unity of bone marrow. *Rev Hematol*, *13*(1), 8–11.

Bhagat, T. D., Zhou, L., Sokol, L., Kessel, R., Caceres, G., Gundabolu, K., … Verma, A. (2013). MiR-21 mediates hematopoietic suppression in MDS by activating TGF-β signaling. *Blood*, *121*(15), 2875–2881. https://doi.org/10.1182/blood-2011-12-397067

Bigarella, C. L., Liang, R., & Ghaffari, S. (2014). Stem cells and the impact of ROS signaling. *Development (Cambridge)*, *141*(22), 4206–4218. https://doi.org/10.1242/dev.107086

Blanc, L., Gassart, A. De, Géminard, C., Bette-Bobillo, P., & Vidal, M. (2005). Exosome release by reticulocytes--an integral part of the red blood cell differentiation system. *Blood Cells, Molecules, and Diseases*, *35*(1).

Broudy, V. C., Lin, N. L., Priestley, G. V., Nocka, K., & Wolf, N. S. (1996). Interaction of stem cell factor and its receptor c-kit mediates lodgment and acute expansion of hematopoietic cells in the murine spleen. *Blood*, *88*(1), 75–81. https://doi.org/10.1182/blood.v88.1.75.bloodjournal88175

C H A N, H. S., Saunders, E. F., & Freedman, M. H. (1982). Diamond-Blackfan Syndrome. II. In Vitro Corticosteroid Effect on Erythropoiesis. *Pediatr. Res*, *16*, 477–478. Retrieved from https://www.nature.com/pr/journal/v16/n6/pdf/pr1982130a.pdf

Camaschella, C., & Pagani, A. (2018, August 1). Advances in understanding iron metabolism and its crosstalk with erythropoiesis. *British Journal of Haematology*, Vol. 182, pp. 481–494. https://doi.org/10.1111/bjh.15403

Capellera-Garcia, S., Pulecio, J., Dhulipala, K., Siva, K., Rayon-Estrada, V., Singbrant, S., … Flygare, J. (2016). Defining the Minimal Factors Required for Erythropoiesis through Direct Lineage Conversion. *Cell Reports*, *15*(11), 2550–2562. https://doi.org/10.1016/j.celrep.2016.05.027

Cazzola, M. (2020). Myelodysplastic Syndromes. *New England Journal of Medicine*, *383*(14), 1358–1374. https://doi.org/10.1056/NEJMra1904794

Chande, S., Caballero, D., Ho, B. B., Fetene, J., Serna, J., Pesta, D., … Bergwitz, C. (2020). Slc20a1/Pit1 and Slc20a2/Pit2 are essential for normal skeletal myofiber function and survival. *Scientific Reports*, *10*(1), 1–14. https://doi.org/10.1038/s41598-020-59430-4

Chasis, J. A., & Mohandas, N. (2008). Erythroblastic islands: Niches for erythropoiesis. *Blood*, *112*(3), 470–478. https://doi.org/10.1182/blood-2008-03-077883

Chen-Liang, T.-H. (2021). Prognosis in Myelodysplastic Syndromes: The Clinical Challenge of Genomic Integration. *Journal of Clinical Medicine*, *10*(10), 2052. https://doi.org/10.3390/JCM10102052

Chen, C., Yu, W., Tober, J., Gao, P., He, B., Lee, K., … Tan, K. (2019). Spatial Genome Re-organization between Fetal and Adult Hematopoietic Stem Cells. *Cell Reports*, *29*(12), 4200-4211.e7. https://doi.org/10.1016/j.celrep.2019.11.065

Chlon, T. M., McNulty, M., Goldenson, B., Rosinski, A., & Crispino, J. D. (2015). Global transcriptome and chromatin occupancy analysis reveal the short isoform of GATA1 is deficient for erythroid specification and gene expression. *Haematologica*, *100*(5), 575–584. https://doi.org/10.3324/haematol.2014.112714

Cluzeau, T., McGraw, K. L., Irvine, B., Masala, E., Ades, L., Basiorka, A. A., … List, A. (2017). Pro-inflammatory proteins S100A9 and tumor necrosis factor-α suppress erythropoietin elaboration in myelodysplastic syndromes. *Haematologica*, *102*(12), 2015. https://doi.org/10.3324/HAEMATOL.2016.158857

Costa, L. Da, Mohandas, N., Sorette, M., & Tchernia, G. (2001). Hereditary Spherocytosis and in Immune Hemolytic Anemia. *Cell*, *98*(10), 2894–2899.

Da Costa, L., Leblanc, T., & Mohandas, N. (2020). Diamond-Blackfan anemia. *Blood*, *136*(11), 1262–1273. https://doi.org/10.1182/BLOOD.2019000947

Da Costa, L., O'Donohue, M. F., van Dooijeweert, B., Albrecht, K., Unal, S., Ramenghi, U., … MacInnes, A. W. (2018). Molecular approaches to diagnose Diamond-Blackfan anemia: The EuroDBA experience. *European Journal of Medical Genetics*, *61*(11), 664–673. https://doi.org/10.1016/j.ejmg.2017.10.017

Dai, C. H., Krantz, S. B., Means, R. T., Horn, S. T., & Gilbert, H. S. (1991). Polycythemia vera blood burst-forming units-erythroid are hypersensitive to interleukin-3. *Journal of Clinical Investigation*, *87*(2), 391–396. https://doi.org/10.1172/JCI115009

Dai, Chun Hua, Krantz, S. B., & Zsebo, K. M. (1991). Human Burst-Forming Units-Erythroid Need Direct Interaction With Stem Cell Factor for Further Development. *Blood*, *78*(10), 2493–2497. Retrieved from https://ashpublications.org/blood/article-pdf/78/10/2493/606186/2493.pdf

Daud, H., Browne, S., Al-Majmaie, R., Murphy, W., & Al-Rubeai, M. (2016). Metabolic profiling of hematopoietic stem and progenitor cells during proliferation and differentiation into red blood cells. *New Biotechnology*, *33*(1), 179–186. https://doi.org/10.1016/j.nbt.2015.05.002

DeVilbiss, A. W., Sanalkumar, R., Hall, B. D. R., Katsumura, K. R., de Andrade, I. F., & Bresnick, E. H. (2015). Epigenetic Determinants of Erythropoiesis: Role of the Histone Methyltransferase SetD8 in Promoting Erythroid Cell Maturation and Survival. *Molecular and Cellular Biology*, *35*(12), 2073–2087. https://doi.org/10.1128/mcb.01422-14

Doré, L. C., & Crispino, J. D. (2011, July 14). Transcription factor networks in erythroid cell and megakaryocyte development. *Blood*, Vol. 118, pp. 231–239. https://doi.org/10.1182/blood-2011-04-285981

Doty, R. T., Phelps, S. R., Shadle, C., Sanchez-Bonilla, M., Keel, S. B., & Abkowitz, J. L. (2015). Coordinate expression of heme and globin is essential for effective erythropoiesis. *Journal of Clinical Investigation*, *125*(12), 4681–4691. https://doi.org/10.1172/JCI83054

Dover, G. J., Chan, T., & Sieber, F. (1983). Fetal hemoglobin production in cultures of primitive and mature human erythroid progenitors: differentiation affects the quantity of fetal hemoglobin produced per fetal-hemoglobin-containing cell. *Blood*, *61*(6), 1242–1246. Retrieved from http://www.ncbi.nlm.nih.gov/pubmed/6188507

Draptchinskaia, N., Gustavsson, P., Andersson, B., Pettersson, M., Willig, T.-N., Dianzani, I., … Dahl, N. (1999). The gene encoding ribosomal protein S19 is

mutated in Diamond-Blackfan anaemia. *Nature Genetics* •, *21*, 169. Retrieved from http://genetics.nature.com

Dulmovits, B. M., Appiah-Kubi, A. O., Papoin, J., Hale, J., He, M., Al-Abed, Y., … Blanc, L. (2016). Pomalidomide reverses γ-globin silencing through the transcriptional reprogramming of adult hematopoietic progenitors. *Blood*, *127*(11), 1481–1492. https://doi.org/10.1182/blood-2015-09-667923

Dulmovits, B. M., Hom, J., Narla, A., Mohandas, N., Blanc, L., Opin, C., & Author, H. (2017). Characterization, regulation and targeting of erythroid progenitors in normal and disordered human erythropoiesis HHS Public Access Author manuscript. *Curr Opin Hematol*, *24*(3), 159–166. https://doi.org/10.1097/MOH.0000000000000328

Dutt, S., Narla, A., Lin, K., Mullally, A., Abayasekara, N., Megerdichian, C., … Ebert, B. L. (2011). Haploinsufficiency for ribosomal protein genes causes selective activation of p53 in human erythroid progenitor cells. *Blood*, *117*(9), 2567–2576. https://doi.org/10.1182/blood-2010-07-295238

Ebert, B. L., Lee, M. M., Pretz, J. L., Subramanian, A., Mak, R., Golub, T. R., & Sieff, C. A. (2005). An RNA interference model of RPS19 deficiency in Diamond-Blackfan anemia recapitulates defective hematopoiesis and rescue by dexamethasone: Identification of dexamethasone-responsive genes by microarray. *Blood*, *105*(12), 4620–4626. https://doi.org/10.1182/blood-2004-08-3313

Edoh, D., Bosaiko, C. A., & Amuzu, D. (2006). Fetal hemoglobin during infancy and in sickle cell adults. *African Health Sciences*, *6*(1), 51. Retrieved from /pmc/articles/PMC1831961/

Endo, T., Odb, A., Satoh, I., Haseyama, Y., Nishio, M., Koizumi, K., … Sawada, K. ichi. (2001). Stem cell factor protects c-kit+ human primary erythroid cells from apoptosis. *Experimental Hematology*, *29*(7), 833–841. https://doi.org/10.1016/S0301-472X(01)00660-9

Engidaye, G., Melku, M., & Enawgaw, B. (2019). Diamond Blackfan Anemia: genetics, pathogenesis, diagnosis and treatment. *Electronic Journal of the International Federation of Clinical Chemistry and Laboratory Medicine*, *30*, 067–081. Retrieved from http://www.ifcc.org/media/477795/ejifcc2019vol30no1pp067-081.pdf

England, S. J., McGrath, K. E., Frame, J. M., & Palis, J. (2011). Immature

erythroblasts with extensive ex vivo self-renewal capacity emerge from the early mammalian fetus. *Blood*, *117*(9), 2708–2717. https://doi.org/10.1182/blood-2010-07-299743

Farrar, J. E., & Dahl, N. (2011). *Untangling the Phenotypic Heterogeneity of Diamond Blackfan Anemia*. https://doi.org/10.1053/j.seminhematol.2011.02.003

Farrar, J. E., Kang, J., Seidel, N., Lichtenberg, J., Atsidaftos, E., Lipton, J. M., … Bodine, D. M. (2018). Altered Epigenetic Maturation in Early Erythroid Cells from Diamond Blackfan Anemia Patients Treated with Transfusions, Corticosteroids, or in Remission. *Blood*, *132*(Supplement 1), 752–752. https://doi.org/10.1182/BLOOD-2018-99-116994

Fenaux, P., Haase, D., Santini, V., Sanz, G. F., Platzbecker, U., & Mey, U. (2021). Myelodysplastic syndromes: ESMO Clinical Practice Guidelines for diagnosis, treatment and follow-up†☆. *Annals of Oncology*, *32*(2), 142–156. https://doi.org/10.1016/J.ANNONC.2020.11.002

Festing, M. H., Speer, M. Y., Yang, H.-Y., & Giachelli, C. M. (n.d.). *Generation of mouse conditional and null alleles of the type III sodium-dependent phosphate cotransporter PiT-1*. https://doi.org/10.1002/dvg.20577

Flygare, J., Estrada, V. R., Shin, C., Gupta, S., & Lodish, H. F. (2011). HIF1?? synergizes with glucocorticoids to promote BFU-E progenitor self-renewal. *Blood*, *117*(12), 3435–3444. https://doi.org/10.1182/blood-2010-07-295550

Forand, A., Koumakis, E., Rousseau, A., Sassier, Y., Journe, C., Merlin, J. F., … Cohen, I. (2016). Disruption of the Phosphate Transporter Pit1 in Hepatocytes Improves Glucose Metabolism and Insulin Signaling by Modulating the USP7/IRS1 Interaction. *Cell Reports*, *16*(10), 2736–2748. https://doi.org/10.1016/j.celrep.2016.08.012

Franco, R. S. (2012). Measurement of red cell lifespan and aging. *Transfusion Medicine and Hemotherapy : Offizielles Organ Der Deutschen Gesellschaft Fur Transfusionsmedizin Und Immunhamatologie*, *39*(5), 302–307. https://doi.org/10.1159/000342232

Frisan, E., Vandekerckhove, J., De Thonel, A., Pierre-Eugène, C., Sternberg, A., Arlet, J. B., … Fontenay, M. (2012). Defective nuclear localization of Hsp70 is associated with dyserythropoiesis and GATA-1 cleavage in myelodysplastic syndromes. *Blood*, *119*(6), 1532–1542. https://doi.org/10.1182/blood-2011-03-343475

Fujiwara, T. (2017). GATA transcription factors: Basic principles and related human disorders. *Tohoku Journal of Experimental Medicine*, *242*(2), 83–91. https://doi.org/10.1620/tjem.242.83

Ganz, T. (2019). Erythropoietic regulators of iron metabolism. *Free Radical Biology and Medicine*, *133*, 69–74. https://doi.org/10.1016/j.freeradbiomed.2018.07.003

Gao, X., Lee, H.-Y., da Rocha, E. L., Zhang, C., Lu, Y.-F., Li, D., … Lodish, H. F. (2016). TGF-β inhibitors stimulate red blood cell production by enhancing self-renewal of BFU-E erythroid progenitors. *Blood*, *128*(23), 2637–2641. https://doi.org/10.1182/blood-2016-05-718320

Garcia-Manero, G., Chien, K. S., & Montalban-Bravo, G. (2020). Myelodysplastic syndromes: 2021 update on diagnosis, risk stratification and management. *American Journal of Hematology*, *95*(11), 1399–1420. https://doi.org/10.1002/AJH.25950

Gastou, M., Rio, S., Dussiot, M., Karboul, N., Moniz, H., Leblanc, T., … Da Costa, L. (2017). The severe phenotype of Diamond-Blackfan anemia is modulated by heat shock protein 70. *Blood Advances*, *1*(22), 1959–1976. https://doi.org/10.1182/bloodadvances.2017008078

Ge, L., Zhang, R. -p., Wan, F., Guo, D. -y., Wang, P., Xiang, L. -x., & Shao, J. -z. (2014). TET2 Plays an Essential Role in Erythropoiesis by Regulating Lineage-Specific Genes via DNA Oxidative Demethylation in a Zebrafish Model. *Molecular and Cellular Biology*, *34*(6), 989–1002. https://doi.org/10.1128/MCB.01061-13

Ge, Liang, Zhang, R., Wan, F., Guo, D., Wang, P., Xiang, L., & Shao, J. (2014). TET2 plays an essential role in erythropoiesis by regulating lineage-specific genes via DNA oxidative demethylation in a zebrafish model. *Molecular and Cellular Biology*, *34*(6), 989–1002. https://doi.org/10.1128/MCB.01061-13

Gidari, A. S., & Levere, R. D. (1979). Glucocorticoid-mediated inhibition of erythroid colony formation by mouse bone marrow cells. *The Journal of Laboratory and Clinical Medicine*, *93*(5), 872–878. https://doi.org/10.5555/URI:PII:0022214379900982

Gillespie, M. A., Palii, C. G., Sanchez-Taltavull, D., Shannon, P., Longabaugh, W. J. R., Downes, D. J., … Brand, M. (2020). Absolute quantification of transcription factors reveals principles of gene regulation in erythropoiesis. *Mol Cell*, *78*(5), 960–974. https://doi.org/10.1016/j.molcel.2020.03.031

Giudice, V., Wu, Z., Kajigaya, S., Cheung, F., Ito, S., Young, N. S., & Heart, N. (2019).

Circulating S100A8 and S100A9 protein levels in plasma of patients with acquired aplastic anemia and myelodysplastic syndromes. *Cytokine*, *113*, 462–465. https://doi.org/10.1016/j.cyto.2018.06.025.Circulating

Gnanapragasam, M. N., McGrath, K. E., Catherman, S., Xue, L., Palis, J., & Bieker, J. J. (2016). EKLF/KLF1-regulated cell cycle exit is essential for erythroblast enucleation. *Blood*, *128*(12), 1631–1641. https://doi.org/10.1182/blood-2016-03-706671

Golde, D. W., Bersch, N., & Cline, M. J. (1976). Potentiation of erythropoiesis in vitro by dexamethasone. *Journal of Clinical Investigation*, *57*(1), 57–62. https://doi.org/10.1172/JCI108269

Gonzalez-Menendez, P., Romano, M., Yan, H., Deshmukh, R., Papoin, J., Oburoglu, L., … Kinet, S. (2021). An IDH1-vitamin C crosstalk drives human erythroid development by inhibiting pro-oxidant mitochondrial metabolism. *Cell Reports*, *34*(5). https://doi.org/10.1016/j.celrep.2021.108723

Greenberg, P., Cox, C., LeBeau, M. M., Fenaux, P., Morel, P., Sanz, G., … Bennett, J. (1997). International Scoring System for Evaluating Prognosis in Myelodysplastic Syndromes. *Blood*, *89*(6), 2079–2088. https://doi.org/10.1182/BLOOD.V89.6.2079

Greenberg, P. L., Tuechler, H., Schanz, J., Sanz, G., Garcia-Manero, G., Solé, F., … Haase, D. (2012). Revised International Prognostic Scoring System for Myelodysplastic Syndromes. *Blood*, *120*(12), 2454–2465. https://doi.org/10.1182/BLOOD-2012-03-420489

Gregory, C. J. (1976). Erythropoietin sensitivity as a differentiation marker in the hemopoietic system: Studies of three erythropoietic colony responses in culture. *Journal of Cellular Physiology*, *89*(2), 289–301. https://doi.org/10.1002/jcp.1040890212

Gregory, Connie J, & Eaves, A. C. (1977). Human Marrow Cells Capable of Erythropoietic Differentiation In Vitro: Definition of Three Erythroid Colony Responses. *Blood*, *49*(6). Retrieved from http://www.bloodjournal.org/content/bloodjournal/49/6/855.full.pdf?sso-checked=true

Gripp, K. W., Curry, C., Haskins Olney, A., Sandoval, C., Fisher, J., Xiao-Ling Chong, J., … Yi, Q. (2014). Diamond-Blackfan Anemia with Mandibulofacial Dystostosis is Heterogeneous, Including the Novel DBA Genes TSR2 and RPS28. *Am J Med*

Genet A, *164*(9), 2240–2249. https://doi.org/10.1002/ajmg.a.36633

Gritz, E., & Hirschi, K. K. (2016, April 1). Specification and function of hemogenic endothelium during embryogenesis. *Cellular and Molecular Life Sciences*, Vol. 73, pp. 1547–1567. https://doi.org/10.1007/s00018-016-2134-0

Grootendorst, S., de Wilde, J., van Dooijeweert, B., van Vuren, A., van Solinge, W., Schutgens, R., … Bartels, M. (2021, February 2). The interplay between drivers of erythropoiesis and iron homeostasis in rare hereditary anemias: Tipping the balance. *International Journal of Molecular Sciences*, Vol. 22, pp. 1–17. https://doi.org/10.3390/ijms22042204

Grover, A., Mancini, E., Moore, S., Mead, A. J., Atkinson, D., Rasmussen, K. D., … Nerlov, C. (2014). Erythropoietin guides multipotent hematopoietic progenitor cells toward an erythroid fate. *The Journal of Experimental Medicine*, *211*(2), 181–188. https://doi.org/10.1084/jem.20131189

Guo, Y., Fu, X., Jin, Y., Sun, J., Liu, Y., Huo, B., … Hu, X. (2015). Histone demethylase LSD1-mediated repression of GATA-2 is critical for erythroid differentiation. *Drug Design, Development and Therapy*, *9*, 3153–3162. https://doi.org/10.2147/DDDT.S81911

Gutiérrez, L., Caballero, N., Fernández-Calleja, L., Karkoulia, E., & Strouboulis, J. (2020). Regulation of GATA1 levels in erythropoiesis. *IUBMB Life*, *72*(1), 89–105. https://doi.org/10.1002/iub.2192

H, E., N, A., D, K.-K., C, C.-O., I, U., M, A., & ET, K. (2015). Determination of PCNA, cyclin D3, p27, p57 and apoptosis rate in normal and dexamethasone-induced intrauterine growth restricted rat placentas. *Acta Histochemica*, *117*(2), 137–147. https://doi.org/10.1016/J.ACTHIS.2014.11.010

H, H., & EP, O. (1992). A history of significant steroid discoveries and developments originating at the Schering Corporation (USA) since 1948. *Steroids*, *57*(12), 617–623. https://doi.org/10.1016/0039-128X(92)90014-Z

Hardy, R. S., Raza, K., & Cooper, M. S. (2020). Therapeutic glucocorticoids: mechanisms of actions in rheumatic diseases. *Nature Reviews Rheumatology*, *16*(3), 133–144. https://doi.org/10.1038/s41584-020-0371-y

Hasan, S., Mosier, M. J., Conrad, P., Szilagyi, A., Gamelli, R. L., & Muthumalaiappan, K. (2018). Terminal maturation of orthochromatic erythroblasts is impaired in burn patients. *Journal of Burn Care and Research*, *39*(2), 286–294. https://doi.org/10.1097/BCR.0000000000000592

Hassan, R. M., & Thurnham, D. I. (1977). Effect of riboflavin deficiency on the metabolism of the red blood cell. *International Journal for Vitamin and Nutrition Research*, *47*(4), 349–355. Retrieved from https://europepmc.org/article/med/591205

Hellström-Lindberg, E., Gulbrandsen, N., Lindberg, G., Ahlgren, T., Dahl, I. M. S., Dybedal, I., … Wisloff, F. (2003). A validated decision model for treating the anaemia of myelodysplastic syndromes with erythropoietin + granulocyte colony-stimulating factor: Significant effects on quality of life. *British Journal of Haematology*, *120*(6), 1037–1046. https://doi.org/10.1046/j.1365-2141.2003.04153.x

Hellström-Lindberg, E., Tobiasson, M., & Greenberg, P. (2020). Myelodysplastic syndromes: moving towards personalized management. *Haematologica*, *105*(7), 1765–1779. https://doi.org/10.3324/HAEMATOL.2020.248955

Hewitt, K. J., Sanalkumar, R., Johnson, K. D., Keles, S., Bresnick, E. H., Opin, C., & Author, H. (2014). Epigenetic and genetic mechanisms in red cell biology. *Curr Opin Hematol*, *21*(3), 155–164. https://doi.org/10.1097/MOH.0000000000000034

Hoffman, R., Tong, J., Brandt, J., Traycoff, C., Bruno, E., Srour, E. F., … Mcniece, I. (1993). The in vitro and in vivo effects of stem cell factor on human hematopoiesis. *Stem Cells*, *11*(2 S), 76–82. https://doi.org/10.1002/stem.5530110813

Hong, W., Nakazawa, M., Chen, Y. Y., Kori, R., Vakoc, C. R., Rakowski, C., & Blobel, G. A. (2005). FOG-1 recruits the NuRD repressor complex to mediate transcriptional repression by GATA-1. *EMBO Journal*, *24*(13), 2367–2378. https://doi.org/10.1038/sj.emboj.7600703

Hu, J., Liu, J., Xue, F., Halverson, G., Reid, M., Guo, A., … An, X. (2013). Isolation and functional characterization of human erythroblasts at distinct stages: implications for understanding of normal and disordered erythropoiesis in vivo. *Blood*, *121*(16), 3246–3253. https://doi.org/10.1182/blood-2013-01-476390

Hu, X., Eastman, A. E., & Guo, S. (2019). Cell cycle dynamics in the reprogramming of cellular identity. *FEBS Letters*, *593*(20), 2840–2852. https://doi.org/10.1002/1873-3468.13625

Hu, Y., An, Q., Sheu, K., Trejo, B., Fan, S., & Guo, Y. (2018, April 20). Single cell multi-omics technology: Methodology and application. *Frontiers in Cell and Developmental Biology*, Vol. 6. https://doi.org/10.3389/fcell.2018.00028

Huang, E., Nocka, K., Beier, D. R., Chu, T. Y., Buck, J., Lahm, H. W., … Besmer, P. (1990). The hematopoietic growth factor KL is encoded by the SI locus and is the ligand of the c-kit receptor, the gene product of the W locus. *Cell*, *63*(1), 225–233. https://doi.org/10.1016/0092-8674(90)90303-V

Huang, H., Xu, C., Gao, J., Li, B., Qin, T., Xu, Z., … Xiao, Z. (2020). Severe ineffective erythropoiesis discriminates prognosis in myelodysplastic syndromes: analysis based on 776 patients from a single centre. *Blood Cancer Journal*, *10*(8), 83. https://doi.org/10.1038/S41408-020-00349-4

Huang, N. J., Lin, Y. C., Lin, C. Y., Pishesha, N., Lewis, C. A., Freinkman, E., … Lodish, H. (2018). Enhanced phosphocholine metabolism is essential for terminal erythropoiesis. *Blood*, *131*(26), 2955–2966. https://doi.org/10.1182/blood-2018-03-838516

Huang, X., Shah, S., Wang, J., Ye, Z., Dowey, S. N., Man Tsang, K., … Cheng, L. (2014). Extensive Ex Vivo Expansion of Functional Human Erythroid Precursors Established From Umbilical Cord Blood Cells by Defined Factors. *Molecular Therapy*, *22*(2), 451–463. https://doi.org/10.1038/mt.2013.201

Hwang, Y., Futran, M., Hidalgo, D., Pop, R., Iyer, D. R., Scully, R., … Socolovsky, M. (2017). Global increase in replication fork speed during a p57KIP2-regulated erythroid cell fate switch. *Science Advances*, *3*(5), 1–16. https://doi.org/10.1126/sciadv.1700298

Iskander, D., Psaila, B., Gerrard, G., Chaidos, A., Foong, H. E., Harrington, Y., … Karadimitris, A. (2015). Elucidation of the EP defect in Diamond-Blackfan anemia by characterization and prospective isolation of human EPs. *Blood*, *125*(16), 2553–2557. https://doi.org/10.1182/blood-2014-10-608042

Ito, K., Chung, K. F., & Adcock, I. M. (2006). Update on glucocorticoid action and resistance. *Journal of Allergy and Clinical Immunology*, *117*(3), 522–543. https://doi.org/10.1016/j.jaci.2006.01.032

Iturri, L., Freyer, L., Biton, A., Dardenne, P., Lallemand, Y., & Gomez Perdiguero, E. (2021). Megakaryocyte production is sustained by direct differentiation from erythromyeloid progenitors in the yolk sac until midgestation. *Immunity*, *54*(7), 1433-1446.e5. https://doi.org/10.1016/j.immuni.2021.04.026

Jaako, P., Debnath, S., Olsson, K., Modlich, U., Rothe, M., Schambach, A., … Karlsson, S. (2014). Gene therapy cures the anemia and lethal bone marrow failure in a mouse model of RPS19-deficient Diamond-Blackfan anemia.

Haematologica, *99*(12), 1792–1798. https://doi.org/10.3324/HAEMATOL.2014.111195

Ji, P., Yeh, V., Ramirez, T., Murata-Hori, M., & Lodish, H. F. (2010). Histone deacetylase 2 is required for chromatin condensation and subsequent enucleation of cultured mouse fetal erythroblasts. *Haematologica*, *95*(12), 2013–2021. https://doi.org/10.3324/haematol.2010.029827

JS, B., JR, M., JA, M., JE, C., LK, J., AE, M., … HA, D. (2018). Glutamine via α-ketoglutarate dehydrogenase provides succinyl-CoA for heme synthesis during erythropoiesis. *Blood*, *132*(10), 987–998. https://doi.org/10.1182/BLOOD-2018-01-829036

Justus, D., Yan, H., Hale, J., Blanc, L., Bitaudeau, F., Petit, V., … Narla, M. (2019). Evaluating Metabolic Regulation of Human Erythropoiesis By Profiling Nutrient Transporter Expression. *Blood*, *134*(Supplement_1), 342–342. https://doi.org/10.1182/BLOOD-2019-124380

Kaneko, H., Shimizu, R., & Yamamoto, M. (2010). GATA factor switching during erythroid differentiation. *Current Opinion in Hematology*, 1. https://doi.org/10.1097/MOH.0b013e32833800b8

Kang, Y., Kim, Y. W., Yun, J., Shin, J., & Kim, A. R. (2015). KLF1 stabilizes GATA-1 and TAL1 occupancy in the human β-globin locus. *Biochimica et Biophysica Acta - Gene Regulatory Mechanisms*, *1849*(3), 282–289. https://doi.org/10.1016/j.bbagrm.2014.12.010

Kapur, R., Chandra, S., Cooper, R., McCarthy, J., & Williams, D. A. (2002). Role of p38 and ERK MAP kinase in proliferation of erythroid progenitors in response to stimulation by soluble and membrane isoforms of stem cell factor. *Blood*, *100*(4), 1287–1293. https://doi.org/10.1182/blood.v100.4.1287.h81602001287_1287_1293

Karayel, Ö., Xu, P., Bludau, I., Velan Bhoopalan, S., Yao, Y., Ana Rita, F. C., … Mann, M. (2020). Integrative proteomics reveals principles of dynamic phosphosignaling networks in human erythropoiesis. *Molecular Systems Biology*, *16*(12), 1–22. https://doi.org/10.15252/msb.20209813

Kassouf, M. T., Hughes, J. R., Taylor, S., McGowan, S. J., Soneji, S., Green, A. L., … Porcher, C. (2010). Genome-wide identification of TAL1's functional targets: Insights into its mechanisms of action in primary erythroid cells. *Genome Research*, *20*(8), 1064–1083. https://doi.org/10.1101/gr.104935.110

Katsumura, K. R., & Bresnick, E. H. (2017). The GATA factor revolution in hematology. *Blood*, *129*(15), 2092–2102. https://doi.org/10.1182/blood-2016-09-687871

Khajuria, R. K., Munschauer, M., Ulirsch, J. C., Fiorini, C., Ludwig, L. S., McFarland, S. K., … Sankaran, V. G. (2018). Ribosome Levels Selectively Regulate Translation and Lineage Commitment in Human Hematopoiesis. *Cell*, *173*(1), 90-103.e19. https://doi.org/10.1016/j.cell.2018.02.036

Kim, A., & Nemeth, E. (2015, May 27). New insights into iron regulation and erythropoiesis. *Current Opinion in Hematology*, Vol. 22, pp. 199–205. https://doi.org/10.1097/MOH.0000000000000132

Kim, C. H., Chen, M. F., & Coleman, A. L. (2017). Adjunctive steroid therapy versus antibiotics alone for acute endophthalmitis after intraocular procedure. *The Cochrane Database of Systematic Reviews*, *2017*(2). https://doi.org/10.1002/14651858.CD012131.PUB2

Kim, M. Y., Yan, B., Huang, S., & Qiu, Y. (n.d.). *Regulating the Regulators: The Role of Histone Deacetylase 1 (HDAC1) in Erythropoiesis*. https://doi.org/10.3390/ijms21228460

Kim, S. T., Lee, S. K., & Gye, M. C. (2011). Cyclic Changes in the Expression of p57kip2 in Human Endometrium and its Regulation by Steroid Hormones in Endometrial Stromal Cells In Vitro: *Reproductive Sciences*, *19*(1), 92–101. https://doi.org/10.1177/1933719111414209

Kohrogi, K., Hino, S., Sakamoto, A., Anan, K., Takase, R., Araki, H., … Nakao, M. (2021). LSD1 defines erythroleukemia metabolism by controlling the lineage-specific transcription factors GATA1 and C/EBPa. *Blood Advances*, *5*(9), 2305–2318. https://doi.org/10.1182/BLOODADVANCES.2020003521

Kolbus, A., Blazques-Domingo, M., Carotta, S., Bakker, W., Auer, H., Luedemann, S., … Beug, H. (2003). Cooperative signaling between cytokine receptors and the glucocorticold receptor in erythroblast renewal: Molecular analysis by expression profiling. *Blood*, *102*(9), 3136–3146. https://doi.org/10.1182/blood-2003-03-0923.Supported

Korolnek, T., & Hamza, I. (2015). Macrophages and iron trafficking at the birth and death of red cells. *Blood*, *125*(19), 2893–2897. https://doi.org/10.1182/blood-2014-12-567776

Koumakis, E., Millet-Botti, J., Benna, J. El, Leroy, C., Boitez, V., Codogno, P., … Forand, A. (2019). Novel function of PiT1/SLC20A1 in LPS-related inflammation

and wound healing. *Scientific Reports*, *9*(1), 1–15. https://doi.org/10.1038/s41598-018-37551-1

Koury, M. J., & Bondurant, M. C. (1991). The mechanism of erythropoietin action. *Am J Kidney Dis*.

Koury, Mark J. (2015). Tracking erythroid progenitor cells in times of need and times of plenty. *Experimental Hematology*, *44*(8). https://doi.org/10.1016/j.exphem.2015.10.007

Koury, S. T., Koury, M. J., & Bondurant, M. C. (1989). Cytoskeletal distribution and function during the maturation and enucleation of mammalian erythroblasts. *Journal of Cell Biology*, *109*(6 I), 3005–3013. https://doi.org/10.1083/jcb.109.6.3005

Kubasch, A. S., Fenaux, P., & Platzbecker, U. (2021). Development of luspatercept to treat ineffective erythropoiesis. *Blood Advances*, *5*(5), 1565–1575. https://doi.org/10.1182/BLOODADVANCES.2020002177

Kuhikar, R., Khan, N., Philip, J., Melinkeri, S., Kale, V., & Limaye, L. (2020). Transforming growth factor β1 accelerates and enhances in vitro red blood cell formation from hematopoietic stem cells by stimulating mitophagy. *Stem Cell Research & Therapy*, *11*(1), 71. https://doi.org/10.1186/s13287-020-01603-z

KuhnViktoria, DiederichLukas, IV, K. C. S., M., K., LückstädtWiebke, PankninChristina, … M., C.-K. (2017). Red Blood Cell Function and Dysfunction: Redox Regulation, Nitric Oxide Metabolism, Anemia. *Https://Home.Liebertpub.Com/Ars*, *26*(13), 718–742. https://doi.org/10.1089/ARS.2016.6954

Kumarswamy, R., Volkmann, I., & Thum, T. (2011). Regulation and function of miRNA-21 in health and disease. *RNA Biology*, *8*(5), 706–713. https://doi.org/10.4161/rna.8.5.16154

Kumkhaek, C., Aerbajinai, W., Liu, W., Zhu, J., Uchida, N., Kurlander, R., … Rodgers, G. P. (2013). MASL1 induces erythroid differentiation in human erythropoietin-dependent CD34+ cells through the Raf/MEK/ERK pathway. *Blood*, *121*(16), 3216–3227. https://doi.org/10.1182/BLOOD-2011-10-385252

Lahlil, R., Lécuyer, E., Herblot, S., & Hoang, T. (2004). SCL Assembles a Multifactorial Complex That Determines Glycophorin A Expression. *Molecular and Cellular Biology*, *24*(4), 1439–1452. https://doi.org/10.1128/mcb.24.4.1439-1452.2004

Lee, H.-Y., Gao, X., Barrasa, M. I., Li, H., Elmes, R. R., Peters, L. L., & Lodish, H. F.

(2015). PPAR-α and glucocorticoid receptor synergize to promote erythroid progenitor self-renewal. *Nature*, *522*(7557), 474–477. https://doi.org/10.1038/nature14326

Lee, H., Crocker, P. R., Key, S. W. N., Mason, D. Y., Gordon, S., Weatheralu, D. J., & Al, L. E. E. E. T. (1988). Isolation and Immunocytochemical characterization of human bone marrow stromal macrophages in hemopoietic clusters. *Journal of Experimental Medicine*, *168*(September), 1193–1198.

Lévesque, J.-P., Summers, K. M., Bisht, K., Millard, S. M., Winkler, I. G., & Pettit, A. R. (2021). Macrophages form erythropoietic niches and regulate iron homeostasis to adapt erythropoiesis in response to infections and inflammation. *Experimental Hematology*, (September). https://doi.org/10.1016/j.exphem.2021.08.011

Li, H., Natarajan, A., Ezike, J., Barrasa, M. I., Le, Y., Feder, Z. A., … Lodish, H. F. (2019). Rate of Progression through a Continuum of Transit-Amplifying Progenitor Cell States Regulates Blood Cell Production. *Developmental Cell*, *49*(1), 118-129.e7. https://doi.org/10.1016/j.devcel.2019.01.026

Li, J., Hale, J., Bhagia, P., Xue, F., Chen, L., Jaffray, J., … An, X. (2014). Isolation and transcriptome analyses of human erythroid progenitors: BFU-E and CFU-E. *Blood*, *124*(24), 3636–3645. https://doi.org/10.1182/blood-2014-07-588806

Liang, R., & Ghaffari, S. (2016). Advances in Understanding the Mechanisms of Erythropoiesis in Homeostasis and Disease. *Br J Haematol.*, *174*(5), 661–663. https://doi.org/10.1111/bjh.14194.Advances

Liang, R., Menon, V., Qiu, J., Arif, T., Renuse, S., Lin, M., … Ghaffari, S. (2021). Mitochondrial localization and moderated activity are key to murine erythroid enucleation. *Blood Advances*, *5*(10), 2490–2504. https://doi.org/10.1182/BLOODADVANCES.2021004259

Ling, T., Birger, Y., Stankiewicz, M. J., Ben-Haim, N., Kalisky, T., Rein, A., … Crispino, J. D. (2019). Chromatin occupancy and epigenetic analysis reveal new insights into the function of the GATA1 N terminus in erythropoiesis. *Blood*, *134*(19), 1619–1631. https://doi.org/10.1182/BLOOD.2019001234

Liu, H., Bi, W., Wang, Q., Lu, L., & Jiang, S. (2015). Receptor binding domain based HIV vaccines. *BioMed Research International*, *2015*, 594109. https://doi.org/10.1155/2015/594109

Liu, J., Guo, X., Mohandas, N., Chasis, J. A., & An, X. (2010). Membrane remodeling during reticulocyte maturation. *Blood*, *115*(10), 2021–2027.

https://doi.org/10.1182/blood-2009-08-241182

Liu, L., Sánchez-Bonilla, M., Crouthamel, M., Giachelli, C., & Keel, S. (2013). Mice lacking the sodium-dependent phosphate import protein, PiT1 (SLC20A1), have a severe defect in terminal erythroid differentiation and early B cell development. *Experimental Hematology*, *41*(5), 432-443.e7. https://doi.org/10.1016/J.EXPHEM.2013.01.004

Liu, Q., Davidoff, O., Niss, K., & Haase, V. H. (2012). Hypoxia-inducible factor regulates hepcidin via erythropoietin-induced erythropoiesis. *Journal of Clinical Investigation*, *122*(12), 4635–4644. https://doi.org/10.1172/JCI63924

Liu, Y., Dahl, M., Debnath, S., Rothe, M., Smith, E. M., Grahn, T. H. M., … Karlsson, S. (2020). Successful gene therapy of Diamond-Blackfan anemia in a mouse model and human CD34+ cord blood hematopoietic stem cells using a clinically applicable lentiviral vector. *Haematologica*, *106*. https://doi.org/10.3324/HAEMATOL.2020.269142

Lodish, H., Flygare, J., & Chou, S. (2010). From stem cell to erythroblast: Regulation of red cell production at multiple levels by multiple hormones. *IUBMB Life*, *62*(7), 492–496. https://doi.org/10.1002/iub.322

Lu, S. J., & Lanza, R. (2019). Cell Therapy for Blood Substitutes. *Principles of Regenerative Medicine*, 923–936. https://doi.org/10.1016/B978-0-12-809880-6.00052-7

Lu, S. J., Park, J. S., Feng, Q., & Lanza, R. (2009). Red Blood Cells. *Essentials of Stem Cell Biology*, 217–222. https://doi.org/10.1016/B978-0-12-374729-7.00025-1

Lu, Y.-C., Sanada, C., Xavier-Ferrucio, J., Wang, L., Zhang, P.-X., Grimes, H. L., … Resources, Y.-C. L. (2018). The Molecular Signature of Megakaryocyte-Erythroid Progenitors Reveals a Role for the Cell Cycle in Fate Specification HHS Public Access. *Cell Rep*, *25*(8), 2083–2093. https://doi.org/10.1016/j.celrep.2018.10.084

Ludwig, L. S., Gazda, H. T., Eng, J. C., Eichhorn, S. W., Thiru, P., Ghazvinian, R., … Sankaran, V. G. (2014). Altered translation of GATA1 in Diamond-Blackfan anemia. *Nature Medicine*, *20*(7), 748. https://doi.org/10.1038/NM.3557

Luo, S.-T., Zhang, D.-M., Qin, Q., Lu, L., Luo, M., Guo, F.-C., … Wei, Y.-Q. (2017). The Promotion of Erythropoiesis via the Regulation of Reactive Oxygen Species by Lactic Acid. *Scientific Reports 2017 7:1*, *7*(1), 1–12. https://doi.org/10.1038/srep38105

M, D., S, W., Y, L., S, D., M, B., K, S., … S, K. (2021). Bone marrow transplantation without myeloablative conditioning in a mouse model for Diamond-Blackfan anemia corrects the disease phenotype. *Experimental Hematology*, *99*, 44-53.e2. https://doi.org/10.1016/J.EXPHEM.2021.06.002

Malleret, B., Xu, F., Mohandas, N., Suwanarusk, R., Chu, C., Leite, J. A., … Russell, B. (2013). Significant Biochemical, Biophysical and Metabolic Diversity in Circulating Human Cord Blood Reticulocytes. *PLoS ONE*, *8*(10). https://doi.org/10.1371/journal.pone.0076062

Manwani, D., & Bieker, J. J. (2008). The Erythroblastic Island. *Curr Top Dev Biol*, *82*, 23–53. https://doi.org/10.1016/S0070-2153(07)00002-6.

Manz, M. G., Miyamoto, T., Akashi, K., & Weissman, I. L. (2002). Prospective isolation of human clonogenic common myeloid progenitors. *Proceedings of the National Academy of Sciences of the United States of America*, *99*(18), 11872–11877. https://doi.org/10.1073/pnas.172384399

Martin, F. H., Suggs, S. V., Langley, K. E., Lu, H. S., Ting, J., Okino, K. H., … Zsebo, K. M. (1990). Primary structure and functional expression of rat and human stem cell factor DNAs. *Cell*, *63*(1), 203–211. https://doi.org/10.1016/0092-8674(90)90301-T

Matsumoto, A., Takeishi, S., Kanie, T., Susaki, E., Onoyama, I., Tateishi, Y., … Nakayama, K. I. (2011). p57 Is Required for Quiescence and Maintenance of Adult Hematopoietic Stem Cells. *Cell Stem Cell*, *9*(3), 262–271. https://doi.org/10.1016/J.STEM.2011.06.014

Matsuzaki, T., Aisaki, K. I., Yamamura, Y., Noda, M., & Ikawa, Y. (2000). Induction of erythroid differentiation by inhibition of Ras/ERK pathway in a Friend murine leukemia cell line. *Oncogene 2000 19:12*, *19*(12), 1500–1508. https://doi.org/10.1038/sj.onc.1203461

McGrath, K., & Palis, J. (2008). Ontogeny of erythropoiesis in the mammalian embryo. *Current Topics in Developmental Biology*, *82*, 1–22. https://doi.org/10.1016/S0070-2153(07)00001-4

Mcleod, D. 1, Shreeve, M. M., & Axelrad, A. A. (1974). Improved Plasma Culture System for Production of Erythrocytic Colonies In Vitro: Quantitative Assay Method for CFU-E. *Blood*, *44*(4), 1974. Retrieved from https://ashpublications.org/blood/article-pdf/44/4/517/578743/517.pdf

McNiece, I. K., Langley, K. E., & Zsebo, K. M. (1991). Recombinant human stem cell

factor synergises with GM-CSF, G-CSF, IL-3 and epo to stimulate human progenitor cells of the myeloid and erythroid lineages. *Experimental Hematology*, *19*(3), 226–231. Retrieved from https://pubmed.ncbi.nlm.nih.gov/1704845/

Medyouf, H., Mossner, M., Jann, J. C., Nolte, F., Raffel, S., Herrmann, C., … Nowak, D. (2014). Myelodysplastic cells in patients reprogram mesenchymal stromal cells to establish a transplantable stem cell niche disease unit. *Cell Stem Cell*, *14*(6), 824–837. https://doi.org/10.1016/j.stem.2014.02.014

Mel, H., Prenant, M., & Mohandas, N. (1977). Reticulocyte motility and form: studies on maturation and classification. *Blood*, *49*(6), 1001–1009. https://doi.org/10.1182/blood.v49.6.1001.1001

Miccio, A., Wang, Y., Hong, W., Gregory, G. D., Wang, H., Yu, X., … Blobel, G. A. (2010). NuRD mediates activating and repressive functions of GATA-1 and FOG-1 during blood development. *EMBO Journal*, *29*(2), 442–456. https://doi.org/10.1038/emboj.2009.336

Migliaccio, G., Migliaccio, A. R., Druzin, M. L., Giardina, P. J. V., Zsebo, K. M., & Adamson, J. W. (1992). Long-term generation of colony-forming cells in liquid culture of CD34+ cord blood cells in the presence of recombinant human stem cell factor. *Blood*, *79*(10), 2620–2627. https://doi.org/10.1182/blood.v79.10.2620.2620

Migliaccio, Giovanni, Migliaccio, A. R., Druzin, M. L., Giardina, P. V., Zsebo, K. M., & Adamson, J. W. (1991). Effects of recombinant human stem cell factor (SCF) on the growth of human progenitor cells in vitro. *Journal of Cellular Physiology*, *148*(3), 503–509. https://doi.org/10.1002/jcp.1041480324

Mikdar, M., Gonzalez-Menendez, P., Cai, X., Zhang, Y., Serra, M., Dembélé, A. K., … Azouzi, S. (2021). The equilibrative nucleoside transporter 1 (ENT1) is critical for nucleotide homeostasis and optimal erythropoiesis. *Blood*, *137*(25), 3548–3562. https://doi.org/10.1182/blood.2020007281

Miller, J. L. (2013). Iron deficiency anemia: A common and curable disease. *Cold Spring Harbor Perspectives in Medicine*, *3*(7), 1–13. https://doi.org/10.1101/cshperspect.a011866

Miura, Y., Miura, O., Ihle, J. N., & Aoki, N. (1994). Activation of the mitogen-activated protein kinase pathway by the erythropoietin receptor. *Journal of Biological Chemistry*, *269*(47), 29962–29969. https://doi.org/10.1016/s0021-9258(18)43975-0

Miyake, T., Kung, C. K. H., & Goldwasser, E. (1977). Purification of human erythropoietin. *Journal of Biological Chemistry*, *252*(15), 5558–5564. https://doi.org/10.1016/s0021-9258(19)63387-9

Miyawaki, K., Iwasaki, H., Jiromaru, T., Kusumoto, H., Yurino, A., Sugio, T., … Akashi, K. (2017). Identification of unipotent megakaryocyte progenitors in human hematopoiesis. *Blood*, *129*(25), 3332–3343. https://doi.org/10.1182/blood-2016-09-741611

Mochizuki-Kashio, M., Shiozaki, H., Suda, T., & Nakamura-Ishizu, A. (2021). Mitochondria turnover and lysosomal function in hematopoietic stem cell metabolism. *International Journal of Molecular Sciences*, Vol. 22. https://doi.org/10.3390/ijms22094627

Mohandas, N., & Prenant, M. (1978). Three-dimensional model of bone marrow. *Blood*, *51*(4), 633–643. https://doi.org/10.1182/blood.v51.4.633.633

Moras, M., Hattab, C., Gonzalez-Menendez, P., Fader, C. M., Dussiot, M., Larghero, J., … Ostuni, M. A. (2021). Human erythroid differentiation requires VDAC1-mediated mitochondrial clearance. *Haematologica*. https://doi.org/10.3324/haematol.2020.257121

Mori, Y., Chen, J. Y., Pluvinage, J. V., Seita, J., & Weissman, I. L. (2015). Prospective isolation of human erythroid lineage-committed progenitors. *Proceedings of the National Academy of Sciences*, *112*(31), 9638–9643. https://doi.org/10.1073/pnas.1512076112

Mosegaard, S., Dipace, G., Bross, P., Carlsen, J., Gregersen, N., & Olsen, R. K. J. (2020). Riboflavin Deficiency—Implications for General Human Health and Inborn Errors of Metabolism. *International Journal of Molecular Sciences*, *21*(11). https://doi.org/10.3390/IJMS21113847

Munugalavadla, V., & Kapur, R. (2005, April 1). Role of c-Kit and erythropoietin receptor in erythropoiesis. *Critical Reviews in Oncology/Hematology*, Vol. 54, pp. 63–75. https://doi.org/10.1016/j.critrevonc.2004.11.005

Muta, K., Krantz, S. B., Bondurant, M. C., & Wickrema, A. (1994). Distinct Roles of Erythropoietin, Insulin-like Growth Factor 1, and Stem Cell Factor in the Development of Erythroid Progenitor Cells. *The Journal of Clinical Investigation,*. Retrieved from https://pdfs.semanticscholar.org/4c1a/847c5b78f03cb62a748e287cf3309b8711ca.pdf?_ga=2.71946129.328112179.1588004663-525492501.1585599095

Myers, J. A., Couch, T., Murphy, Z., Malik, J., Getman, M., & Steiner, L. A. (2020). The histone methyltransferase Setd8 alters the chromatin landscape and regulates the expression of key transcription factors during erythroid differentiation. *Epigenetics and Chromatin*, *13*(1). https://doi.org/10.1186/s13072-020-00337-9

Nagata, Y., & Maciejewski, J. P. (2019). The functional mechanisms of mutations in myelodysplastic syndrome. *Leukemia*, *33*(12), 2779. https://doi.org/10.1038/S41375-019-0617-3

Nandakumar, S. K., Ulirsch, J. C., & Sankaran, V. G. (2016, April 1). Advances in understanding erythropoiesis: Evolving perspectives. *British Journal of Haematology*, Vol. 173, pp. 206–218. https://doi.org/10.1111/bjh.13938

Narla, A., Vlachos, A., & Nathan, D. G. (2011). Diamond Blackfan Anemia Treatment: Past, Present, and Future. *Seminars in Hematology*, *48*(2), 117–123. https://doi.org/10.1053/j.seminhematol.2011.01.004

Nemeth, E. (2008, May). Iron regulation and erythropoiesis. *Current Opinion in Hematology*, Vol. 15, pp. 169–175. https://doi.org/10.1097/MOH.0b013e3282f73335

Notta, F., Zandi, S., Takayama, N., Dobson, S., Gan, O. I., Wilson, G., … Dick, J. E. (2016). DISTINCT ROUTES OF LINEAGE DEVELOPMENT RESHAPE THE HUMAN BLOOD HIERARCHY ACROSS ONTOGENY Europe PMC Funders Group. *Science*, *351*(6269). https://doi.org/10.1126/science.aab2116

Nowak, R. B., Papoin, J., Gokhin, D. S., Casu, C., Rivella, S., Lipton, J. M., … Fowler, V. M. (2017). Tropomodulin 1 controls erythroblast enucleation via regulation of F-actin in the enucleosome. *Blood*, *130*(9), 1144–1155. https://doi.org/10.1182/blood-2017-05-787051

Oburoglu, L., Romano, M., Taylor, N., & Kinet, S. (2016). Metabolic regulation of hematopoietic stem cell commitment and erythroid differentiation. *Current Opinion in Hematology*, Vol. 23, pp. 198–205. https://doi.org/10.1097/MOH.0000000000000234

Oburoglu, L., Tardito, S., Fritz, V., De Barros, S. C., Merida, P., Craveiro, M., … Taylor, N. (2014). Glucose and glutamine metabolism regulate human hematopoietic stem cell lineage specification. *Cell Stem Cell*, *15*(2), 169–184. https://doi.org/10.1016/j.stem.2014.06.002

Oburoglu, L., Tardito, S., Fritz, V., Phanie, S., De Barros, C., Merida, P., … Taylor, N. (2014). Cell Stem Cell Article Glucose and Glutamine Metabolism Regulate

Human Hematopoietic Stem Cell Lineage Specification. *Stem Cell*. https://doi.org/10.1016/j.stem.2014.06.002

Ogawa, S. (2019). Genetics of MDS. *Blood*, *133*(10), 1049–1059. https://doi.org/10.1182/blood-2018-10-844621

Okano, M., Bell, D. W., Haber, D. A., & Li, E. (1999). DNA methyltransferases Dnmt3a and Dnmt3b are essential for de novo methylation and mammalian development. *Cell*, *99*(3), 247–257. Retrieved from http://www.ncbi.nlm.nih.gov/pubmed/10555141

Oneal, P. A., Gantt, N. M., Schwartz, J. D., Bhanu, N. V, Lee, Y. T., Moroney, J. W., … Miller, J. L. (2006). *Fetal hemoglobin silencing in humans*. https://doi.org/10.1182/blood-2006-04

Orgebin, E., Lamoureux, F., Isidor, B., Charrier, C., Ory, B., Lézot, F., & Baud'huin, M. (2020). Ribosomopathies: New Therapeutic Perspectives. *Cells*, *9*(9). https://doi.org/10.3390/CELLS9092080

Ouled-Haddou, H., Messaoudi, K., Demont, Y., dos Santos, R. L., Carola, C., Caulier, A., … Garçon, L. (2020). A new role of glutathione peroxidase 4 during human erythroblast enucleation. *Blood Advances*, *4*(22), 5666–5680. https://doi.org/10.1182/bloodadvances.2020003100

Palis, J. (2014). Primitive and definitive erythropoiesis in mammals. *Frontiers in Physiology*, *5*, 3. https://doi.org/10.3389/fphys.2014.00003

Papoff, P., Christensen, R. D., Harcum, J., & Li, Y. (1998). In vitro effect of dexamethasone phosphate on hematopoietic progenitor cells in preterm infants. *Archives of Disease in Childhood. Fetal and Neonatal Edition*, *78*(1), F67-9. Retrieved from http://www.pubmedcentral.nih.gov/articlerender.fcgi?artid=1720743&tool=pmcentrez&rendertype=abstract

Park, S., Hamel, J. F., Toma, A., Kelaidi, C., Thépot, S., Campelo, M. D., … Fenaux, P. (2017). Outcome of lower-risk patients with myelodysplastic syndromes without 5q deletion after failure of erythropoiesis-stimulating agents. *Journal of Clinical Oncology*, *35*(14), 1591–1597. https://doi.org/10.1200/JCO.2016.71.3271

Passegué, E., Wagers, A. J., Giuriato, S., Anderson, W. C., & Weissman, I. L. (2005). Global analysis of proliferation and cell cycle gene expression in the regulation of hematopoietic stem and progenitor cell fates. *Journal of Experimental Medicine*, *202*(11), 1599–1611. https://doi.org/10.1084/jem.20050967

Peschle, C., Mavilio, F., Carè, A., Migliaccio, G., Migliaccio, A. R., Salvo, G., … Mastroberardino, G. (1985). Haemoglobin switching in human embryos: Asynchrony of ζ → α and ε → γ-globin switches in primitive and definitive erythropoietic lineage. *Nature*, *313*(5999), 235–238. https://doi.org/10.1038/313235a0

Platzbecker, U. (2019). Treatment of MDS. *Blood*, *133*(10), 1096–1107. https://doi.org/10.1182/blood-2018-10-844696

Platzbecker, U., Kubasch, A. S., Homer-Bouthiette, C., & Prebet, T. (2021). Current challenges and unmet medical needs in myelodysplastic syndromes. *Leukemia*. https://doi.org/10.1038/s41375-021-01265-7

Pop, R., Shearstone, J. R., Shen, Q., Liu, Y., Hallstrom, K., Koulnis, M., … Socolovsky, M. (2010). A key commitment step in erythropoiesis is synchronized with the cell cycle clock through mutual inhibition between PU.1 and S-phase progression. *PLoS Biology*, *8*(9). https://doi.org/10.1371/journal.pbio.1000484

Pronk, C. J. H., Rossi, D. J., Månsson, R., Attema, J. L., Norddahl, G. L., Chan, C. K. F., … Bryder, D. (2007). Elucidation of the Phenotypic, Functional, and Molecular Topography of a Myeloerythroid Progenitor Cell Hierarchy. *Cell Stem Cell*, *1*(4), 428–442. https://doi.org/10.1016/j.stem.2007.07.005

Pronk, E., & Raaijmakers, M. H. G. P. (2019). The mesenchymal niche in MDS. *Blood*, *133*(10), 1031–1038. https://doi.org/10.1182/BLOOD-2018-10-844639

Psaila, B., Barkas, N., Iskander, D., Roy, A., Anderson, S., Ashley, N., … Roberts, I. (2016). Single-cell profiling of human megakaryocyte-erythroid progenitors identifies distinct megakaryocyte and erythroid differentiation pathways. *Genome Biology*, *17*(1). https://doi.org/10.1186/s13059-016-0939-7

Qiu, J., Gjini, J., Arif, T., Moore, K., Lin, M., & Ghaffari, S. (2021). Using mitochondrial activity to select for potent human hematopoietic stem cells. *Blood Advances*, *5*(6), 1605–1616. https://doi.org/10.1182/BLOODADVANCES.2020003658

Quigley, J. G., Yang, Z., Worthington, M. T., Phillips, J. D., Sabo, K. M., Sabath, D. E., … Abkowitz, J. L. (2004). Identification of a human heme exporter that is essential for erythropoiesis. *Cell*, *118*(6), 757–766. https://doi.org/10.1016/j.cell.2004.08.014

Remy, I., Wilson, I. A., & Michnick, S. W. (1999). Erythropoietin receptor activation by a ligand-induced conformation change. *Science (New York, N.Y.)*, *283*(5404), 990–993. https://doi.org/10.1126/SCIENCE.283.5404.990

Rhodes, M. M., Kopsombut, P., Bondurant, M. C., Price, J. O., & Koury, M. J. (2008). Adherence to macrophages in erythroblastic islands enhances erythroblast proliferation and increases erythrocyte production by a different mechanism than erythropoietin. *Blood*, *111*(3), 1700. https://doi.org/10.1182/BLOOD-2007-06-098178

Ribeil, J. A., Zermati, Y., Vandekerckhove, J., Cathelin, S., Kersual, J., Dussiot, M., … Hermine, O. (2007). Hsp70 regulates erythropoiesis by preventing caspase-3-mediated cleavage of GATA-1. *Nature*, *445*(7123), 102–105. https://doi.org/10.1038/nature05378

Richard, A., Vallin, E., Romestaing, C., Roussel, D., Gandrillon, O., & Gonin-Giraud, S. (2019). Erythroid differentiation displays a peak of energy consumption concomitant with glycolytic metabolism rearrangements. *PLoS ONE*, *14*(9). https://doi.org/10.1371/journal.pone.0221472

Richard, C., & Verdier, F. (2020). Transferrin Receptors in Erythropoiesis. *International Journal of Molecular Sciences*, *21*(24), 1–16. https://doi.org/10.3390/IJMS21249713

Rio, S., Gastou, M., Karboul, N., Derman, R., Suriyun, T., Manceau, H., … Da Costa, L. (2019). Regulation of globin-heme balance in Diamond-Blackfan anemia by HSP70/GATA1. *Blood*, *133*(12), 1358–1370. https://doi.org/10.1182/blood-2018-09-875674

Rivella, S. (2019). Iron metabolism under conditions of ineffective erythropoiesis in β-Thalassemia. *Blood*, *133*(1), 51–58. https://doi.org/10.1182/blood-2018-07-815928

Romanello, K. S., Teixeira, K. K. L., Silva, J. P. M. O., Nagamatsu, S. T., Bezerra, M. A. C., Domingos, I. F., … Cunha, A. F. (2018). Global analysis of erythroid cells redox status reveals the involvement of Prdx1 and Prdx2 in the severity of beta thalassemia. *PLoS ONE*, *13*(12), 1–19. https://doi.org/10.1371/journal.pone.0208316

Roodman, G. D., Lee, J., & Gidari, A. S. (1983). Effects of dexamethasone on erythroid colony and burst formation from human fetal liver and adult marrow. *British Journal of Haematology*, *53*(4), 621–628. Retrieved from http://www.ncbi.nlm.nih.gov/pubmed/6830705

Sallman, D. A., & List, A. (2019). The central role of inflammatory signaling in the pathogenesis of myelodysplastic syndromes. *Blood*, *133*(10), 1039–1048.

https://doi.org/10.1182/BLOOD-2018-10-844654

Samuelsson, M. K. R., Pazirandeh, A., Davani, B., & Okret, S. (1999). p57(Kip2), A glucocorticoid-induced inhibitor of cell cycle progression in HeLa cells. *Molecular Endocrinology*, *13*(11), 1811–1822. https://doi.org/10.1210/mend.13.11.0379

Sanada, C., Xavier-Ferrucio, J., Lu, Y.-C., Min, E., Zhang, P.-X., Zou, S., … Krause, D. S. (2016). Adult human megakaryocyte-erythroid progenitors are in the CD34+CD38mid fraction. *Blood*, *128*(7), 923–934. https://doi.org/10.1182/blood-2016-01-693705

Sanada, Chad, Xavier-Ferrucio, J., Lu, Y.-C., Min, E., Zhang, P.-X., Zou, S., … Krause, D. S. (2016). Adult human megakaryocyte-erythroid progenitors are in the CD34 + CD38 mid fraction. *Blood*, *128*, 923–933. https://doi.org/10.1182/blood-2016-01-693705

Sankaran, V. G., Ghazvinian, R., Do, R., Thiru, P., Vergilio, J.-A., Beggs, A. H., … Gazda, H. T. (2012). Exome sequencing identifies GATA1 mutations resulting in Diamond-Blackfan anemia. *The Journal of Clinical Investigation*, *122*(7), 2439. https://doi.org/10.1172/JCI63597

Sathyanarayana, P., Dev, A., Fang, J., Houde, E., Bogacheva, O., Bogachev, O., … Wojchowski, D. M. (2008). EPO receptor circuits for primary erythroblast survival. *Blood*, *111*(11), 5390–5399. https://doi.org/10.1182/blood-2007-10-119743

Sawada, K., Glick, A. D., Civin, C. I., Krantz, S. B., Kans, J. S., Dessypris, E. N., … Civin, C. 1. (1987). Purification of human erythroid colony-forming units and demonstration of specific binding of erythropoietin. *J Clin Invest*, *80*(2), 357. https://doi.org/10.1172/JCI113080

Sawada, K., Krantz, S. B., Dessypris, E. N., Koury, S. T., & Sawyer, S. T. (1989). Human Colony-forming Units-Erythroid Do Not Require Accessory Cells, but Do Require Direct Interaction with Insulin-like Growth Factor I and/or Insulin for Erythroid Development. *JCI*. Retrieved from https://pdfs.semanticscholar.org/d66d/579a882f1a75f018c45acdbc86309cdd80b3.pdf?_ga=2.97092127.1889065387.1588972179-525492501.1585599095

Schmidt, E. K., Fichelson, S., & Feller, S. M. (2004). PI3 kinase is important for Ras, MEK and Erk activation of Epo-stimulated human erythroid progenitors. *BMC Biology*, *2*(1), 1–12. https://doi.org/10.1186/1741-7007-2-7/FIGURES/7

Schneider, R. K., Schenone, M., Ferreira, M. V., Kramann, R., Platzbecker, U., Büsche, G., … Ebert, B. L. (2016). Rps14 haploinsufficiency causes a block in

erythroid differentiation mediated by S100A8/S100A9. *Nature Medicine*, *22*(3), 288–297. https://doi.org/10.1038/nm.4047.Rps14

Sen, T., Chen, J., & Singbrant, S. (2021). Decreased PGC1β expression results in disrupted human erythroid differentiation, impaired hemoglobinization and cell cycle exit. *Scientific Reports*, *11*(1). https://doi.org/10.1038/s41598-021-96585-0

Seu, K. G., Papoin, J., Fessler, R., Hom, J., Huang, G., Mohandas, N., … Kalfa, T. A. (2017). Unraveling macrophage heterogeneity in erythroblastic islands. *Frontiers in Immunology*. https://doi.org/10.3389/fimmu.2017.01140

Sevilla, L. M., Jiménez-Panizo, A., Alegre-Martí, A., Estébanez-Perpiñá, E., Caelles, C., & Pérez, P. (2021). Glucocorticoid Resistance: Interference between the Glucocorticoid Receptor and the MAPK Signalling Pathways. *International Journal of Molecular Sciences*, *22*(18). https://doi.org/10.3390/IJMS221810049

Sheng, Y., Ma, R., Yu, C., Wu, Q., Zhang, S., Paulsen, K., … Qian, Z. (2021). Role of c-Myc haploinsufficiency in the maintenance of HSCs in mice. *Blood*, *137*(5), 610–623. https://doi.org/10.1182/blood.2019004688

Siatecka, M., & Bieker, J. J. (2011). The multifunctional role of EKLF/KLF1 during erythropoiesis. *Blood*, *118*(8), 2044–2054. https://doi.org/10.1182/blood-2011-03-331371

Sperling, A. S., Gibson, C. J., & Ebert, B. L. (2016). The genetics of myelodysplastic syndrome: from clonal haematopoiesis to secondary leukaemia. *Nature Reviews Cancer*, *17*(1), 5–19. https://doi.org/10.1038/nrc.2016.112

Stadhouders, R., Cico, A., Stephen, T., Thongjuea, S., Kolovos, P., Baymaz, H. I., … Soler, E. (2015). Control of developmentally primed erythroid genes by combinatorial co-repressor actions. *Nature Communications*, *6*, 1–17. https://doi.org/10.1038/ncomms9893

Steensma, D. P. (2015). Myelodysplastic Syndromes: Diagnosis and Treatment. *Mayo Clinic Proceedings*, *90*(7), 969–983. https://doi.org/10.1016/j.mayocp.2015.04.001

Stellacci, E., Di Noia, A., Di Baldassarre, A., Migliaccio, G., Battistini, A., & Rita Migliaccio, A. (2009). Interaction between the glucocorticoid and the erythropoietin receptors in human erythroid cells. *Exp Hematol*, *37*(5), 559–572. https://doi.org/10.1016/j.exphem.2009.02.005

Stephenson, J. R., Axelrad, A. A., Mcleod, D. L., & Shreeve, M. M. (1971). Induction of

Colonies of Hemoglobin-Synthesizing Cells by Erythropoietin In Vitro. *PNAS*, *68*(7), 1542–1546. Retrieved from https://www.pnas.org/content/pnas/68/7/1542.full.pdf

Suresh, S., Rajvanshi, P. K., & Noguchi, C. T. (2020). The Many Facets of Erythropoietin Physiologic and Metabolic Response. *Frontiers in Physiology*, *10*. https://doi.org/10.3389/fphys.2019.01534

Suzuki, M., Kobayashi-Osaki, M., Tsutsumi, S., Pan, X., Ohmori, S., Takai, J., … Yamamoto, M. (2013). GATA factor switching from GATA2 to GATA1 contributes to erythroid differentiation. *Genes to Cells*, *18*(11), 921–933. https://doi.org/10.1111/gtc.12086

Suzuki, N., Ohneda, O., Takahashi, S., Higuchi, M., Mukai, H. Y., Nakahata, T., … Yamamoto, M. (2002). Erythroid-specific expression of the erythropoietin receptor rescued its null mutant mice from lethality. *Blood*, *100*(7), 2279–2288. https://doi.org/10.1182/blood-2002-01-0124

Takubo, K., Nagamatsu, G., Kobayashi, C. I., Nakamura-Ishizu, A., Kobayashi, H., Ikeda, E., … Suda, T. (2013). Regulation of glycolysis by Pdk functions as a metabolic checkpoint for cell cycle quiescence in hematopoietic stem cells. *Cell Stem Cell*, *12*(1), 49–61. https://doi.org/10.1016/j.stem.2012.10.011

Tallack, M. R., Keys, J. R., Humbert, P. O., & Perkins, A. C. (2009). EKLF/KLF1 controls cell cycle entry via direct regulation of E2f2. *Journal of Biological Chemistry*, *284*(31), 20966–20974. https://doi.org/10.1074/jbc.M109.006346

Teodorescu, P., Pasca, S., Dima, D., Tomuleasa, C., & Ghiaur, G. (2020). Targeting the Microenvironment in MDS: The Final Frontier. *Frontiers in Pharmacology*, *11*(July), 1–10. https://doi.org/10.3389/fphar.2020.01044

Timmermans, S., Souffriau, J., & Libert, C. (2019). A general introduction to glucocorticoid biology. *Frontiers in Immunology*, Vol. 10. https://doi.org/10.3389/fimmu.2019.01545

Toma, A., Kosmider, O., Chevret, S., Delaunay, J., Stamatoullas, A., Rose, C., … Dreyfus, F. (2016). Lenalidomide with or without erythropoietin in transfusion-dependent erythropoiesis-stimulating agent-refractory lower-risk MDS without 5q deletion. *Leukemia*, *30*(4), 897–905. https://doi.org/10.1038/leu.2015.296

Tomc, J., & Debeljak, N. (2021). Molecular insights into the oxygen-sensing pathway and erythropoietin expression regulation in erythropoiesis. *International Journal of Molecular Sciences*, *22*(13). https://doi.org/10.3390/ijms22137074

Trowbridge, J. J., & Starczynowski, D. T. (2021). Innate immune pathways and inflammation in hematopoietic aging, clonal hematopoiesis, and MDS. *Journal of Experimental Medicine*, *218*(7). https://doi.org/10.1084/JEM.20201544

Tusi, B. K., Wolock, S. L., Weinreb, C., Hwang, Y., Hidalgo, D., Zilionis, R., … Socolovsky, M. (2018). Population snapshots predict early haematopoietic and erythroid hierarchies. *Nature*. https://doi.org/10.1038/nature25741

Tyagi, A., Gupta, A., Dutta, A., Potluri, P., & Batti, B. (2020). A Review of Diamond-Blackfan Anemia: Current Evidence on Involved Genes and Treatment Modalities. *Cureus*, *12*(8). https://doi.org/10.7759/CUREUS.10019

Varricchio, L., & Migliaccio, A. R. (2014). The role of glucocorticoid receptor (GR) polymorphisms in human erythropoiesis. *American Journal of Blood Research*, *4*(2), 53–72. Retrieved from http://www.ncbi.nlm.nih.gov/pubmed/25755906

Varricchio, L., Tirelli, V., Masselli, E., Ghinassi, B., Saha, N., Besmer, P., & Migliaccio, A. R. (2012). The Expression of the Glucocorticoid Receptor in Human Erythroblasts is Uniquely Regulated by KIT Ligand: Implications for Stress Erythropoiesis. *Stem Cells and Development*, *21*(15), 2852–2865. https://doi.org/10.1089/scd.2011.0676

Venugopal, S., Mascarenhas, J., & Steensma, D. P. (2021). Loss of 5q in myeloid malignancies – A gain in understanding of biological and clinical consequences. *Blood Reviews*, *46*, 100735. https://doi.org/10.1016/J.BLRE.2020.100735

Verma, A., Suragani, R. N. V. S., Aluri, S., Shah, N., Bhagat, T. D., Alexander, M. J., … Kumar, R. (2020). Biological basis for efficacy of activin receptor ligand traps in myelodysplastic syndromes. *Journal of Clinical Investigation*, *130*(2), 582–589. https://doi.org/10.1172/JCI133678

von Lindern, M, Zauner, W., Mellitzer, G., Steinlein, P., Fritsch, G., Huber, K., … Beug, H. (1999). The glucocorticoid receptor cooperates with the erythropoietin receptor and c-Kit to enhance and sustain proliferation of erythroid progenitors in vitro. *Blood*, *94*(2), 550–559.

von Lindern, Marieke, Schmidt, U., & Beug, H. (2004). Control of erythropoiesis by erythropoietin and stem cell factor: a novel role for Bruton's tyrosine kinase. *Cell Cycle (Georgetown, Tex.)*, *3*(7), 876–879. https://doi.org/10.4161/cc.3.7.1001

Wang, F., Ni, J., Wu, L., Wang, Y., He, B., & Yu, D. (2019). Gender disparity in the survival of patients with primary myelodysplastic syndrome. *Journal of Cancer*, *10*(5), 1325–1332. https://doi.org/10.7150/jca.28220

Wang, L., Di, L., & Noguchi, C. T. (2014, August 23). Erythropoietin, a novel versatile player regulating energy metabolism beyond the erythroid system. *International Journal of Biological Sciences*, Vol. 10, pp. 921–939. https://doi.org/10.7150/ijbs.9518

Wang, W., Horner, D. N., Chen, W. L. K., Zandstra, P. W., & Audet, J. (2008). Synergy between erythropoietin and stem cell factor during erythropoiesis can be quantitatively described without co-signaling effects. *Biotechnology and Bioengineering*, *99*(5), 1261–1272. https://doi.org/10.1002/bit.21677

Wang, Z. Q., Auer, B., Stingl, L., Berghammer, H., Haidacher, D., Schweiger, M., & Wagner, E. F. (1995). Mice lacking ADPRT and poly(ADP-ribosyl)ation develop normally but are susceptible to skin disease. *Genes & Development*, *9*(5), 509–520. https://doi.org/10.1101/gad.9.5.509

Watowich, S. S. (2011). The erythropoietin receptor: Molecular structure and hematopoietic signaling pathways. *Journal of Investigative Medicine*, *59*(7), 1067–1072. https://doi.org/10.2310/JIM.0b013e31820fb28c

Watts, D., Gaete, D., Rodriguez, D., Hoogewijs, D., Rauner, M., Sormendi, S., & Wielockx, B. (2020). Hypoxia pathway proteins are master regulators of erythropoiesis. *International Journal of Molecular Sciences*, *21*(21), 1–18. https://doi.org/10.3390/ijms21218131

WAUGH, R. E., MCKENNEY, J., BAUSERMAN, R. G., BROOKS, D. M., VALERI, C. R., & SNYDER, L. M. (1995). *Surface Area and Volume Changes During Maturation of Reticulocytes in the Circulation of the Baboon*.

Weiler, S. R., Mou, S., DeBerry, C. S., Keller, J. R., Ruscetti, F. W., Ferris, D. K., … Linnekin, D. (1996). JAK2 is associated with the c-kit proto-oncogene product and is phosphorylated in response to stem cell factor. *Blood*, *87*(9), 3688–3693. https://doi.org/10.1182/blood.v87.9.3688.bloodjournal8793688

Wessely, O., Deiner, E. M., Beug, H., & Von Lindern, M. (1997). The glucocorticoid receptor is a key regulator of the decision between self-renewal and differentiation in erythroid progenitors. *EMBO Journal*, *16*(2), 267–280. https://doi.org/10.1093/emboj/16.2.267

Wickrema, A., Krantz, S. B., Winkelmann, J. C., & Bondurant, M. C. (1992). Differentiation and Erythropoietin Receptor Gene Expression in Human Erythroid Progenitor Cells. *Blood*. Retrieved from http://www.bloodjournal.org/content/bloodjournal/80/8/1940.full.pdf

Wielockx, B., Grinenko, T., Mirtschink, P., & Chavakis, T. (2019). Hypoxia Pathway Proteins in Normal and Malignant Hematopoiesis. *Cells*, *8*(2), 155. https://doi.org/10.3390/cells8020155

Wilkinson-White, L., Gamsjaeger, R., Dastmalchi, S., Wienert, B., Stokes, P. H., Crossley, M., … Matthews, J. M. (2011). Structural basis of simultaneous recruitment of the transcriptional regulators LMO2 and FOG1/ZFPM1 by the transcription factor GATA1. *Proceedings of the National Academy of Sciences of the United States of America*, *108*(35), 14443–14448. https://doi.org/10.1073/pnas.1105898108

Witthuhn, B. A., Quelle, F. W., Silvennoinen, O., Yi, T., Tang, B., Miura, O., & Ihle, J. N. (1993). JAK2 associates with the erythropoietin receptor and is tyrosine phosphorylated and activated following stimulation with erythropoietin. *Cell*, *74*(2), 227–236. https://doi.org/10.1016/0092-8674(93)90414-L

Wu, H., Liu, X., Jaenisch, R., & Lodish, H. F. (1995). Generation of committed erythroid BFU-E and CFU-E progenitors does not require erythropoietin or the erythropoietin receptor. *Cell*, *83*(1), 59–67. https://doi.org/10.1016/0092-8674(95)90234-1

Wu, W., Morrissey, C. S., Keller, C. A., Mishra, T., Pimkin, M., Blobel, G. A., … Hardison, R. C. (2014). Dynamic shifts in occupancy by TAL1 are guided by GATA factors and drive large-scale reprogramming of gene expression during hematopoiesis. *Genome Research*, *24*(12), 1945–1962. https://doi.org/10.1101/gr.164830.113

Xavier-Ferrucio, J., & Krause, D. S. (2018, August 1). Concise Review: Bipotent Megakaryocytic-Erythroid Progenitors: Concepts and Controversies. *Stem Cells*, Vol. 36, pp. 1138–1145. https://doi.org/10.1002/stem.2834

Ximeri, M., Galanopoulos, A., Klaus, M., Parcharidou, A., Giannikou, K., Psyllaki, M., … Papadaki, H. A. (2010). Effect of lenalidomide therapy on hematopoiesis of patients with myelodysplastic syndrome associated with chromosome 5q deletion. *Haematologica*, *95*(3), 406–414. https://doi.org/10.3324/haematol.2009.010876

Xin, Z., Pu, L., Gao, W., Wang, Y., Wei, J., Shi, T., … Guo, C. (2017). Riboflavin deficiency induces a significant change in proteomic profiles in HepG2 cells OPEN. *Scientific Reports*, (7). https://doi.org/10.1038/srep45861

Xue, L., Galdass, M., Gnanapragasam, M. N., Manwani, D., & Bieker, J. J. (2014). Extrinsic and intrinsic control by EKLF (KLF1) within a specialized erythroid niche.

Development. https://doi.org/10.1242/dev.103960

Yamada, O., & Kawauchi, K. (2013). The role of the JAK-STAT pathway and related signal cascades in telomerase activation during the development of hematologic malignancies. *JAK-STAT*. https://doi.org/10.4161/jkst.25256

Yamamoto, R., Morita, Y., Ooehara, J., Hamanaka, S., Onodera, M., Rudolph, K. L., … Nakauchi, H. (2013). Clonal analysis unveils self-renewing lineage-restricted progenitors generated directly from hematopoietic stem cells. *Cell*. https://doi.org/10.1016/j.cell.2013.08.007

Yan, H., Hale, J., Jaffray, J., Li, J., Wang, Y., Huang, Y., … Blanc, L. (2018). Developmental Differences Between Neonatal and Adult Human Erythropoiesis. *American Journal of Hematology*, *93*, 494–503. https://doi.org/10.1002/ajh.25015

Yan, H., Wang, Y., Qu, X., Li, J., Hale, J., Huang, Y., … An, X. (2017). Distinct roles for TET family proteins in regulating human erythropoiesis. *Blood*, blood-2016-08-736587. https://doi.org/10.1182/blood-2016-08-736587

Yoshida, H., Kawane, K., Koike, M., Mori, Y., Uchiyama, Y., & Nagata, S. (2005). Phosphatidylserine-dependent engulfment by macrophages of nuclei from erythroid precursor cells. *Nature*, *437*(7059), 754–758. https://doi.org/10.1038/nature03964

Yuan, W., Cai, W., Zhou, W., Han, Z., Lei, J., Zhuang, J., … Wu, X. (2020). Master regulator genes and their impact on major diseases. *Peer J*. https://doi.org/10.7717/peerj.9952

Zemanova, Z., Brezinova, J., Svobodova, K., Lhotska, H., Izakova, S., Sarova, I., … Michalova, K. (2018). Variability in the extent of del(5q) and its clinical implication in myelodysplastic syndromes (MDS). *Https://Doi.Org/10.1200/JCO.2018.36.15_suppl.E19025*, *36*(15_suppl), e19025–e19025. https://doi.org/10.1200/JCO.2018.36.15_SUPPL.E19025

Zermati, Y., Fichelson, S., Valensi, F., Freyssinier, J. M., Rouyer-Fessard, P., Cramer, E., … Hermine, O. (2000). Transforming growth factor inhibits erythropoiesis by blocking proliferation and accelerating differentiation of erythroid progenitors. *Experimental Hematology*, *28*(8), 885–894. https://doi.org/10.1016/S0301-472X(00)00488-4

Zeuner, A., Francescangeli, F., Signore, M., Venneri, M. A., Pedini, F., Felli, N., … De Maria, R. (2011). The Notch2-Jagged1 interaction mediates stem cell factor signaling in erythropoiesis. *Cell Death and Differentiation*, *18*(2), 371–380.

https://doi.org/10.1038/cdd.2010.110

Zeuner, Ann, Pedini, F., Signore, M., Testa, U., Pelosi, E., Peschle, C., & De Maria, R. (2003). Stem cell factor protects erythroid precursor cells from chemotherapeutic agents via up-regulation of Bcl-2 family proteins. *Blood*, *102*(1), 87–93. https://doi.org/10.1182/blood-2002-08-2369

Zhang, J., Khvorostov, I., Hong, J. S., Oktay, Y., Vergnes, L., Nuebel, E., … Teitell, M. A. (2011). UCP2 regulates energy metabolism and differentiation potential of human pluripotent stem cells. *EMBO Journal*, *30*(24), 4860–4873. https://doi.org/10.1038/emboj.2011.401

Zhang, Y., Wang, L., Dey, S., Alnaeeli, M., Suresh, S., Rogers, H., … Noguchi, C. T. (2014, June 10). Erythropoietin action in stress response, tissue maintenance and metabolism. *International Journal of Molecular Sciences*, Vol. 15, pp. 10296–10333. https://doi.org/10.3390/ijms150610296

Zhao, B., Liu, H., Mei, Y., Liu, Y., Han, X., Yang, J., … Ji, P. (2019). Disruption of erythroid nuclear opening and histone release in myelodysplastic syndromes. *Cancer Medicine*, *8*(3), 1169. https://doi.org/10.1002/CAM4.1969

Zhao, B., Mei, Y., Yang, J., & Ji, P. (2016). EPO-regulated oxidative stress negatively affects enucleation during terminal erythropoiesis. *Experimental Hematology*, *44*(10), 975–981. https://doi.org/10.1016/j.exphem.2016.06.249.Erythropoietin-regulated

Zhou, L., McMahon, C., Bhagat, T., Alencar, C., Yu, Y., Fazzari, M., … Verma, A. (2011). Reduced SMAD7 leads to overactivation of TGF-β signaling in MDS that can be reversed by a specific inhibitor of TGF-β receptor I kinase. *Cancer Research*, *71*(3), 955–963. https://doi.org/10.1158/0008-5472.CAN-10-2933

Zhou, L., Nguyen, A. N., Sohal, D., Ma, J. Y., Pahanish, P., Gundabolu, K., … Verma, A. (2008). Inhibition of the TGF-β receptor I kinase promotes hematopoiesis in MDS. *Blood*, *112*(8), 3434–3443. https://doi.org/10.1182/blood-2008-02-139824

Zou, P., Yoshihara, H., Hosokawa, K., Tai, I., Shinmyozu, K., Tsukahara, F., … Suda, T. (2011). p57Kip2 and p27Kip1 Cooperate to Maintain Hematopoietic Stem Cell Quiescence through Interactions with Hsc70. *Cell Stem Cell*, *9*(3), 247–261. https://doi.org/10.1016/J.STEM.2011.07.003

Zwifelhofer, N. M., Cai, X., Liao, R., Mao, B., Conn, D. J., Mehta, C., … Bresnick, E. H. (2020). GATA factor-regulated solute carrier ensemble reveals a nucleoside transporter-dependent differentiation mechanism. *PLoS Genetics*, *16*(12

December), 1–26. https://doi.org/10.1371/journal.pgen.1009286